

**MIOCENE BASIN EVOLUTION OF THE ISPARTA ANGLE,
SOUTHERN TURKEY**

Rachel Flecker

*Thesis submitted for the degree of
Doctor of Philosophy*

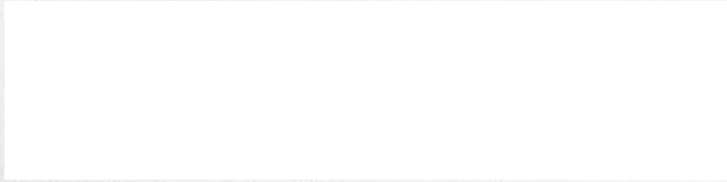
*University of Edinburgh
1995*



To Lara and Brontë

DECLARATION

I declare that this thesis has been written by myself and is the result of my own research, except where contributions have been stated and duly acknowledged.



Rachel Flecker

Acknowledgements

This project was set up and supervised by Alastair Robertson and John Underhill at Edinburgh University and André Poisson at Orsay (Paris XI) where I spent some part of every year. Alastair and André both came into the field with me and contributed greatly both to the academic content of this thesis and also to my enjoyment of fieldwork in Turkey. All three of my supervisors have read this thesis and I am particularly grateful to them all for their prompt response to my chapters as the deadline for the end of the project drew near.

Perhaps the greatest debt of any fieldwork project is owed to those who brave the heat, the bug-ridden water and the outrageous driving to come and field assist. Toby Harris, James Flecker, Mike Metcalf, Mark Hodson, Elizabeth Pickett and Lawrence Miles have all left an indelible mark on this Ph.D. visible only in my note book and on my sample bags, but permeating unseen throughout.

In Edinburgh my research has been facilitated by the help and guidance of the following people: Pedder Aspen, Mike Shaw, Nicky McEwan, Helena Jack, Diana Batey, Janet Cuthill, Yvonne Cooper, Geof Angell, Shane Voss and Ian Chisholm. I received similar support from the team in Batiment 504 in Orsay and would like to thank Geneviève Roche in particular. Rob Ellam, Anne and Vinney (East Kilbride), Brian Rosen (Natural History Museum) and Carla Müller all provided essential technical expertise.

The Turkish aspect of this project would have been so much more difficult had it not been for the endless help of Mustafa Gerger (Pepsi factory, Antalya) who managed the bureaucracy of exporting rocks and renewing visas with great good humour and patience. I would like to thank Celal Sengör for introducing me to Musafer and providing logistical support from Istanbul Technical University. The hospitality and friendship of those I met in Turkey is unforgettable and I can't wait to go back in a few months time and see them all. Particular mention must be made of the people at Unals Kebab Salonu, Feyvsi, Atilla, Halide, and Timor, Ida and Ece Üstömer.

Useful discussions have been had with the following people: John Dixon, Roger Scrutton, Dick Kroon, Bill Austin, Olivier Monod, Dominique Frizon de Lamotte, Graham Williams, Peter Clift and past and present members of the Tethyan Group. Jon Turner constructed and explained the subsidence curves presented here. I have been particularly fortunate to be writing up at the same time as Anne Payne and Clare Glover. Their knowledge of different regions/times of the Eastern Mediterranean and their support and encouragement throughout the painful business of finishing has been invaluable.

Finally my thanks Phil and Paul for their tolerance; to Flatmate Flem for his yummy meals and enthusiasm and to the KB supper club for their solidarity in adversity: John, Sandra, Jon, Anne, Clare, Jo. As I write, Jerry is checking and formatting my references and La is sticking on page numbers. Thanks too, to Sprout for the flowers.

ABSTRACT

The study of basins developed on top of older suture zones is demonstrably important in the Tethyan region where rifting and convergence have occurred repeatedly from the Mesozoic to the present-day. In southern Turkey, three Miocene basins developed in the Isparta Angle suture zone. Two of these, the Aksu and Köprü basins, are orientated north-south, parallel to pre-Miocene lineaments in the basement (e.g. Antalya Complex). These basins are underlain by a mosaic of deformed Mesozoic carbonate platforms, deep-sea sediments and ophiolitic units. The Manavgat basin, to the east, overlies Permian meta-carbonates (Alanya Massif) deformed by NW-SE trending basement structures. The northern margin of the Manavgat basin, in the south-east of the area, is also orientated NW-SE, but it was open to the Mediterranean Sea to the south.

Prior to Burdigalian-Langhian transgression, a thick (~1.5km) succession of predominantly continental conglomerates and sandstones accumulated in the south of the Aksu and Köprü basins (Kizildag Formation). Coeval thrusting of the Lycian Nappes on the western limb of the Isparta angle is inferred to have induced block faulting of the foreland, exploiting pre-existing basement weaknesses and generating accommodation space.

In the Manavgat basin palaeocurrents and south-to-north diachroneity of transgression demonstrate that the Alanya Massif formed a palaeogeographic high to the north of the basin. This was colonised by coral and algal fringing reefs, which shed abundant shallow-water debris, deposited as calcarenites in Langhian times (Oymapinar Limestone). Elsewhere, to the south and west, Late Burdigalian-Langhian patch reefs developed within coastal fan-delta conglomeratic sequences. Detailed study of the interaction between coral growth and clastic influx reveals that relative sea level rise outstripped sediment influx at this time.

Extensional faulting during the Langhian in the Manavgat basin generated numerous micro-faults which trend parallel to NW-SE basement lineaments. This faulting led to the deposition of localised talus (Çakallar Formation) and formation of an asymmetrical horst-graben structure. Reef deposition was abruptly terminated and 3-500m of Serravallian planktic foraminiferal marls (Geceleme Formation) then accumulated as post-rift fill. In the Aksu and Köprü basins, a correlative transition from shallow-water carbonates to deeper-water turbidite deposition (Karpuzçay Formation) is observed.

Palaeocurrents from the Köprü basin suggest that N-S striking lineaments in the basement funnelled sediment southwards in the north of the basin, but had little topographic expression in the south.

In the Early Tortonian, the Geceleme Formation in the Manavgat basin passed rapidly up into slumped siltstones, sandstones and coarse conglomerates, containing large (~10m) detached blocks of Alanya Massif metacarbonate. Debris-flow processes dominated the deposition of this succession (Karpuzçay Formation) and together with foraminiferal studies, document uplift and infill of the basin during Tortonian-Messinian times. In the north of the Aksu and Köprü basins, uplift caused a transition from Karpuzçay turbidites to shallow-marine fan-delta conglomerates with rare patch reefs.

At the end of the Miocene, a compressional event caused the reactivation of the N-S striking lineaments in the Isparta Angle and small-scale inversion of the horst-graben structure in the Manavgat basin. East- and west-vergent faults and large -scale recumbent folds deformed Miocene and basement rocks. Compressional forces, oblique or orthogonal to the N-S fabric of the Isparta Angle, could have been generated both by movement of the Lycian Nappes to the north-west and westward escape of the Anatolian block. On a more regional scale, the Isparta Angle basins appear to be part of a transtensional system which linked the Aegean arc to the west with the Cyprus arc to the east.

ÖZ

Mezozoik'ten günümüze kadar süregelen riftlerin ve konverjansların sürekli olarak meydana geldiği Tetis bölgesindeki eski kenet kuşaklarında gelişmiş havzaların incelenmesi önemli bir yer tutmaktadır. Türkiye'nin güneyinde, Isparta açısı kenet kuşağında üç Miyosen yaşlı havza gelişmiştir. Bunlardan ikisi, Aksu ve Köprü havzaları, temel kayaç içerisindeki Miyosen öncesi çizgiselliklere (lineamentlere) paralel olarak (Antalya kompleksi) Kuzey-Güney yönündedirler. Bu havzalar deforme olmuş Mezozoik karbonat platformları, denizel sedimanlar ve ofyolitler birliğinden oluşan bir mozaik üzerine oturmuştur. Doğuda Manavgat havzası, KB-GD yönlü temel kayaç yapıları tarafından deforme olmuş permien yaşlı meta-karbonatları (Alanya masifi) örtmüştür. Bölgenin güney doğusunu oluşturan Manavgat havzasının kuzey kenarı yine KB-GD yönündedir, fakat güneyde Akdeniz'e açılmıştır.

Burdigaliyan-Langhiyan transgresiyonundan önce Aksu ve Köprü havzalarının güneyinde kumtaşı ve karasal karbonat ağırlıklı kalın (~1.5km) bir çökeltme (Kızıldağ Formasyonu) meydana gelmiştir. Lysiyen naplarının eşzamanlı batıdaki Isparta açısına bindirmeleri, var olan yumuşak temel kayaçlardan yararlanarak ve gerekli sahayı oluşturarak ön ülke blok deformasyonunu doğurmasından anlaşılmaktadırlar.

Manavgat havzasındaki paleo-yapılar ve güneyden kuzeye doğru transgresiyon diyakroneiti, Alanya masifinin havzanın kuzey kesiminde yüksek paleo-cografik yapıları meydana getirdiğini göstermektedirler. Bu, Langhiyan yaşlı kalkarenit gibi depolanmış bolca sığ-su kırsıtlı olarak çökelmiş (Oymapınar kireçtaşı) kenar resifli depolar ve algler tarafından istila edilmiştir. Öte yandan güneye ve batıya doğru, üst Burdigaliyan-Langhiyan parça resifi delta yelpazeli iri konglomeratik sekanslar içerisinde gelişmiştir. Resif depoları ile bolca detritik malzemenin arasındaki ilişkinin detaylı incelenmesi, göreceli olarak su düzeyinin yükselmesi sedimanların depolanmasına oranından daha fazla olduğunu göstermektedir.

Manavgat havzasında Langhiyan boyunca extensif deformasyon KB-GD doğrultulu temel kayaç çizgiselliklerine paralel olarak pek çok mikro-fay meydana getirmiştir. Bu faylanma, yamaç deposuna (Cakallar formasyonu) ve asimetrik horst-graben yapısında bir formasyona olanak sağlar. Resif deposu aniden sona ermiş ve 3-500 m kalınlığında Serravalliyan yaşlı planktik foraminiferaylı marnlar (Geceleme formasyonu) rift çökeltme sonrası şeklinde çökelmiştir. Aksu ve Köprü havzalarında sığ denizel karbonatlardan derin deniz turbidit deposuna (Karpuzçay Formasyonu) doğru bir korelatif geçiş gözlenmiştir. Köprü havzasından itibaren paleo-yapılar havzanın kuzeyinden güneyine doğru kanalise

olmuş temel kayaç sedımanları içerisinde K-G yönlü çizgiselliklere işaret ederken güneyde küçük topografik yapılara sahiptir.

Erken Totonıyan'da Manavgat havzasında Geceleme Formasyonu hızlı bir biçimde çökelmiş kıltaşı, kumtaşı ve iri taneli kongromeralara ~10m kalınlığında Alanya masifi meta-karbonatlarından kopan bir blok ihtiva ederek geçmektedir. Kırıntılı-akışkan süreçleri bu sıralı depolanmaya (Karpuz Formasyonu) hakim olmuşlardır ve foraminiferal etudlerle birlikte havzanın Tortonoyan-Messiniyan'da yükseldiğini ve depolandığını kanıtlamaktadır. Aksu ve Köprü havzalarının güneyinde yükselmeler Karpuzçay turbuditlerinin siğ denizel delta yelpase kongromelara geçişleri ile birlikte az miktarda parça resiflerini meydana getirmektedir.

Miyosen sonunda, bir kompresif safha, Isparta açısında K-G yönlü çizgisellikleri ve Manavgat havzasında hors-graben yapısının küçük ölçekli terslenimini tekrar harekete geçirmiştir. Dogu-Batı uzanımlı faylar ile büyük ölçekli yatık kıvrımlar Miyosen yaşlı seriyi ve temel kayaçları deforme etmişlerdir. Kompresif kuvvetler, Isparta açısının K-G yapısına oblik veya diagonal olarak Lysiyan napının kuzey doğuya doğru ile Anadolu blokunun batıya doğru hareketlerinden dolayı meydana gelmiş olabilirler. Daha geniş ölçekli bir bölgede, Isparta açısı havzaları batıda Ege arkı ve doğuda Kıbrıs arkı ile ilişki sağlayan transgresif sistemin bir parçası görünümündedirler.

TABLE OF CONTENTS

Chapter 1	Introduction	
1.1	Context	1
1.2	Plate tectonic setting of the Eastern Mediterranean	1
1.4	An overview	11
1.5	General Aims	11
1.7	Thesis organisation	14
Chapter 2	Stratigraphy	
2.1	Introduction	17
2.2	Lithostratigraphy, biostratigraphy and isotopic dates	17
2.3	Historical development of existing stratigraphic framework	21
2.4	Revised Stratigraphy	23
Chapter 3	Biogenic Carbonates	
3.1	Context	32
3.2	Geographical distribution	32
3.3	Organisation of the chapter	32
3.4	Previous work	34
3.5	Classification	36
3.6	Facies description	41
3.6.1	Reef facies	41
3.6.1.1	Domal coral framestone	42
3.6.1.2	Porites bafflestone	48
3.6.1.3	Fan coral framestone	51
3.6.1.4	Porites rudstone	55
3.6.1.5	Summary of reef sub-facies	58
3.6.2	Off-Reef facies	58
3.6.2.1	Coral floatstone	60
3.6.2.2	Rhodolithic calcarenites	66
3.6.2.3	Reef talus	69
3.6.2.4	Summary of off-reef sub-facies	74
3.6.3	Reef-associated facies in coarse clastic environments.	74
3.6.3.1	Echinoid-scapopod grainstone	74
3.6.3.2	Oyster packstone	77
3.6.3.3	Gastropod grainstone/wackestone	78
3.6.3.4	Oyster bafflestone	79
3.6.3.5	Summary of reef-associated sub-facies	81
3.6.4	Carbonate shelf facies	81
3.6.4.1	Planktic foraminiferal marl	81
3.6.4.2	Operculina packstones/grainstones	84
3.6.4.3	Calcirudites	85
3.6.4.4	Summary of shelf sub-facies	85
3.7	Model of sub-facies location.	88
3.8	Discussion	88
3.8.1	The Mid-Miocene hiatus in shallow-water carbonate production	88
3.8.2	Coral zonation	89
3.8.3	Spatial morphology of reefs	92
3.9	Conclusions	95

Chapter 4	Sediment Gravity Flows and the Karpuzçay Formation	
4.1	Context	97
4.2	Organisation of this chapter	97
4.3	Temporal and Spatial distribution	97
4.4	Previous work	98
4.5	Facies description	102
4.5.1	Aksu Basin	102
4.5.1.1	Texture and composition	102
4.5.1.2	Processes of deposition	108
4.5.1.3	Palaeocurrent analysis	113
4.5.1.4	Temporal and spatial variations	117
4.5.2	Köprü Basin	118
4.5.2.1	Texture and composition	120
4.5.2.2	Interpretation	126
4.5.2.3	Palaeocurrent analysis	126
4.5.2.4	Spatial and temporal variations	128
4.5.3	Manavgat basin	129
4.5.3.1	Texture and composition	132
4.5.3.2	Interpretation	141
4.5.3.3	Spatial and temporal variations	147
4.5.3.4	Palaeocurrent analysis	153
4.7	Summary interpretation and reclassification of the Karpuzçay Formation	153
4.8	Correlation of the Karpuzçay Formation across the Isparta Angle	155
4.9	Conclusions	159

Chapter 5	Fan-Delta Sedimentation, Process and Controls: the Aksu and Kizildat Formations	
5.1	Context	160
5.2	Organisation of this chapter	160
5.3	Temporal and Spatial distribution	161
5.4	Previous work	161
5.4.1	The conglomerate successions	161
5.4.2	Lacustrine limestone	165
5.5	Facies description	165
5.5.1	Sub-facies association A	165
5.5.1.1	Clast-supported angular conglomerate.	165
5.5.1.2	Clast-supported conglomerates and coarse sandstones	168
5.5.1.3	Matrix-supported conglomerates	173
5.5.1.4	Laminated sandstones	178
5.5.1.5	Calcretes and associated fine-grained sediments	179
5.5.1.6	Interpretation of sub-facies association A	182
5.5.2	Sub-facies association B	185
5.5.2.1	Organic rich horizons	185
5.5.2.2	Green clays	189
5.5.2.3	Laminated limestone and lime mud	190
5.5.2.4	Gastropod siltstones	194
5.5.2.5	Limestone breccia	195
5.4.2.6	Interpretation of sub-facies association B	200
5.5.3	Sub-facies association C	203
5.5.3.1	Echinoid-scapopod facies	203
5.5.3.2	Porites bafflestones	204
5.5.3.3	High angle, cross-bedded conglomerates	209
5.5.3.4	Interpretation of sub-facies association C.	218
5.5.4	Sub-facies association D	218
5.5.4.1	Clast-supported conglomerates	220

	5.5.4.2	Matrix-supported conglomerates	222
	5.5.4.3	Fossiliferous and cross-bedded sandstones	224
	5.5.4.4	Interpretation of sub-facies association D	225
5.6		Provenance and Palaeocurrent data	225
	5.6.1	The Manavgat basin	228
	5.6.2	The Aksu and Köprü basins	230
5.7		General interpretation of the sedimentary system.	233
5.8		Classification of the fan delta systems	235
5.9		Controls on fan-delta development	235
	5.9.1	Climate	237
	5.9.2	Tectonics	239
	5.9.3	Eustacy	241
5.10		Conclusions	243

Chapter 6

Strontium Isotope Dating

6.1		Context	245
6.2		Introduction to Strontium dating	245
6.3		Application of $^{87}\text{Sr}/^{86}\text{Sr}$ dating technique to the Miocene of the study area and the correction for radiogenic Sr	246
6.4		Methodology	247
	6.4.1	Sample selection	247
	6.4.2	Cleaning methods	253
	6.4.3	Chemistry	253
	6.4.4	Mass Spectrometry	254
	6.4.5	Calculations	255
6.5		Results	257
	6.5.1	Assessment of the validity of the ages	257
	6.5.1.1	Comparison of the two Sr sea water curves	257
	6.5.1.2	Foraminiferal samples	261
	6.5.1.3	Macrofossil samples	261
	6.5.2	Ages of the shallow water carbonates and the transgression surface	263
	6.5.2.1	Lower-Middle Miocene	264
	6.5.2.2	Upper Miocene	266
6.6		Diagenesis	266
6.8		Conclusions	268

Chapter 7

Structure and Tectonic Context

7.1		Context	270
7.2		Organisation of this chapter	270
7.3		Introduction	271
7.4		Previous work	271
7.5		Deformational structures	279
	7.5.1	The Manavgat basin	279
	7.5.1.1	Basement and basal Miocene structures	279
	7.5.1.2	Evidence of brittle fracture in Miocene sediments	280
	7.5.1.3	Folding of Miocene sediments	296
	7.5.1.4	Interpretation and basin evolution	300
	7.5.2	The Köprü and Aksu basins	305
	7.5.2.1	Basement and basal Miocene structures	305
	7.5.2.2	Basin bounding faults and faults within Miocene sediments	306
	7.5.2.3	Folding of Miocene sediments	313
	7.5.2.4	Interpretation	317
7.6		Tectonic context	321
	7.6.1	Formation of the Miocene basins	321
	7.6.1.1	Post-Langhian anticlockwise rotation of the Bey Daglari and	321

		extension in the Manavgat basin.	321
	7.6.1.2	Subduction related extension on the upper plate of the Hellenic-Cyprus system	325
	7.6.2	Emplacement of the Lycian Nappes and the Aksu Phase	326
	7.6.3	Evidence for a later Susuz Dag Phase of southward transport	329
7.7		Conclusions	330
Chapter 8		Regional Comparisons and Conclusions	
8.1		Introduction	332
8.2		Regional comparisons	332
	8.2.1	Kas basin, outboard of the Lycian Nappes, SW Turkey	332
	8.2.2	Adana basin, north-east corner of Mediterranean, SE Turkey	337
	8.2.3	Northern Cyprus	341
	8.2.4	Southern Cyprus	342
	8.2.5	Crete, north of the Hellenic trench	343
8.3		The relative importance of tectonics (local and regional) versus eustasy in controlling sedimentation	347
	8.3.1	Closure of Neotethys	350
Conclusions			352
References			356
Appendices			
1		XRD analysis on coral samples from the Köprü and Manavgat basins	I
2		Strontium dating table	II
3.A.1		Nannoplankton from the Ahmetler Section samples, Manavgat basin	IV
3.A.2		Nannoplankton from the Aksu, Köprü and Manavgat basins (with the exception of the Ahmetler section)	VI
3.B		Counts of benthic and planktic foraminifer from the Ahmetler section, Manavgat basin	X
3.C		Coral indication	XI
4.A.1		Conglomerate analysis from the Kizildag Formation in the Manavgat basin	XII
4.A.2		Conglomerate analysis from the Kizildag Formation and the Aksu Formation in the Köprü basin	XIV
4.B.1		Typical values for point counted marls from the Manavgat and Köprü basins	XVI
4.B.2		Typical point counts from the Karpuzçay Formation sandstones of the Köprü, Aksu and Manavgat basins	XVII
5.1		Akseki Road Section	XVIII
5.2		Stratigraphic location of samples used for nannoplankton analysis and Sr dating	XXXV
6		Backstripping	XLI

LIST OF FIGURES

Chapter 1

1.1	Regional plate setting of the Mediterranean Sea	2
1.2	Map of the north-eastern Mediterranean showing the location of the main suture zones and tectonic units. Inset showing the Isparta Angle and the three Miocene basins within it.	3
1.3	Isparta Angle area and tectonic units mentioned in the text	5
1.4	More detailed map of the Isparta Angle	7
1.5	Alternative models of the formation of the Antalya Complex	9
1.6	Satellite photograph of the area	12
1.7	Diagram showing the overlap of the formations in the three chapters	16

Chapter 2

2.1	Location map of places mentioned in the text	18
2.2	Biostratigraphic chart	19
2.3	Areas of Isparta Angle covered by previous workers.	22
2.4	Chronostratigraphic chart showing the relationship of the various formations from Akay <i>et al.</i> (1985)	28
2.5	Modified stratigraphic framework used during this study	31

Chapter 3

3.1	Location map of all carbonate deposits and sections referred to in text.	33
3.2	Thin section photo of speckly and deformed carbonate.	39
3.3	Sketch of channel in reef south of Yesilbag	43
3.4	Alarahan section showing different vertical coral zonation in its 4 reefs.	45
3.5	Photograph of the irregular massive <i>Montastrea</i> build up at Kesme.	46
3.6	Photograph of spaced <i>Porites</i> bafflestone with interstitial grit.	46
3.7	South Kargi log correlated to east of tunnel log	49
3.8	East of tunnel photomontage with sketch beneath.	52
3.9	Photograph of <i>Tarbellastrea</i> framestone.	53
3.10	Photograph of stick <i>Porites</i> framestone at Yesilbag	53
3.11	SEM photograph of skeletal fibres of aragonite in Dumanli coral.	63
3.12	Photograph of abraded <i>Favites neglecta</i> and well preserved and less abraded <i>Heliastrea oligophylla</i>	64
3.14	Bedded calcarenites banking up against Alanya Massif basement with marked palaeotopography.	67
3.15	Rhodolithic algae forming round a flat <i>Porites</i> nucleus.	67
3.16	Oymapinar log of the shallow-water carbonate section showing multiple talus horizons.	70
3.17	Photograph of the cemented top of the Akseki road talus horizon and the loose rubble beneath.	72
3.18	Echinoid-Scaphopod facies with algal rhodoliths encrusting Mesozoic limestone pebble.	72
3.19	Scaphopods parallel to laminations.	76
3.20	Pteropod moulds in planktic foraminiferal marls.	76
3.21	Depositional model of the biogenic carbonates	87
3.22	Reef zonation of coral morphology (after Hayward 1982a).	91
3.23	Geological map of the Manavgat basin.	94

Chapter 4

4.1	Base map with outcrop pattern and localities mentioned in the text	99
4.2	Base map with Akay's dates for the Karpuzçay on them.	101
4.3	Photograph of overturned sandstone and siltstone beds of the Karpuzçay Formation.	103
4.4	Photograph of Karpuzçay formation turbidites indicating a silt to sand transition	103
4.5	Log of the succession shown in Figure 4.3	104
4.6	Log of the succession shown in Figure 4.4,	105
4.7	Idealised Bouma (1962) sequence of sedimentary structures in a turbidite bed.	110
4.8	Classification of sediment gravity flows in terms of their flow rheology and particle support mechanism	111
4.9	Origin of traction carpets during high-density turbidity flow	111
4.10	Palaeocurrent directions measured in the Aksu basin from the Karpuzçay formation.	116
4.11	Contrasting conglomerate concentrations in logs of the Karpuzçay Formation for the north and south of the Aksu basin.	119
4.12	Photograph of a channel in Karpuzçay Formation, central Köprü basin.	121
4.13	Photograph of rip-up clasts in a sandstone unit from the Karpuzçay Formation, central Köprü basin.	121
4.14	Photograph of a bored coal fragment in a Karpuzçay Formation siltstone unit	124
4.15	Photograph of a slumped horizon overlain by a channelised sandstone, overlain by a debris flow containing a detached block of Alanya Massif metacarbonate from the Karpuzçay Formation	124
4.16	Köprü basin palaeocurrent rose diagrams.	124
4.17	Schematic palaeogeographic reconstruction of the Köprü basin	127
4.18	Summary log of the Ahmetler section.	131
4.19	Triangular diagram plotting the relative proportions of Alanya Massif metacarbonate, Miocene shallow-water carbonate and lithic clasts in conglomerates and debris flows from the Çakallar, Geceleme and Karpuzçay Formations	134
4.20	Photograph of a unit with a clast-supported, imbricated basal layer and an upper layer of matrix-supported conglomerate from the Karpuzçay Formation.	137
4.21	Photograph of a large water escape structure intruding into an imbricated conglomerate,	137
4.22	Photograph of a large load structure located in the Messinian of the Karpuzçay Formation	139
4.23	Photograph of layered bioturbation.	139
4.24	Chart of ichnofacies assemblages related to water depth	140
4.25	Photograph of the "snapped beds" where both ductile and brittle deformation have occurred during deposition of the overlying conglomerate unit	142
4.26	Characteristics of submarine debris flows (Nemec and Steel, 1984).	146
4.27	Benthic/planctic foraminiferal ratios for the Ahmetler section, Manavgat basin	148
4.28	Sedimentation rates for the Ahmetler, Alarahan and Oymapinar sections in the Manavgat basin.	151
4.29	Correlation of Manavgat basin sections.	152
4.30	Rose diagrams of the palaeocurrents directions in the Manavgat basin.	154

4.31	Schematic sketches representing the development of the Isparta Angle throughout the period of Karpuzçay Formation deposition.	156
4.32	North west- south east correlation diagram of the Isparta Angle.	157
4.33	Subsidence curves for the Alarahan, Ahmetler and Oymapinar section, Manavgat basin.	158

Chapter 5

5.1	Geographical area covered by exposure of the Aksu Formation and the localities mentioned in the text.	162
5.2	The names and inferred ages of the basal conglomerate succession in the Manavgat basin.	163
5.3	Tortonian angular clast-supported conglomerate banked up against the Kapikaya (after Gutnic et al., 1979)	166
5.4	Photograph of some of the mega-clasts in the angular conglomerate at Kapikaya, north Aksu basin.	166
5.5	Photograph and field sketch of channelised red conglomerates directly overlying basement melange	170
5.6	Photograph, sketch log and rose diagrams for the Aspendos section	172
5.7	Typical features of subaerial mass-flow deposits (After Nemec and Steel, 1984).	177
5.8	Morphologies of calcrete.	180
5.9	Evidence of roots in a medium sandstone	181
5.10	Log and interpretation of the Bozburun coal section, north west Koprü basins, with rose diagrams derived from measurements of the cross-bedded conglomerates.	186
5.11	Log of the Yaylaalan transition section from continental conglomerates through lagoonal facies to shallow-water marine limestones. Photograph of bioturbated limemud from this section.	187
5.12	Location map of the Kepezbelenli section on the northern margin of the Manavgat basin	191
5.13	Log of the Kepezbelenli section and a thin section photograph of the laminated limestone facies from this locality.	192
5.14	Photograph of limestone breccia at Kesme unconformably overlying Mesozoic carbonates.	196
5.15	Interbedded limestone breccia and polymict conglomerate at Kesme gorge	196
5.16	Breach in the Kirkkavak fault to the west of Dumanli in the north of the Koprü basin.	198
5.17	Log and photographs of the transition between limestone breccia and polymict conglomerate at the Kesme gorge locality, North Koprü basin.	199
5.18	Generalised model of the depositional environments and processes active in producing lagoonal and lacustrine sediments in the study area.	202
5.19	Photomontage showing the five reef successions at South Kargi interbedded with coarse alluvial red clastics.	206
5.20	Correlation of the logged sections at South Kargi, central Aksu basin and a facies model	207
5.21	Cartoon of rising sea level versus sediment influx in Porites bafflestone environments.	208
5.22	Photograph of the high-angle cross-bedded conglomerates at Bozburun, north west Koprü basin.	
5.23	The twelve major proto-type deltas suggested by Postma (1990).	212
5.24	Schematic diagrams of conical and Gilbert-type deltas (after Nemec, 1990b).	214

5.25	Field sketch of high angle cross-bedded conglomerates and reef limestones at Alarahan, south Manavgat basin	216
5.26	Model of the fan-delta shoreline facies preserved in the study area.	219
5.27	Photograph of the parallel bedded conglomerates at Bucakkoyu, west Kopru basin.	221
5.28	Outcrop sketch of the most proximal part of an underwater conical delta abutting against a palaeofault scarp of the Capo dell'Armi horst, Messinian Strait, Italy	223
5.29	Cross-laminated sandstones and gravels north of Yesilbag, north east Kopru basin Aksu Formation.	221
5.30	Provenance data from the Manavgat basin	227
5.31	Palaeocurrent data from the lower conglomerate succession in the Manavgat basin.	229
5.32	Triangular diagram of the conglomerates from the Kopru and Aksu basins.	231
5.33	Bar chart of the radiolarian chert distribution through out the Kopru basin.	231
5.34	Palaeocurrent data from the Aksu conglomerates in the Aksu and Kopru basins.	232
5.35	Geographic areas covered by different conglomerate groups of the Kizildag and Aksu Formations.	236
5.36	Conceptual framework for a comparative study of both modern and ancient delta systems	238
5.37	Eustatic sea level curve for the Miocene (Haq <i>et al.</i> , 1988)	242

Chapter 6

6.1	SEM photograph of a benthic foraminifera showing excellent preservation of skeletal structure	248
6.2	SEM photograph of a foraminifera which has been filled with diagenetic calcite rhombs.	248
6.3	Graph of Sr ratio versus age showing the two linear regressions of Miller <i>et al.</i> (1991) and the 5th order polynomial best fit of Hodell and Woodruff (1994).	256
6.4	Sr ages measured for the foraminiferal samples compared with their nannoplankton zones.	258
6.5	Graph of Sr ratio versus age showing the errors on the data for the linear regression of Miller <i>et al.</i> (1991) for the Lower Miocene and the 5th order polynomial best fit of Hodell and Woodruff (1994).	260
6.6	Sr ages measured for the non-foraminiferal samples using the linear regression of Miller <i>et al.</i> (1991)	265

Chapter 7

7.1	Map of a) north-eastern Mediterranean and b) Southern Turkey showing the tectonic units around the field area	272
7.2	More detailed map of the Isparta Angle showing the north-south structural lineaments within the Antalya Complex.	273
7.3	Model from Kissel <i>et al.</i> (1993) of the evolution of the Isparta Angle.	275
7.4	Diagram illustrating the geometry of a lateral culmination fold on a south-vergent blind thrust as envisaged by Frizon de Lamotte <i>et al.</i> (1995).	278
7.5	Location map of the places mentioned in the text	281
7.6	Geological map of the Manavgat basin with stereonet of fault data	283
7.7	Model of two extensional events to explain the normal fault distribution in the Lower-Mid and Upper Miocene succession.	284

7.8	Photograph of the normal offsets and transpressional slickensides on the faults at the Akseki Road locality.	285
7.9	Model of the changes in fault type affecting the Manavgat basin from Lower Miocene to recent times.	287
7.10	Geological map of the Manavgat basin showing the orientation of the west verging syncline and anticline in the east of the basin.	289
7.11	Schematic representation of outcrop data of joint development in the Çakallar formation south of Alarahan. A stereonet projection of the poles to these fractures is also shown with poles to bedding and π -girdle of the west-verging anticline.	290
7.12	Sections from the limbs of the folds in the east of the Manavgat basin, hung from the bottom of the Karpuzçay formation.	292
7.13	Schematic cross-section across the Manavgat basin indicating the possible structure of the basin at the end of deposition of the Geceleme formation.	295
7.14	a) Cross-section across the Manavgat basin taken from Akay (1985). b) Schematic reconstruction of the cross-section.	297
7.15	Theoretical generation of slickenside orientations	299
7.16	Schematic cross-section across the Manavgat at the end of the compressional event at the Mio-Pliocene boundary.	301
7.17	Subsidence curve for the Ahmetler section of the Manavgat basin with a theoretical (uniform stretching) subsidence curve fitted to it .	304
7.18	Geological map of the central region of the study area.	307
7.19	Stereonet projections of faults measured from the sub-basins located on top of the Mesozoic promontory a) NE-SW striking normal faults; b) the scattered orientation of the reverse faults.	308
7.20	Stereonet projections of fault data from the eastern parts of the Kopru and Aksu basins.	311
7.21	a) Stereonet projections of fault plane data from Kargi and Pinargözü from Frizon de Lamotte <i>et al.</i> (1995); b) Stereonet projections from the Pinargozu fault zone collected during this study.	312
7.22	a) Structural map and b) interpretative cross-section of the Aksu and Köprü basins (from Frizon de Lamotte <i>et al.</i> , 1995). c)interpretative cross-section from field observation presented in this study.	314
7.23	Photograph of the nose of the Bozburun Dag recumbent fold.	315
7.24	Photo-montage looking north from the Pinargozu pass	316
7.25	Photomontage and sketch of recumbent fold in Mesozoic carbonate and Miocene sediments near Akbas, SW Köprü basin.	318
7.26	Stereonet projections of fold axes from the eastern side of the Köprü basin and from well defined fault zones at Pinargozu in the west of the Köprü basin and at Kargi in the Aksu basin.	319
7.27	Sketches illustrating the rotation of broken parallel slats (Taymaz <i>et al.</i> , 1991).	323
7.28	Model proposed by Price and Scott (1994) modifying behaviour of the broken slat model (Taymaz <i>et al.</i> , 1991) at the eastern margin of the Aegean extensional region to accommodate observed structures in the Burdur region.	323
7.29	Model of the development of extension in the study area during the Langhian-Burdigalian	324
7.30	Early Miocene plate tectonic reconstruction of the Aegean-Lycian-Cyprus systems.	327
7.31	Diagram showing the possible role of the Isparta Angle as a transform zone linking the Hellenic and Cyprus subduction systems.	328
7.32	Model of the interaction between westward escape of Turkey and the dying breaths of the emplacement of the Lycian Nappes	331

Chapter 8

8.1	Model of the Miocene emplacement of the Lycian Nappes with respect to the Dariören-Kas basin	335
8.2	Palaeogeographic model of the Lower Miocene sedimentary basins on top of the Bey Daglari	336
8.3	Stratigraphy, sea level and tectonic interpretation of the Miocene sediments of the Adana basin	338
8.4	Map of the tectonic units of Cyprus.	340
8.5	Calculation for roll-back	346
8.6	Sea level curves for the Manavgat and combined Köprü and Aksu basins.	348
8.7	Comparison of Isparta Angle sea level curves with a curve from the Adana basin (Gürbüz, 1993) and the eustatic sea level curve generated by Haq <i>et al.</i> (1988).	349

List of Tables

Chapter 2

2.1	Chart of stratigraphic information for the Kizildag Formation	24
2.2	Chart of stratigraphic information for the Oymapinar limestone, Çakallar and Geceleme Formations	25
2.3	Chart of stratigraphic information for the Karpuzçay Formation	26
2.4	Chart of stratigraphic information for the Aksu Formation	27
2.5	Table showing the names of important sections in the Manavgat basin used by previous workers and those used in this study in an attempt to avoid confusion.	29
2.6	Table showing the division of the Karpuzçay, Aksu and Kizildag Formations into a series of formation groups reflecting the environment of deposition	30

Chapter 3

3.1	Chart of stratigraphic information for the Oymapinar Limestone, Çakallar Formation and Geceleme Formation.	35
3.2	Table showing difference in dates from Akay, Flecker <i>et al</i> , Monod, Dumont, Bizon and this study.	37
3.3	Diagram showing the facies and sub-facies of Akays carbonate classification.	39
3.4	Table of reef sub-facies, listing their characteristic fauna and the localities at which they can be found.	41
3.5	Summary of information and interpretation of reef sub-facies	59
3.6	Table of off-reef sub-facies, listing their characteristic fauna and the localities at which they can be found.	60
3.7	Table of names and ages of the corals found at Karapinar	62
3.8	Summary of information and interpretation of off-reef sub-facies	73
3.9	Table of reef-associated sub-facies, listing their characteristic fauna and the localities at which they can be found.	74
3.10	Summary of information and interpretation of reef-associated sub-facies	80
3.11	Table of shelf sub-facies, listing their characteristic fauna and the localities at which they can be found.	81
3.12	Table of depth diagnostic benthic foraminifera found in the planktic foraminiferal marls.	83
3.13	Summary of information and interpretation of shelf sub-facies.	86

Chapter 4

4.1	Description and classification of medium-sand to clay grade units from the Aksu, Köprü and Manavgat basins, in terms of low- and high-density turbidity currents (after Pickering <i>et al.</i> , 1989).	114
4.2	Description and classification of coarse sand and conglomerate units from the Aksu, Köprü and Manavgat basins in terms of high-density turbidity currents (after Pickering <i>et al.</i> , 1989).	115
4.3	Description and classification of matrix-supported conglomerates in terms of debris-flow processes (Pickering <i>et al.</i> , 1989).	144
4.4	Description and classification of clast-supported conglomerates in terms of high-density turbidity currents (Pickering <i>et al.</i> , 1989).	145

Chapter 5

5.1	List of the sub-facies in sub-facies association A, their localities and formations.	167
5.2	Criteria for distinguishing between streamflood and braided stream deposits (Modified after Steel and Wilson, 1976).	172
5.3	Table of the differences between subaqueous and subaerial debris flows.	176
5.4	Summary of the features of sub-facies association A.	183
5.5	List of the sub-facies in sub-facies association B, their localities and formations.	185
5.6	Differences between the limestone breccia at Kesme and the megabreccia at Kapikaya.	200
5.7	Summary of the features of sub-facies association B.	201
5.8	List of the sub-facies in sub-facies association C, their localities and formations.	203
5.9	Distinguishing features of Gilbert-type delta foresets and channel mouth bars (Nemec, 1990).	211
5.10	Summary of the features of sub-facies association C.	217
5.11	List of the sub-facies in sub-facies association D, their localities and formations.	218
5.12	Summary of the features of sub-facies association D.	226
5.13	Summary of the interpretation of individual sub-facies and the sub-facies associations as a whole.	234
5.14	Sub-division of the Aksu and Kizildag Formations (Akay, 1985; Akay <i>et al.</i> , 1985) into formation groups.	235

Chapter 6

6.1	Table showing the type of carbonates found in samples used for $^{87}\text{Sr}/^{86}\text{Sr}$ analysis and the sediment in which they were preserved.	249
6.2	List of the fauna used for $^{87}\text{Sr}/^{86}\text{Sr}$ analysis.	252
6.4	Measured values of $^{87}\text{Sr}/^{86}\text{Sr}$ and the ages calculated using the Lower Miocene regression from Miller <i>et al.</i> (1991) for the <i>Porites</i> sp. samples in the Alarahan section.	262
6.5	Measured values of $^{87}\text{Sr}/^{86}\text{Sr}$ and the ages calculated using the Lower Miocene regression from Miller <i>et al.</i> (1991) for algal samples in the Ahmetler section. The results are arranged in stratigraphic order, e.g. lowest sample at the bottom of the table.	262
6.6	Measured values of $^{87}\text{Sr}/^{86}\text{Sr}$ and the ages calculated using the Lower Miocene regression from Miller <i>et al.</i> (1991) for oyster samples in the Kargi section. The results are arranged in stratigraphic order, e.g. lowest sample at the bottom of the table.	263

Chapter 7

7.1	Thickness variations and a summary of the main rock types making up the Miocene formations folded in the east of the Manavgat basin.	294
7.2	Tabulation of the timing and tectonic events affecting the Manavgat basin. Evidence from the basin is also listed.	302

Chapter 8

8.1	Summary of sedimentation information from previous chapters	333
-----	---	-----

Chapter 1

INTRODUCTION

1.1 Context

The Mediterranean Sea lies along a complex zone of convergence between the Eurasian and Turkish plates to the north and the African, Arabian and Indo-Australian plates to the south. This boundary is marked today by the Alpine-Himalayan orogenic belt (Fig. 1.1). Palaeozoic-Recent fragments preserved within, or on the margins of this suture contain partial records of its history. In the Eastern Mediterranean intensive study of these fragments has been carried out with a view to reconstructing the nature of past and present collision, which in this area is complicated by the presence of a number of micro-plates along the suture zone (Robertson *et al.*, 1991b). Much of this work has focused either on the very young, neotectonic setting of the area, or on its Mesozoic-Early Tertiary history. A number of Miocene basins exposed in south coastal Turkey, document the evolution of the northern margin of the Mediterranean at this time. Three of these, The Aksu, Köprü and Manavgat basins are situated at the junction between two arcuate orogenic belts, the Hellenides and Taurides (Fig. 1.2), in a zone known as the Isparta Angle (Blumenthal, 1963). Study of these Mid-Tertiary basins is essential in trying to bridge the gap in knowledge between Mesozoic-Early Tertiary models and the present day tectonic configuration.

1.2 Plate tectonic setting of the Eastern Mediterranean

The Eastern Mediterranean has a prolonged history of convergence involving the closure of a large Palaeozoic ocean (Palaeotethys) whose suture lies within northern Turkey (e.g. Pickett, 1994, Üstömer, 1993) and the initiation and closure of smaller oceans (Neotethys) during the Mesozoic and Cenozoic (e.g. Robertson and Dixon, 1984). The location of the present-day convergent zone in the Eastern Mediterranean is well established. Continental collision (Bitlis) and strike slip movement is

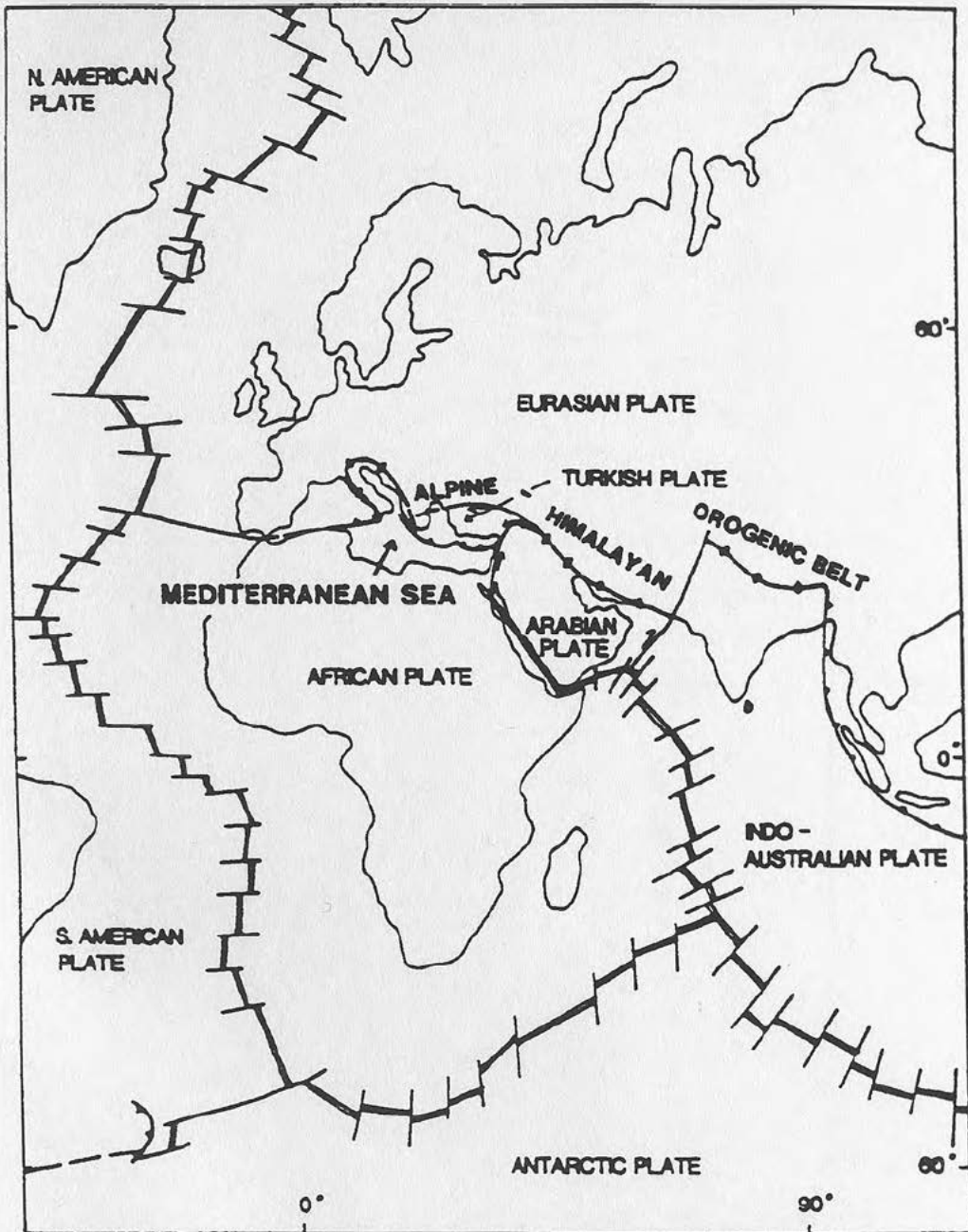


Figure 1.1 Regional plate setting of the Mediterranean Sea.

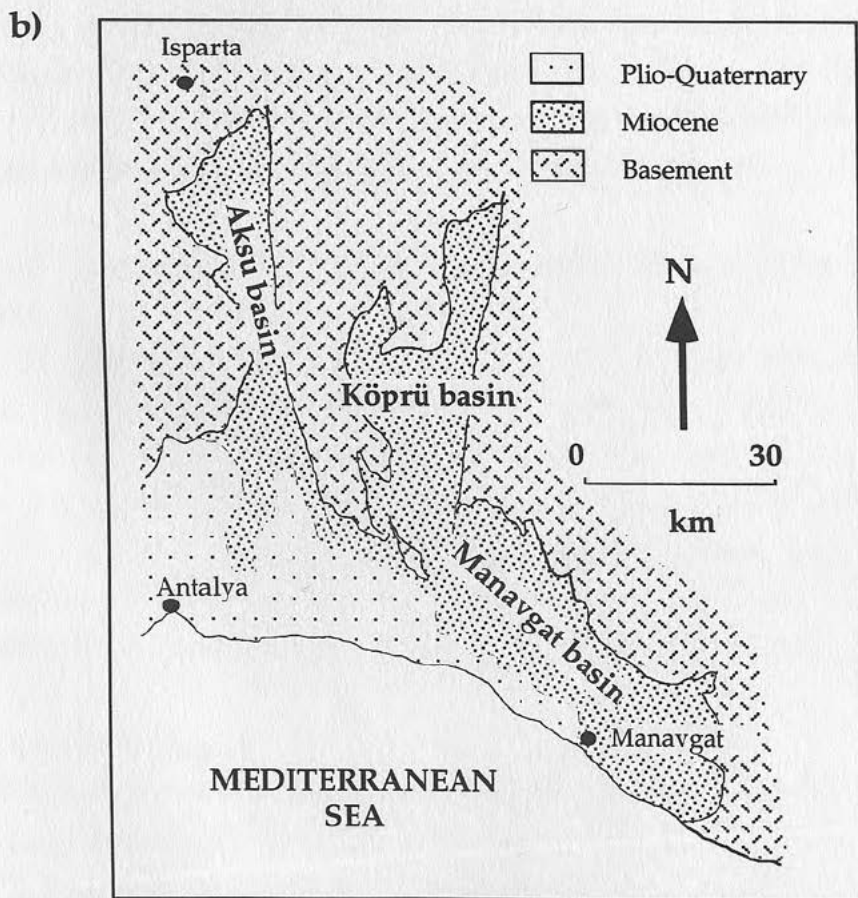
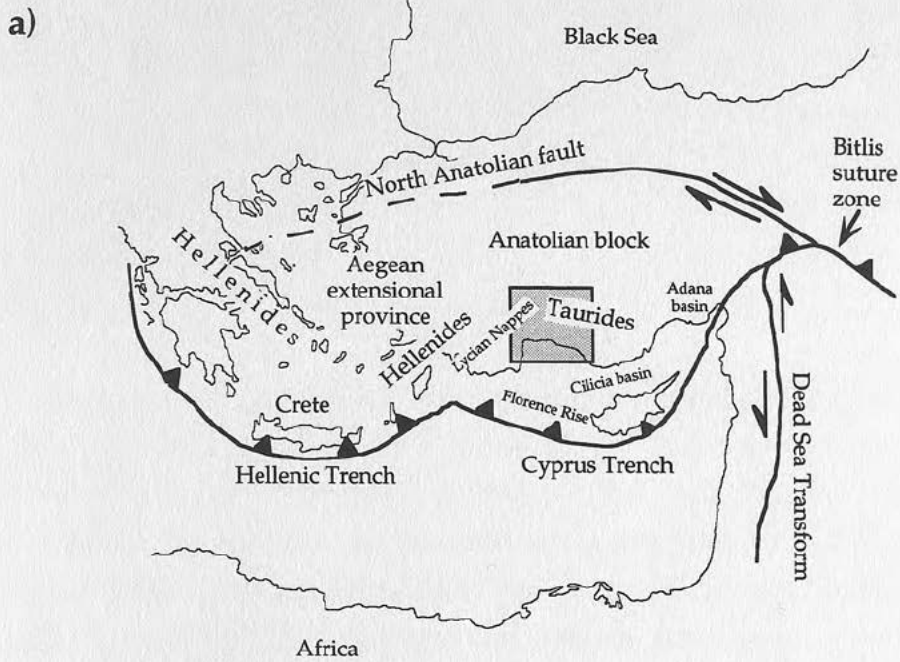


Figure 1.2 Map of a) the north-eastern Mediterranean showing the main suture zones and tectonic units; b) Neogene sediments of the Isparta Angle showing the three basins studied in this project.

occurring (North and East Anatolian Faults) in the far east of the Mediterranean. In the west, subduction is taking place on the Hellenic arc while the Aegean Sea undergoes extension. The segment of the Hellenic-Cyprus arc which lies to the south of Isparta Angle is less well delineated (Jackson and McKenzie, 1984), but the general consensus is that some combination of subduction and strike-slip motion are taking place in an arcuate zone to the south of Cyprus.

Pre-Miocene subduction in this area is thought to have been taken place along the Kyrenia Range in Cyprus, to the north of the present location (Robertson and Woodcock 1986). The connection between this subduction system and the Hellenic arc is not at all well defined given the present plate configuration, still less for the Oligocene and earlier. One possibility is that the Hellenic arc system continued onto land up the front of the Lycian Nappes which form the western arm of the Isparta Angle (Poisson, 1984). From here the Hellenic arc might have been connected to the Cyprus system along a suture zone located within the Isparta Angle itself (Robertson and Grasso, in press).

1.3 Structural framework and geological history of the Isparta Angle

The heterogeneous rocks of the Isparta Angle have been studied by many workers over the last three decades. Interest has focused on the complex mosaic of allochthonous and relatively autochthonous Mesozoic successions. These can be divided into six broad groups (Lycian Nappes, Bey Daglari, Antalya Complex, Anamas-Akseki platform, Beysehir-Hoyran-Hadim Nappes and Alanya Massif) located on figure 1.3. The dominant characteristics of each are summarised below:

Lycian Nappes

This extensive nappe system includes Mesozoic carbonate, radiolarites, sandstones and ophiolitic rocks (Graciansky, 1972; Poisson, 1977a). It is thought to have been emplaced during the Mid-Tertiary forming a foreland flexural basin to the south and south-east (Hayward, 1982b). Further thrusting of the Lycian system is thought to have recurred around the Mid-Miocene, deforming the Lower Miocene sediments in the flexural basin (Gutnic *et al.*, 1979; Hayward, 1982) and causing a

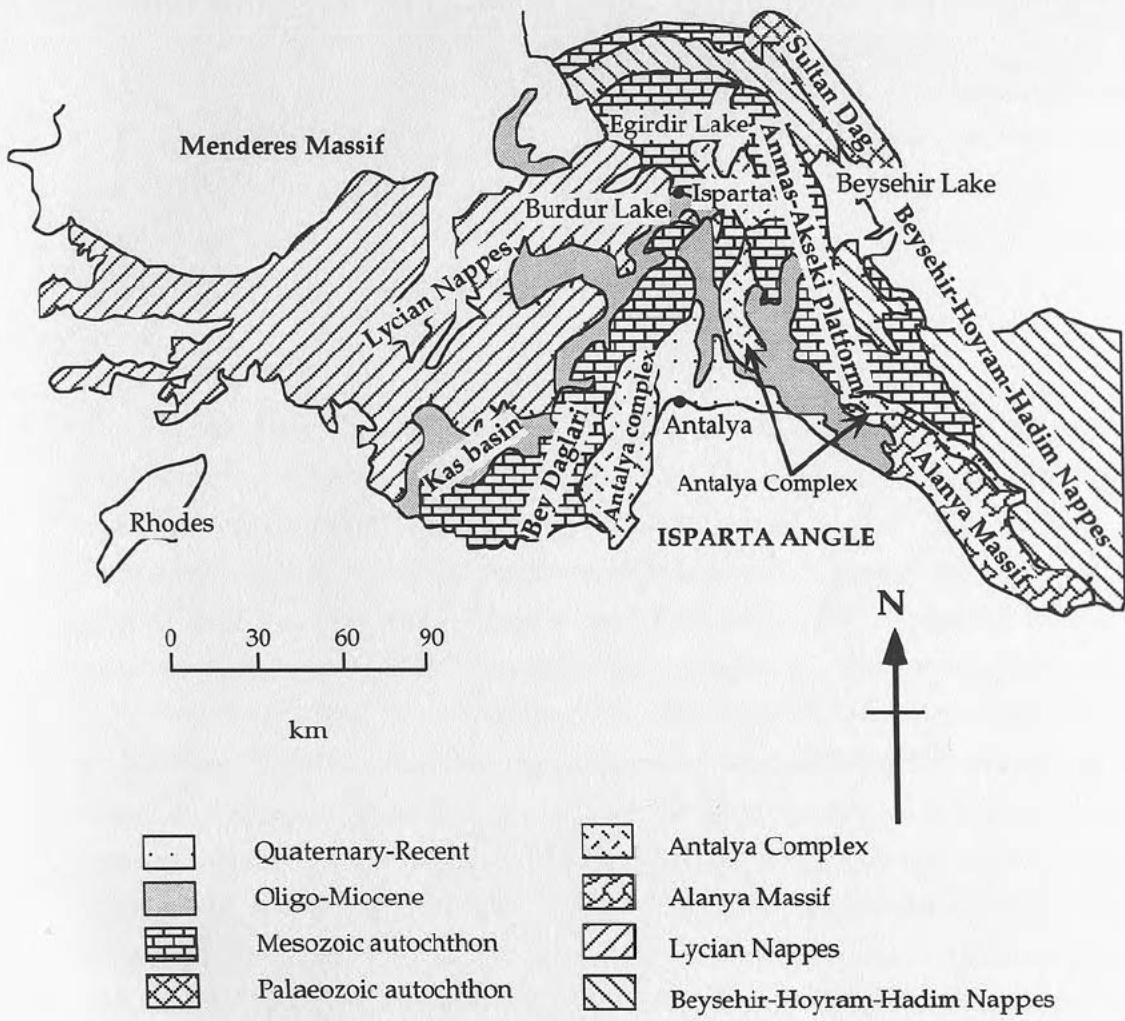


Figure 1.3 Map of the Isparta Angle region and the tectonic units described in the text.

widespread remagnetisation event out-board of the nappes (Morris and Robertson, 1993). The Lycian Nappes front and parallel flexural basin strike approximately NE-SW marking the western boundary of the Isparta Angle. Active thrusting of the Lycian system was terminated in the Late Miocene (Hayward, 1982b). The internal structure of the Lycian Nappes and their emplacement style and direction are still controversial issues. These questions are currently being investigated in a Ph.D. project undertaken by A. Collins at Edinburgh University.

Bey Daglari

The Bey Daglari-Susuz Dag Cretaceous carbonate platform forms most of the western margin of the Aksu basin. It has generally been viewed as relatively autochthonous (Poisson, 1977; Gutnic *et al.*, 1979; Poisson and Robertson, 1990) and is unmetamorphosed. Palaeomagnetic studies (Kissel and Poisson, 1987; Morris and Robertson, 1993) suggest that it has rotated anticlockwise by 30° since the Langhian. This rotation has been genetically linked to thrusting in the Lycian Nappes (Morris and Robertson, 1993) and the formation of the NNE-SSW trending Bey Daglari anticline (Kissel *et al.*, 1993). Palaeocurrent studies of Miocene sediments in a small basin overlying the eastern flank of the Bey Daglari (Hayward and Robertson, 1982; Fig. 1.4) suggest that sediment was derived from the Antalya Complex to the east. Subsidence of the eastern flank of the Bey Daglari is thought to have been induced by flexural subsidence due to lithospheric loading by the Lycian Nappes (Fig. 8.1; Hayward and Robertson, 1982; Hayward, 1982b). Termination of sedimentation in the Late Miocene resulted from the westward emplacement of the Antalya Complex on top of Mid-Miocene sediments along a basal thrust (Hayward and Robertson, 1982; Hayward, 1982b).

Antalya Complex

Perhaps the most contentious debate surrounding the Isparta Angle focuses on the Antalya Complex. Originally named, the Antalya Nappes (Lefevre, 1967), this unit mainly consists of Palaeozoic-Maastrichtian sandstones, shales, carbonates, radiolarites and ophiolitic rocks. The argument centres on the origin and emplacement of the Antalya Complex (e.g. Dumont *et al.*, 1972; Monod, 1977; Poisson, 1977a; Woodcock and Robertson, 1977b; Gutnic *et al.*, 1979; Ricou *et al.*, 1979;

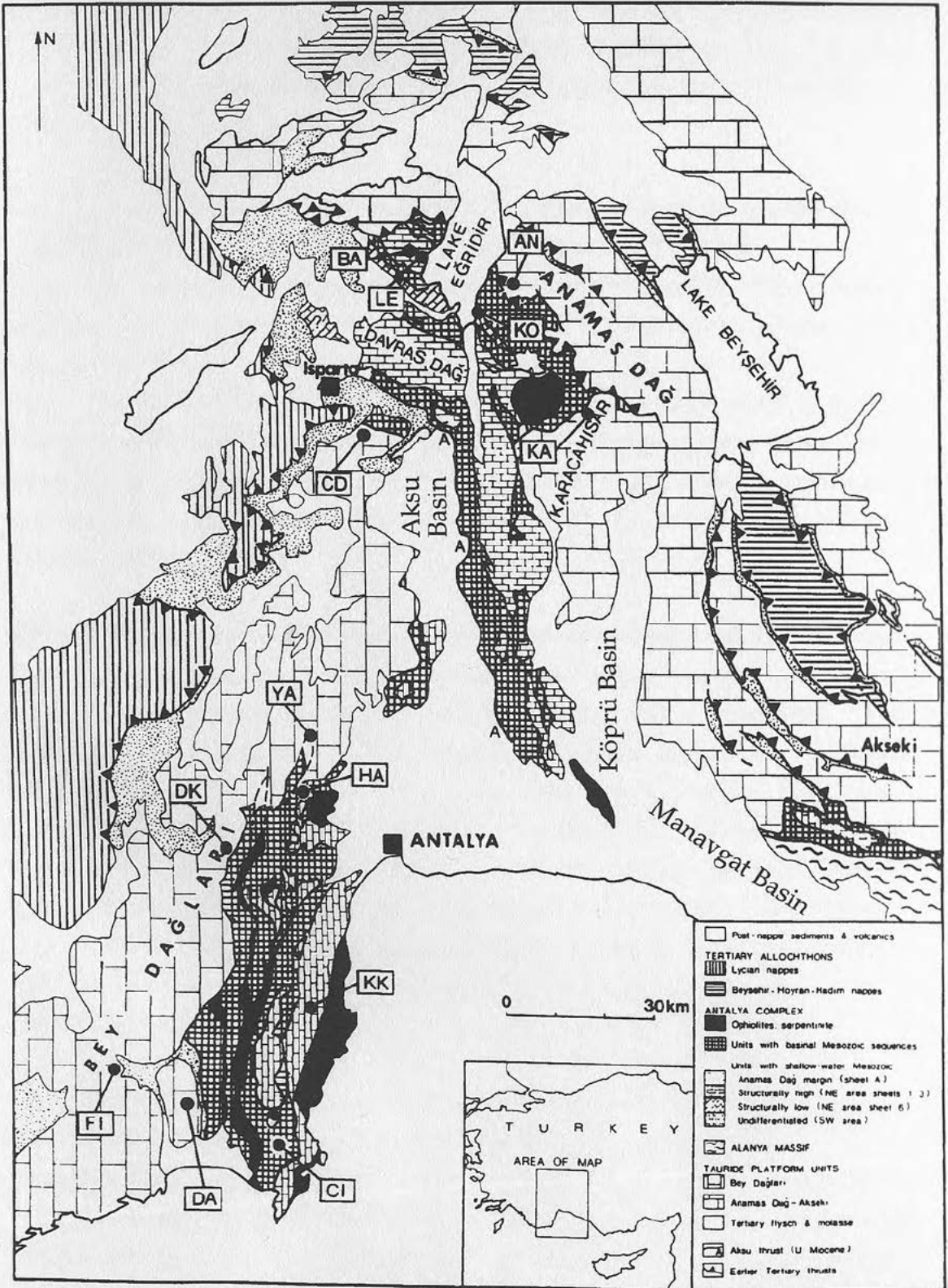


Figure 1.4 A more detailed map of the Isparta Angle showing the north-south structural lineaments within the Antalya Complex and the location of the palaeomagnetic sites of Morris and Robertson (1993). Modified from Waldron (1984).

Woodcock and Robertson, 1979; Hayward, 1984; Robertson and Woodcock, 1980; 1982; Poisson, 1984; Ricou *et al.*, 1984; Waldron, 1984; 1986; Marcoux *et al.*, 1989; Robertson, 1993) the alternative tectonic models for which are summarised below and illustrated in figure 1.5 (Robertson, 1993):

- ◆ The Antalya Complex was rooted far to the north and thrust southwards from a single Neotethyan ocean (Ricou *et al.*, 1974; 1975; 1979; Marcoux *et al.*, 1989);
- ◆ The Antalya Complex had its origins in a southerly Neotethyan (Pamphylian) basin and was thrust northward by tens to hundreds of kilometres (Dumont *et al.*, 1972; Monod, 1976; 1977);
- ◆ The Antalya Complex was routed within the Isparta Angle either in a deep marine basin (Poisson, 1984) or in palaeogeographically complicated ocean basins within which Antalya units were thrust relatively short distances outwards on to neighbouring carbonate platforms (Robertson and Woodcock, 1980; 1982; 1984; Waldron, 1981; 1984a; b; Robertson 1993).

With reference to the present study the emplacement of the Antalya Complex may be of great importance in terms of the underlying lithospheric weaknesses that govern the fabric of the basement. The north-south orientation of the Köprü and Aksu basins for instance parallel structural trends within the Antalya Complex (Fig. 1.4). According to the theory which supports an origin of the Complex within the Isparta Angle (internal), these lineaments are the sites of Triassic rifting and Early Tertiary collision and thrust emplacement. The theories of an external origin of the Antalya Complex either to the north or south, rely on complicated thrusting patterns to produce the dominant north-south structural trend.

Exposure of this unit occurs in the far south west of the Isparta Angle, on the basement promontory dividing the Köprü and Aksu basins, to the south of Lake Egirdir and in a thin strip to north of the Manavgat basin. Poisson *et al.* (1983) showed that the Antalya Complex was essentially emplaced prior to the Oligocene in the central part of the Isparta Angle, earlier than in the south-western segment, where Hayward and Robertson (1982) suggested that final emplacement occurred in the Late Miocene (see Bey Daglari above). Palaeomagnetic studies carried out by

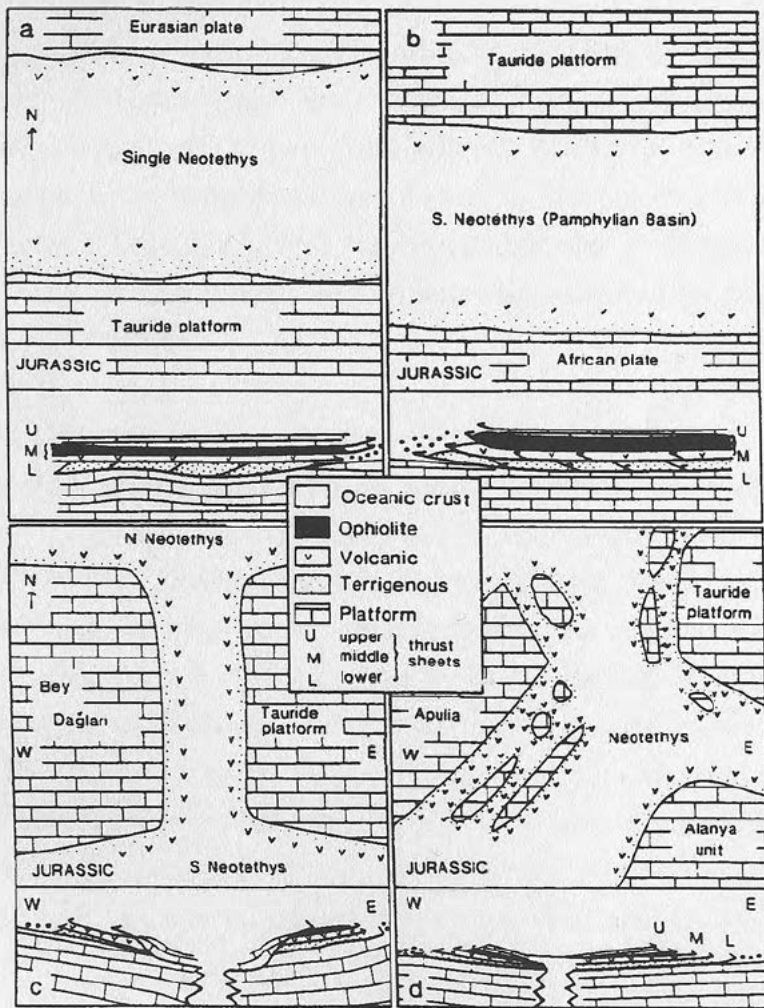


Figure 1.5 Alternative tectonic interpretations of the Antalya units, based loosely on published concepts: a) thrust from the north from a single Neotethyan ocean basin (Ricou et al., 1974; 1975; 1979; Marcoux et al., 1989); b) thrust from a southerly Neotethyan ocean basin (Dumont et al., 1972; Monod, 1976; 1977); c) thrust from a deep marine basin within the Isparta Angle (Poisson, 1977; 1984); d) an origin as a palaeogeographically complicated small ocean basin within the Isparta Angle; units were thrust relatively short distances outwards onto adjacent carbonate platforms (Robertson and Woodcock, 1980; 1982; 1984; Waldron, 1981; 1984a and b). Diagram taken from Robertson (1993).

Morris and Robertson (1993) suggest that the anticlockwise rotation suffered by the Bey Daglari during the Mid-Late Miocene also affected the south-western segment of the Antalya Complex, causing west-vergent thrusting.

Anamas-Akseki Platform

Anamas-Akseki platform, like the Bey Daglari is considered to be a relatively autochthonous unit (Monod, 1977) comprising dominantly Mesozoic carbonate. It forms the eastern border of the Köprü basin and the basement to the Manavgat basin in its far north-western corner. Morris and Robertson (1993) indicated that the Anamas-Akseki Platform in the north of the Isparta Angle was also affected by Mid-Late Miocene anticlockwise rotation.

Beysehir-Hoyran-Hadim Nappes

The Beysehir-Hoyran-Hadim Nappes (BHH) consist mainly of Upper Palaeozoic-Lower Tertiary carbonate, sandstone and ophiolitic rocks (Monod, 1977). Arcuate thrust belts trending north-south in the north and NW-SE in the south characterise the Beysehir-Hoyran-Hadim Nappes which mark the eastern arm of the Isparta Angle and border the Anamas-Akseki platform to the west. Narrow exposures of Eocene flysch parallel these thrusts indicating flexural loading at this time. Palaeomagnetic evidence from this area (Kissel *et al.*, 1993) suggests that the BHH nappes underwent 40° of clockwise rotation in the Upper Eocene to Oligocene, but there is no indication that subsequent movement has occurred.

Alanya Massif

The Alanya Massif consists mainly of Permian meta-carbonates (Özgül, 1983; Okay and Özgül, 1984). Its structure is complex and still not clearly understood, but it is of great interest as it contains blueschist metamorphic facies and thus is indicative of the high-pressure low-temperature metamorphism associated with subduction zones. It borders the north-eastern part of the Manavgat basin and is exposed at the core of an anticline within the basin itself. It is thought to have been emplaced onto the Antalya Complex to the north during the Early Eocene (Monod, 1977; Okay and Özgül, 1984). Detailed field assessment of the internal

structure of the Alanya Massif has been carried out (Robertson, unpublished data). This suggests that many of the structures within the unit parallel the NW-SE trend of its northern margin.

1.4 An overview

The Isparta Angle represents a long-lived suture zone across which episodic compression and extension took place. There is evidence both of rifting and collision throughout the Mesozoic and Early Tertiary successions preserved within the area. Miocene sequences too, on a smaller scale, document the generation of accommodation space and subsequent uplift and erosion. Even today, neotectonic graben systems such as the Kovada graben to the south of Lake Egirdir in the north of the area are concentrated within the Isparta Angle. The Plio-Quaternary evolution within the angle is the subject of a Ph.D. project currently being carried out by C. Glover at Edinburgh University. Significantly, much of the deformational structures within the Isparta Angle, dating from the Early Mesozoic to the present-day, are orientated north-south. Figure 1.6 is a satellite photograph showing the strong north-south grain to the fabric of the region.

1.5 General Aims

- ◆ To study in detail the sedimentological character of the Miocene succession within the Isparta Angle in order to construct facies models during basin evolution;
- ◆ To assess the structural development of the three Miocene basins within the Isparta Angle and compare them;
- ◆ To evaluate the role of eustatic sea level change in controlling sedimentation;
- ◆ To examine the tectonic implications of these studies with respect to both the evolution of the Isparta Angle as a whole and regional tectonic history of the Eastern Mediterranean during the Miocene.

1.6 Techniques used

The major data base for this project comes from field-based studies which

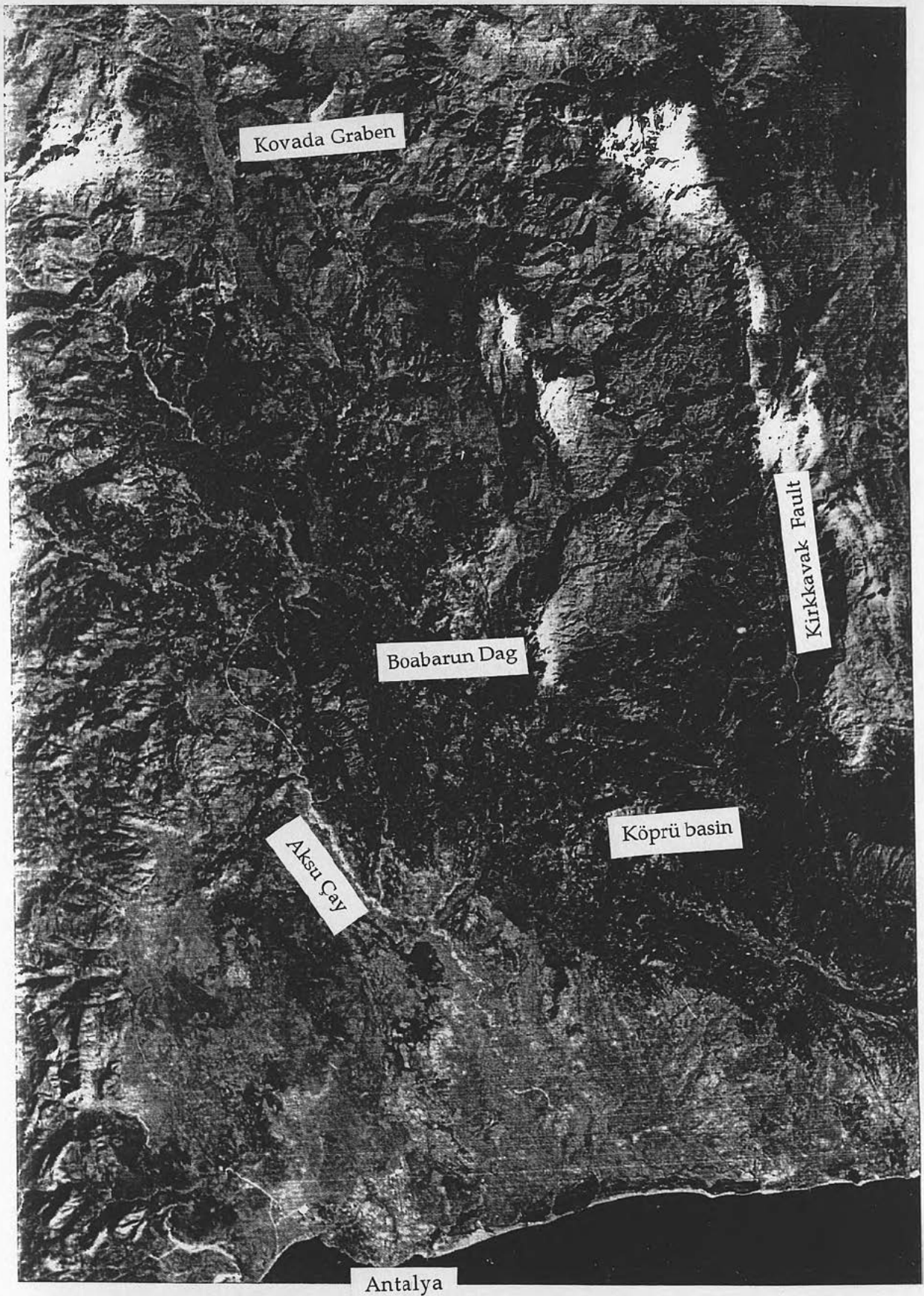


Figure 1.6 Satellite photograph of part of the area showing the strong north-south grain to the fabric of the Isparta Angle.

were carried out during a total of 8 months fieldwork over three years. The geological map of Miocene-Quaternary sediments of the Aksu, Köprü and Manavgat basins produced by Akay and Uysal (1985) as part of his M.T.A. report was used extensively as a guide to the area. Detailed sedimentological logging on various scales was used as a fundamental tool for examining intra- and inter-basin evolution. This was combined with extensive palaeocurrent analysis and provenance studies on the conglomerates where over 100 clasts were recorded for each locality. Where high tectonic dips required, palaeocurrent data were corrected for tilt.

Much of the data base produced by Akay and Uysal (1985) in his study of the area was of a biostratigraphic nature. The current study has expanded his work, using nannoplankton biostratigraphy undertaken with Dr. C. Müller, coral identification carried out with the help of Dr. B. Rosen (Natural History Museum) and strontium isotope stratigraphy. Isotope work was planned in order to assess the age of shallow-water carbonates, which through the paucity or absence of diagnostic foraminifera or nannoplankton, proved difficult to date. It was carried out at the Scottish Universities Research and Reactor Centre in East Kilbride under the guidance of Dr. R. Ellam. The sample preparation and methodology of this technique is described in chapter 6.

Prior to the isotope work a detailed diagenetic study of the biogenic carbonate was required. This involved XRD analysis of coral samples to ascertain the relative quantities of primary aragonite and secondary calcite. Samples of coral were first drilled from a fresh hand specimen and washed in ethanol standing in an ultrasound bath for at least half an hour. After removal, the samples were rinsed and dried and ground to a fine powder using a pestle and mortar. XRD analysis was then carried out and compared to standards containing known compositions of aragonite and low-Mg calcite.

Diagenetic studies of the foraminifera used for Sr isotope analysis were attempted, by first examining washed samples picked at 63μ under a binocular microscope and later using a scanning electron microscope at Stuttgart University, Germany. Each foraminifer was mounted on a stub

with conductive graphite mounting material, or a double sided sticky tab prior to gold-coating.

General diagenetic and textural features of the carbonates and sandstones were investigated using standard thin section microscopy and acetate peels. Poorly lithified samples were first impregnated with resin. Point counting of selected sandstones was undertaken as part of provenance investigations. Over 300 points were counted initially and the percentages recorded. A further 100 points were then counted and the total percentages calculated. If the difference for each grain-type between 300 and 400 point counts was less than 5%, then the 400 value was accepted. If however, the difference was greater than 5%, then a further 100 point counts was carried out. This process was repeated until the difference between values over a 100 point count differential was less than 5%.

1.7 Thesis organisation

The introductory chapter is followed by a chapter outlining the stratigraphic framework used in this study. Chapters 3-5 give detailed descriptions, interpretations and models for the sediments seen. They also discuss larger scale issues relevant to the study of similar sediments and processes. Chapter 6 documents the isotopic dating study carried out on biogenic carbonates within the area. Chapter 7 examines the structural evidence for the initiation and evolution of the three basins and discusses the various models put forward. The implications of the work described in previous chapters are summarised in chapter 8. The basins are compared with other Miocene basins within in the Mediterranean and placed in the wider context of the Eastern Mediterranean evolution. The major conclusions are then listed.

Chapters 3-5 describing the sediments of the three Miocene basins are not divided up on the basis of formations. Instead each of the chapters is written from the point of view of examining the fundamental processes involved. Thus, chapter 3 is written from the perspective of the role of biogenic components in carbonate deposition; chapter 4 is written with the mode of deposition of turbiditic sediments foremost in mind and

chapter 5 examines the sediments from the perspective of an interactive fan-delta system. As a result of this method of organisation a certain amount of overlap between chapters occurs. Porites bafflestones described in chapter 3 for instance are crucial in the interpretation of coastal fan-delta sediments discussed in chapter 5. When repetition of this kind is needed, a brief summary of the salient points is given and the reader is referred back to the original description for more detailed information if required. Figure 1.7 is a schematic representation of the overlap of the formations into the three chapters. Information concerning the previous work on the sediments is outlined at the beginning of the relevant chapter.

In justification of this organisational structure, it was felt that to describe the sediments purely on the basis of stratigraphic divisions would have superimposed an arbitrary framework on the study, not valid when considering interactive basinal processes. It is hoped therefore that the approach used will facilitate both the understanding of the integrated depositional and preservational systems active during the Miocene and subsequent publication.

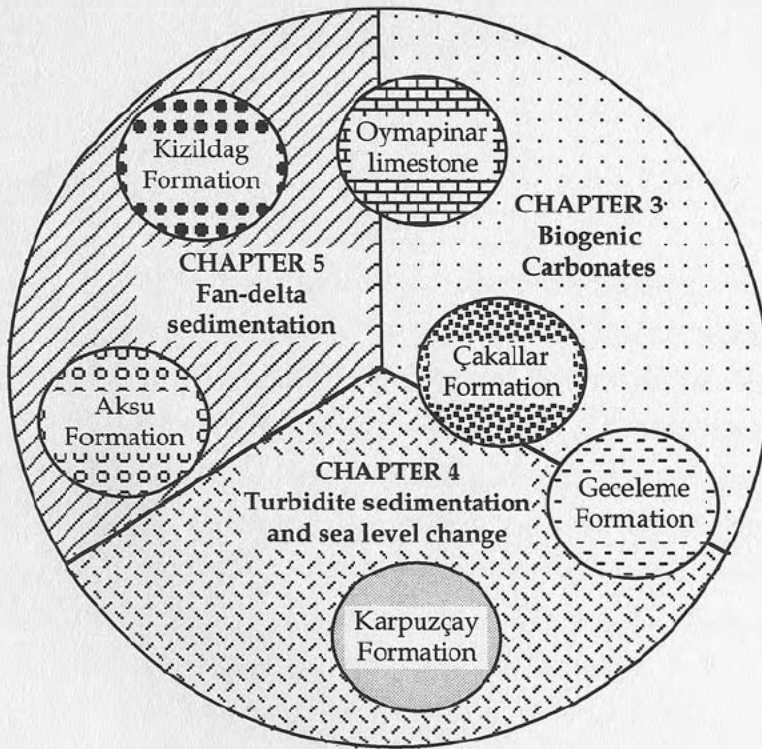


Figure 1.7 Diagram showing the overlap of the formations within the three descriptive chapters. Note that the ornament used here for each formation is the same throughout the thesis.

Chapter 2

STRATIGRAPHY

2.1 Introduction

This chapter describes the time scale used throughout the study and points out the assumptions made in relying on biostratigraphic data. It goes on to introduce information published by previous workers on the Miocene stratigraphy of the area. The most comprehensive of these studies was undertaken by Akay and Uysal (1985) and the stratigraphy used in this thesis is based primarily on the one they produced. Revisions of some of the formation classification have been carried out however and these are described below. Figure 2.1 is a location map showing the position of places mentioned in the text.

2.2 Lithostratigraphy, biostratigraphy and isotopic dates

Figure 2.2 is a chart of the ages of Miocene nannoplankton zones with respect to the record of magnetic polarity from Berggren *et al.* (1985). Set against this is the time scale used by Haq *et al.* (1988) when constructing the global eustatic sea level curve. The Berggren time scale is used throughout this study, but as much of the discussion focuses on the role of eustasy in controlling sedimentation, comparison with the eustatic curve and other relative sea level curves which use the Haq time scale must be treated with a little caution. Minor discrepancies as a result of differences between the ages of stage boundaries occur, but these are thought to be insignificant in the context of the resolution of the curve itself

New biostratigraphic information is listed in Appendix 3. Nannoplankton ages for sections measured during this study were carried out by Dr. C. Müller and can be found in Appendix 3a. This information was combined with data from previous studies of the Miocene sediments of this area (Bizon *et al.*, 1974; Dumont, 1974; Poisson, 1977; Monod, 1977;

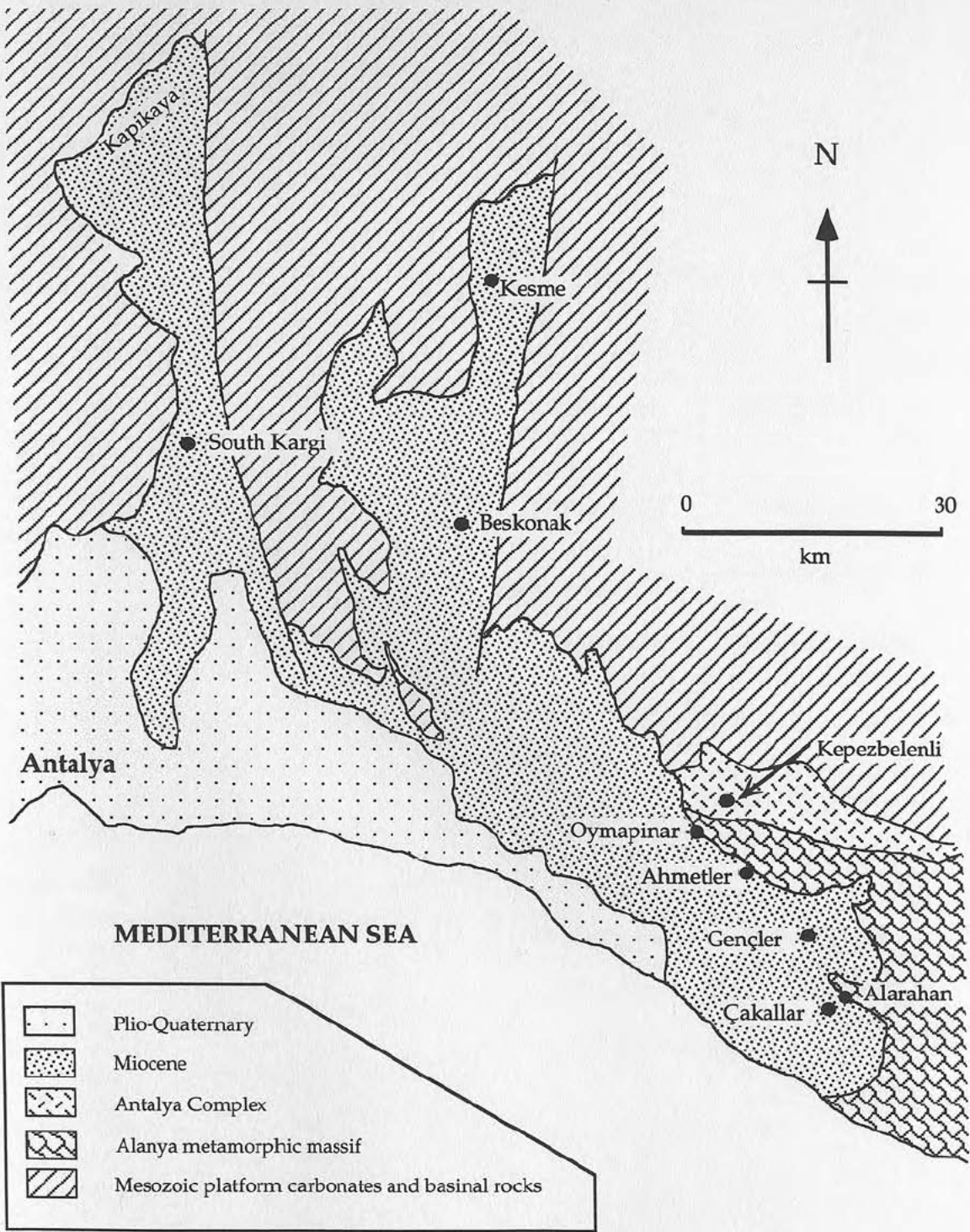


Figure 2.1. Location map of type sections mentioned in tables 2.2, 2.3, 2.4 and 2.6.

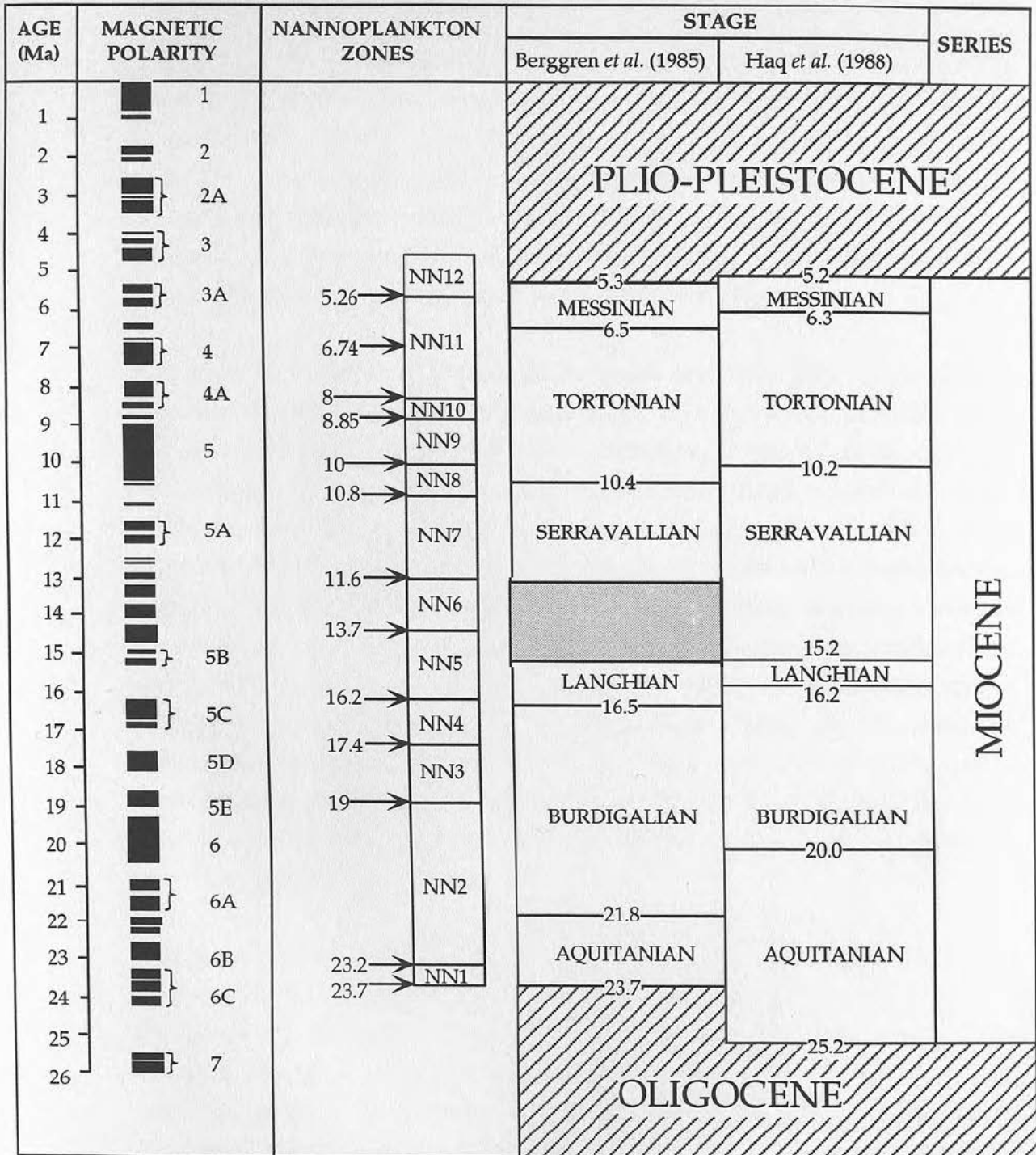


Figure 2.2 Biostratigraphic chart showing the correlation of nannoplankton zones with magnetostratigraphy (after Berggren *et al.*, 1985). The stage boundaries used throughout this thesis are those of Berggren *et al.* (1985), but Haq *et al.*'s (1988) stratigraphic framework is also shown because it is against this that the eustatic sea level curve discussed in the text was constructed.

Akay and Uysal, 1985; Akay *et al.*, 1985). Much, though not all of this focuses on foraminiferal biostratigraphy.

Lithostratigraphic correlation without the age framework provided here by nannoplankton and foraminiferal biostratigraphy and strontium isotope dating would have been both a difficult process and hard to justify. Facies vary laterally and it can be demonstrated that completely different depositional processes were active synchronously in different parts of the Isparta Angle. It is only through using well defined ages that secure correlation is possible and basin evolution clarified.

With this in mind it is important to point out that large parts of the successions studied here were deposited in continental environments and are very poorly dated as a result. The base of the Miocene sequence for instance, is only clearly dated in the few places where the basal sediments were deposited in a marine environment and it has been suggested that the thick successions of undated continental conglomerates in parts of the Köprü and Aksu basins may be Oligocene in age (Akay *et al.*, 1985). It was felt that pinning down lithostratigraphic relationships and dating them where possible would be a more effective method of dealing with this gap in the data base than setting out to date the continental sediments directly given the time constraint of three years. Further work on this aspect of continental sediments in the Isparta Angle would enhance palaeogeographic reconstructions of both the Miocene and Plio-Quaternary.

One final note of caution concerning the stratigraphic framework used here concerns redeposition and will be considered again in chapter 4 where this information is most extensively used. The bulk of the samples found to contain nannoplankton or planktic foraminifera and used for dating, came from the Geceleme and Karpuzçay Formations. The possibility that the fine-grained fractions of these formations, sampled for the purpose of age reconstruction were redeposited by low-density turbidity flows cannot be excluded. Indeed, in the case of the Karpuzçay Formation it is extremely unlikely that even the finest material sampled here represents background sedimentation and there is clear evidence that at least parts of the Geceleme Formation are the

products of redeposition. Does this invalidate the biostratigraphic framework outlined below? It would be reasonable to expect a miscorrelation between the biostratigraphic results and the lithostratigraphy observed in the field if it did. In fact this very rarely happens suggesting that although redepositional processes are active, they are not sufficiently effective to significantly reorganise the stratigraphy above the level of biostratigraphic resolution. To obtain an independent view on this problem, Sr isotopes were measured both on *in situ* reef carbonates (Oymapinar limestone) and on foraminifera from the overlying Geceleme and Karpuzçay Formations. The sequential nature of the results suggests that reliance may be placed on biostratigraphic data.

2.3 Historical development of existing stratigraphic framework

By far the greatest debt is owed to Ergün Akay (see Akay and Uysal, 1985) who, in a team of French and Turkish geologists, first studied the Neogene sediments within the Isparta Angle as a whole, and set up the stratigraphy, which, though refined during this study, remains in place. Prior to his work many authors had dabbled in the Miocene stratigraphy particularly concentrating on the Manavgat basin partly because of its relative geological simplicity, but also due to the ease of access (e.g., Bizon *et al.*, 1974). Blumenthal (1947) was the first to document Miocene stratigraphy in the area. He was followed in the 1970s by a wave of French geologists who mapped the entire Isparta Angle (Dumont, 1974; Marcoux, 1976; Poisson, 1977; Monod, 1977; Ricou 1979) and who triggered the debate over the Antalya Complex in the early eighties which has made the area famous (Robertson, 1993 for review). Although their work concentrated on the Mesozoic successions, all of them studied the overlying Neogene sediments in passing and between them they contributed greatly to the data base of information concerning Miocene sedimentation. Figure 2.3 is an outline map of the Isparta Angle showing the areas covered by the various workers who looked at some aspect of Miocene stratigraphy. Without the detailed knowledge and help of two of these people, Dr. O. Monod and particularly Dr. A. Poisson, this thesis would be much the poorer and less well understood by the author.

Previous work concerning each of the six formations described in this

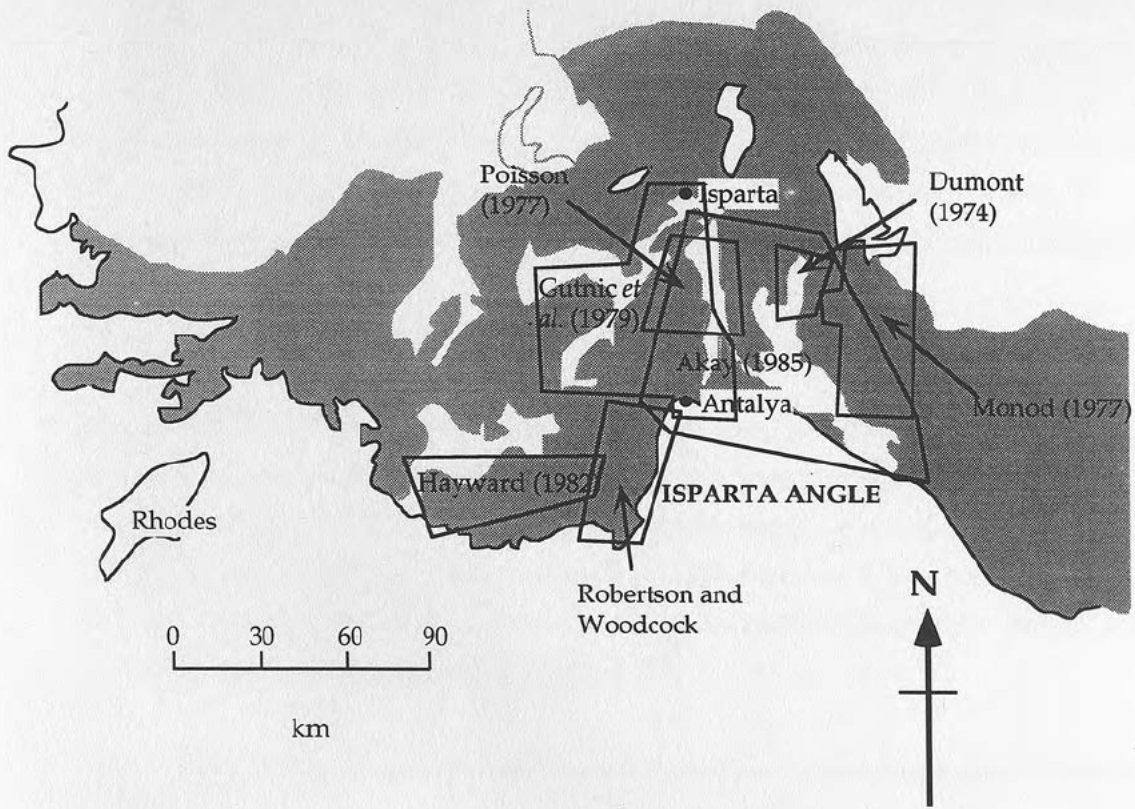


Figure 2.3 Map of the Isparta Angle region showing the areas covered by previous studies who worked (at least partially) on Miocene sediments.

thesis are outlined at the beginning of the chapter in which they first feature. The minor complication of changing formation names is clarified in tables 2.1, 2.2, 2.3 and 2.4. More difficult to immediately master when perusing the literature are the changing names of the principal sections in the Manavgat basin. These are summarised in table 2.5 along with the names used in this study which relate to the geographical locality of the section and are aimed at reducing confusion.

2.4 Revised Stratigraphy

Figure 2.4 is the chronostratigraphic chart produced by Akay *et al.*, (1985) summarising the relationships between the formations across the Isparta Angle. Much of this stratigraphic framework provided an excellent template on which to base a detailed assessment of the basin evolution through facies analysis. The following modifications have been made however and are illustrated in figure 2.5:

- ◆ The Aksu Conglomerate Formation which, in the Akay scheme occurs throughout the Miocene succession in all three basins (Fig. 2.4) has been split up into two main formations, the Aksu Formation and the Kizildag Formation (tables 2.4 and 2.1 respectively). The justification for doing this is based on the increase of biostratigraphic and lithostratigraphic resolution which revealed that there is little evidence for continuous conglomerate deposition throughout the Miocene. Instead, conglomerate successions appear to be concentrated in the Lower Miocene (Kizildag Formation) and Upper Miocene (Aksu Formation).
- ◆ These two formations have been further divided into a number of members reflecting the differing environments of deposition (table 2.6).
- ◆ One of these members has been drawn from the work of Monod (1972; 1977) on the northern margin of the Manavgat basin. He found and classified lacustrine limestone within Lower Miocene conglomerates (Kizildag Formation) and called it Calcaire de Kepez after a nearby village. This limestone was not documented by Akay, but has been reintroduced into the classification used for this study as a formation group of the Kizildag Formation (table 2.1).
- ◆ Akay and Uysal (1985) classified the coarse debris flow-dominated succession in

Table 2.1 Chart of stratigraphic information for the Kizildag Formation

Formation	Member	Synonymy	Type locality	Lower contact	Upper contact	Description	Age
Kizildag Formation	Kargi Member	Aksu Formation (Akay and Uysal, 1985; Akay <i>et al.</i> , 1985); Conglomerats de Tepekli (Monod, 1977)	Kargi, south-west Aksu basin	Unconformable on Mesozoic basement	Conformably overlain by Oymapinar limestone. Apparently conformably overlain by Karpuzçay Formation	Clast-supported conglomerates and coarse, sometimes laminated, reddened sandstones, interbedded with calccrete	? Aquitanian/Burdigalian ? - Langhian.
	Calcaire de Kepez	Calcaire de Kepez (Monod, 1972;1977)	Kepezbelenli, north of the northern margin of the Manavgat basin	Unconformable on Mesozoic radiolarites. Conformable on Kargi Group conglomerates	Conformably overlain by both Kargi Group conglomerates and Oymapinar limestone	Laminated, lacustrine limestone	? Burdigalian
	Tepekli Member		South Kargi, south central Aksu basin and Aspendos, south Köprü basin	Conformable on Kargi Group conglomerates	Overlain conformably either by Oymapinar limestone or Kargi Group conglomerates	High angle cross-bedded conglomerates, with interbedded Porites baffle stones or rhodolith bearing grits	Burdigalian-Langhian

Table 2.2 Chart of stratigraphic information for the Oymapinar limestone, Çakallar and Geceleme Formations

Formation	Synonymy	Type locality	Lower contact	Upper contact	Description	Age
Geceleme Formation	Geceleme Formation (Akay and Uysal, 1985; Akay <i>et al.</i> , 1985); Geceleme Formation (Blumenthal, 1947; Monod, 1977)	Gençler, along the old road north from the coast to Akseki, Manavgat basin	Disconformity with Oymapinar limestone and Çakallar Formation	Conformable and gradual transformation over 20m to Taskesigi Group or more rarely, the Karpuzçay Formation	Planktic foraminiferal marls and rare wedge shape calcirudites	Latest Burdigalian ?-Langhian
Çakallar Formation	Çakallar Formation (Akay and Uysal, 1985; Akay <i>et al.</i> , 1985)	Çakallar, near Alarahan, south-east Manavgat basin	Conformable with Oymapinar limestone	Disconformably overlain by Geceleme Formation or Karpuzçay Formation	Calcirudites interbedded with marls and sandstones. Blocky talus sometimes present	Latest Burdigalian ?- Langhian
Oymapinar Limestone	Oymapinar limestone (Akay and Uysal, 1985; Akay <i>et al.</i> , 1985); Calcaire d'Oymapinar (Monod, 1972)	Oymapinar, northern margin of the Manavgat basin	Unconformable on Alanya Massif along the north-eastern margin of the Manavgat basin. Conformable on Kizildag Formation elsewhere	Conformably overlain by Çakallar Formation locally. Sometimes small angular disconformity below Karpuzçay Formation and Geceleme Formation	Shallow-water biogenic carbonates including coral and algal reefs.	Burdigalian-Langhian. Diachronous from south to north in the Manavgat basin

Table 2.3 Chart of stratigraphic information for the Karpuzçay Formation

Formation	Member	Synonymy	Type locality	Lower contact	Upper contact	Description	Age
Karpuzçay Formation	Beskonak Member	Karpuzçay Formation (Akay and Uysal, 1985; Akay <i>et al.</i> , 1985); Beskonak Formation (Degirmenci, 1992)	North of Beskonak, central Köprü basin	Angular disconformity associated with sections of faulted Oymapinar limestone, e.g. Deniztepesi. Otherwise apparently conformable on Kizildag Formation	?Conformably overlain by Aksu Formation, only rarely seen. Unconformably overlain by Pliocene sediments in the south	Sandstone-siltstone turbidites. Rare conglomerate channels	Serravallian-Middle Messinian
	Taskesigi Member		Along the road from the coast to Akseki, near Taskesigi, Manavgat basin	Conformable on Geceleme Formation	Unconformably overlain by Lower Pliocene sediments	Debris flows containing large detached blocks, conglomerates, sandstones and slumped silts	Tortonian-Middle Messinian

Table 2.4 Chart of stratigraphic information for the Aksu Formation

Formation	Member	Synonymy	Type locality	Lower contact	Upper contact	Description	Age
Aksu Formation	Kapakaya Member	Aksu Conglomerate (Akay and Uysal, 1985; Akay <i>et al.</i> , 1985)	Kapakaya, far north of Aksu basin	Unconformable on Mesozoic basement.	Probably conformable passing up into Kesme Group	Coarse, reddened conglomerates and sandstones. Local evidence of fault generation	Tortonian- ?Messinian
	Kesme Member	Conglomérats de Kesme (Dumont, 1974)	Kesme, far north-east of Köprü basin	Unconformable on Mesozoic basement.	Not seen	Clast-supported conglomerates and fossiliferous, cross-bedded sandstones.	Tortonian- ?Messinian

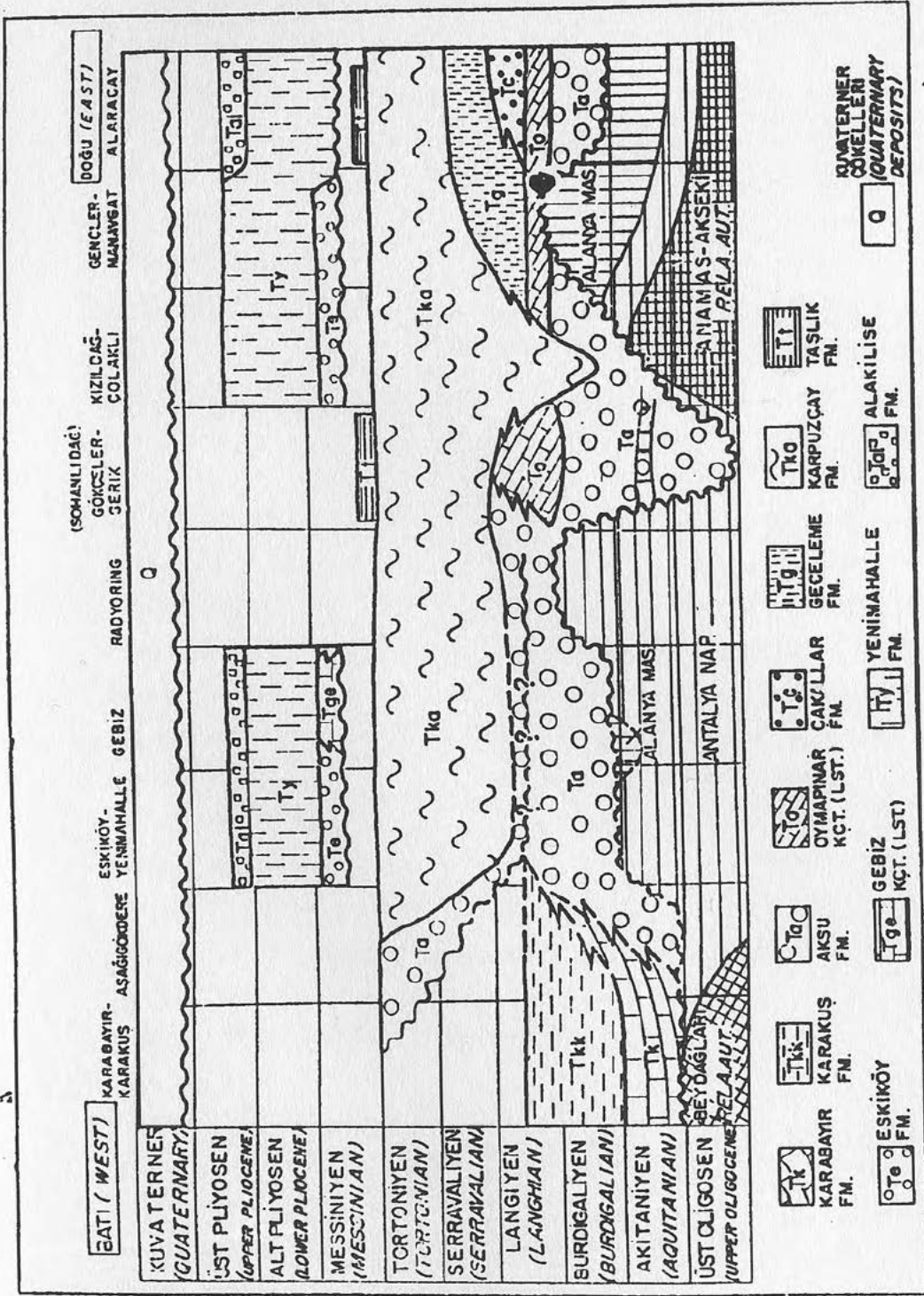


Figure 2.4 Composite stratigraphic framework of the Neogene sediments of the Isparta Angle from Akay et al. (1985). Note that the Karabayır and Karakuş Formations outcrop in the flexural basin to the north-west of the Aksu basin. These formations are not discussed here.

Table 2.5 List of sections used by previous workers which have been renamed to avoid confusion in the present study.

Name of Author	Section name	Section name in this study
Monod (1977), Bizon <i>et al.</i> (1974)	Manavgat section	Oymapinar section
Monod (1977)	Alara Çay section	Alarahan section
Blumenthal (1947 &1951), Monod (1977), Akay and Uysal (1985), Akay <i>et al.</i> (1985)	Gecereme/Gençler section	Akseki road section
Akay and Uysal (1985), Akay <i>et al.</i> (1985)	Manavgat section	Ahmetler section

the Tortonian-Messinian of the Manavgat basin as Karpuzçay Formation. This succession is completely different from any other exposure of his Karpuzçay Formation in which horizons coarser than sandstone are rare. More detailed field study of the debris-flow dominated sequence revealed that it is laterally discontinuous even within the Manavgat basin, although definition of its margins is difficult due to the similarity of the finer-grained components to the "standard" Karpuzçay Formation. The coarse horizons by which this sequence can be recognised appear to be concentrated in a narrow north-south zone ~10km across. This zone has been loosely termed the Akseki corridor in this study because the succession is so well exposed along the new road to Akseki from the coast. The Karpuzçay Formation has been divided into two groups (table 2.3) to distinguish between the debris-flow dominated succession (Taskesigi group), and the finer-grained turbidites (Beskonak group). This re-classification has implications for the origin of the Akseki corridor and these are discussed in chapters 4 and 7.

General definitions, descriptions and ages of the formations used in this study of the Miocene sediment of the Isparta Angle are given in tables 2.1, 2.2, 2.3 and 2.4. A modified stratigraphic framework is shown in figure 2.5 to accommodate the revised formation classification and more detailed biostratigraphic and lithostratigraphic study.

Table 2.6 Re-classification of the Aksu Conglomerate Formation and Karpuzçay Formation (Akay and Uysal, 1985; Akay et al., 1985) and the division into members used in this study.

Environment	Sub-environment	Karpuzçay Formation	Aksu Formation	Kizildag Formation
Continental	Alluvial		Kapikaya	Kargi
	Lagoonal and Lacustrine			Calcaire de Kepez
Marine	Shoreline		Kesme	Tepekli
	Shelf	Taskesigi Beskonak		

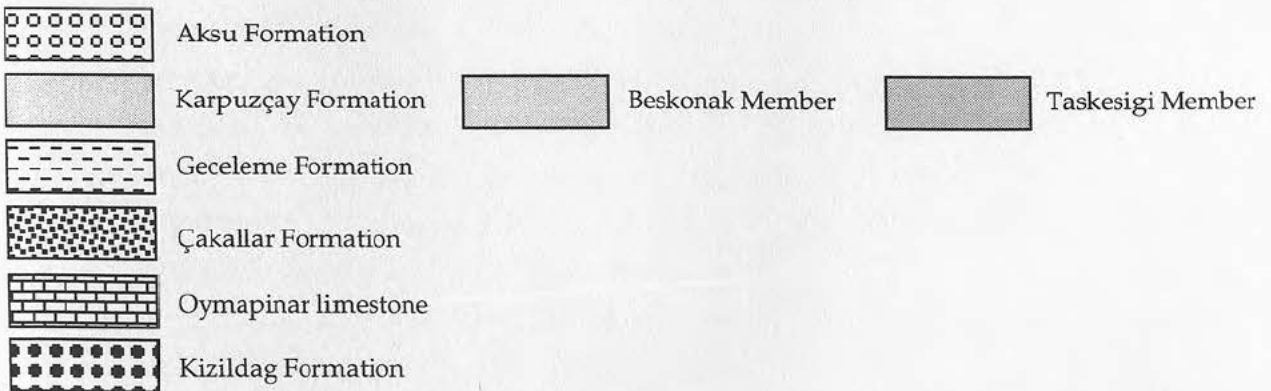
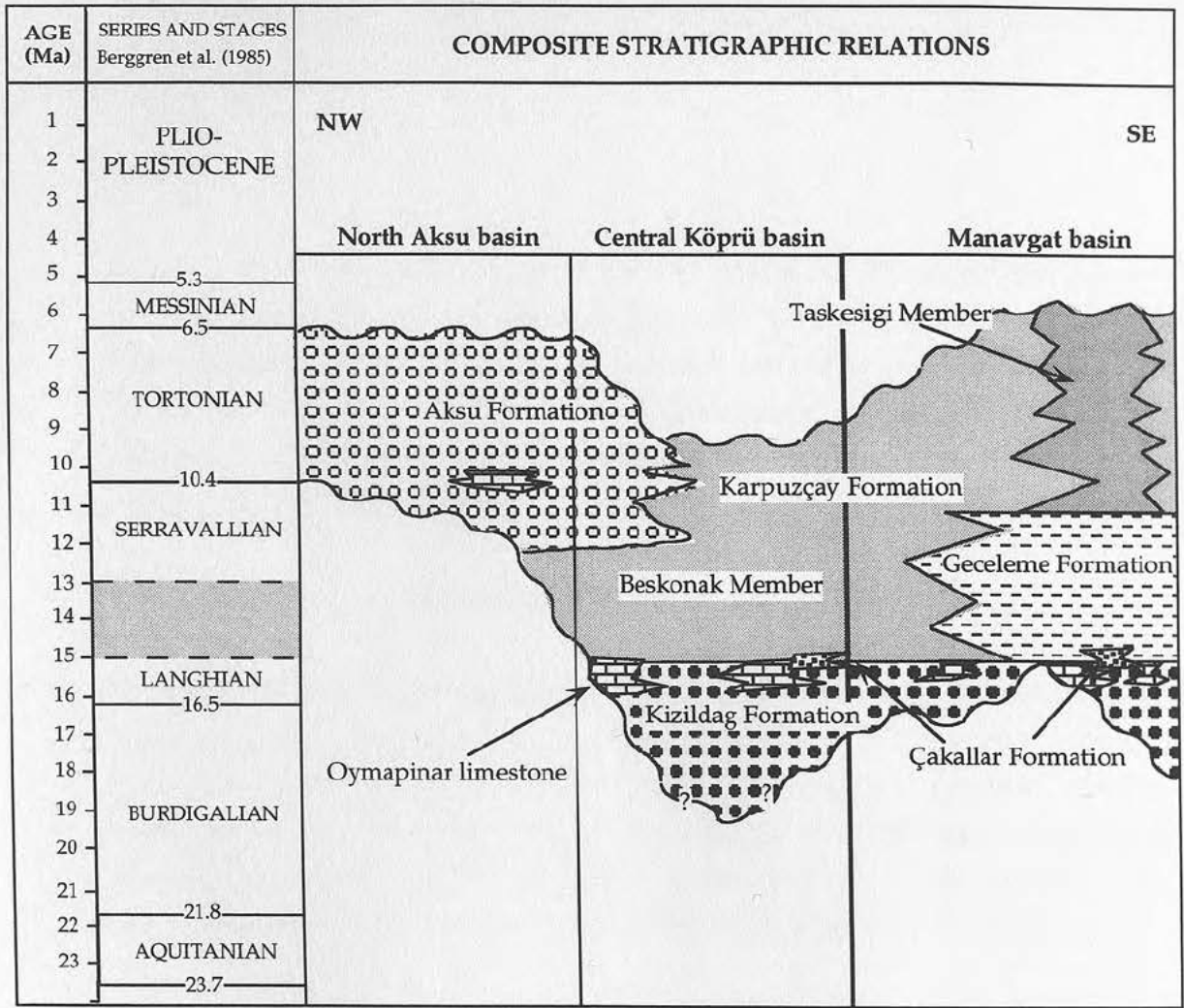


Figure 2.5 Modified stratigraphic framework (after Akay et al., 1985) used during this study.

Chapter 3

BIOGENIC CARBONATES

3.1 Context

Important information about the early stages of the sedimentary and tectonic evolution of the Aksu, Köprü and Manavgat basins is derived from biogenic carbonates. These occur at two stratigraphic levels in the Miocene: Lower-Mid Miocene and Tortonian. Crucially, the Lower Miocene carbonates occur at, or just above the basal unconformity and mark a basin-wide relative sea level rise.

3.2 Geographical distribution

Biogenic carbonates, primarily coral and algal-rich reefs, calcarenites and planktic foraminiferal marls, are found throughout the study area (Fig. 3.1.) The distribution of shallow water carbonates is uneven however, with concentrations of reef and reef related material occurring in the central and eastern parts of the Manavgat basin and more sparsely along the western and northern margins of both the Köprü and Aksu basins.

3.3 Organisation of the chapter

After a brief outline of the information gained from previous work on the area (section 3.4) the assumptions on which the classification used in this thesis for the biogenic carbonates is stated and the rocks divided into facies groups and sub-divided into sub-facies (section 3.5). The facies groups are dealt with in turn (section 3.6) with each sub-facies described and interpreted in terms of its dimensions, content, matrix and cement. A summary chart is given at the end of each facies group and a model of the environments of sub-facies deposition given in section 3.7. Broader topics related to the biogenic carbonates in the study area as a whole, are discussed at the end of the chapter (section 3.8) and the conclusions are listed in section 3.9. Diagenetic alteration of biogenic components is

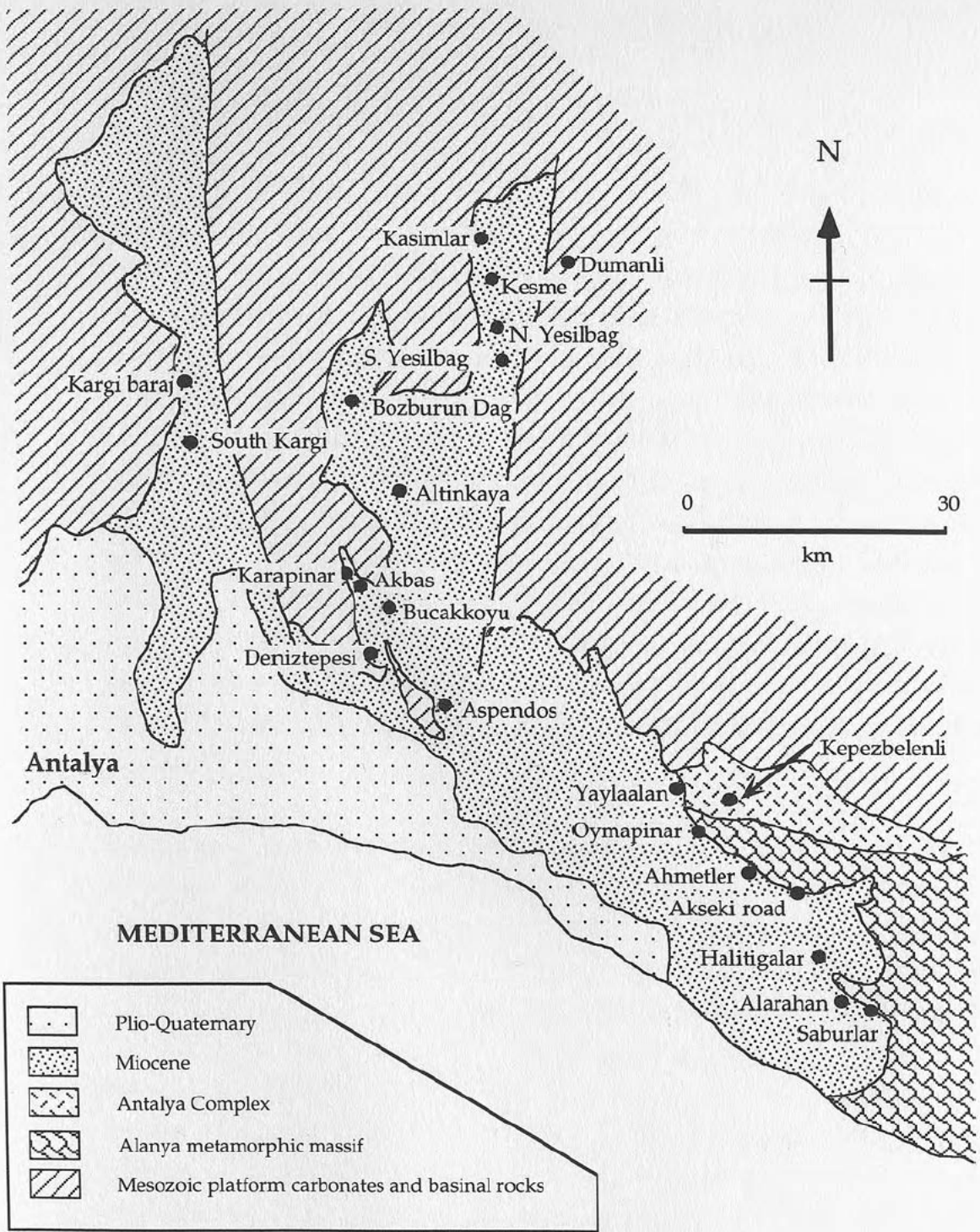


Figure 3.1. Location map of the biogenic carbonate sections referred to in the text.

touched on here, but is discussed more fully in chapter 6.

3.4 Previous work

Table 3.1 displays general information about the principal formations discussed in this chapter: the Oymapinar Limestone; the Çakallar Formation and the Geceleme Formation. The ages of these formations have been deduced from their stratigraphic position and age diagnostic micro-fossil assemblages (Bizon *et al.*, 1974; Dumont, 1974; Poisson, 1977; Monod, 1977; Akay and Uysal, 1985; Akay *et al.*, 1985; Flecker *et al.*, 1995; this study). They occur in the Lower-Mid Miocene (Burdigalian-Langhian) and are predominantly exposed in the Manavgat basin and in the south of the Aksu and Köprü basins. Rare lenses of reef limestone can be found in the north of the Aksu and Köprü basins and these are thought to be Tortonian in age (Akay and Uysal, 1985; Dumont, 1974). Akay classified these Upper Miocene reefs as part of the Aksu Formation. During this study, the Aksu Formation was subdivided and the Tortonian reef limestone lenses are now classified as part of the Kesme Group (Table 2.4).

The Oymapinar Limestone in the Manavgat basin has an upper age limit of Upper Burdigalian to Mid-Langhian as defined by the nannoplankton (Akay *et al.*, 1985 and Flecker *et al.* 1995) and foraminiferal (Akay 1985) ages of the overlying marls. Problems with dating the reefs themselves particularly in the Manavgat basin have dogged attempts to define an age for the lower boundary, since no foraminifera have been found within the shallow water carbonates that denotes an age any more precise than Lower Miocene. Blumenthal (1947) first recognised and dated these carbonates as Lower Miocene and they were subsequently correlated with the Aquitanian Karabayir Formation (Poisson and Poignant, 1974) of the Dariören-Kas basin to the west (Fig. 1.3). Monod (1972) first named the limestones calcaire d'Oymapinar. Using the presence of *Praeorbulina glomerosa* found in a marl towards the top of the Oymapinar section, Monod (1977) indicates a Burdigalian to Langhian age, but suggests that the absence of benthic foraminifera characteristic of the Burdigalian such as *Miogypsina* and *Lepidocyclina* indicate that the Oymapinar Limestone is more likely to be Langhian. Bizon *et al.* (1974) date a number of

3.1 Chart of stratigraphic information for the Oymapinar limestone, Çakallar and Geceleme Formations

Formation	Synonymy	Type locality	Lower contact	Upper contact	Description	Age
Geceleme Formation	Geceleme Formation (Akay & Uysal, 1985; Akay et al., 1985); Geceleme Formation (Blumenthal, 1947; Monod, 1977)	Gençler, along the old road north from the coast to Akseki, Manavgat basin	Disconformity with Oymapinar limestone and Çakallar Formation	Conformable and gradual transformation over 20m to Taskesigi Group or more rarely, the Karpuzçay Formation	Planktic foraminiferal marls and rare wedge shape calcirudites	Latest Burdigalian ?-Langhian
Çakallar Formation	Çakallar Formation (Akay & Uysal, 1985; Akay et al., 1985)	Çakallar, near Alarahan, south-east Manavgat basin	Conformable with Oymapinar limestone	Disconformably overlain by Geceleme Formation or Karpuzçay Formation	Calcirudites interbedded with marls and sandstones. Blocky talus sometimes present	Latest Burdigalian ?- Langhian
Oymapinar Limestone	Oymapinar limestone (Akay & Uysal, 1985; Akay et al., 1985); Calcaire d'Oymapinar (Monod, 1972)	Oymapinar, northern margin of the Manavgat basin	Unconformable on Alanya Massif along the north-eastern margin of the Manavgat basin. Conformable on Kizildag Formation elsewhere	Conformably overlain by Çakallar Formation locally. Sometimes small angular disconformity below Karpuzçay Formation and Geceleme Formation	Shallow-water biogenic carbonates including coral and algal reefs.	Burdigalian-Langhian. Diachronous from south to north in the Manavgat basin

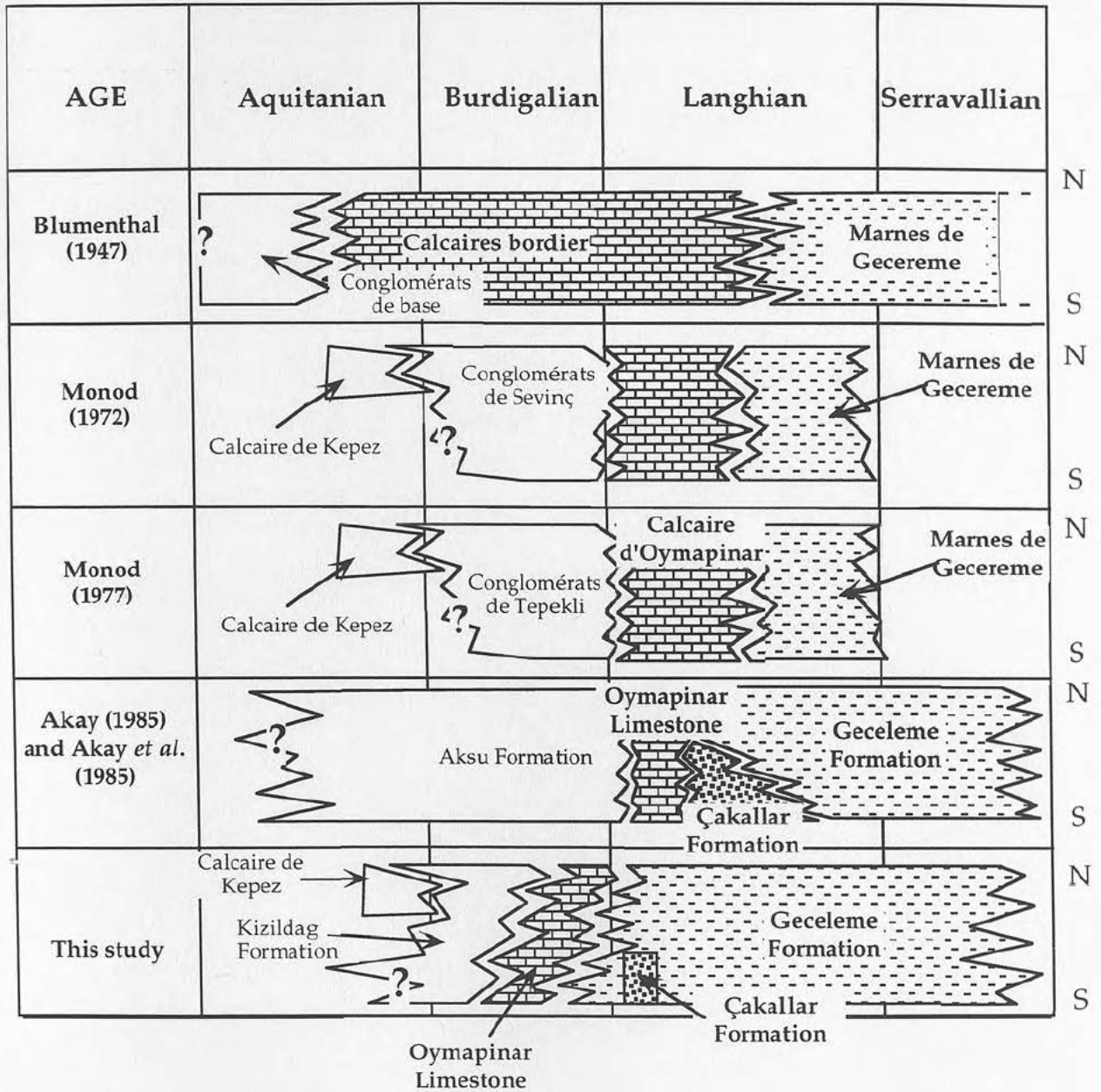
Tertiary sections in south coastal Turkey using planktic foraminifera. The basal marls in the Ahmetler section (Table 2.5) are dated as being Mid-Langhian while those of the Alarahan section to the south are Lower Langhian. Akay and Uysal (1985) also proposed a Langhian age for the Oymapinar Limestone, but more recent work on the nannoplankton in the Ahmetler section (Flecker *et al.* 1995) indicates that the lowest horizons of the overlying marls contain genera specific to the Upper Burdigalian in an assemblage which also contains *Praeorbulina glomerosa*, the planktic foraminifera diagnostic of the Burdigalian Langhian boundary (Berggren *et al.*, 1985). This indicates that although the Burdigalian fauna must be reworked, their presence suggests that some of the Oymapinar Limestone was deposited in the Burdigalian. In an attempt to resolve the issue of whether Burdigalian limestone is preserved, independent strontium isotopic dates on the reef limestone were obtained. The results of this work are reported in Chapter 6.

The ages of the Çakallar and Geceleme Formations were also defined by Akay and Uysal (1985) using both planktic foraminifera and nannoplankton analysis, as Langhian and Langhian-Serravallian respectively. A summary of the different interpretations of the Lower Miocene carbonate stratigraphy in the area is given in table 3.2. Note that authors prior to Akay and Uysal (1985) did not document the presence of the Çakallar Formation.

3.5 Classification

A rock is classified as a carbonate if it contains more than 50% carbonate minerals. In the Anatalya region, however, classification of many carbonate-rich rocks is complicated by the huge volumes of older (generally Mesozoic) carbonate that are eroded from the surrounding basement hinterland and redeposited during the Miocene. Sticking to the literal definition of a carbonate rock, my entire thesis would have to go into this chapter as nearly every sandstone, siltstone and conglomerate is over 50% carbonate, not including the cement which is ubiquitously carbonate in either micritic or sparite form (Folk, 1959; 1962). From the point of view of looking at the dominant processes involved in the deposition of these rocks it makes little sense to lump the carbonate

Table 3.2 Table showing the various names and inferred ages of the biogenic carbonate succession in the Manavgat basin. For each box, the south of the basin is at the bottom and the north at the top. Thus a south-north diachronous transgression is suggested as part of this study.



grains derived from the erosion of the basement together with those carbonate grains derived from Miocene carbonate-forming environments. Thus, where possible the two have been treated separately and the basement carbonate grains referred to as terrestrial detritus along with quartz and other lithic fragments e.g. mica, chert, pyroxene, opaques, feldspar, chlorite and igneous fragments. In practical terms in thin section this is relatively straightforward since the bulk of the basement carbonate grains contain abundant, small speckely inclusions, appearing dirty in comparison to younger carbonate grains and they frequently display deformation twinning under cross polars (Fig. 3.2).

The formation names and broad definitions of Akay *et al.* (1985) are retained in this study, but independent of these, the biogenic carbonates are divided into four broad facies groups: reef facies; off-reef facies; reef-associated carbonate facies and shelf carbonate facies (see Table 3.3).

Reef facies are distinguished from off-reef facies by the presence of an *in situ* coral (or rarely algal) framestone. In general terms, framework coral or algae bind together both biogenic material and clastic sediment.

Off-reef facies include rocks which derive the bulk of their constituent parts from the reef framestone e.g. redeposited coral rudstones. Prolific quantities of off-reef facies are found in a continuous strip parallel to the northern margin of the Manavgat basin.

Rocks containing *in situ* or redeposited bioclasts, which are not derived from the reef framework are classified as *reef-associated carbonate facies* e.g. benthic foraminiferal packstones. The bulk of these rocks are found in close spatial association with reef or off-reef accumulations.

Biogenic carbonate rocks showing little influence of shallow water carbonate production (i.e. containing <50% shallow-water detritus) are classified as *shelf carbonate facies* e.g. planktic foraminiferal wackestones.

In this study these four facies groups have been further subdivided into 14 sub-facies (see Table 3.3). These sub-facies transgress the boundaries of

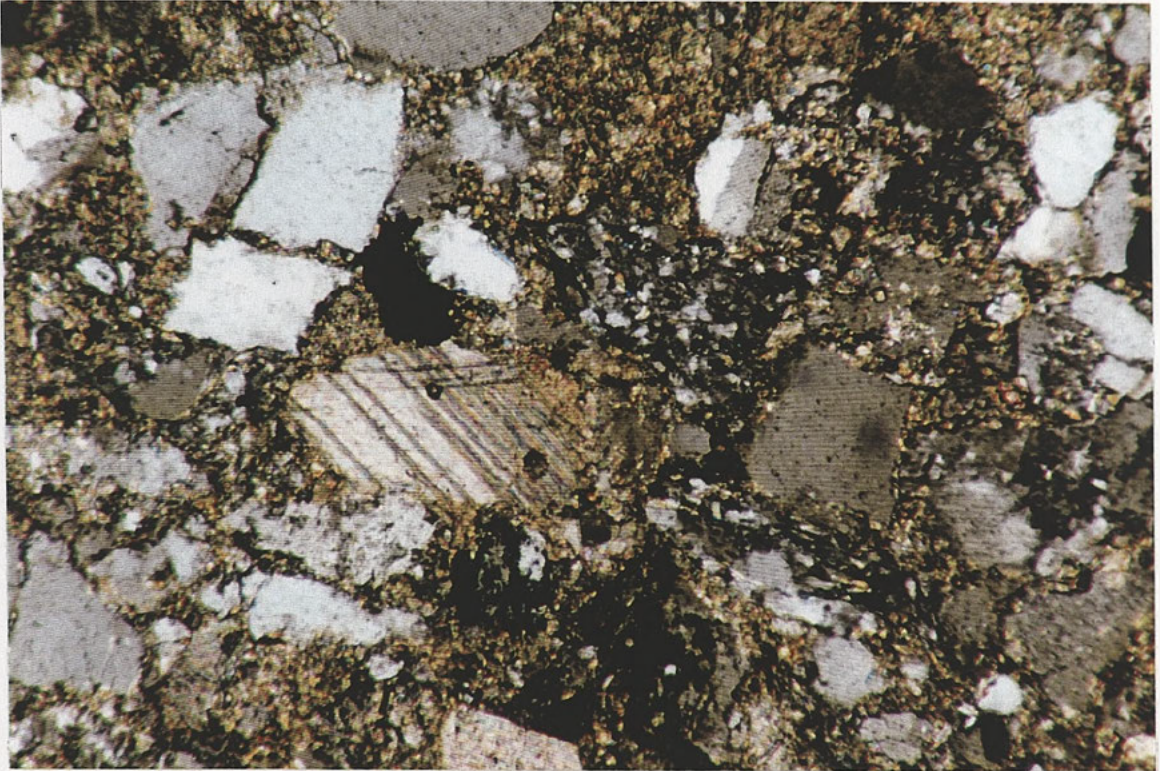


Figure 3.2 Thin section photo of speckly and deformed carbonate grains in a heterogeneous sandstone.

Table 3.3 Chart showing the overlap between Akay and Uysal's carbonate Formations and the facies and sub-facies used in this chapter.

Akay and Uysal (1985) Terms	Reef Facies			Off-reef Facies			Reef-associated Facies			Shelf Facies	
Reef lenses in the Aksu Formation	Domal coral framestone	Porites bafflestone	Fan coral framestone	Porites rudstone	Calcarenite	Coral floatstone	Oyster packstone	Gastropod wackestone	Echinoid-scapopod grainstone		
Oymapinar Limestone											
Çakallar Formation					Reef talus					Planktic foraminiferal marl	Calcirudites
Geceleme Formation											

both formations and facies. Sub-facies have been classified using Dunham's (1962) classification scheme and including the boundstone subdivision suggested by Embry and Klovan (1971).

3.6 Facies description

3.6.1 Reef facies

Table 3.4 Table of reef sub-facies, listing their characteristic fauna and the localities at which they can be found (Fig. 3.1).

Sub-facies	Characteristic fauna	Localities
Domal coral framestone	<i>Porites</i> <i>Montastrea</i>	South Yesilbag Alarahan Kasimlar-Kesme Saburlar Oymapinar
Porites bafflestone	<i>Porites</i>	South Kargi South Yesilbag
Fan coral framestone	<i>Tarbellastrea</i> <i>Porites</i>	South Kargi North Yesilbag
Porites rudstone	<i>Porites</i> algae shell fragments	South Kargi South Yesilbag Altinkaya

The study of modern reefs has revealed that coral type, location and morphology are controlled by a myriad of environmental factors such as salinity, temperature, nutrient supply, light, turbulence, relative sea level change as well as substrate type and sediment flux. In the rock record, preservation of such controls is minimal and most environmental factors can only be tentatively inferred. Substrate and sediment type, because of their high preservation potential, in the past have been credited with controlling coral type, morphology and location in the interpretation of fossil reefs. Although some studies of modern reefs do indicate that such factors can control reef composition, (e.g. Fagerstrom, 1987 in the Caribbean and Acredo *et al.*, 1989) many authors now think that other environmental controls are generally more important as well

as controls such as species replacement (Barnes and Hughes, 1982). It is therefore extremely difficult to draw any firm conclusions about what controlled the location, species and morphology of fossil corals. Bearing this in mind however, in describing the reef facies, associations between fossils and the sediment have been noted and a few, very tentative conclusions drawn. The implications of the interaction between coarse clastic environments and reef carbonate growth are discussed more fully in chapter 5.

3.6.1.1 Domal coral framestone

Dimensions and sediment associations

Domal coral framestones are found all over the study area, but constitute a small percentage of total reef exposure. Framestone horizons are generally 2-3m thick. Laterally, where exposed, units either wedge out on to basement (e.g. Ahmetler) or conglomerate highs over 12 to 20m (e.g. Alarahan) or exhibit a gradual transition to calcarenite (e.g. Kasimlar-Kesme reef). Vertical transitions tend to be abrupt as almost all domal coral framestones are overlain by coarse conglomerates with erosive bases. An example of this can be seen just south of Yesilbag. Here, a pronounced channel structure 2m in depth divides two outcrops of domal coral framestone (Fig. 3.3). The corals do not terminate at the channel margins, but appear to have grown out into the main channel conduit which is now filled with siltstones, mudstones and reef debris. The framestone on the Kasimlar-Kesme road by contrast is overlain by a fine grained conglomerate. Parts of the irregular top to the domal coral surface can be seen protruding up into this conglomerate. At Saburlar, marls that overlie the domal coral framestone horizon have been subsequently eroded, exposing an undulating top surface of the harder domal corals beneath.

Corals

The domal corals found in this facies can be up to 20cm in diameter and, at Saburlar, they protrude 5-10cm from the matrix. Domal coral species varies between localities, but by far the most dominant coral type is *Porites sp.* Poritid morphology is variable. The following main types of morphology occur commonly in reef frameworks:

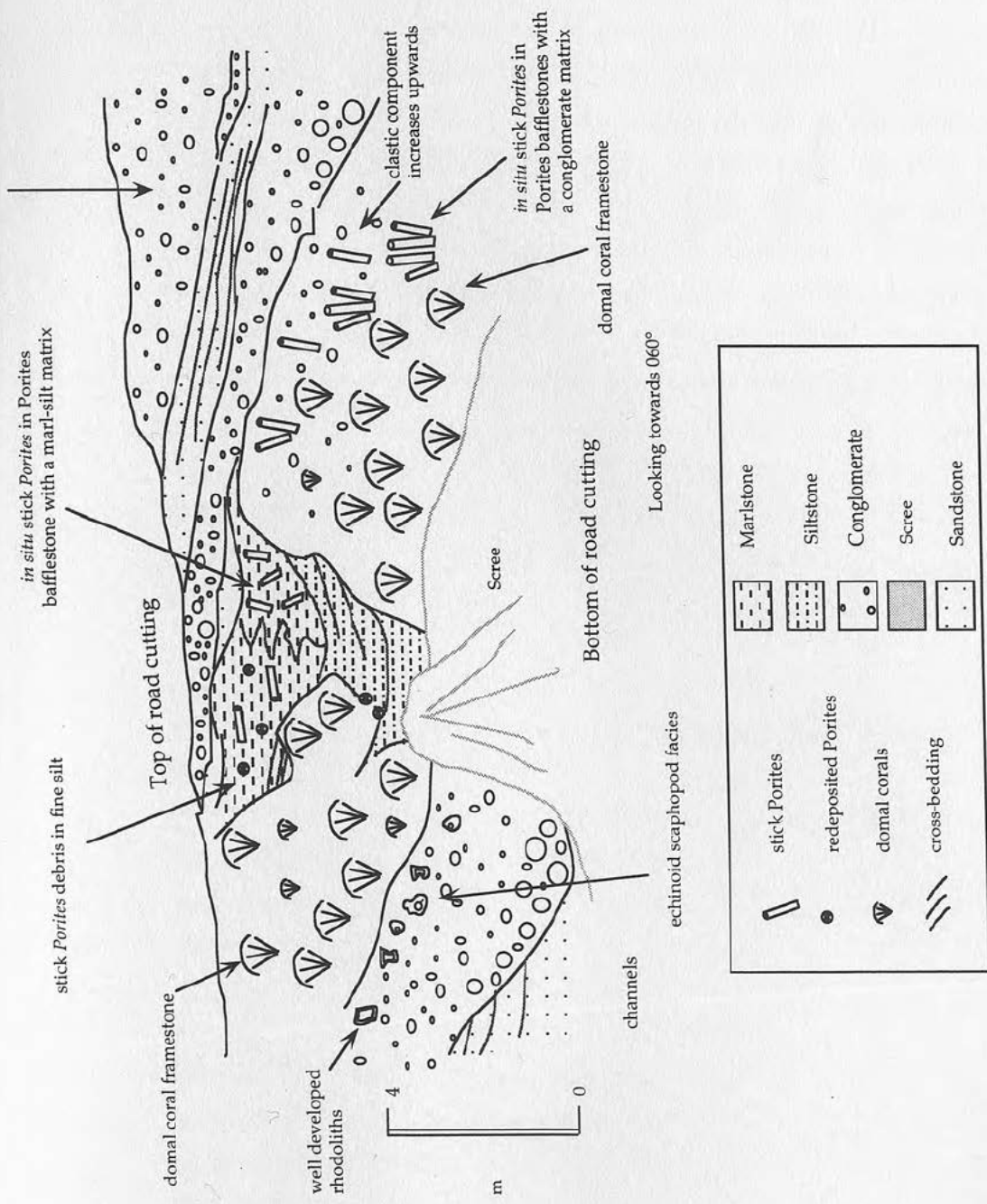


Figure 3.3 Schematic sketch of the reef at South Yesilbag. Note the increase of stick Porites and correlative decrease in domal corals with increasing clastic content. See also the two different sorts of bafflestone matrix visible at this locality, conglomerate and fine-grained silt. The silt bafflestone appears to be confined within a channel of finer grained material, which from its relationship with the coral framestones and the overlying clastics suggests that the coral growth influence the structure of a coeval channel for fine grained sediments.

- ◆ *Domal* - approximating hemispherical shape, 5-10cm across;
- ◆ *Tabular* - flattened or dish-shaped, 5-20cm;
- ◆ *Sticks* - rods, sometimes branching when in situ, length 2-15cm, diameter 2-5cm.

There are four individual coral-framestone horizons exposed in the Alarahan section (Fig. 3.4). In the lowest of these (reef 1) at the base of the framestone, domal *Porites* corals are interspersed with tabular *Porites* colonies. The framestone passes up over 2m into a reef talus facies containing disorientated fragments of domal *Porites* and rare *Tarbellastrea* and *Porites* stick coral. Stick *Porites* dominate the base of reef 2 with *in situ* domal corals (again dominantly *Porites*) distributed amongst them higher in the section. This reef is abruptly terminated by an erosion surface and overlain by a channelised conglomerate. Reef 3 is similar to reef 2 in that stick *Porites* coral dominates at the base. Towards the top of this reef however domal *Porites* corals become much more prolific and are the dominant morphology. The top of the reef is not exposed. Just below the base of the highest reef (reef 4), a detached block of domal coral framework limestone a metre in length, is seen suspended within cross-bedded conglomerates. The base of the reef itself contains concentrated domal corals. Stubby stick *Porites* are also abundant and become more dominant up section, with domal corals dispersed amongst abundant stick *Porites*.

The Kesme reef displays the greatest diversity of *in situ* coral found within the study area. It is dominated by large, ridged, spreading structures of *Montastrea* (Fig. 3.5), but it also contains tabular and domal *Porites* and *Tarbellastrea*. One sample of the *Montastrea* was submitted for x-ray diffraction analysis and this indicated that all coral in the sample had been completely converted from primary aragonite to low magnesium calcite.

Matrix

At Saburlar and Alarahan (Fig. 3.1) the abundant framework interstices are infilled with a coarse, poorly sorted bioclastic matrix rich in echinoid spines and body fossils, abundant large algal fragments, brachiopods and the large benthic foraminifera *Operculina*. Non-bioclastic fragments

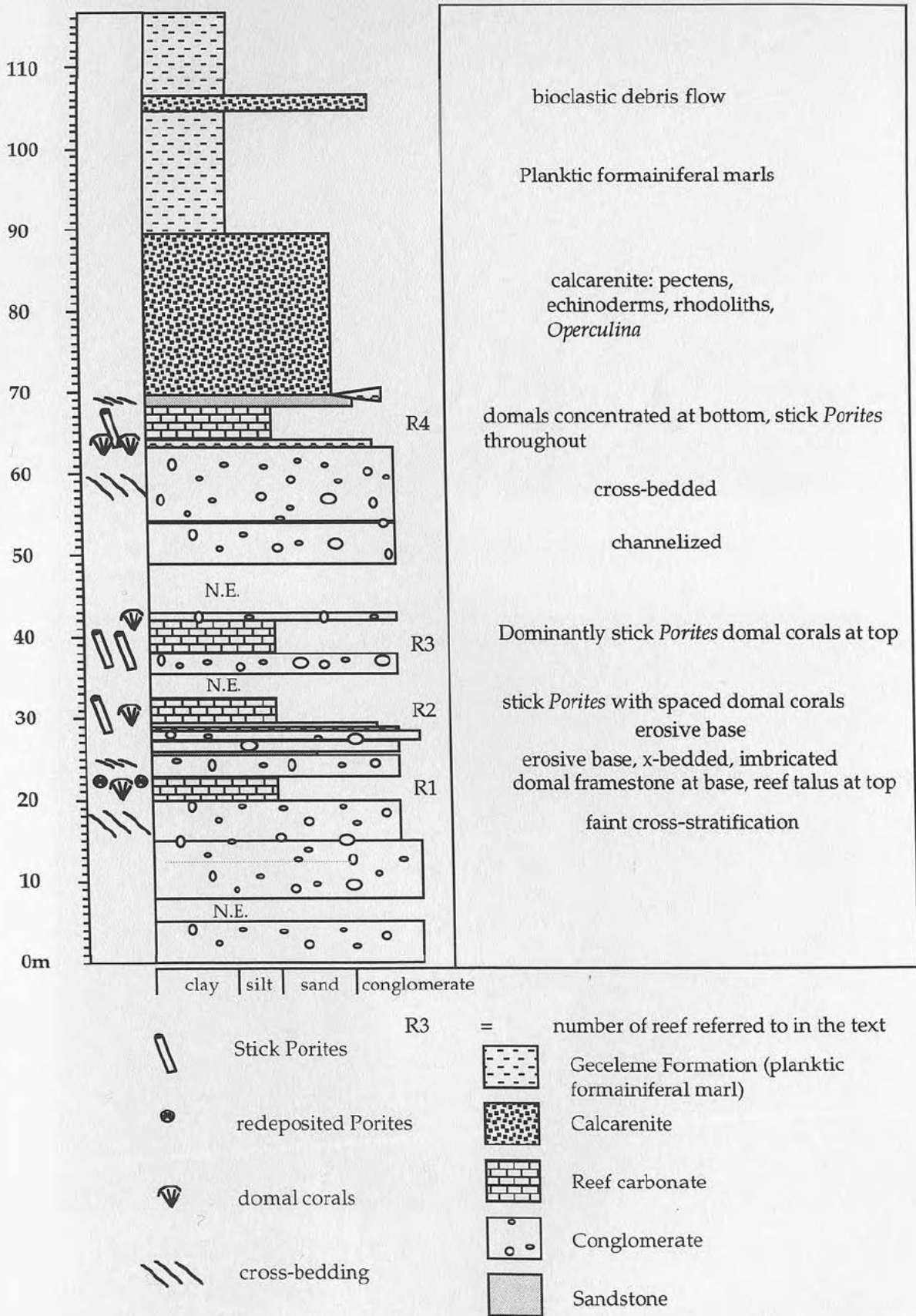


Figure 3.4 Alarahan section from the south-east of the Manavgat basin, showing the different vertical stratigraphies in the 4 reefs. Note also that the onset of deposition of planktic foraminiferal marls marks the termination both of reefs and the coarse clastic sedimentation.



Figure 3.5 Photograph of the irregular massive *Montastera* build-up at Kesme.



Figure 3.6 Photograph of spaced *Porites* bafflestone with interstitial micro-conglomerate.

include red chert, sandstone, carbonate grains containing abundant opaques. At Kesme (Fig. 3.1), because of the more massive framework structure, there is little matrix and the colonies of *Montastrea* appear to be largely supported by the close packed nature of neighbouring corals. What matrix there is however is dominantly micrite with miliolids and rare quartz (Dumont, 1974). Dark-grey micro-conglomeratic matrix infills the open framework structure at Yesilbag making up 20-30% of the rock.

Ages

The Saburlar and Alarahan sections have a Langhian age inferred from the Langhian nannoplankton and planktic foraminifera found in the overlying marls (Akay 1985; Akay *et al.*, 1985). The Yesilbag reef lies close to the boundary between the Serravallian Karpuzçay Formation (Akay and Uysal, 1985) and the overlying Tortonian Aksu Formation (Dumont, 1974). This reef and the Kasimlar-Kesme reef to the north are considered to be Tortonian because they are interbedded in the Aksu Formation.

Interpretation

The Miliolids found in the matrix in the Kasimlar-Kesme reef indicate a low energy environment of deposition (Martin *et al.* 1989). The structure of this *Montastrea* reef however is very different from that seen elsewhere. Where the abundance and grain size of the matrix is relatively coarse, this may suggest a relatively high-energy environment of deposition, e.g. strong currents causing break-up and reworking of reef components.

The high terrigenous content of the matrix and the conglomerate channel structures both in and above the domal-coral framestone at Yesilbag suggest that sediment influx, probably from a local fluvial source, was also active. The non-erosive nature of the margins of this channel within the framestone may indicate that coral growth patterns influenced the finer grained sediment pathways. The interaction of coral growth in a clastic environment is discussed more fully in section 5.6.3.2.

Despite displaying the highest diversity of *in situ* coral in the study area, the Kasimlar-Kesme reef is still low diversity in comparison to the coral diversity seen in the Ziqlag Formation in Israel (Esteban 1979) which is

also of Tortonian age. Follows (1990) however, describes a similar diversity restriction of Tortonian corals (*Montastrea*, *Tarbellastrea* and *Porites*) in the Koronia Member in Cyprus. The possible reasons for this restriction are discussed further in section 3.8.2.

3.6.1.2 *Porites* bafflestone

Dimensions and sediment associations

Porites bafflestone horizons identified in the study area are 2-3m thick. At South Kargi (Fig. 3.1), differing concentrations of stick *Porites* occur in stacked bafflestone beds such that the total thickness of the bafflestones is over 6.5m. The beds cannot be traced out laterally, but are absent from a tunnel cutting section 100m to the east (Fig. 3.7). Sediment between coral sticks is coarse sand to micro-conglomerate grade. At South Kargi the uppermost bafflestone bed is abruptly terminated by an erosion surface.

There are two distinct bafflestones in the reef just south of Yesilbag: one with a medium-grained conglomerate matrix and the other with a muddy matrix. The latter of these is located in the upper part of the channel structure (Fig. 3.3), wedging out against the channel margin to the east and passing laterally into a silty coral floatstone to the west.

Coral

The bafflestones studied here are all exclusively *Porites*. The dominant *Porites* morphology is a stick-like form 2-3cm in diameter, up to 10cm in length and variously spaced from other sticks (Fig. 3.6). The orientation of these sticks is vertical to sub-vertical in the Kargi and Yesilbag sections where conglomerate or coarse micro-conglomerate is the associated matrix. More horizontal sticks are seen in the silt matrix bafflestone at Yesilbag. Coral concentration in the bafflestones varies from 30-70%.

Matrix

Throughout the bafflestones at Kargi, changes in grain size and composition of the matrix are clearly visible as bedding. Coral sticks pass undisturbed through these boundaries. The matrix here, is made of angular fragments of red, radiolarian chert and limestone as well as biogenic fragments including algal debris and echinoid spines. The

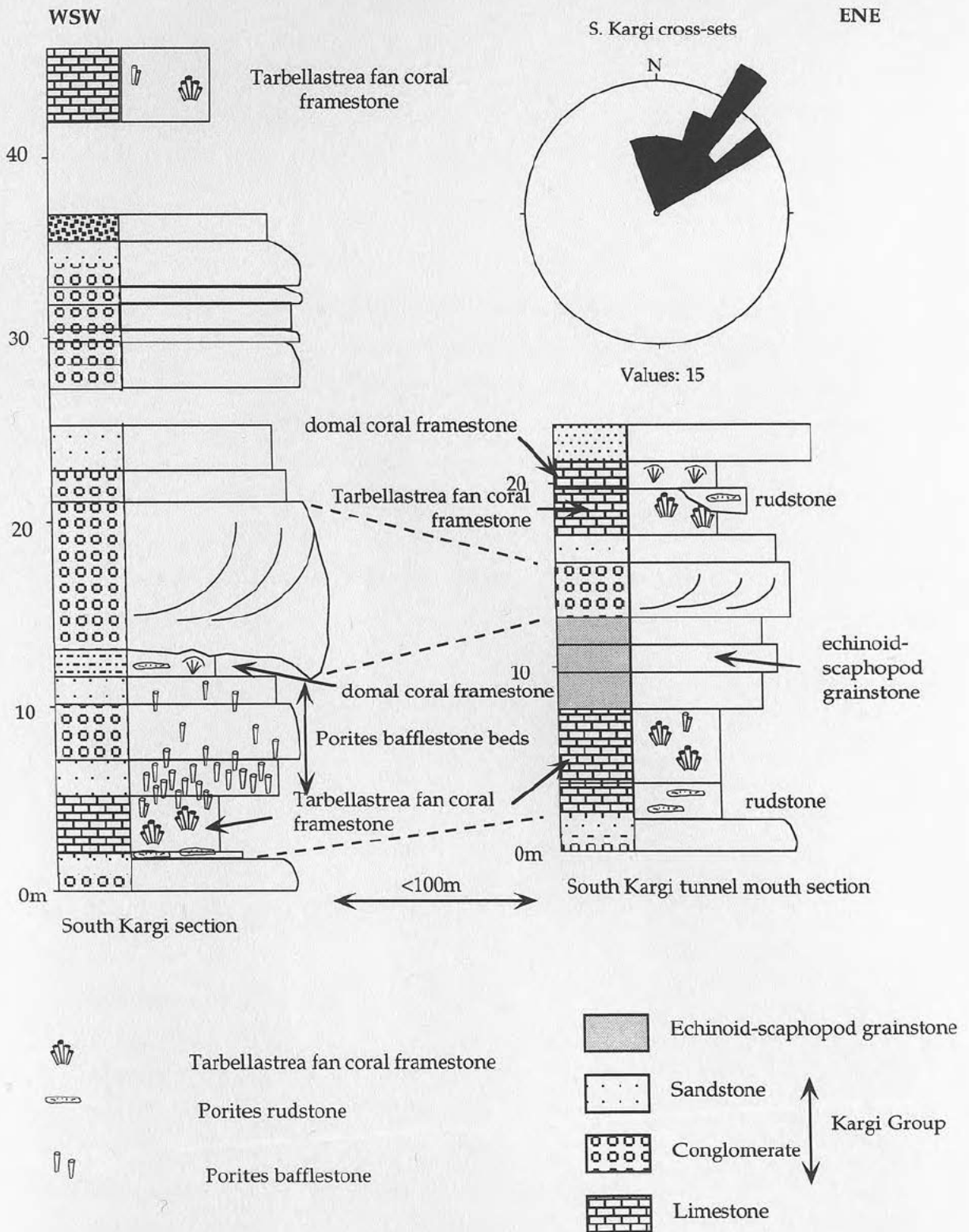


Figure 3.7 Tentative correlation of the logged sections at South Kargi, central Aksu basin, and palaeocurrent data measured from the cross-bedded conglomerates. Note the rapid lateral facies changes in reef framestones.

grainsize is dominantly silt to fine sand, but it increases to micro-conglomerate grade towards the top of the lowermost *Porites* bafflestone bed (Fig. 3.6 and 3.7). At Yesilbag both the matrix types (conglomerate and siltstone) have similar compositions to the matrix at South Kargi. In the conglomerate the larger limestone clasts are well rounded and algal debris is abundant. This contrasts with the angularity of the micro-conglomeratic matrix at South Kargi.

Interpretation

Martin *et al.* (1989) found a close association of *Porites* coral with siltstone in the Tortonian reefs of south east Spain and it is possible that sediment flux is one of the factors controlling the exclusive colonisation of stick *Porites* in these bafflestones. As well as being tolerant to environments of high terrestrial sedimentation, *Porites* has also been observed to colonise areas of low salinity, low temperature and reduced water circulation in modern reefs (Marshall and Orr 1931, Manton 1935, Wells 1954 and Scoffin and Stoddart 1978). Thus the factor controlling *Porites* dominance may be low salinity associated with a high fluvial input rather than the sediment itself, or a combination of the two. Equally likely however, is that the matrix infilled the spacious coral framework after the coral had grown. Evidence supporting this is the observation that individual stick corals appear to pass through lithological boundaries. In this case, it would be difficult to argue that sediment influx and low salinity alone were dominant factors controlling coral type. The bafflestone located within the channel structure at Yesilbag may be an exception to this.

The correlation between the orientation of the *Porites* sticks and the coarseness of the grainsize may be explained by the stability of the substrate. Martin *et al.* (1989) observed in south east Spain, that many of the *Porites* colonies embedded in silt appeared to have toppled over having reached a certain size (see section 3.6.1.3). The coarser packing of the micro-conglomeratic matrix at Yesilbag and South Kargi may have better supported the *Porites* than the finer, more mobile silt observed at Yesilbag where more horizontally orientated coral sticks were found. Given that the silt bafflestone occurs within a channel structure however,

it is also possible that some of the horizontal *Porites* sticks may be redeposited.

3.6.1.3 Fan coral framestone

Dimensions and sediment associations

The fan coral framestone horizons found at South Kargi (Fig. 3.1) and to the north of Yesilbag are all between 4 and 6m thick. Variations in thickness occur along a single horizon at South Kargi where the lower framestone is at least a metre thicker in the tunnel cutting than it is 100m to the west in the main South Kargi section (Fig. 3.7). The tunnel cutting also exposes another fan coral horizon a few metres higher up the section which is absent to the west. This horizon has a wedge-shaped geometry which passes laterally into a Poritid rudstone containing abundant tabular *Porites*, both *in situ* and redeposited (Fig. 3.8). In South Kargi all the fan coral framestones overlie *Porites* rudstone horizons. They pass upwards into sand and micro-conglomerate rich *Porites* bafflestones with a rather abrupt transition, or are terminated by an erosion surface.

Fan coral framestones along the track north of Yesilbag (Fig. 3.1) are interbedded with sandstones, conglomerates, and siltstones. The framestones are occasionally observed passing into a more spaced *Porites* bafflestone. Poor exposure does not enable lateral relationships to be observed.

Corals

There are two distinct types of fan coral framestone: one composed entirely of *Tarbellastrea* as can be seen at South Kargi and the other exclusively *Porites*. The latter is observed along the track to Kesme, north of Yesilbag (Fig. 3.1).

The *Tarbellastrea* colonies at South Kargi are cone shaped. They are composed of bunches of sticks spreading upwards and outwards and at the same time thickening so that there is virtually no space between individual sticks. Colonies can reach over 3m in height and appear to compete for space with neighbours (Fig. 3.9) In the South Kargi section, well exposed *Tarbellastrea* colonies all appear to grow from a single level



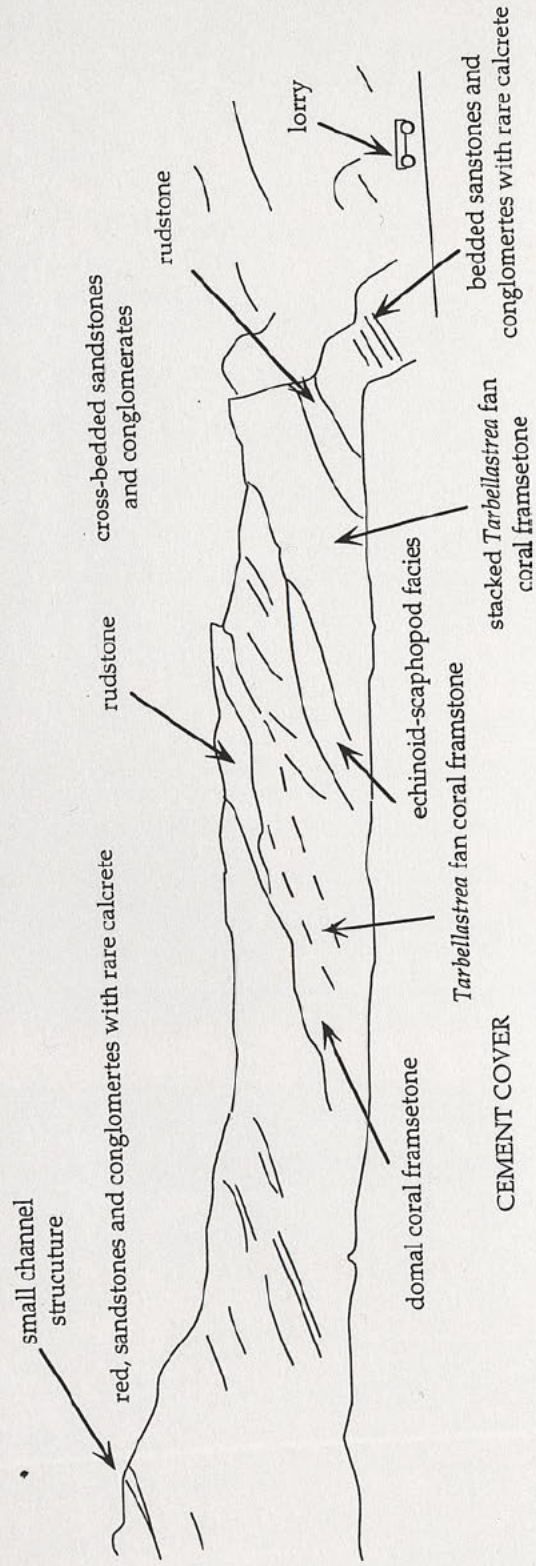


Figure 3.8 Photomontage and interpretive sketch of the patch-reef and Kargi Group conglomerates in the tunnel section at South Kargi, central Aksu basin. Figure 3.7 shows a log of this section correlated to the main South Kargi section to the west.

Figure 3.9
Photograph of
Tarbellastrea
fan coral
framestone.



Figure 3.10 Photograph of stick Porites framestone at Yesilbag

at the top of the rudstone horizon (Fig. 3.7). 100m to the east however, the tunnel cutting through the same section reveals a series of *Tarbellastrea* cones on top of one another.

The *Porites* fan corals are similar in morphology to the *Tarbellastrea* colonies, but they are less closely packed and much smaller, reaching a maximum vertical height of only 15-20cm. In contrast to the *Tarbellastrea* framework, where there is little displaced coral, *in situ* *Porites* colonies are in the minority. They sit within a dense mêlée of disoriented colonies and single *Porites* sticks (Fig. 3.10).

Matrix

As a result of the close packed structure of the *Tarbellastrea* framework, the amount of sediment contained within it is minimal. The *Porites* colonies have more space between individual sticks varying between 5-15% silt to sand grade matrix.

Interpretation

According to Martin *et al.* (1989), the degree to which the *Tarbellastrea* cone structures open out is related to water depth i.e. the deeper the water the tighter and narrower the cone structure. Braga and Martin (1988) note micro atoll shapes covered in iron oxides preserved at the top of colonies which reach sea level. These features are not developed at South Kargi suggesting that relative sea level rise was rapid enough to prevent corals from reaching sea level. Furthermore, the *Tarbellastrea* cones are relatively narrow, supporting a deeper water interpretation. The *Porites* fan coral framestones by contrast have a much wider cone geometry and although there is no clear evidence of micro atoll structure development they may have developed much closer to sea level.

The average growth rate estimated for modern reef corals is 7-8m/1000 yrs (Geister, 1983 and Johnson *et al.*, 1986). Thus, even the individual *Tarbellastrid* colonies in the main South Kargi section which are over 3m in height may well have grown in under half a century. This growth rate has implication for the rate of relative sea level rise which is discussed in section 3.8 and further in chapter 5.

The cause of the total domination of one species of coral in these framestones may well be biotic factors. Martin *et al.* (1989) suggests that interspecific aggression, susceptibility to predation and colony overgrowth may have caused the *Tarbellastrea* domination observed in south east Spain. *Porites* domination of the Yesilbag reefs may be related to the Late Miocene age of the reefs (see section 3.6.1.1) and will be discussed further in section 3.8.2.

The close packed nature of the *Tarbellastrea* framestone, results in little sediment being retained within the structure. This might initially suggest that the sediment input at this time was low. However, structures as tall as these colonies are require support in order to prevent their top heavy structures from falling over (Scoffin 1987). The outcrop evidence suggests that rather than being supported in sediment, neighbouring colonies, by virtue of the competition for space, supported each other in a close-packed structure with few inter-colony interstices. This is similar to the *Tarbellastrea* frameworks studied by Martin *et al.* (1989). It is difficult to draw any firm conclusions concerning sediment flux during growth of *Tarbellastrea* fan-coral framestones as their topography may well have affected sediment dispersal patterns. This is discussed further in chapter 5.

Conical shaped stick colonies of *Porites* have been documented by Martin *et al.* (1989) in the Tortonian reefs of south east Spain. These corals anchor themselves directly into the silt substrate. The authors indicate that the silt was not lithified at the time of coral growth allowing colonies of *Porites* to topple over and become embedded in silt without suffering mechanical abrasion characteristic of firmly cemented corals which have been dislodged by wave or current action. This may well be what has caused the mixture of *in situ* and displaced *Porites* colonies visible along the track north of Yesilbag. A relatively high sediment influx is envisaged for this environment.

3.6.1.4 *Porites* rudstone

Dimensions and sediment associations

Porites rudstones occur at two horizons within the South Kargi section.

Towards the bottom of the section, rudstone overlies the interbedded red conglomerates, sandstones, siltstones and calcrete horizons of the Kargi Group (Kizildag Formation; chapter 5). The coarse sandstone to microconglomerate substrate below the rudstone displays a weak palaeotopography, but there is no evidence of boring or encrustation. The rudstone itself varies in thickness from 50cm to 2m over a distance of 100m. To the east, the tunnel cutting reveals a wedge shaped *Tarbellastrea* fan coral framework passing laterally into *Porites* rudstone (Figs. 3.7 and 3.8). A higher rudstone horizon further up the main South Kargi section occurs above *Porites* bafflestone. The transition from the underlying bafflestone is abrupt and marked by the termination of the stick *Porites* and a change in the nature of the matrix.

The rudstone horizon at Altinkaya (Fig. 3.1) is only 50cm thick and is sandwiched between a conglomerate and a coral floatstone. Lateral variations in bed thickness were not observed.

Coral

The *in situ* coral at South Kargi is exclusively *Porites* with flat or dish-shaped forms. The concentration of coral increases up the rudstone section and corals generally become more domal in shape. Some redeposited stick-shaped coral fragments are found lying horizontally at the base of the rudstone horizon. Many of these are encrusted with coralline red algae. In the tunnel cutting, the majority of the coral in the rudstone horizon, though larger, appears to be redeposited.

At Altinkaya, the morphology of the *Porites* rudstone is stick-like. The clasts are much smaller than those at South Kargi with the largest coral clasts being up to 3 cm in length. Once again the long axes of the clasts lie approximately along the plane of bedding, but this bed presents a much more chaotic appearance than the rudstones in the South Kargi section. None of the *Porites* at Altinkaya appears to be in life position.

Matrix and diagenesis

There is a change in the matrix associated with the bottom of the lower most rudstone horizon at South Kargi. Here, polyolithic microconglomerate (radiolarite, carbonate and igneous fragments as well as

abundant shallow-water carbonate debris) gradually grades into the white silt matrix of the rudstone. This silt contains as clasts, small angular chert, bioclastic detritus including abundant algal fragments, and carbonate grains. The transition to a more bioclastic dominated matrix is mirrored in the upper rudstone although the grainsize is here rather coarser (fine sand). The percentage of matrix varies within and between rudstone horizons, but rarely constitutes more than 40%. In the tunnel cutting however, the base of the rudstone horizon has only 30% matrix, but it increases upwards until the coral clasts are only just in contact with each other and the rock resembles a floatstone rather than a rudstone.

The percentage of matrix found at Altinkaya is 50-60% with the coral clasts only just in contact with each other in the plane of exposure. Silt intraclasts of comparable size are also found. The silt matrix is dominated by bioclastic detritus including algal fragments, echinoid spines, benthic foraminifera with agglutinated tests, mollusc and brachiopod shell fragments. The subsidiary terrigenous component consists of rare angular quartz grains, opaques and carbonate grains which show deformation lamellae under cross-polars. Micrite envelopes on the coral clasts and on the other biogenic components are locally coated in microspar and clay minerals.

Interpretation

Particular morphologies and species of coral are characteristic of early colonising assemblages. Flat and dish-shaped coral structures have large surface areas of attachment providing better stability on sandy substrates and in high energy environments (Scoffin 1972). The presence of some *Porites* sticks lying horizontally at the base of the rudstone horizon in the Kargi section, may indicate either that stick *Porites* colonies were forming here as in SE Spain (Martin *et al.*, 1989) on an unlithified substrate or that a nearby established reef was shedding stick *Porites* material. Two pieces of evidence mitigate against the second hypothesis:

- ◆ The transition from continental to marine sedimentation is just below the rudstone horizon;
- ◆ Palaeocurrent data from the cross-bedded conglomerates indicate that fluvial input was from the W-SW.

The evidence concerning the hardness of the substrate prior to coral colonisation is mixed. The gentle palaeotopography preserved on the surface of the underlying micro-conglomerate may suggest that there had been some lithification of the substrate before coral colonisation. The absence of borings on the top of the micro-conglomerate however, indicates that the upper surface was not hard. The presence of redeposited horizontal sticks of *Porites* within the rudstone may also indicate a soft substrate such that nearby stick-Poritids toppled over due to substrate instability (Martin *et al.* 1989). Mechanical erosion and redeposition of stick *Porites* colonies could also be responsible for these however, and the encrusted nature of the corals argues in favour of this as Martin *et al.* (1989) indicate that immediate burial in silt due to the toppling of a stick *Porites* colony prevents extensive encrustation and abrasion from occurring.

Although coralline red algae are found encrusting individual coral clasts and *in situ* coral and as the main constituent of the bioclastic component in the matrix, algae only very rarely occurs as *in situ* laminated mats. It can therefore be interpreted as a secondary framework builder (Scoffin, 1987).

3.6.1.5 Summary of reef sub-facies

A summary table of the information discussed and interpreted above is given in table 3.5.

3.6.2 Off-Reef facies

Table 3.6 below displays the off-reef sub-facies, listing their characteristic fauna and the localities at which they can be found (Fig. 3.1).

Generally, transitions from reef to off-reef facies are abrupt as preserved in a vertical section. Where exposed however, lateral transitions are gradational over 5 to 100 metres. This is a result of the reefs exerting a control on the surrounding facies development (e.g. Scoffin 1987.)

Table 3.5 Summary of information and interpretation of reef sub-facies

Sub-facies	Coral type	Matrix	Energy level	Sediment dispersal pattern	Water depth/sea level change
Domal coral framestone	<i>Porites</i>	20-30% chert, sandstone, carbonate, bioclasts	Moderate-high	found in muddy channel	Photic zone, but no evidence of corals reaching sea level
	<i>Montastrea</i>	Very little	Low	may have formed in areas of low sediment influx	Photic zone, but no evidence of corals reaching sea level
Porites bafflestone	<i>Porites</i>	Sandstone/micro-conglomerate	High	Traps sediment (see chapter 5 for more information)	Relative sea level rise > sediment influx. No evidence of sea surface
Fan coral framestone	<i>Porites</i>	Siltstone	High	May trap some sediment	Relatively shallow
	<i>Tarbellastrea</i>	Very little	?	Topography may have influenced sediment dispersal patterns	Relatively deep? Instantaneous sea level rise > 8m/1000yrs
Porites rudstone	<i>Porites</i>	30-60% Siltstone-micro-conglomerate chert, sandstone, carbonate, high concentration of bioclastic components	High	Colonising colony. May suggest period of low sediment influx	?

Table 3.6 Table of off-reef sub-facies, listing their characteristic fauna and the localities at which they can be found (Fig. 3.1).

Sub-facies	Characteristic fauna	Localities
Coral floatstone	Various coral types Gastropods	Dumanli Altinkaya Karapinar
Rhodolithic calcarenite	Algal rhodoliths various shallow-water biogenic fragments	Yaylaalan Ahmetler Alarahan Kepezbelenli Akseki Road Deniztepesi Bucakköyü Saburlar Oymapinar
Reef talus	Coral Molluscs	Oymapinar Deniztepesi Akseki Road

3.6.2.1 Coral floatstone

Dimensions and sediment associations

At Altinkaya (Fig. 3.1), a coral floatstone overlies the Porites rudstone described above. The floatstone horizon is 50cm thick and contains large coral clasts up to 10cm across, oysters and algae, all chaotically orientated. The floatstones at Dumanli (Fig. 3.1) are interbedded with sandstones, conglomerates and rare, thin *in situ* coral framestones. The floatstones wedge out passing into coral and gastropod packstones towards the west and into macro-fossil poor marls and sandstones to the east. The section at Karapinar is just over 18m long and contains 4 individual floatstone horizons.

Corals

Two coral samples from the Dumanli section was submitted by Dr. J. P. Cuif for Sr measurements using an energy dispersive spectroscopic

microprobe (LINK system). The mean Sr values for these two samples were 0.7% and 0.65%. These values are far closer to the percentages expected in living Scleractinid aragonite (approximately 0.8%) than they are for diagenetic low-Mg calcite (0.02%; Scoffin, 1987). SEM photographs taken of these same samples revealed good preservation of skeletal fibres (Fig. 3.11). There has been some preferential dissolution along organic-rich growth lines, but there is no evidence of general calcitization, (C. Cuif pers. comm. 1994).

The Karapinar floatstones contain a diverse coral assemblage. Table 3.7 lists the species of coral found and their stratigraphical ranges as determined by Chevalier (1961). The coral assemblage found here indicates a Lower Miocene (Aquitanian-Burdgalian) age for the reef. This has important implications for the age of the previously undated underlying conglomerates (see chapters 5 and 6).

Many of the corals collected from the Karapinar section show good preservation of the detailed skeletal structure in hand specimen (Fig. 3.12a), (B. Rosen pers. com., 1993). Of these coral specimens two samples (26J.217.4a and 26J.217.4c) were ground up for x-ray diffraction analysis to determine whether primary aragonite was still present. Sample 26J.217.4a (*Heliastrea oligophylla*) contained approximately 55% aragonite (see Appendix 1). Sample 26J.217.4c (*Favites neglecta*; Fig. 3.12b) was found to have been completely transformed to low-Mg calcite. In hand specimen the Favid appears smoothed and abraded (Fig. 3.12b) and in thin section the skeletal structure can be seen to have been completely destroyed and replaced by irregular dirty calcite crystals. The Heliastrid, by contrast, retains some of the prismatic crystal structure within the coral skeleton.

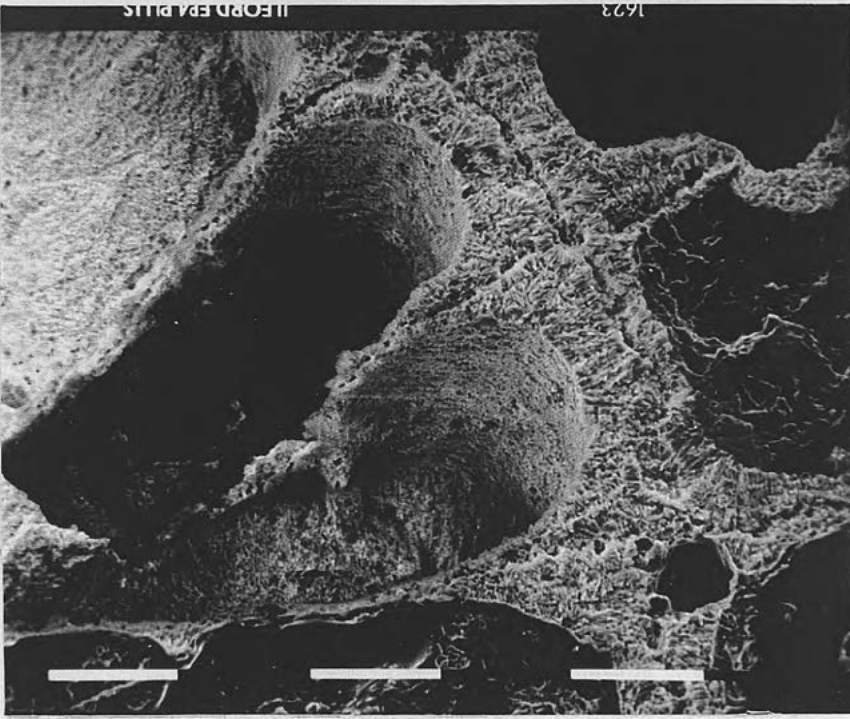
Matrix and Diagenesis

At Altinkaya coral clasts are suspended in a fine to medium-grained sandstone matrix. Smaller bioclasts include echinoid spines, brachiopod fragments showing punctate like structures, benthic foraminifera with agglutinated tests, gastropods and organic fragments. Terrigenous quartz and deformed carbonate grains are scattered liberally through out, constituting 10-20% of the matrix. The coral clasts have a thin, well defined micrite envelope around the skeletal structure which has been

NAME	Aquitanian	Burdigalian	Langhian	Serravallian	Tortonian
<i>Heliastrea oligophylla</i>	—————				
<i>Favites neglecta</i>	—————				
<i>Tarbellastrea carryensis</i>		—————			
<i>Tarbellastrea ellisiana</i>		—————			
<i>Caulastria matheroni</i>		—————			
<i>Porites</i> sp.	—————				

Table 3.7. List of the coral species found in the patch reefs on the western margin of the Köprü basin and their age ranges. The species found in these reefs allowed them to be dated as Early Miocene in age (Chevalier, 1961; B. Rosen pers. com. 1993).

a)



b)

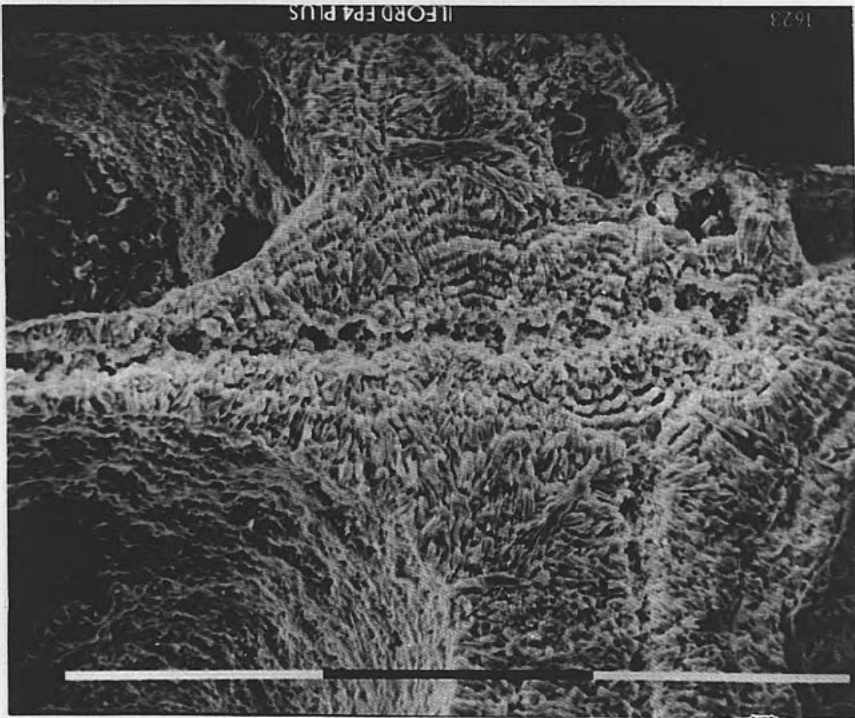
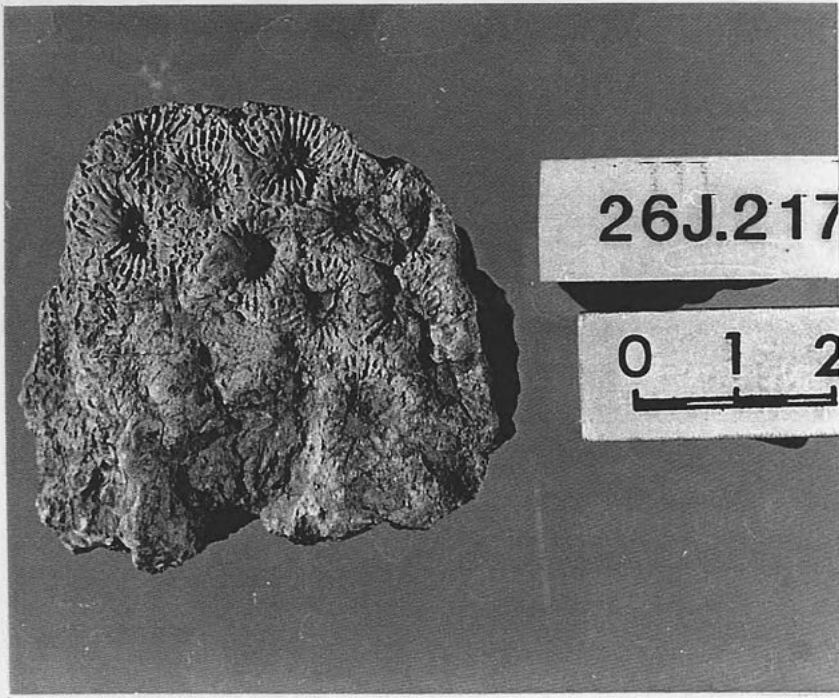


Figure 3.11 SEM photograph of skeletal fibres of aragonite in a Dumanli coral, north Köprü basin. Note the preferential dissolution along organic growth lines and the good morphological preservation of aragonite fibres (Photographs: C. Cuif, 1994).

a)



b)

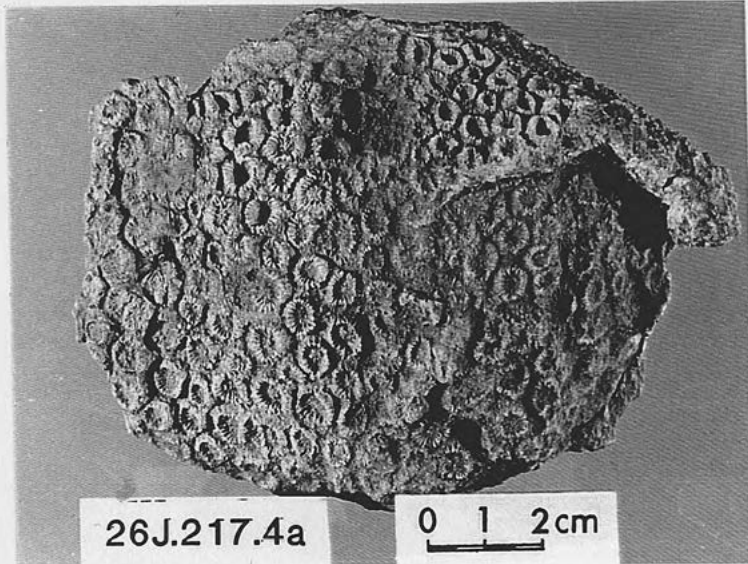


Figure 3.12 Photograph of a) abraded *Favites neglecta* and well preserved and b) less abraded *Heliastrea oligophylla* (Chevallier, 1961)

replaced by large, equant crystals of neomorphic spar. Smaller stubby, prismatic crystals of sparry calcite coat the micritic envelopes, but the bulk of both matrix and cement is micrite. The matrix at Dumanli is uniformly fine-grained and argillaceous and has yielded a Serravallian age from nannoplankton analysis (C. Müller pers. com., 1994.)

At Karapinar by contrast, the matrix of the floatstones varies from coarse-grained sandstone to argillaceous marls and corals. Gastropods and brachiopods are also found within the floatstones, but are a subsidiary component. Planktic foraminifera are extremely rare. Wood and plant fragments in various states of preservation are found abundantly in some of the floatstone horizons. Thin sections cut perpendicular and parallel to growth direction reveal that the pore spaces in the coral have been variously filled with micrite and drusy sparite, with opaques concentrated round the edges of the spar grains.

Karapinar corals showing sharply defined calice and septal structure including sample 26J.217.4a, are almost entirely found within a silt to mud grade matrix. These horizons are argillaceous, but the grains identified at the size range 63-200 μ are almost entirely carbonate, (see Appendix 4.)

Interpretation

Two possible depositional processes may have been active in forming the coral floatstones found in the study area.

- 1) Mechanical abrasion of a raised reef structure leading to periodic shedding of coral debris down slope into a quieter water area accumulating finer grained sediment. This may have occurred at Dumanli, where the correlative reef is still preserved up slope.
- 2) Redeposition of fragmented coral by debris flows generated by storms or faulting events. This seems particularly likely when shallow-water material is found interbedded with deeper-water components which appear to have been deposited by turbiditic currents (e.g. chapter 4). At Altinkaya and Karapinar, no *in situ* reef structure now remains and although this does not preclude the possibility of deposition having occurred as described above, debris flow processes may also have been active.

There is an apparent relationship between the grain size of the matrix and the preservation of primary structure and chemistry in coral. All the coral samples which have retained primary aragonite were sampled from fine-grained clay-rich rocks and it seems likely that the argillaceous nature of the matrix restricted diagenetic fluid flux. Matrix with coarser grain sizes, have a higher quantity of chert and quartz and are likely not only to have a smaller quantity of clay minerals due to the higher energy of deposition required, but also a greater volume of pore network allowing post-depositional flux of fluids and aiding diagenetic transformation. Coarser grain sizes also may account for the increased abrasion on coral samples found associated with them.

On a larger scale, Scoffin (1987) indicates that rock composition may be a function of whether shallow marine limestones undergo burial after a regression or transgression. Exposure caused by a regression leads to diagenetic change in an open system resulting in flushing out of Sr^{2+} and Mg^{2+} ions. Burial caused by a transgression is more likely to result in a closed system i.e. shallow water carbonates become covered in argillaceous marls and clays which prevent high fluid flux. In this case the isotopic concentrations of the constituents are more likely to be preserved.

3.6.2.2 Rhodolithic calcarenites

Dimensions

Rhodolithic calcarenites are the most abundant shallow water carbonate facies found in the study area making up approximately 60% of all shallow water carbonate exposure. Technically, the majority of the rocks classified are having a dominant grain size $>2\text{mm}$, but there is an infinite range from micro-conglomeratic calcirudites with clasts of rhodolithic algae, coral and shells, to calcilutites with a dominant grain size $<63\mu$. Sorting and maturity of the carbonate grains are also infinitely varied. The calcarenites are often well bedded on a scale of 0.5-2m (Fig. 3.14) and occasionally show cross bedding.



Figure 3.14 Bedded calcarenites banking up against Alanya Massif basement with marked palaeotopography, Ahmetler section, Manavgat basin.



Figure 3.15 Rhodolitic algae forming round a flat *Porites* nucleus, Ahmetler section Manavgat, basin.

Composition and diagenesis

Calcarenite composition varies from bioclastic sandstones to calcarenites with a negligible terrigenous component. There is apparently no systematic variation of terrigenous input, (individual sections contain a range of terrigenous percentages) except in the north of the Manavgat basin. Here, calcarenites found on top of the Alanya Massif contain some Alanya Massif limestone and schist fragments, but no other detrital clasts.

Coralline red algae of the *Amphiroa* and *Lithothamnium* types, is almost always present in large quantities making up 10-70% of calcarenites point counted. Occasionally whole rhodoliths are preserved as at Ahmetler. Here, fragmented strands of algae are found with rhodoliths several centimetres in diameter which have generally nucleated on fragments of Poritid coral (Fig. 3.15). Whole rhodoliths are rare in calcarenite facies (see echinoid-scapopod facies, 3.6.3.1 below). The vast bulk of algal material appears as variously micritized fragments. At Halitigalar algal fragments show a complete gradation between fragments with well preserved structure to structureless peloids. Where well preserved, the cells within the algal structure are filled, either with micrite or spar. Conceptacles are also generally spar filled.

Other fauna, including molluscs, coral, brachiopods, echinoids, and benthic foraminifera, found in horizons containing whole rhodoliths are almost always in a fragmentary state. Locally however, 4-8 entire individual echinoids (Clypeasterids) are found in close proximity to each other (e.g. Ahmetler; Ballibucak; Fig. 3.1). Calcarenites found interbedded with planktic foraminiferal marls also contain planktic foraminifera. These tend to be far less fragmented than the shallow water components.

Cements are generally dominated by micrite, but spar is common within the larger pore spaces and particularly in the upper chambers of benthic foraminifera and gastropods. Various developed micrite envelopes are common on all calcarenite clasts.

Interpretation

Algal rhodoliths in Bermuda form today at depths of 3-5m (Orzag-Sperber *et al.*, 1977). The environment in which they are found is one of high-

energy and with constantly agitated conditions. It is probable fauna other than these rhodoliths have been transported and this helps to explain the advanced state of abrasion and fragmentation that they have suffered.

Algal-rich calcarenites in which there are no whole rhodoliths are also interpreted as having occurred in high energy environments. The common association of coral, and the rich diversity of biota indicates that redeposited reef material is the probable source. The lack of any terrigenous component other than Alanya Massif material in the Ahmetler and Akseki road sections is indicative of the localised source area in this region. The implications of this are discussed in section 5.7. The sorting and maturity of grains is probably a function of the energy of the environments and the length of time the sediment is exposed.

3.6.2.3 Reef talus

The most widespread and prominent reef talus horizon occurs at the boundary between shallow water carbonates (Oymapinar Limestone) and shelf carbonate facies (Geceleme Formation). Good examples of these are found in the Akseki road section, Oymapinar and at Deniztepesi (Fig. 3.1). In these localities talus horizons between 2 and 6m thick overlie *in situ* reef framestones and wedge out over 500m to a kilometre. The talus is always overlain by planktic foraminiferal marls, (Geceleme Formation) or turbidites (Karpuzçay Formation). At Deniztepesi, where the talus forms a prominent cliff, these marls overlie it with an angular discordance. The Oymapinar section (Fig. 3.16) contains three separate talus horizons interbedded with *in situ* reef framestones, calcarenites and bioclastic sandstones. The upper most of these is also overlain by deeper water marls with an angular disconformity.

Composition

The Akseki road section is perhaps the most spectacular of the talus outcrops as it contains huge blocks of domal coral framestone up to 3.5m in diameter. The poorly sorted nature of the clasts means that many of the larger ones protrude from the bed and stick up into overlying marls which have passively filled around them. This section is associated with abundant normal faulting which is discussed in section 7.5.1.2. The

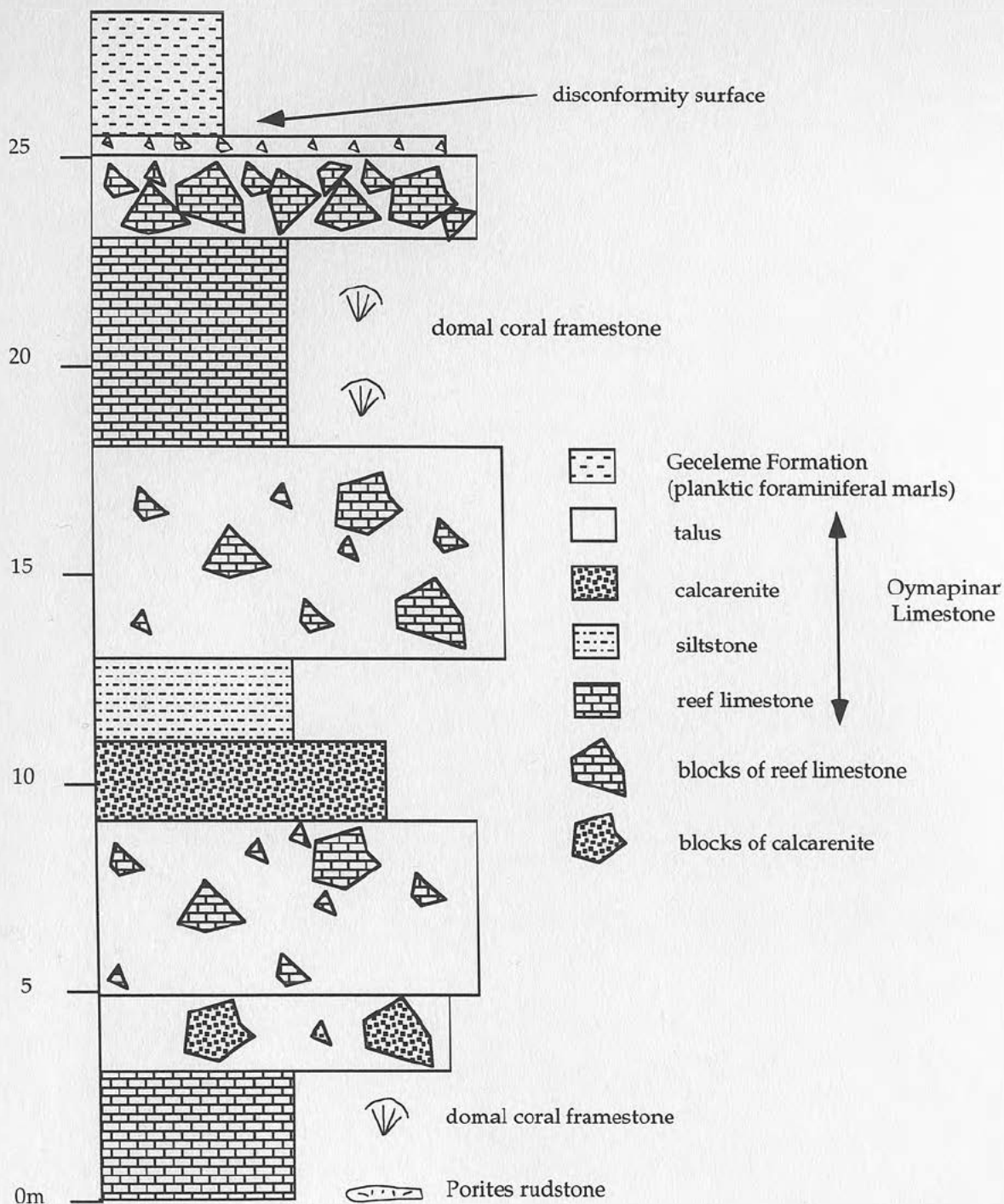


Figure 3.16 Log of the type section locality of the Oymapinar Limestone at Oymapinar, northern margin of the Manavgat basin. The dominant in situ facies is domal coral framestone, but the section also contains multiple talus horizons often comprising disorientated blocks of coral-rich reef limestone. At the top of the section a talus horizon is overlain by the planktic foraminiferal marls of the Geceleme Formation with a clear disconformity.

Oymapinar talus horizons as well as containing disorientated blocks of domal coral framestone also contain abundant oysters and gastropods. Deniztepesi by contrast is a talus composed of coral-poor limestone, dominated by algae.

Matrix and diagenesis

The Akseki road talus is well exposed in a stream bed and has a carbonate cemented top up to half a metre thick (Fig. 3.17). Beneath this the talus is a loose rubble, except where faults dissect it. In contrast to this the lower talus horizons at Oymapinar have abundant white silt micritic matrix. The uppermost talus at Oymapinar resembles that at the Akseki road section.

Interpretation

The process of deposition in the lower talus horizons at Oymapinar may be similar to those of the coral floatstones i.e. mechanical and bio-erosion of reef framework depositing into a deeper, quieter water silt dominated environment. It is possible that the talus horizons which occur at the interface between shallow carbonate deposition and the planktic foraminiferal marls were fault generated. The following evidence supports this interpretation:

- ◆ The presence of an angular unconformity marking the transition from shallow to deeper water;
- ◆ The absence of matrix;
- ◆ The very angular nature of the blocks;
- ◆ The spatial correlation of talus and Çakallar Formation with areas containing numerous faults (section 7.5.1.2);
- ◆ Thickness variations across the Manavgat basin (section 7.5.1.2).

Note however that much talus can be generated by the fast growth of coral due to rapid relative sea level rise. As rapid relative sea level rise would be predicted in association with extension generated faulting, the talus described here may have been formed by both processes and it would be difficult to distinguish between them.



Figure 3.17 Photograph of the cemented top of the Akseki road talus horizon and the loose rubble beneath, Manavgat basin.



Figure 3.18 Echinoid-Scaphopod facies with algal rhodolith encrusting Mesozoic limestone pebble, Aspandos section, west Köprü basin.

Table 3.8 Summary of information and interpretation of off-reef sub-facies.

Sub-facies	Components	Matrix	Cement	Preservation	Water depth	Mode of deposition
Coral floatstone	Various corals	clay	poorly lithified	Primary aragonite preserved in corals	?	Rock fall (and/or debris flow)
	Coral and other shallow water components	sandstone	Poorly lithified	Corals replaced with secondary Low-Mg calcite	?	Debris flow
Rhodolithic calcarenite	Biogenic reef components Generally little terrigenous material	micrite	Micrite and spar	Secondary replacement	Shallow water, shelf environment	Current reworking
Reef talus	Reef framestone blocks Local basement in north of Manavgat basin	none	surficial carbonate cement	Coral aragonite replaced by secondary calcite	?	Rock fall/fault generated talus

3.6.2.4 Summary of off-reef sub-facies

A summary table of the information discussed and interpreted above is given in table 3.8.

3.6.3 Reef-associated facies in coarse clastic environments.

Table 3.9 Table of reef-associated sub-facies, listing their characteristic fauna and the localities at which they can be found (Fig. 3.1).

Sub-facies	Characteristic fauna	Localities
Echinoid-scapopod grainstone	Echinoids scaphopods algal rhodoliths <i>Operculina</i>	Aspendos South Yesilbag
Oyster packstone	Oysters	Kesme North Yesilbag
Gastropod wackestone	Gastropods	North Yesilbag Bozburun Dag
Oyster bafflestone	Oysters	Kargi Baraj

3.6.3.1 Echinoid-scapopod grainstone

Dimensions and localities

The largest outcrop of this sub-facies occurs to the north of the ruins of Aspendos (Fig. 3.1). Here an 11m interval of echinoid-scapopod grainstone persist for several hundred metres, passing up into algal limestone (Fig. 5.6). The exposure south of Yesilbag is associated with the channel structure sketched in figure 3.3 and is limited laterally by it. The thickness of the horizon here is only 2m and it passes up in to domal coral framestone.

Fauna and flora

This very distinctive facies consists of a coarse micro-conglomerate with abundant whole and fragmented scaphopods, echinoids, large benthic foraminifera including *Operculina* and, more rarely, algal rhodoliths up to 5cm in diameter.

These rhodoliths encrust rounded pebbles most commonly veined grey Mesozoic limestone (Fig. 3.18). Individual layers of algae can be clearly seen encrusting first the clast and then other algal layers and included matrix. They are irregular in shape and individual layers do not encircle the clast, but can be traced out to their terminations, which are often abrupt and ragged. Although algal encrustation is visible on many of the micro-conglomerate clasts, the biggest rhodoliths are developed on clasts significantly larger than average.

The orientations of scaphopods and echinoids are for the most part, random. In just a few places however, millimetre scale, graded laminations can be seen and scaphopods have been deposited parallel to these, (Fig. 3.19) The scaphopod most commonly found here is *Dentalium* (Upper Cretaceous-Recent) with its prominent longitudinal ribs. When entire, specimens can reach over 10cm in length. The majority of the scaphopods occur here as large fragments. Entire clypeastrids (minus their spines) are fairly common. Their distribution tends to be rather clustered. These are infaunal or semi-infaunal detritus feeders.

Terrigenous components

The proportions of detrital components of the echinoid-scaphopod facies varies from place to place, but the components themselves remain fairly constant. In order of volumetric importance they include grey and fawn crystalline limestone sometimes veined, red and green chert, grey sandstone and yellow silt. The chert is generally subangular to angular, whilst the other grains are rounded to well rounded.

Interpretation

No columnar rhodoliths are found here, just laminar ones which form in Bermuda today by overturning on a sandy substrate (Orzag-Sperber *et al.* 1977). The preservation of these large and delicate structures in such a coarse clastic environment shows that they have not been transported. Rhodoliths of a comparable size and structure have been documented from the Miocene of the Meso-Hellenic Trough in northern Greece (Wilson, 1993). The large number of entire echinoid and scaphopod fossils found in this facies indicates that these creatures also inhabited



Figure 3.19 Scaphopods parallel to grit-silt laminations. Randomly orientated scaphopods can be seen in the overlying sediment, Aspendos section, south-west Köprü basin.

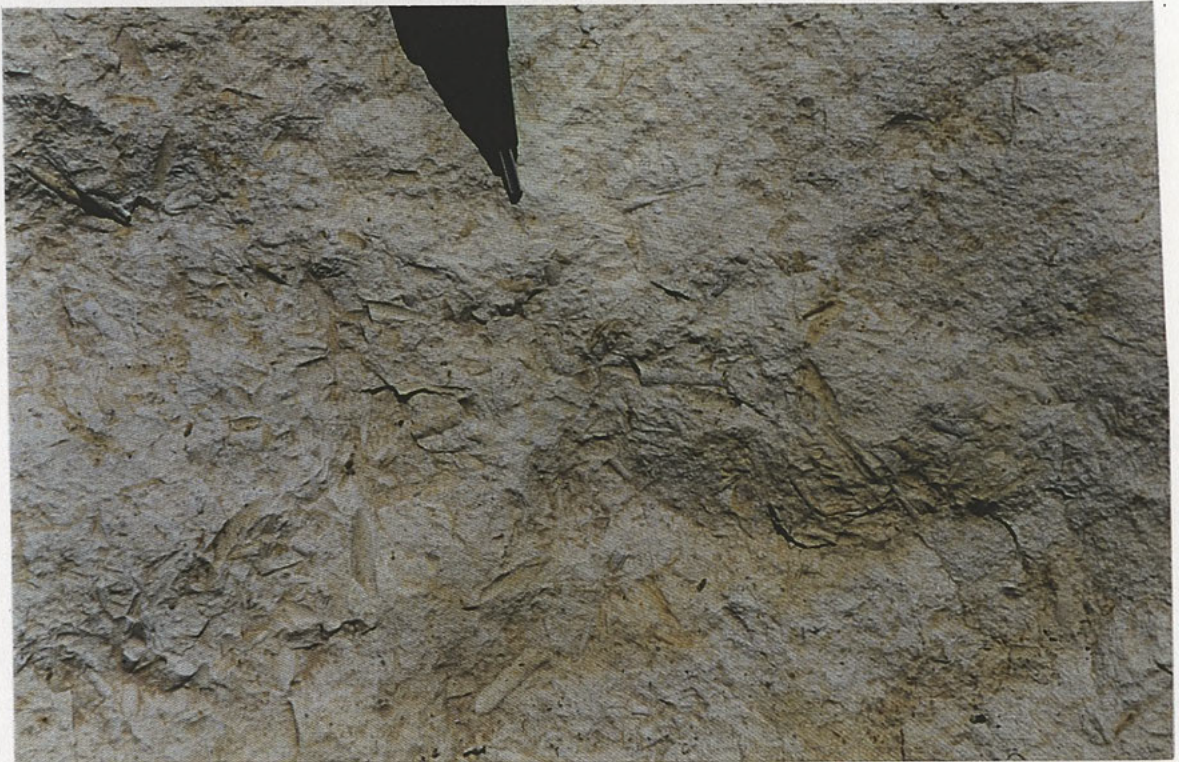


Figure 3.20 Pteropod moulds in planktic foraminiferal marls, Akseki road section, Manavgat basin.

this coarse grained environment. Scaphopods are deposit feeders which live with the wider end of the shell embedded in the sediment. Their presence is in accordance with the interpretation of a shallow marine environment subject to periodic sweeping by currents.

3.6.3.2 Oyster packstone

Dimensions

This sub-facies was first described by Dumont (1974). He noted that although individual horizons are of limited lateral extent, several similar beds occur at different localities at about the same stratigraphic level in the Kesme area (Fig. 3.1). The morphology of the beds is often channelised and interbedded with fossil poor sandstones, siltstones and rare conglomerates. Beds generally are less than a metre thick and consist of silts to medium grained sandstone with abundant, large oysters.

Fauna and flora

The two valves of the oysters are generally separated although little abrasion of the shell is visible. The abundance of oysters varies dramatically from being so concentrated that they constitute over 50% of the rock and are in contact with each other, as can be seen along the Kesme-Yesilbag road, to being more sparsely distributed so that the clasts are matrix supported as can be seen between Kasimlar Kesme. In this latter case other fauna particularly gastropods and burrowing bivalves are common. Wood is also associated and on the Kasimlar-Kesme road and some of these fragments reach 20cm in length. The oysters show good alignment sub-parallel to bedding irrespective of whether they are in contact with each other. Some of the gastropods show a similar alignment, but the burrowing bivalves cut across this trend and appear to be *in situ*.

Matrix

The matrix to this sub-facies is yellow and is dominated by angular chert and limestone fragments. It is generally poorly lithified and argillaceous.

Interpretation

The dislocation and alignment of the oyster valves indicates that they have been reworked. The concentration of redeposited fauna presumably reflects the concentration in the source area and the volume of sediment and post-depositional current winnowing. This source area is likely to have been a marginal, shallow-marine setting, allowing the inclusion of fairly large fragments of wood. The channelised nature of these bodies and the size of some of the larger oysters which were transported as clasts, indicates that the current was probably a high energy one. Subsequent burrowing may have occurred in periods of quiescence.

3.6.3.3 Gastropod grainstone/wackestone

Dimensions and age

This sub-facies resembles the oyster packstone in terms of its matrix composition, bed morphology and texture. It is best exposed along the Kesme-Yesilbag road, but it is also found a few metres above a coal horizon to the north of the Bozburun Dag col, near Pinargözü (Fig. 5.10). At Kesme, gastropod wackestones are interbedded with sandy marls the nannoplankton which have yielded an Upper Miocene age (C. Müller, pers. com., 1994). This confirms the Tortonian age proposed by Dumont (1974) from the planktic foraminifera from interbedded horizons.

Fauna

The dominant fauna are gastropods identified by Dumont (1974) as *Cerithidae* sp. Other fauna found within these fossil rich beds include bivalves, rare oysters and brachiopods and the benthic foraminifera *Alveolina*.

Matrix

At Kesme cross-laminated micro-conglomeratic sandstones and laminated silts showing water escape structures are also associated with gastropod wackestones. The gastropods here occur either in winnowed horizons with a fine sand matrix or in argillaceous marls where they show no preferred orientation and are well spaced. At Bozburun Dag however, the matrix is siltstone-micro-conglomerate.

Interpretation

The interpretation of this sub-facies is similar to that for the oyster packstone facies. Deposition by high-energy currents and subsequent winnowing of finer sediments is likely to have caused the grainstones, whilst debris flow processes may have deposited the wackestones.

3.6.3.4 Oyster bafflestone

Dimensions

This sub-facies has only been identified in one locality. A hundred metres north of the Kargi baraj, oyster-rich limestones are exposed overlying Jurassic limestones with a marked palaeotopography. The sequence has a very limited lateral extent. 50m along strike to the south a debris flow with clasts up to a metre in diameter is exposed banked up against the basement. Half a kilometre to the north a small coral patch reef is exposed at the same horizon.

Fauna

The basement limestone is heavily bored, by small, *Lithophaga*-like borings. Planar-bedded, bored limestones, variably rich in oysters onlap on to the basement. Half a metre above the base of the section and rooting partly on the underlying oyster-rich limestones and partly on the basement, an oyster dome, 50cm in height and 20cm in diameter is located. The oysters are rigidly cemented on to each other producing a framework in which interstitial sediment is trapped. Laterally, the dome passes abruptly into fossiliferous limestone with abundant tubular structures. The sequence is overlain by interbedded marls and sandstones.

Interpretation

This unusual facies has been interpreted as having grown *in situ*. The bored nature of both the basement and underlying oyster-rich limestones indicates exposure and rapid lithification. The small quantity of terrigenous material found in the oyster-rich limestones suggests efficient channelling was active in the area, leading to rapid lateral changes in facies visible at this locality.

Table 3.10 Summary of information and interpretation of reef-associated sub-facies.

Sub-facies	Components	Matrix	Cement	Preservation	Water depth	Mode of deposition
Echinoid-scapopod grainstone	Echinoids, scapopods algal rhodoliths benthic foraminifera angular chert and rounded limestone	Micrite	Micrite and rare spar in algal conceptules	Micrite envelopes developed	Shallow, probably within wave base	Periodic influx of sediment reworked by currents (?waves?)
Oyster packstone	Oysters Gastropods Wood Chert and limestone	Clay-rich	Poorly lithified Micrite	Altered oyster chemistry (see chapter 6)	Relatively shallow and near shore	Debris flow? subsequently winnowed
Gastropod grainstone/wackestone	Gastropods Benthic foraminifera bivalves Oysters terrigenous carbonate	micro-conglomerate to clay	Micrite and spar	Micrite envelopes developed	relatively shallow	Winnowing by currents Some current deposition
Oyster bafflestone	Oysters Shallow-water debris Lithophaga-like borings	micrite	spar	Bored Altered oyster chemistry (see chapter 6)	Shallow	Cementation

3.6.3.5 Summary of reef-associated sub-facies

A summary table of the information discussed and interpreted above is given in table 3.10.

3.6.4 Carbonate shelf facies

Table 3.11 Table of shelf sub-facies, listing their characteristic fauna and the localities at which they can be found (Fig. 3.1).

Sub-facies	Characteristic fauna	Localities
Planktic foraminiferal marl	Planktic foraminifera pteropods rare benthic foraminifera and rare echinoid spines	Alarahan Ahmetler Saburlar Akseki Road
Operculina packstone/grainstone	<i>Operculina</i> echinoids	Halitigalar Alarahan
Calcirudites	Algae foraminifera echinoid spines	Akseki Road Alarahan Ahmetler

3.6.4.1 Planktic foraminiferal marl

Dimensions

A thick succession (>330m) of this facies occurs throughout the Manavgat basin. Although the majority of the marls appear to be laterally extensive, rare, better lithified horizons show a wedge-shaped geometry. The Ahmetler succession (Fig. 3.1) is interspersed with rare calcarenite and calcirudite horizons some of which contain large (several metres in diameter) detached blocks of Alanya Massif limestone.

Fauna

The facies consists of a fine grained carbonate-rich marl with an abundance of planktic foraminifera and more sparse benthic foraminifera. Occasionally horizons contain abundant pteropod moulds (Fig. 3.20) e.g. in the Ahmetler section and just above the talus at Akseki road. The abundance of the planktic foraminifera in these marls ranges from less than 1% to over 20% as calculated by point counting of washed,

disaggregated samples. (These figures do not include the clay mineral content; see Appendix 4). Where the foraminifera are most abundant i.e. along the Alarahan-Çakallar road and at the junction of the Ahmetler road with the road to Akseki, the dominant species is *Orbulina sp* and this can constitute over 60% of the planktic foraminifera. Other planktic foraminifera commonly found include *Globorotalia* and *Globigerinoides*. Monod (1977) reports the following species:

Globigerinoides bisphericus
Globigerinoides subquadratus
Globigerinoides trilobus
Globoquadrina altisoira
Globoquadrina dehiscens
Globoquadrina langhiana
Globorotalia obesa
Globorotalia scitula praescitula
Praeorbulina glomerosa glomerosa
Praeorbulina transitoria
Praeorbulina glomerosa curva

Table 3.12 below lists the benthic foraminifera found in these horizons and the water depths at which they are commonly found. The preservational detail of many of these foraminifera, both benthic and planktic, is good (W. Austin pers. com. 1994). Some benthic foraminifera however appear to have suffered abrasion and part of the test ornamentation may be obscured making identification difficult. Where large quantities of benthic foraminifera occur this is most likely to be the case. Shallow water debris, such as echinoid spines and gastropods are also often found in greater concentrations in these horizons which also tend to be those displaying better lithification and wedge-shaped geometries.

Detrital components

The terrigenous components in these marls are overwhelmingly dominated by carbonate grains and clay minerals. The carbonate can constitute 100% of grains point counted after washing, although rare quartz and other lithic fragments are more common. In the Ahmetler

section, the lower part of the marl sequence contains virtually no terrigenous material other than carbonate and clay minerals.

Table 3.12 Table of depth diagnostic benthic foraminifera found in the planktic foraminiferal marls. Depths derived from living foraminifera according to Murray (1973); Boltorskoy and Wright (1976); Murray (1991).

Name	Water depth in meters
<i>Ammonia</i>	0-50
<i>Amphistegina</i>	5-20
<i>Bolivina</i>	0-3000
<i>Bulimina</i>	0-3000
<i>Cancris</i>	50-150
<i>Elphidium</i>	0-50
<i>Melonis</i>	3-1000
<i>Nonion</i>	0-180
<i>Operculina</i>	0-70
<i>Planorbulina</i>	0-50
<i>Rosalina</i>	0-100
<i>Ulvigerina</i>	100->4500

Interpretation

The abundance of planktic foraminifera and relative scarcity of benthic foraminifera and shallow-water dwellers indicates that the environment of deposition was deeper water relative to the reef, off-reef and reef-associated facies described above. The fine-grained sediment and planktic fauna may well have collected out of suspension in the water column. The benthic foraminifera listed in table 3.12 which are thought to be indicative of water depth suggest that the environment of deposition was still not particularly deep, corresponding to inner shelf (0-70m; e.g. Murray, 1993). Most of the benthic foraminifera listed however occur in horizons which also contain shallow-water debris (e.g. echinoid spines, algae). It is suggested that these horizons represent redeposition of shallow-water material (probably by low-density turbidity currents, see chapter 4) and the benthic foraminifera within them can therefore only

act as a minimum water depth indicator. The difference in lithification of these horizons may also be related to the different mode of deposition i.e. by a current rather than from suspension.

3.6.4.2 Operculina packstones/grainstones

Dimensions

Horizons of operculina packstone are up to 2m thick and laterally inextensive. They are well exposed at the base of the calcarenites in the Alarahan section and at Halitigalar.

Fauna

The large benthic foraminifera *Operculina* sp. can constitute from 10-70% of the rock. Its large flattened disc-shaped tests which are in contact with each other often show a parallel to sub-parallel alignment. Horizons are often algal-rich and contain whole, well preserved echinoids, as well as other benthic foraminifera with agglutinated tests.

Matrix and diagenesis

The matrix to these packstones is always a fine grained micrite, its percentage being dependent on the quantity of *Operculina* present. Micrite envelopes are visible on foraminifera tests and most of the cement appears to be micritic. Rarely however, syntaxial overgrowths on echinoid spines are visible.

Interpretation

These *Operculina* packstones have been interpreted as foraminiferal shoals similar to those identified by Samuel (1994) in Indonesia. They form in shallow marine conditions where currents winnow and sort material leading to the packstone or grainstone texture. Micritic envelopes on the foraminifera indicate that they were at the sediment-water interface long enough for boring to occur. Similar foraminiferal shoals have been recognised from the Miocene of Cyprus (Eaton, 1987).

3.6.4.3 Calcirudites

Dimensions

These calcirudites occur within the planktic marl successions as spaced, wedge-shaped horizons, laterally discontinuous on a scale of several kilometres. They vary in thickness between 50cm and up to 5 m although some of the detached blocks within them may be considerably larger than the thickness of the horizon in which it sits.

Components

The calcirudites are dominated by shallow water debris including coral, coralline limestone, algal-rich calcarenite, echinoid spines and benthic foraminifera. Intraformational marl is also a common constituent. Terrigenous components in the lower part of the Ahmetler sequence are restricted to Alanya Massif limestone and schist. These form the large detached blocks which are entrained within some of the calcirudite horizons. Much of the debris within these horizons is angular.

Matrix

The matrix is very similar to the planktic foraminiferal marls in which these calcirudites are interbedded. It constitutes micrite with abundant planktic foraminifera. The percentage of matrix varies, but it can make up to 40%.

Interpretation

The marked textural immaturity of these calcirudites, their poor sorting and abundant matrix of a different composition suggests that they were deposited either by rock-fall or debris flow processes. The presence of huge detached blocks of Alanya Massif basement several kilometres from the present day outcrop suggests that deposition by debris flow processes is more likely. The nature of the Miocene carbonate material within them indicates that the source area was an area of shallow-water carbonate production.

3.6.4.4 Summary of shelf sub-facies

A summary table of the information discussed and interpreted above is

Table 3.13 Summary of information and interpretation of shelf sub-facies.

Sub-facies	Components	Matrix	Cement	Preservation	Water depth	Mode of deposition
Planktic foraminiferal marls	Foraminifera pteropods shallow-water debris terrigenous carbonate	micrite and clay	Poorly lithified	Some diagenetic alteration of foraminifera (see chapter 6)	Minimum = inner shelf (0-70m), probably more than this	Partly out of suspension, partly by turbiditic redeposition
Operculina packstone/wackestone	Operculina echinoids terrigenous carbonate grains	micrite	Poorly lithified Micrite and some spar	Micrite envelopes on foraminifera	Shallow, forming foraminiferal shoals	Current sweeping and winnowing
Calcirudites	Shallow-water components Large blocks of locally derived basement	clay-rich marl with planktic forams	Micrite and spar	Micrite envelopes developed	Minimum = inner shelf (0-70m), probably deeper	Deposition by debris flow processes

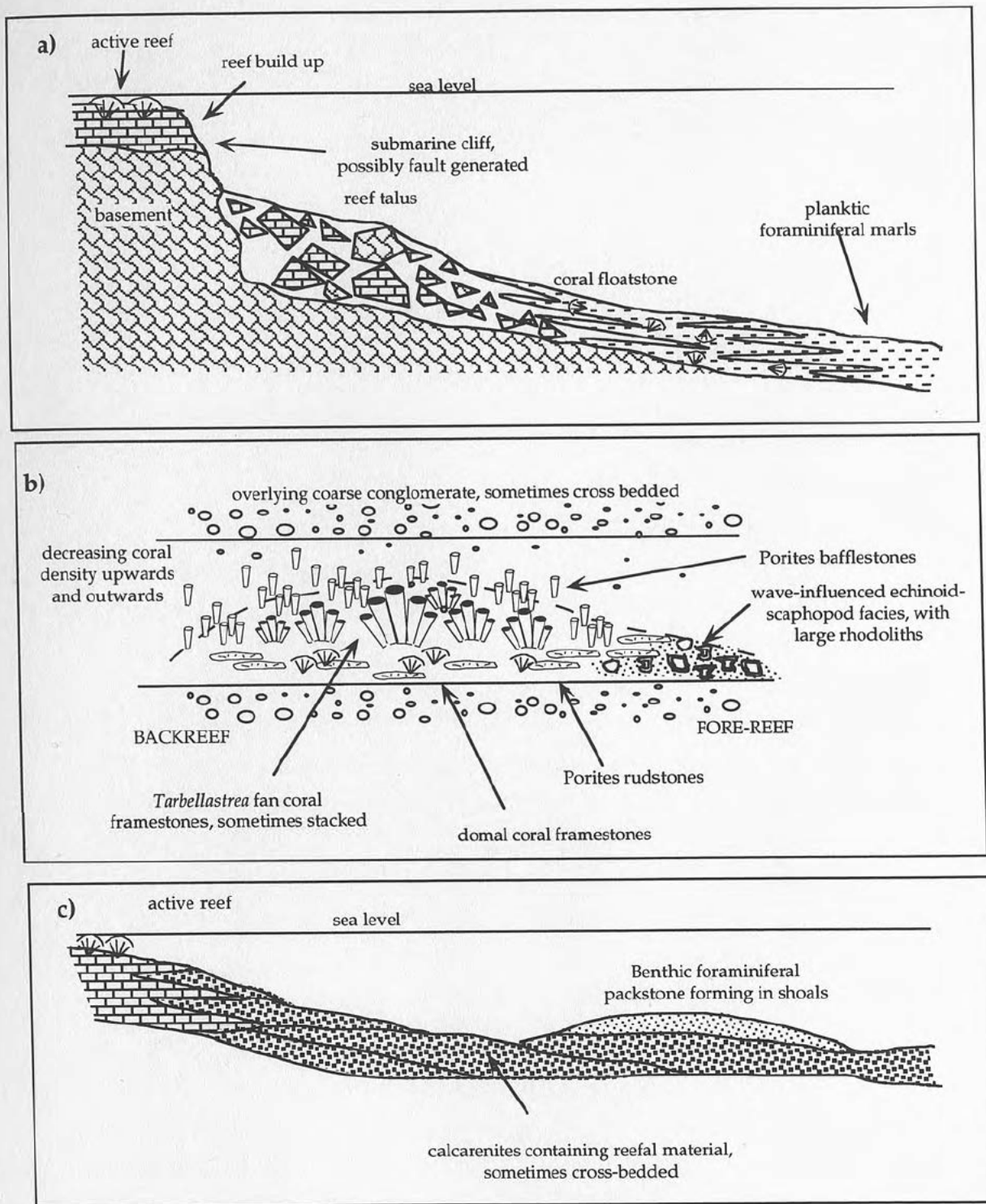


Figure 3.21 Depositional models for the deposition of the various biogenic carbonates discussed in the text.

given in table 3.13.

3.7 Model of sub-facies location.

Figure 3.21 is a model indicating the likely locations of the formations of the sub-facies discussed above.

3.8 Discussion

3.8.1 *The Mid-Miocene hiatus in shallow-water carbonate production*

The shallow-water carbonates in the study area are restricted to two distinct periods of time: the Early Miocene (Burdigalian-Langhian) and the Late Miocene (Tortonian). There is no evidence of shallow-water carbonate build-ups in the intervening period. This hiatus poses two questions. First, what caused the termination of the Lower Miocene shallow-water carbonates? And second, what allowed shallow-water carbonate production to start again in the Tortonian?

In Cyprus the Miocene reefs have a similar chrono-stratigraphic relationship (Follows 1990) to those in the study area and it was tentatively suggested that the Mid-Miocene hiatus in reef growth (Chevalier 1961) was a result of eustatic sea level rise (Follows 1990).

In the Antalya region however, it is difficult to assess the role of eustasy as no section contains both Lower and Upper Miocene reefs with a complete succession between. The Manavgat basin for instance, does comprise a complete succession from Upper Burdigalian to Messinian age, but it does not contain any Tortonian shallow-water carbonates. At first glance however, a eustatic sea level rise might appear to account for the termination of the Lower Miocene shallow-water carbonates. According to the sea level curve in Haq *et al.* (1988) the most rapid sea level rise occurring during the Langhian is approximately 75m over about 0.5 million years (Fig. 4.25). This of course represents average, not instantaneous sea level rise. If eustasy did drown the reefs then according to Geister (1983) and Johnson *et al.* (1986) instantaneous sea level rise must have been >7-8m/1000 yrs. The resolution of the eustatic curve (Haq *et al.*, 1988) is not sufficient to conclusively decide whether or not

this is likely.

Post-hiatus colonisation in the Tortonian is also problematic. Tortonian reefs are concentrated in the north of the study area. Particularly in the far north they overlie thin sequences of continental conglomerates covering the basement. The shallow-water carbonates here, such as those seen at North Yesilbag and Kesme, can be clearly interpreted as a result of relative sea level rise. To the south however, the continuous sequence exposed in the Manavgat basin is entirely marine from the Langhian onwards. The benthic/planktic foraminiferal ratios here (Fig. 4.21) indicate overall shallowing water depths from Early Langhian times. Thus, any concrete evidence of a relative rise in sea level is localised even within the study area. The structural implications of this intra-basinal difference are discussed more fully in chapter 8.

If not eustatic sea level change, then what? Control over modern reef location is now thought to be shared amongst many factors most which are not preserved in the fossil record e.g. salinity, temperature, nutrient supply, light, turbulence, substrate type and sediment flux. A combination of these factors is likely to have controlled the Mid-Miocene shallow-water carbonate hiatus. However, *relative* sea level change has not been ruled out as a possible controlling factor. A rapid tectonic subsidence might result in sufficient relative sea level rise to drown shallow-water carbonate production and this possibility is discussed further in section 7.5.2.1. What can to a certain extent be discounted is the control substrate and sediment flux have over the location of shallow-water carbonate deposition. For instance, it is difficult to argue that the high rate of muddy sedimentation in the Manavgat basin in the Tortonian precluded coral colonisation when areas such as South Yesilbag indicate that *Porites* colonisation was possible at the same time in apparently far more adverse conditions i.e. within a mud dominated channel.

3.8.2 *Coral zonation*

The general paucity of coral species in the Mediterranean during the entire Miocene, but particularly in the Late Miocene was first discussed by

Chevalier (1961). Lydendyk *et al.* (1972) proposed that tectonic movement in the Far East blocked the eastward flowing current from the Indo-Pacific to the Mediterranean at the end of the Oligocene. This resulted in gradual cooling of the Mediterranean and caused selective coral extinctions. As a result the Eastern Mediterranean corals lack the diversity of the Indo-Pacific province (Chevalier 1977).

The dominant coral in the study area is *Porites*. Previous authors working on Miocene Mediterranean corals have also observed a *Porites* domination (e.g. Follows 1990). Frost (1981) indicates that the reason for *Porites* being the dominant "pioneer" coral in the Miocene of the Mediterranean is due to the ability of its planula larvae to settle on mobile wave swept sandy substrates and the ability of the corallites to free themselves from the constant rain of sedimentary particles. In the South Kargi section, subordinate early colonisers of unstable substrates, such as *Acropora* and *Goniopora* (Frost 1981) are absent from the pioneering colonies. This may indicate that other environmental factors were adverse to coral colonisation as well as an unstable substrate. *Porites* has long been observed for being especially tolerant to adverse environmental conditions such as low salinity, low temperature, high terrigenous sedimentation and reduced water circulation (Marshall and Orr, 1931; Manton, 1935; Wells, 1954; Scoffin and Stoddart, 1978). In the South Kargi region, where the coral rudstones directly overlie coarse fluvial clastics and interbedded calcretes (see chapter 5) it seems likely that the fluvial influence was great and that therefore as well as being a high terrigenous sedimentation environment, the salinity was at least periodically lower than normal sea water.

However the South Kargi section is unusual in displaying vertical zonation in coral type. Most of the reefs studied had no systematic pioneering community that was significantly different from overlying framework horizons. A similar observation was made by Hayward (1982b) concerning Lower Miocene reefs of the Kas basin to the west of the study area. He suggested that the reason for this was due to the firm, though unlithified substrate of cobble and pebble gravel.

Hayward (1982a and b) did observe a vertical zonation in coral

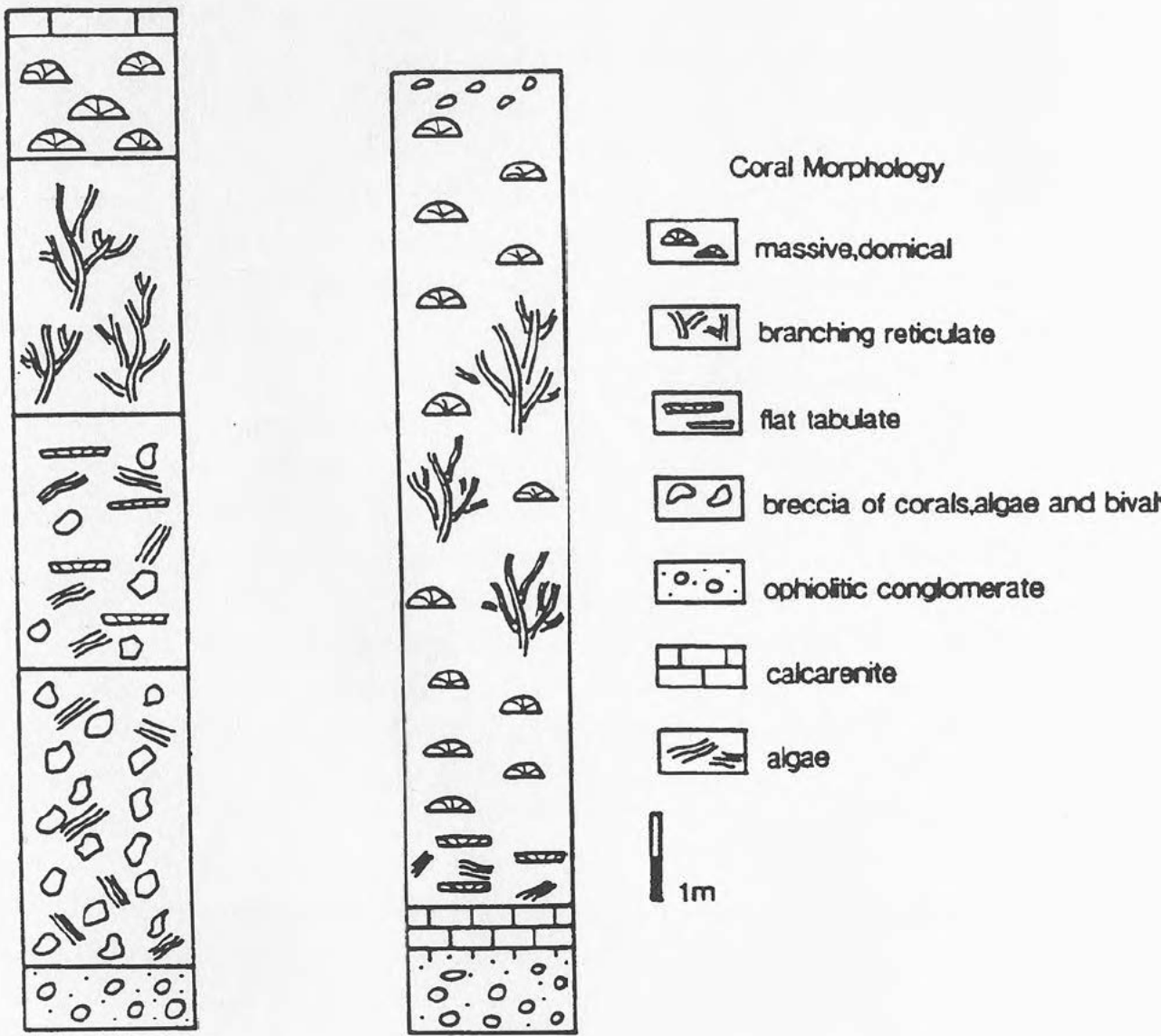


Figure 3.22 Progressive change in coral morphology upwards through central reef framework (Hayward, 1982a and b).

morphology from flat, tabulate-dish forms, through branching, reticulate structures, to massive-domal forms (Fig. 3.22). He interpreted this zonation as being consistent with an increase in hydrodynamic stress. In the Antalya region, no systematic morphological variation in coral structure has been observed and in no reef is the whole of Hayward's morphology zonation exposed. However all of his morphological zones can be identified. For instance, many of the lower coral horizons are rudstones with flat or tabulate forms. The other dominant morphology of basal coral horizons not documented by Hayward, is one of cone-shaped stick *Porites*, most commonly seen north of Yesilbag. A similar colonising *Porites* morphology is documented by Martin *et al.* (1989). The reticulate morphology documented by Hayward (1982a) is similar to the large *Tarbellastrea* fan framework seen at South Kargi, and the massive domal forms resemble those *Montastrea* frameworks exposed at Kesme. The tectonic setting of the Kas basins is that of a flexural foredeep with continual subsidence throughout the period of reef deposition (Hayward 1982a). Hayward (1982a and b) showed that reefs developed the complete morphology in areas of locally low clastic input. The possible reasons for the incomplete development of a similar coral zonation in the Antalya area are:

- ◆ Different tectonic setting, e.g. not such continual subsidence in the Antalya area;
- ◆ Higher clastic input in the Antalya area;
- ◆ Preservational differences.

3.8.3 *Spatial morphology of reefs*

Shallow-water carbonates in the Aksu and Köprü basins are generally exposed for less than a kilometre. Even when linear bodies of Miocene carbonates crop out over several kilometres, such as those seen north of Deniztepesi, in detail these lineaments consist of lenses of shallow-water carbonates which are separated from each other. In almost all cases they are interbedded with coarse clastics, often dominated by conglomerate and are interpreted as patch-reefs. Classically, reef generated carbonates were not thought to be associated with areas of high terrigenous sedimentation. Studies of modern reefs in Jamaica (Wescott and Etheridge 1980) and the Red sea (Gwartzman and Buchbinder 1978,

Hayward 1982a and 1982b) however have shown that this is not necessarily the case.

Hayward (1982b) studied Miocene coral reefs in the Kas basin to the west of the study area using the Red Sea reefs as a modern analogue. He suggested that coarse gravel sediments of alluvial fans provided ideal substrates for coral planulae to settle. He noted that material finer than 60mm was not directly colonised by coral in the Red Sea, and that Miocene reefs were not found in association with well developed claystone suggesting that they were subject to a similar control. He identified periodic run-off as a critical factor in reef development, particularly stressing that the influence of the one or two flash-floods a year experienced in the Red Sea would be restricted to the active portion of the fan. He concluded that lateral confinement of the fluvial system precludes reef development within channels due to the high sedimentation rates. Although this can be generally applied to the Miocene reefs of the Antalya area, Yesilbag, with its *Porites* within a fine grained channel is a notable exception.

In contrast to those of the Aksu and Köprü basins, the shallow-water carbonates in the north of the Manavgat basin occur in a continuous NW-SE striking, linear outcrop (Fig. 3.23). They directly overlie Alanya Massif basement here and very little associated terrigenous material. Further south however, coarse conglomerates underlie and are interbedded with the shallow-water carbonates. Very little reef framework is preserved anywhere in the Manavgat basin, but it is particularly sparse along the northern margin. The evidence for it having existed along this margin is strong however. Displaced blocks in talus horizons such as those exposed at the Akseki road section bear witness to its framework structure, but equally convincing is the large quantities of reef-derived carbonate material, particularly calcarenite, that line the basin margin. The Alanya Massif has been uplifted since the Lower Miocene and the shallow-water carbonates now dip at about 50 degrees to the south. The absence of fluvial conglomerates on top of the Alanya Massif where it forms the northern margin to the Manavgat basin indicates that it was a palaeotopographic high during the Lower Miocene and this is borne out by palaeocurrent measurements from the

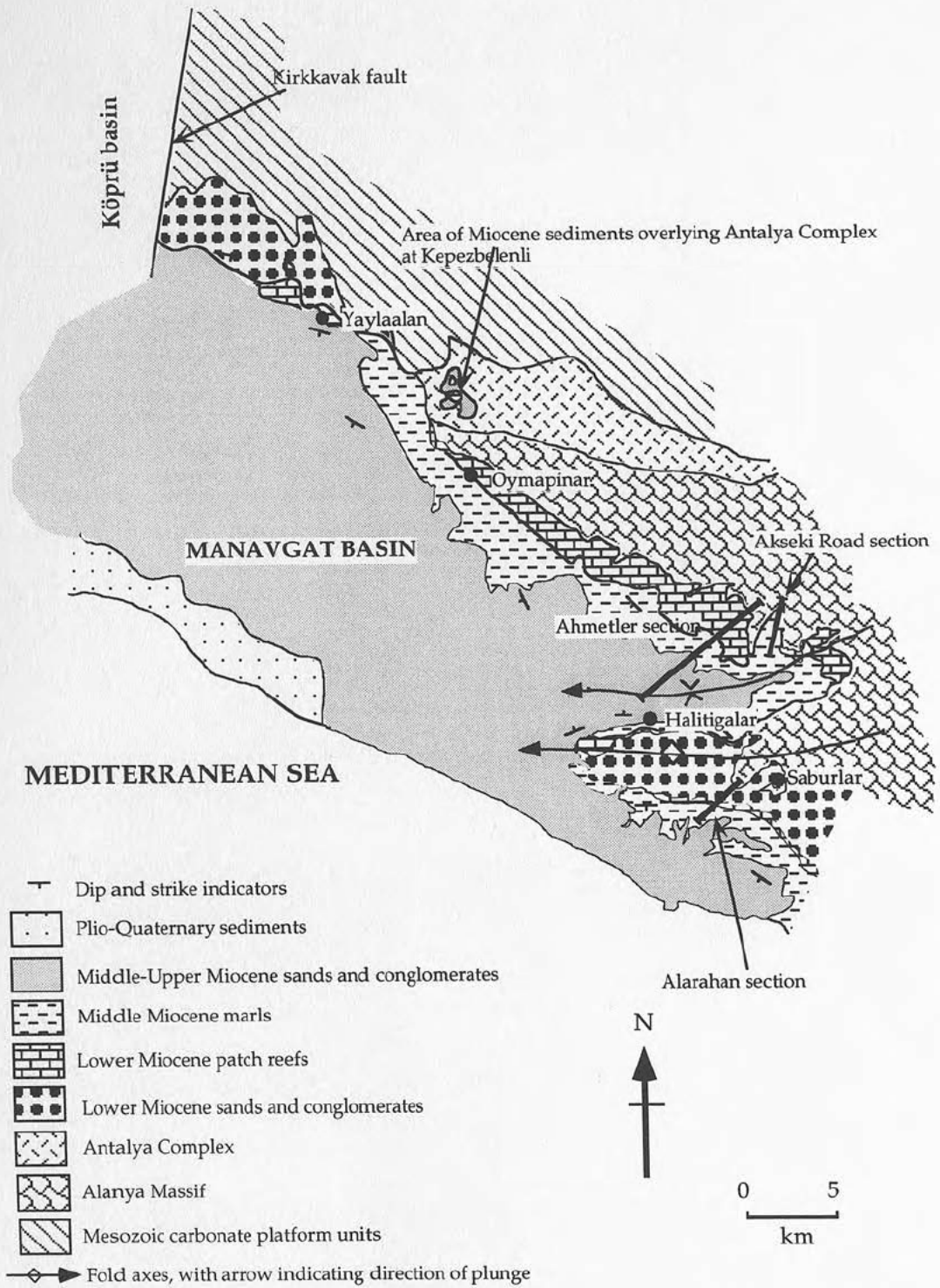


Figure 3.23. Simplified geological map of the Manavgat basin showing the open folding in the south-east of the basin and the location of the principal localities mentioned in the text.

lowermost conglomerates in the south, none of which indicate flow from the Massif to the south (Fig. 5.33). It seems possible therefore that the reefs directly colonising the Alanya Massif may well have been fringing reefs. Elsewhere in the study area reefs are always interbedded with conglomerate and have limited lateral extent. These have been interpreted as patch-reefs. It is possible to draw the tentative conclusion that high sediment influx and/or processes associated with high sediment influx, may have been some of the factors controlling patch-reef development.

3.9 Conclusions

- ◆ Most of the shallow-water carbonates are interpreted as having formed as patch reefs interbedded with coarse terrigenous clastics. Reefs, no longer preserved, but deduced to have colonised the south facing margin of the Alanya Massif in the Manavgat basin however, may have been fringing reefs.
- ◆ Colonisation generally occurs on coarse conglomerates, but is also occasionally associated with silt to mud grade grainsizes.
- ◆ No distinct coral colonising community exists, but particular coral morphologies are associated with the basal colonies, e.g. flat dish-shaped forms and squat reticulate cones.
- ◆ *Porites* is the dominant coral throughout the Miocene of the study area. Minor *Tarbellastrea* and *Montastrea* are important in particular reefs.
- ◆ The full coral zonation of Hayward (1982a and b) is not observed.
- ◆ Sediment influx and associated processes may have controlled the development of patch reefs.
- ◆ Reefs topography have had some influence on sediment dispersal patterns.

- ◆ Porites bafflestones development suggests that relative sea level rise > sediment influx.
- ◆ A hiatus in shallow-water carbonate production exists spanning the Mid-Langhian to Lower Tortonian.
- ◆ The eustatic sea level curve of Haq *et al.* (1988) is not sufficiently high resolution to explain termination of the Lower Miocene reefs in terms of an instantaneous global sea level rise.

Chapter 4

SEDIMENT GRAVITY FLOWS AND THE KARPUZÇAY FORMATION

4.1 Context

Sediment gravity flows deposited units of coarse conglomerate to siltstone grade material (the Karpuzçay Formation) between Langhian and Messinian times. These stratigraphically overlie the shallow-water carbonates described in chapter 3 and indicate a basinward shift in facies. Palaeocurrents, and grain-size changes within the Karpuzçay Formation indicate the geometry of sedimentation patterns and basin morphology in each of the three basins. This has implications for the ultimate controls of the processes of basin formation and evolution.

4.2 Organisation of this chapter

Following a brief outline of the spatial and temporal distribution of the Karpuzçay Formation, a summary of the previous work on these sediments is given in section 4.4. The texture and composition of the Karpuzçay Formation is described and interpreted for each of the three basins taking palaeocurrent directions into account (section 4.5). In the light of this information a comparison of the sediments exposed in the three basins leads to the subdivision of the Karpuzçay Formation into the Beskonak and Taskesigi Members (section 4.6). The discussion is then extended to include sedimentation trends resulting from the correlation of Miocene sequences across the Isparta Angle are noted in section 4.7, prior to the conclusion of the chapter (section 4.8).

4.3 Temporal and Spatial distribution

The majority of the Karpuzçay Formation sediments are exposed on the eastern side of the Köprü basin and in the central part of the Aksu basin. These sediments are mainly Serravallian in age although rare older (Langhian and Upper Burdigalian) and younger (Lower Tortonian)

nannoplankton dates have been derived by previous authors. Exposure of the Karpuzçay Formation is abundant throughout the Manavgat basin, but has a longer age span (Langhian/Lower Serravallian to Upper Messinian). The place names used in the text are indicated on figure 4.1.

4.4 Previous work

Blumenthal (1951) divided the Mio-Pliocene succession found between Alanya and the Köprü Çay into five formations: Conglomérats de base (chapter 5); Calcaire récifal "bordier" (chapter 3); Marnes de Gecereme (Blumenthal 1947; section 3.6.4.1); Molasses gréso-marneuse and lying discordantly above these the Pliocene Conglomérats de Belkis. Monod (1977), studying the same area and using Blumenthal's 1951 classification improved the dating of these formations and as a result modified the classification so that, Les Marnes de Gecereme, and a new formation, La Molasse de Manavgat, were both grouped under the heading of La Molasse Miocène de Manavgat. Monod noted that the pure pelagic sediments (e.g. Marnes de Gecereme) found near the village of Gençler close to the Akseki road section in this study, (table 2.5) were a very restricted facies evolving rapidly into the sediments of the "Molasse". He describes the "Molasse" as being a thick (1000-2000m?) succession of rhythmically-bedded sandstones and marls with lenses of conglomerate. He also indicated a general trend in the grain-size from north to south with the coarsest beds being found to the north close to Beskonak (Fig. 4.1). Using the Oymapinar and Alarahan sections in the Manavgat basin (Fig. 4.1), Monod identified the following foraminiferal zones in the "Molasse". (N.B. zone stages identified using Berggren *et al.*, 1985):

<i>Orbulina suturalis</i>	(Upper Langhian);
<i>Globorotalia mayeri</i>	(Serravallian);
<i>G. menardii</i>	(Serravallian-Tortonian boundary);
<i>G. dutertrei</i>	(Messinian).

In his thesis, Monod (1977) notes the need for further study of the Molasse in the Köprü basin, but leaves the Miocene sediments found there undifferentiated.

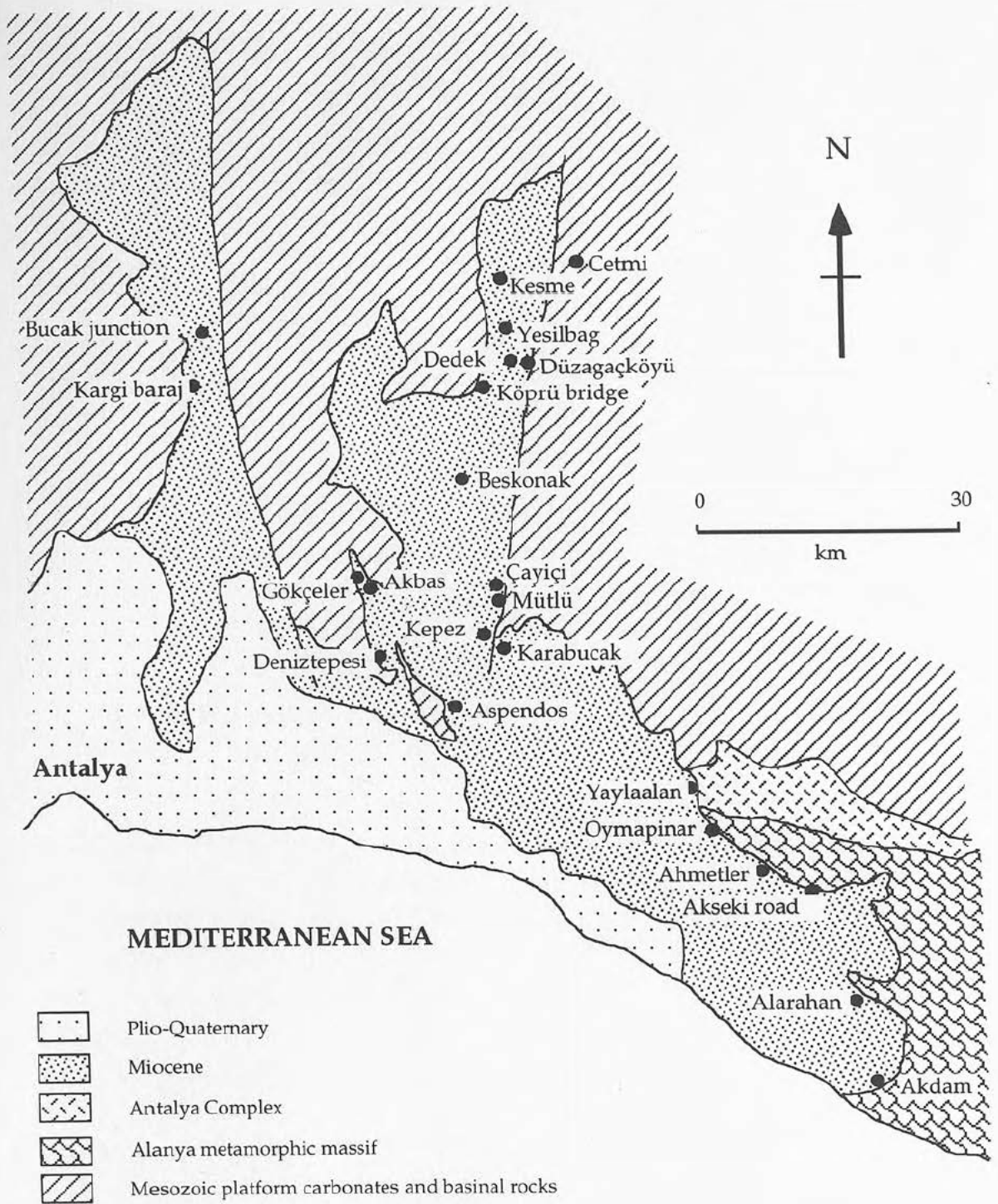


Figure 4.1. Location map of the Karpuzçay Formation exposures referred to in the text.

The work published by Bizon *et al.* (1974) concentrated on the south of the Isparta Angle. They dated the Alarahan and Oymapinar sections (table 2.5) in the Manavgat basin, and the base of the Miocene succession near Apendos in the south of the Köprü basin (Fig. 4.1)

Poisson (1977) used planktic foraminifera to date a semi-continuous section through the Karpuzçay Formation in the Aksu basin near the Kargi baraj (Fig. 4.1). This section overlies Lower Miocene shallow-water carbonates and spans the Serravallian to Lower Tortonian.

Akay & Uysal (1985) and Akay *et al.* (1985) classified "shale-sandstone-conglomerate alternation with occasional volcanic tuff interbeds" as the Karpuzçay Formation. The type section Akay & Uysal (1985) used for the Karpuzçay Formation is in the Manavgat basin, located along the road from the coast towards Akseki (Ahmetler section; Fig 4.1; table 2.5; sections 4.6 and 2.4; table 2.3). The formation is named after the river Karpuzçay, above which the road runs and means literally the "watermelon" river formation.

Sections within the Aksu and Köprü basins are often structurally complex such that the resultant dating of this formation in these two basins is rather patchy. The Manavgat basin sections are simpler and generally well dated. Figure 4.2 shows the locations of the sections dated by Akay & Uysal (1985), Akay *et al.* (1985), Bizon *et al.* (1974) and Poisson (1977), and the dates that they derived from the study of planktic foraminifera. The salient features of this diagram are listed below:

- ◆ The Karpuzçay Formation in the Aksu basin spans Burdigalian to Messinian times. Exposures are generally younger in the north of the basin, although rare Messinian dates are derived from the far south, juxtaposed against the oldest turbidite exposures in this structurally complex area.
- ◆ All dated sections in the Köprü basin are Latest Burdigalian-Langhian (NN4-NN5).
- ◆ The Karpuzçay Formation in the Manavgat basin spans the Langhian-Messinian (NN5-NN11b).

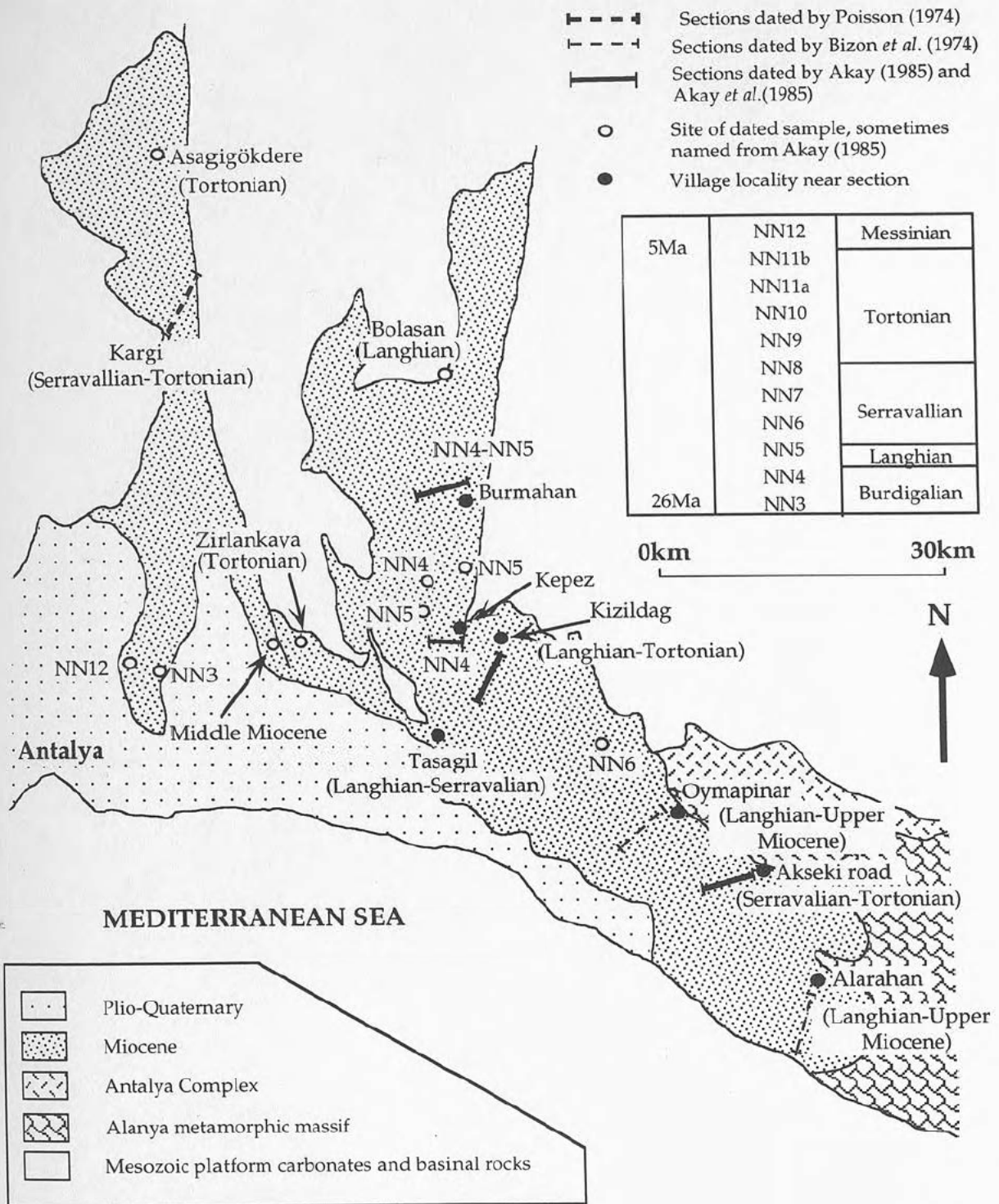


Figure 4.2 Location and dates of the Karpuzçay Formation sections and samples from Poisson (1974), Bizon *et al.* (1974), Akay (1985) and Akay *et al.* (1985). The ages of the nannoplankton zones are taken from Berggren *et al.* (1985).

Flecker *et al.* (1995) date the Ahmetler section using nannoplankton. Over 700m of interbedded conglomerates, sandstones, siltstones and marls show progressive younging from the north (Burdigalian/Langhian; section 3.3) to south (Messinian).

4.5 Facies description

4.5.1 Aksu Basin

The Karpuzçay Formation outcrop is concentrated towards the centre of the Aksu basin, to the north of the Kargi baraj (Fig. 4.1). The best exposure occurs in recent road cuttings along the new road north of the Kargi baraj towards Isparta, but due to the steep slopes of these cuttings and the rather crumbly nature of the rock, colluvium formation is rapid and the superb clarity of the turbidite exposure here will probably not be visible in a couple of years time.

Where the base of the Karpuzçay Formation is exposed, it overlies thin, laterally discontinuous Langhian shallow-water carbonates (Oymapinar Limestone; chapter 3) or passively onlaps Mesozoic basement limestone. The relationship of the lower contact of this formation is only observed in the west of the Aksu basin. The upper contact of the Karpuzçay Formation appears to be gradational into Tortonian conglomerates and sandstones with interbedded, small patch reefs (Aksu Formation; chapter 5).

4.5.1.1 Texture and composition

Thickness:

The thickness of the individual beds in the Karpuzçay Formation of the Aksu basin vary from a few centimetres to nearly a metre. Most of the thickest beds are either coarse sandstones and conglomerates or massive siltstones.

Bed shape:

Parallel sided geometries dominate the bed-shapes of the Aksu basin Karpuzçay Formation (Figs. 4.3, 4.4, 4.5 and 4.6). Some parallel bedded



Figure 4.3 Photograph of overturned sandstone and siltstone beds of the Karpuzçay Formation, 1.7km north of the Kargi baraj site, central Aksu basin. (Younging direction to the right).



Figure 4.4 Photograph of Karpuzçay formation turbidites 2.7km north of the Kargi baraj, central Aksu basin. The exposure here indicates a transition from silt dominated turbidites to more sand rich turbidites and back to silt dominated ones again. (The car is pointing in the younging direction.)

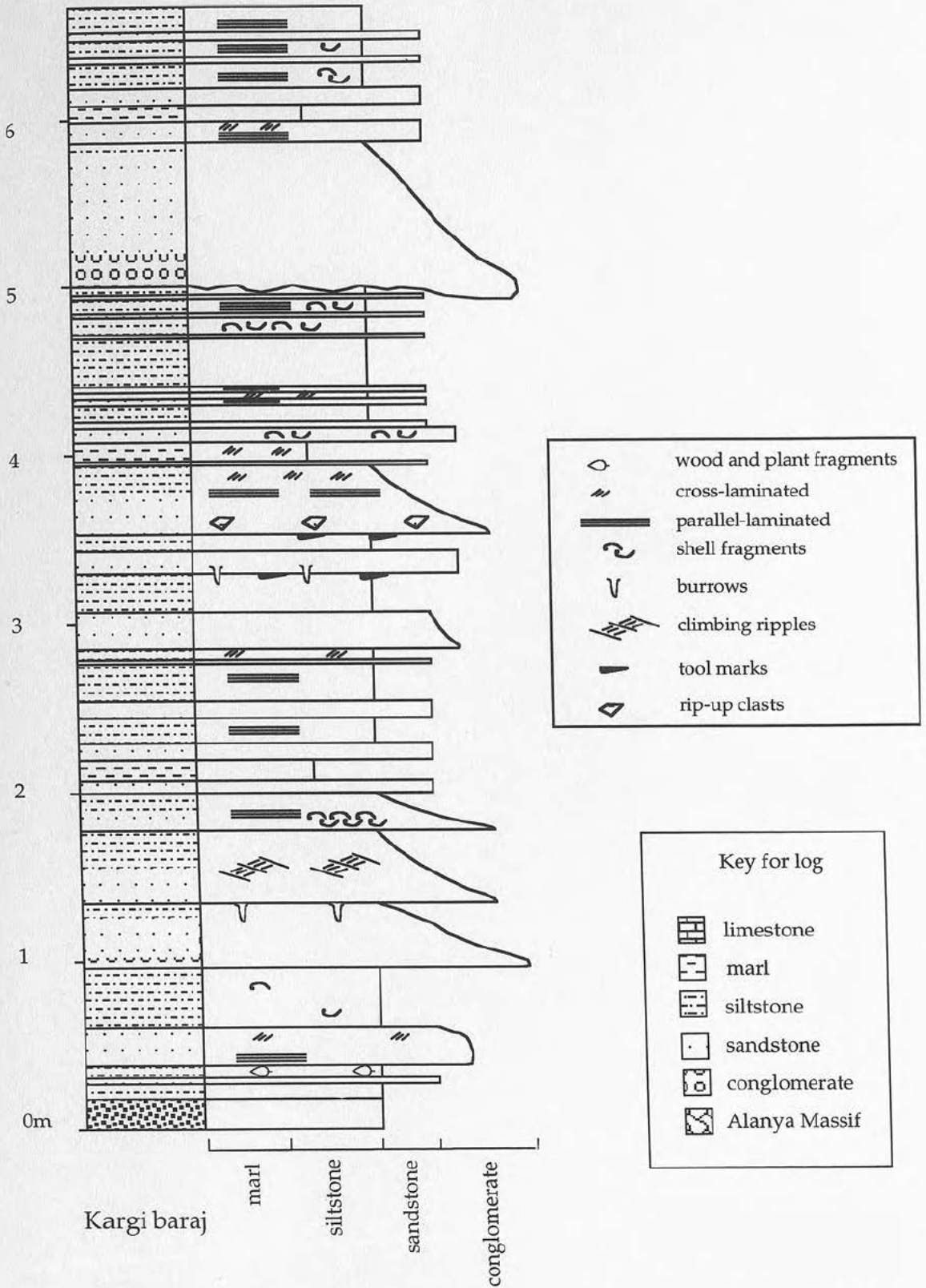


Figure 4.5 Log of the part of the succession shown in figure 4.3, Kargi baraj, central Aksu basin.

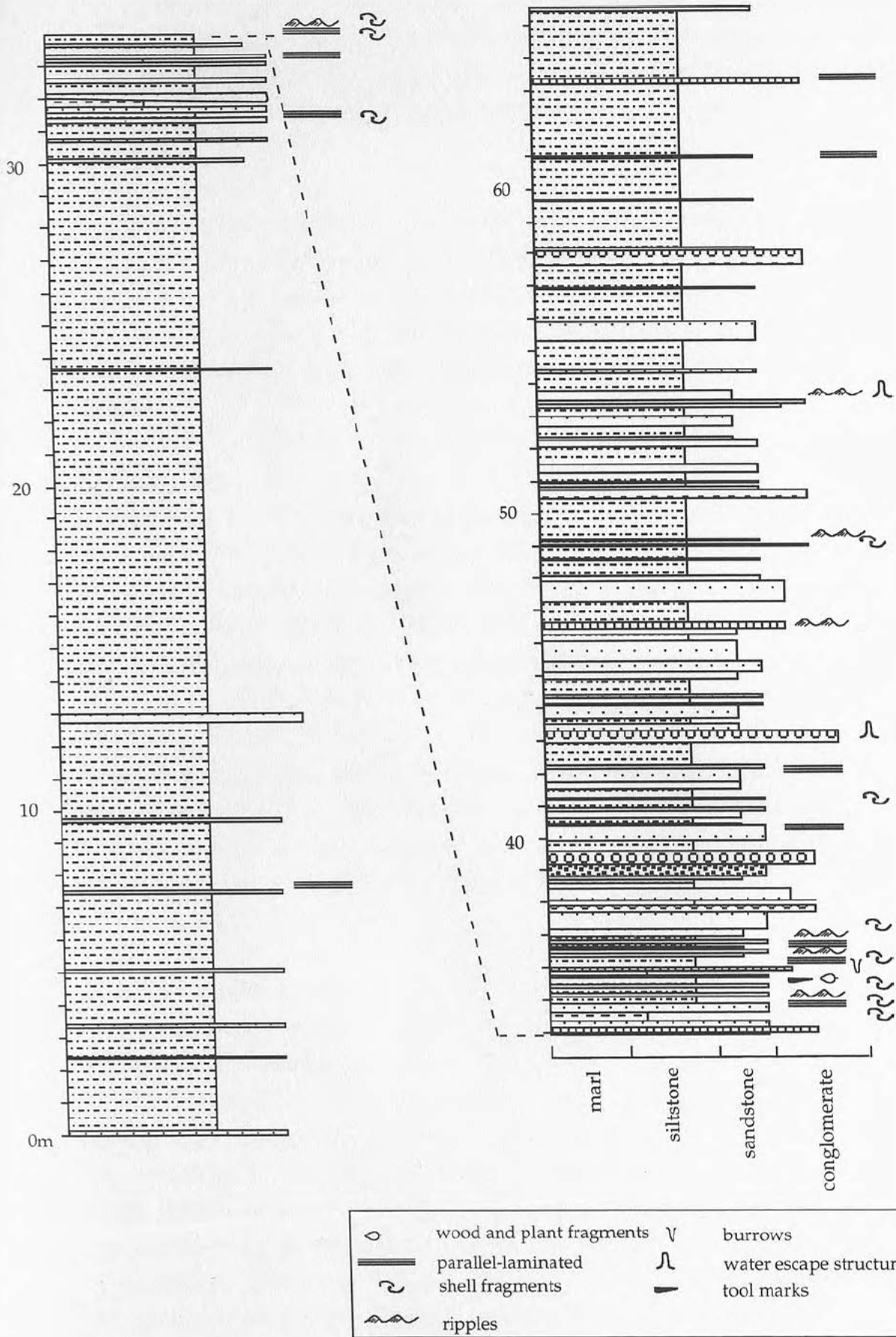


Figure 4.6 Log of the succession shown in figure 4.4, Kargi baraj, central Aksu basin. For key see figure 4.5.

sand units can be traced laterally over a hundred metres where the exposure permits. Gradual changes in bed thickness were observed in association with beds displaying basal scour. However, complete wedging out of beds was not observed on the scale of 100m.

Grain size:

The grain-size varies from relatively rare occurrences of fine-grained conglomerates with pebbles up to a few centimetres in diameter, to rare mudstones. Most Karpuzçay Formation exposures in the Aksu basin are siltstone dominated, but examples of equal sandstone and siltstone domination are exposed just to the north of the Kargi baraj site (Figs. 4.4 and 4.6).

Composition:

Terrigenous clasts within the conglomerates include: red and green chert; basement limestone (fawn, white and grey) and rather rare igneous fragments which are generally serpentized basalts. The sandstones contain similar material (Appendix 4). Biogenic components are dominated by plant debris, but concentrations of shell fragments are also common. In thin section these are overwhelmingly dominated by mollusc debris including oyster fragments although brachiopod fragments have also been identified. Rare entire gastropods are found particularly within the coarser sands and conglomerates. The micropaleontological content of the coarser-grained units is low, but planktic foraminifera and nannoplankton have been identified in the siltstones and mudstones.

Sorting:

The terrigenous components of individual units tend to be moderately to well sorted except in the particularly structureless sandstone-conglomerate beds. Biogenic debris generally forms larger clasts than the terrigenous components and this is particularly obvious towards top of fine sand units where plant debris is concentrated. Concentrations of shell debris appear both as coarse clasts in the basal part of massive sandstones and as winnowed lags associated with laminated and rippled sandstones. Very occasionally, shell fragments are found scattered rather randomly through more massive siltstones.

Grading:

Most of the sand-grade beds display normal grading. Inverse grading is occasionally observed in the lower parts of sandy conglomerates. The thicker bedded siltstone to mudstone units, by contrast, tend not to show grading. However, some of the thickest siltstone units, on detailed inspection are found to be made of millimetre scale silt-mud couplets with which subtle normal grading is associated.

Clast alignment:

Abundant plant debris, generally found towards the top of sandstone units shows distinct bedding parallel alignment, generally with an orientation within that plane. Imbrication within the conglomerates is also relatively common and rose diagrams from measurements on imbricated pebbles are discussed in section 4.5.1.3.

Structures:

Parallel laminations occur commonly in both sandstones and siltstones.

Cross laminations are also common. Most of the cross lamination is seen in section and appears to have a single flow direction. Where rippled surfaces are exposed, as at the junction between the Kargi-Isparta road and the road east from Bucak (11km north of the Kargi baraj site; Fig. 4.1) however, the evidence is equivocal and some of the ripples may be wave rather than current generated. Palaeocurrent measurements taken from the ripples in this locality are discussed in section 4.5.1.3. Climbing ripples are also found, but are much more rare.

Both the laminations and ripples are picked out generally by grain-size differences although occasionally compositional variations in the abundance of plant fragments pick out parallel laminations.

Water escape structures are found associated with sandstones passing rapidly into siltstones. They are generally small and rare.

Burrows, both horizontal and vertical occur throughout the Karpuzçay Formation although concentrations are more obvious both at the very

tops and bottoms of beds. Thick beds where burrows are visible on the bottom of the unit often completely lack structures further up. This may indicate that intensive bioturbation has completely destroyed all structures, save its own traces at the very bottom, where the burial level was potentially too deep for extensive biogenic activity. Concentrations at the top of beds may indicate that sufficient time elapsed between the deposition of one unit and the next for burrowing to occur, but not for it to have caused the destruction of all structures including its own traces. Horizons with well preserved sedimentary structures, but no burrows may indicate periods of low oxygen content both in the upper centimetres of the sediment and in the water just overlying it (Chamberlain 1978; Plaziat, 1984).

Tool marks, generally grooves or prods are found on the bases of many of the coarser sandstone units particularly where they overlie siltstones. Palaeocurrent directions measured from the tool marks in the Aksu basin are discussed in section 4.5.1.3.

Slumps are found throughout the Karpuzçay Formation and indicate an east-dipping palaeoslope to the basin.

4.5.1.2 Processes of deposition

The features of the sediments described above can be interpreted terms of the mechanisms of sediment gravity flows (Middleton and Hampton, 1973). Some of them could also be interpreted in terms of storm deposits. Aigner and Reineck (1982) distinguished shelf storm sand layers from turbidites using the following criteria:

- ◆ Wave-ripple cross-lamination;
- ◆ Wave-rippled top surface;
- ◆ *In situ* shallow-marine shelf fauna in interbedded shale layers;
- ◆ Marked increase in the bioturbation of storm sand layers from proximal to distal settings;
- ◆ Association with shallow-water facies.

Wave-rippled surfaces only occur in one locality in the Aksu basin. Here, they represent rippled top-surfaces of sandy units in a sequence which is significantly coarser than the Karpuzçay Formation elsewhere in the basin. This sequence may indeed represent at least partial deposition by storm-generated currents. Other successions studied in the Aksu basin however, failed to reveal structures characteristic of storm deposits. Hummocky cross-stratification (e.g. Dott and Bourgeois, 1982) for example, was not observed in the basin. Shallow-water fauna are only found as lags in the base of sandstone units, never *in situ* in the finer-grained layers. The absence of these typical storm structures suggests that although storm processes may have affected some of the deposits in the Aksu basin, there is little evidence that they were the dominant mechanism of deposition.

A brief summary of the depositional processes involved in sediment gravity flows and the formation mechanisms of the characteristic structures observed in Karpuzçay Formation of the Aksu basin, is given below.

Bouma (1962) collected detailed information of the internal characteristics of turbidites from the Maritime Alps in southern France. The Bouma sequence (Fig. 4.7) represents a summary of this information. The sequence was interpreted in relation to the progression of bedforms observed during decelerating flow in flumes (Harms and Fahnestock, 1965; Walker, 1965). Further work suggested that the Bouma sequence is a good model only for medium-grained turbidites deposited by the deceleration of low concentration turbidity currents.

The classification of sediment gravity flows by Lowe (1979) is based on flow rheology (*fluid or plastic*) and particle support mechanism (*turbulence, pore fluid, dispersive pressure and matrix support*; Fig. 4.8). In turbidity currents, grains are suspended by the turbulence of the flow and must therefore be treated in terms of several size populations (see Lowe, 1982 for review). Clay to medium-grained sand particles can be suspended by fluid turbulence alone, largely independent of the concentration and hence can be transported by low-density flows (Pantin, 1979). The vast majority of the turbidites observed in the Aksu basin, fall

	GRAIN SIZE	BOUMA (1962) DIVISIONS	INTERPRETATION
	Mud	E Laminated to homogeneous mud	Deposition from low-density tail of turbidity current ± settling of pelagic or hemipelagic particles
	Silt	D Upper mud/silt laminae	Shear sorting of grains & flocs
	Sand	C Ripples, climbing ripples, wavy or convolute laminae	Lower part of lower flow regime of Simons <i>et al</i> (1965)
		B Plane laminae	Upper flow regime plane bed
	Coarse Sand	A Structureless or graded sand to granule	Rapid deposition with no traction transport, possible quick (liquefied) bed

Figure 4.7 Idealised sequence of sedimentary structures in a turbidite bed (after Bouma, 1962, with interpretation after Harms and Fahnestock, 1965; Walker, 1965; Walton, 1967; Stow and Bowen, 1980).

Flow behaviour	Flow type	Flow character		Sediment support mechanism
Fluid	Fluidal flow	Turbidity current	Fluid Turbulence	Low density turbidity current
		Fluidized flow	Escaping pore fluid (full support)	
Plastic	Debris flow	Liquified flow	Escaping pore fluid (Partial support)	High-density turbidity current
		Grain flow	Dispersive pressure	Mud flow
		Mudflow or cohesive debris flow	Matrix strength/ matrix density	

Figure 4.8. Nomenclature of laminar and turbulent sediment gravity flows based on flow rheology and particle support mechanisms (modified after Lowe, 1979).

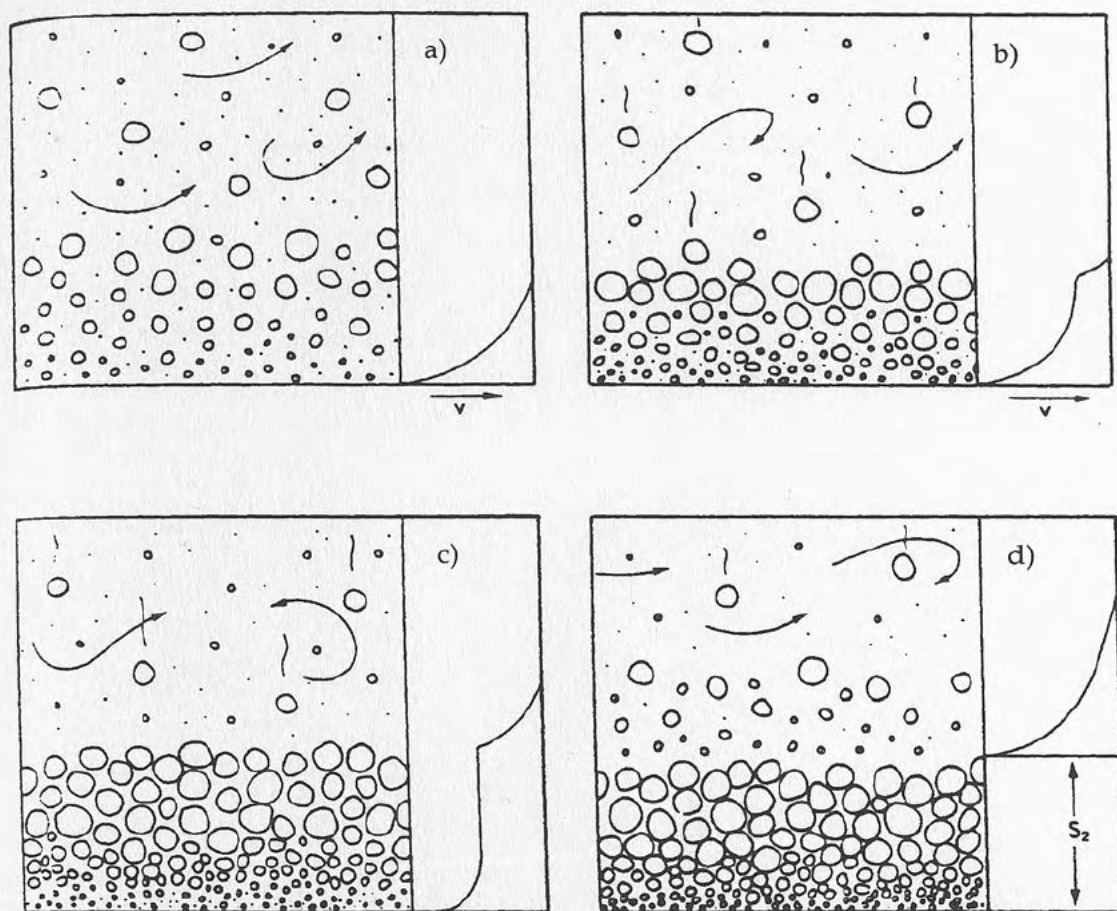


Figure 4.9 Origin of traction carpet layers, with sketches from Lowe (1982) and explanation based on Hiscott and Middleton (1979, 1980): a) Grain interaction at the base of a high-concentration turbidity current produces inverse grading of the flow. b) Continued fallout from suspension produces a dense traction carpet that is supported by dispersive pressure and sheared by the main body of the flow above. c) The upper part of the traction carpet freezes (vertical segment in the velocity profile) with shear being concentrated at the base of the carpet. d) The entire sheared layer ceases to move and becomes welded to the bed. Repetition of this process forms a division of inversely-graded stratification.

within this grainsize population and many of the structures with which they are associated can be formed during the deceleration of a low-density turbid flow (see below). Coarse sand to small pebble-sized gravel however, cannot be entirely suspended within a dilute flow. In high density flows where there is a wide range of particle sizes, the coarser grains can be supported by a combination of turbulence; hindered settling due to their own high concentration and buoyant lift caused by the interstitial mixture of water and finer-grained sediment. Pebble to cobble-sized clasts in concentrations >10-15% can also be supported by dispersive pressure from grain collision (Lowe, 1982). Although the quantity of coarse grained material within the Karpuzçay Formation in the Aksu basin is relatively small, none-the-less, different depositional mechanisms can be inferred from their presence and internal structures.

The process of deposition is mainly a function of a) flow concentration or flow density and b) rate of deposition. Generally more than one process (*Traction sedimentation, suspension sedimentation, frictional freezing and cohesive freezing*) is operative either synchronously or serially during the deposition of an entire unit. Deceleration of a low-density turbid flow, for instance, results in the passage of sediment from suspension to bed load. Sediment is then deposited by traction sedimentation. Bedforms resulting from the combination of these two processes include parallel lamination, ripples and normal grading, features that are characteristic of Bouma division B, C and D (Fig. 4.7) and are commonly found in the Aksu basin turbidites.

High-density turbidity currents with a coarse sand-gravel population, may deposit some load as a sand bed in a slightly unsteady, but fully turbulent flow state. These sediments show traction-related structures, e.g. flat lamination or oblique cross-stratification and high-density turbidity currents are locally erosive, causing scour structures. As flow unsteadiness increases, suspended load becomes increasingly concentrated towards the base of the flow, and, particularly in coarser size fractions, a basal layer is formed and maintained by dispersive pressure due to grain collision. This layer is known as a traction carpet (Dzulynski and Sanders, 1962) and leads to the formation of inversely graded coarse-grained layers.

When it freezes, due to continued sediment fallout from the overlying flow, a new carpet forms on top and the process is repeated (Fig. 4.9).

In cohesive mudflows (or debris flows), grains are supported by the cohesiveness and buoyancy of a sediment-water matrix rather than by turbulence. In some of these flows, the clasts are not truly suspended in the matrix, but the buoyancy and lubrication (preventing frictional locking) provided by the sediment-water mix, allows them to bounce and roll down-slope whilst remaining more or less in contact with other clasts. The features produced by such flows are variable and may depend on whether the flow was turbulent at some point during deposition (Enos, 1977). Chaotic units where larger clasts are at least partially suspended in a finer-grained matrix are generally attributed to debris flow processes.

Tables 4.1 and 4.2 indicate the range of structures observed in the Aksu basin. Using the classification scheme of Pickering *et al.* (1989) which is a modified version of the much earlier work by Mutti and Ricci Lucchi (1972), the Karpuzçay Formation has been divided into 6 sub-facies and the probable depositional processes and current types have been identified.

4.5.1.3 Palaeocurrent analysis

Figure 4.10 displays representative rose diagrams measured in the Kargi area plotted against a generalised section which has been derived, in part from Poisson (1977a). A clear bimodal current distribution can be seen; broadly to the east and to the SSE. On closer examination the east and ESE directed current measurements are derived from pebble imbrication, whilst the south to SSE directed palaeocurrents are derived from tool marks. The limited slump data collected from the area indicate that there was a palaeoslope dipping towards the east. Palaeocurrent directions measured on six rippled surfaces in the turbidites at the Bucak junction with the new Isparta-Kargi baraj road indicate a dominantly east directed flow with a subordinate westerly flow direction. As discussed earlier, cross-sections through these rippled surfaces did not indicate

Table 4.1 Description and classification of medium-sand to clay grade units from the Aksu, Köprü and Manavgat basins, in terms of low- and high-density turbidity currents (after Pickering *et al.*, 1989).

Structures	Sub-facies (Pickering <i>et al.</i> 1989)	Bouma divisions (Bouma 1962)	Depositional process	Current type
Tool marks, scour, water-escape, normal grading, parallel laminations, ripples.	C2.1 sand-mud couplets	A-D	Grain-by-grain deposition from suspension. Tractional transport active in Bouma division B and C	High concentration turbidity flow
Generally parallel bedded, normal grading, parallel laminations, ripples	C2.2 sand-mud couplets	B-D	Grain-by-grain deposition from suspension. Tractional transport active	Intermediate strength turbidity flow
Generally parallel bedded, normal grading, parallel laminations in silt	C2.3 sand-mud couplets	C-D	Grain-by-grain deposition from suspension. Tractional transport active	Relatively dilute turbidity flow
Silt-mud laminations, gradational tops and bases	D2.3 Thin silt and mud laminae		Slow uniform deposition from suspension with shear sorting	Low concentration turbidity flow

Table 4.2 Description and classification of coarse sand and conglomerate units from the Aksu, Köprü and Manavgat basins in terms of high-density turbidity currents (after Pickering *et al.*, 1989).

Structures	Sub-facies (Pickering <i>et al.</i> 1989)	Bouma divisions (Bouma 1962)	Depositional process	Current type
Inverse grading, imbrication, massive, water escape, rippled silts at top	B2.1 Parallel- stratified sands		Freezing of traction carpets at base. Intense grain interaction producing imbrication and inverse grading	High concentration turbidity flow
Thicker bedded, flat based, poorly sorted, mudstone intraclasts common	A1.1 Disorganised gravel		freezing on decreasing slopes due to intergranular friction and cohesion	High concentration turbidity currents or debris flows

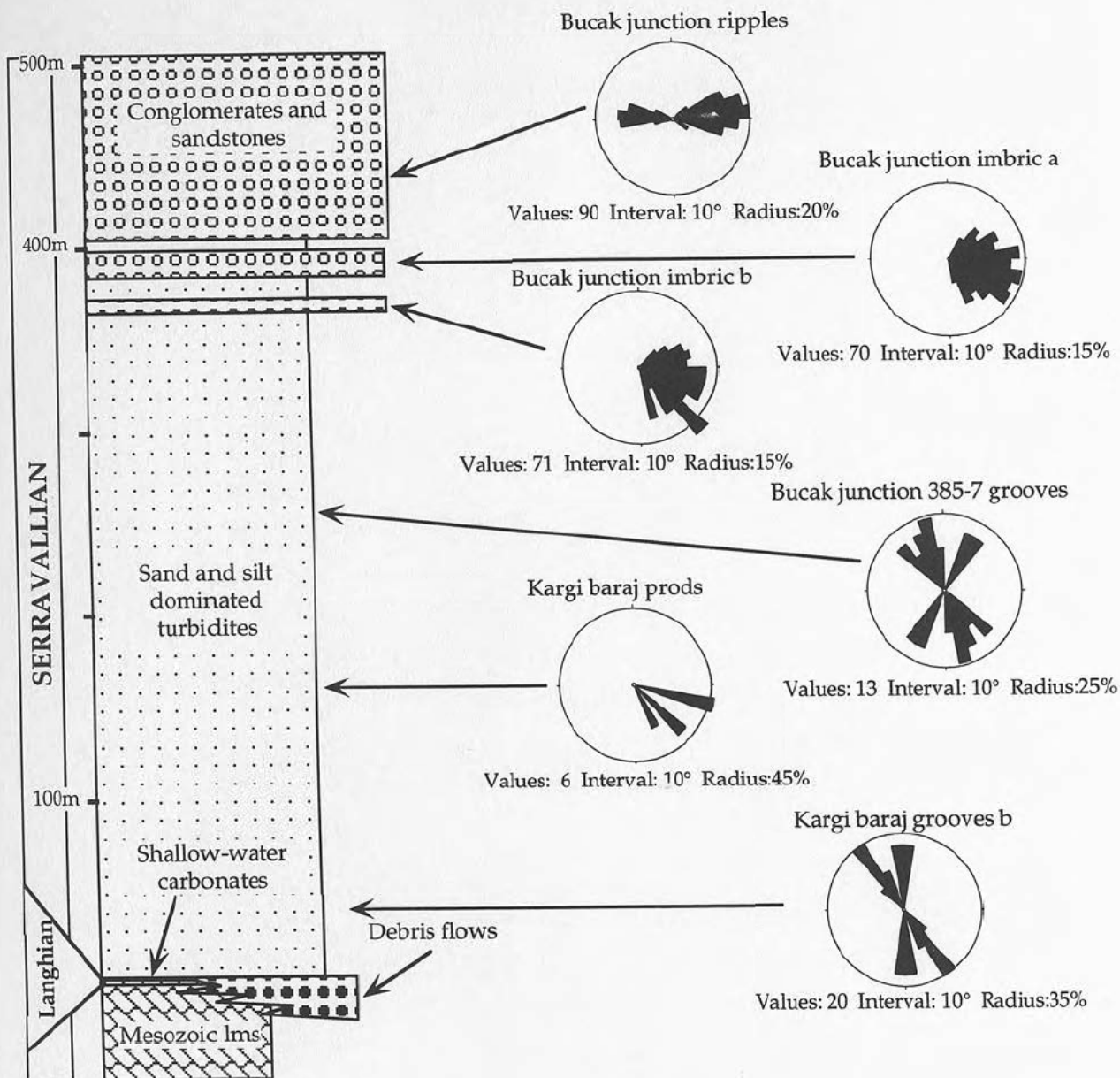


Figure 4.10 A schematic log of the Kargi baraj section, central Aksu basin with palaeocurrent rose diagrams. The ages are derived from Poisson (1977).

unequivocally what sort of current deposited them. The bimodal ripple direction suggests that they were formed by wave action.

Interpretation of the palaeocurrent data can be listed as follows:

- ◆ There is no evidence to suggest that the east margin of the Aksu basin was a major sediment source;
- ◆ Tool marks on the base of sandstone-siltstone units suggest that the turbidites flowed axially, from north to south;
- ◆ Imbrication in conglomeratic units near the Bucak junction indicate derivation from the western margin;
- ◆ Wave ripples are associated with the conglomeratic sequence.

4.5.1.4 Temporal and spatial variations

Dating of this formation in the Aksu basin, due to intense folding and large scale faulting requires detailed sampling and mapping on a scale which was not compatible with the template of the project. Thus, the discussion of temporal relationships within the formation is limited either to broad generalities or relationships visible within a single continuous exposure.

Where redeposition of material is a dominant process in the formation of a sedimentary unit, (e.g. turbidites) biostratigraphic data should be treated with caution. In this case, although the biostratigraphic template is based on nannoplankton which are notoriously easily reworked, the younging to the north trend is likely to be real even if the zones identified in individual samples (particularly the older samples), are inaccurate for the date of deposition of the turbiditic unit. It is therefore assumed that the age of the Karpuzçay Formation in the Aksu basin spans the Late Langhian/Early Serravallian- Lower Tortonian.

The timing of input of the Bucak junction conglomerates from the western margin occurs in the Serravallian. Poisson (1977a) indicates that these conglomerates pass upwards into finer turbidites which are also Serravallian in age, suggesting that the western source of coarse material was both developed and abandoned in a relatively short space of time.

Interpretation of the coarse, often matrix-supported conglomerates in this succession is discussed more fully with reference to the Tortonian and Messinian succession in the Manavgat basin, where this type of deposit is more common (section 4.5.3.2). A tentative interpretation of the episodic nature of the conglomeratic sequence seen at the Bucak junction is that it represents shelf deposition of an ephemeral fan-delta lobe. On a smaller scale (i.e. 100m) a similar pattern of periodic coarse influx can be seen in the finer-grained units near Kargi baraj (Figs. 4.4 and 4.6). This succession may document the formation and abandoning of a sand lobe such as those discussed by Stow (1984).

The Karpuzçay Formation in the north of the Aksu basin is significantly richer in conglomerate than in the south (Fig. 4.11). This may indicate a proximal to distal relationship within the basin from north to south and the north-to-south direction of axial flow inferred from the turbidite palaeocurrents would support this interpretation. However, given the younging trend, the distribution of conglomerate may also represent a shallowing of the basin through time. In this scenario, axial flow from north-to-south would be maintained throughout the Serravallian, but a relative fall in sea level would cause increasingly proximal facies to be deposited near the source area, in the north. The continental and shallow-marine Tortonian facies in the north of the Aksu and Köprü basins discussed in chapter 5 and foraminiferal evidence from the Manavgat basin, support the interpretation of Serravallian shallowing throughout the Isparta Angle.

One further possibility, however, is that the conglomerate-rich Karpuzçay Formation represents a period of active deposition on a fan-lobe, much like that seen in the centre of the basin at the Bucak junction.

4.5.2 Köprü Basin

The outcrop of the Karpuzçay Formation is mainly confined to the east of the basin between the river Köprü and the Kirkkavak fault and to the south of the village of Yesilbag. An important exception to this is the exposure which occurs in the south west of the Köprü basin in the region of the village of Akbas (Fig. 4.1).

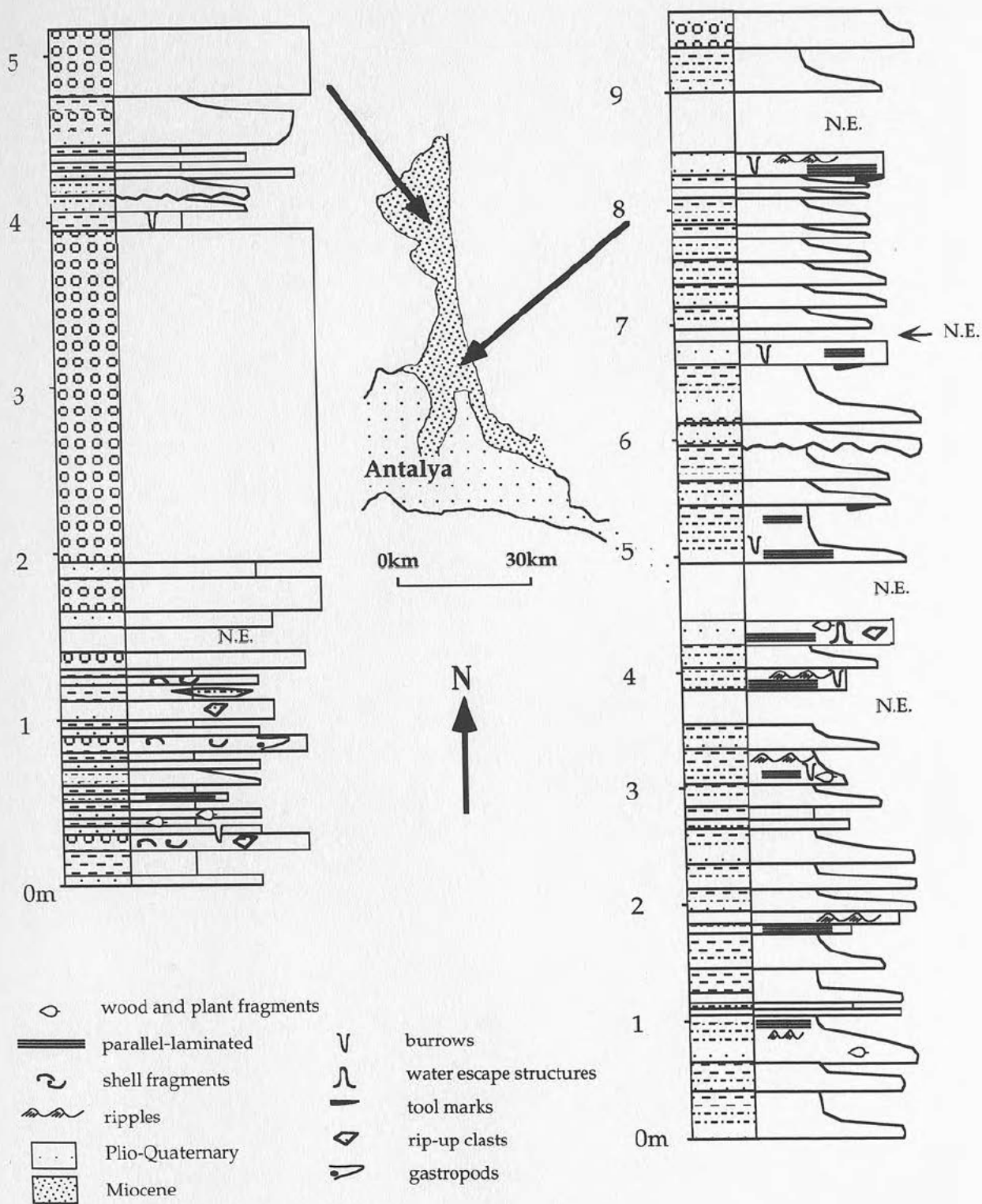


Figure 4.11 Logs of typical Karpuzçay Formation sections from the north and south of the Aksu basin.

Where the base of the Karpuzçay Formation is exposed, it overlies laterally discontinuous Langhian shallow-water carbonates (Oymapinar Limestone; chapter 3) and coarse conglomerates and sandstones (Kizildag Formation; chapter 5) sometimes with a disconformable relationship. The base of the formation is only observed in the south-west of the Köprü basin, near Aspendos and Deniztepesi and in the north where the basin bifurcates, near Ballibucak.. The upper contact of the Karpuzçay Formation is exposed along the road north from Beskonak to Kesme near the village of Yesilbag and appears to be rapidly gradational into Tortonian conglomerates and sandstones with interbedded, small patch reefs (Aksu Formation; chapter 5).

4.5.2.1 Texture and composition

Thickness:

Conglomerate beds in the Köprü basin vary in thickness from a few centimetres at the base of fining upwards sequences, to 50cm thick massive units. Sandstone beds tend to be thinner, generally between 5 and 20cm although much thicker beds are occasionally found. An example of a 75cm thick massive sandstone horizon was observed on the road to Karabucak. Channelised sandstone and conglomerate units such as those located near the junction between the road to Karabucak and the road from the coast to Beskonak are generally in the order of 1-2m thick. Siltstone and mudstone horizons are interbedded on a centimetre scale.

Bed shape:

The vast majority of the Karpuzçay Formation in the Köprü basin consists of parallel bedded units. However, lenticular geometries are far more common in the Köprü basin than in the Aksu basin. Such geometries include: wedging out of coarse horizons (e.g. the micro-conglomerates at Duzagaçköyü); cross-sections through channels (e.g. near the junction between the road to Karabucak and the road from the coast to Beskonak, Fig. 4.12) and rare cross-cutting relationships on a scale of a hundred metres, indicating transverse sections through channels. Most of these bedforms are associated with conglomerate and coarse sandstone.



Figure 4.12 Photograph of a channel in Karpuzçay Formation, central Köprü basin.



Figure 4.13 Photograph of rip-up clasts in a sandstone unit from the Karpuzçay Formation, central Köprü basin.

However, at Çayıçi in a relatively sandstone poor succession, fine sandstone is confined within narrow channels approximately 1m across.

Grain size:

A few broad generalisations can be made concerning the overall grain-size of the turbidites in the Köprü basin:

- ◆ The Akbas syncline area in the west of the basin contains fine grained turbidites, with very rare conglomerates. These have clasts up to about 4cm in diameter and a mean clast size of 0.5cm;
- ◆ The eastern margin of the Köprü basin is also generally conglomerate poor, but the percentage of sand seems to vary unsystematically from 5-90%.
- ◆ Conglomerate-rich units are concentrated in the centre of the basin in association with channel geometries. Here maximum clasts size varies from 5-10cm with a mean of 2-4cm. Rare boulders up to 50cm in diameter are found in a poorly sorted conglomerate to the north west of Beskonak.

Composition:

The clast types found in the conglomerates of the Köprü basin are more varied than those found in the Aksu basin. They include: red, green, black and diagenetic grey chert; pale grey limestone; dark grey limestone with gastropods; white fossiliferous limestone; fawn recrystallised limestone; brown sandstone; green silt; calcarenite; igneous fragments including serpentinite and weathered basalt and intraformational rip-up clasts of mud and silt. Abundant, large rip-up clasts of grey-green silt are also found at the base of sandstone units such as those found near the junction of the road to Kepez and Mütlü with the road to Beskonak (Fig. 4.13).

The terrigenous components of the sandstones are broadly similar to those of the conglomerates, but the sandstones also contain individual quartz grains making up about 25% of the total number of grains (Appendix 4b). Micrite is also a fairly abundant component constituting up to 45%.

Biogenic detritus is a significant component of many sandstone and some conglomerate horizons. One of the most fundamental differences

between the composition of the Aksu basin and the Köprü basin is the quantity and preservational state of the wood and plant fragments. In the Aksu basin the turbidites contain brown plant material, generally concentrated in particular horizons. In the Köprü basin the quantity of organic material is much greater and consists of coal fragments. This may reflect differences in both the nature of the organic material (i.e. more wood rather than leaf detritus influxed into the Köprü basin) and in the burial depth between the two basins. Figure 4.14 is located a few kilometres to the north of Beskonak and shows a siltstone horizon containing a large wood clast (now coal) which has been copiously bored. Organic fragments of various sizes are found in horizons of all grain sizes.

Large pieces of coral included as clasts in conglomerate are also relatively common in the Köprü basin. The most common species found is *Porites* sp., but *Heliastrea* (Vindobonian, Early-Mid Miocene, Chevalier 1961) has also been identified (Appendix 3c). Shells and shell fragments are concentrated in particular horizons the grain-size of which varies from conglomerate to siltstone. At Duzagaçköyü, a shell-rich sandstone contains pectens, oysters, bivalves, gastropods and small bored limestone clasts, whilst 7% of clasts in a pebble conglomerate 50m higher up the section are oysters. A further 2% of clasts in this horizon are gastropods (Appendix 4a).

Sorting and physical maturity:

The physical maturity of the conglomerate clasts in the Köprü basin is sometimes difficult to assess accurately as it is, to some extent, dependent on the relative quantities of chert and limestone. Angular conglomerates rich in chert clasts are not uncommon, but angular limestone conglomerates such as the 50cm thick horizons seen in the Dedek section are rare. Most conglomerates and sandstones contain clasts and grains which are subangular-subrounded.

Sorting of conglomerates varies, but is on the whole poor to moderate. Matrix supported conglomerates are rare, whilst clast-supported conglomerates with abundant matrix are the norm. Grain sorting in the



Figure 4.14 Photograph of a bored coal fragment in a Karpuzçay Formation siltstone unit a few kilometres north of Beskonak, central Köprü basin.

detached block

Figure 4.15 Photograph of a slumped horizon overlain by a channelised sandstone, overlain by a debris flow unit containing a detached block of Alanya Massif metacarbonate from the Karpuzçay Formation, 1km south of the Ahmetler junction, north-eastern Manavgat basin.



channelised sandstone

slump horizon

person for scale

sandstones tends to be moderate to good with the exception of larger clasts near the base of beds.

Grading:

Almost all the grading seen in the basin is normal. Conglomerates located along the Kepez section contain rare examples of inverse grading at the base overlain by subsequent normal grading.

Clast alignment:

As in the Aksu basin, imbrication in the conglomerates is relatively rare. Alignment of organic fragments is less common in the Köprü basin than in the turbidites in the Aksu basin, perhaps due to the larger size of the organic clasts.

Structures:

Parallel laminations in both sandstones and siltstones are common and are well exposed in sandstone near Gökçeler in the Akbas syncline area;

Cross laminations associated with both straight crested and crescent-shaped ripples are common in sandstones. Mega-ripples with a ripple height of 5cm and a wave length of approximately 20cm are found in one locality, a few kilometres south east of the Köprü bridge on the road to Yesilbag. Cross-sets in sandstones at the top of channelised units such as those along the Karabucak section can be up to 1.5m in height;

Water escape structures were observed infrequently;

Bioturbation is abundant in all but the coarsest conglomerates. Both horizontal and vertical tubes are common.

Tool marks found in the Köprü basin include grooves, prods, more rare flutes, load balls and sludge marks.

Slumps are abundant particularly along the eastern margin of the basin. They vary in thickness from a few centimetres to 10m.

4.5.2.2 Interpretation

The Karpuzçay Formation exposed in the Köprü basin closely resembles the succession in the Aksu basin and can be interpreted in terms of high and low-density turbidity currents in a similar way (section 4.5.1.2; tables 4.1 and 4.2).

4.5.2.3 Palaeocurrent analysis

Figure 4.16 shows the locations of representative rose diagrams from the Karpuzçay Formation in the Köprü basin. Slumps are more common in the Köprü basin than in the Aksu basin, but are concentrated along the eastern margin, marked today by the Kirkkavak fault (Fig. 4.16). In the north of the basin the slump directions indicate a palaeoslope dipping towards the west, whilst the main transport direction of the turbidites in the central part of the basin is indicated by measurements of the tool marks which show north-south movement. Sandstone channels associated with these turbidites are exposed in three dimensions on a scale of 3-5m in central parts of the basin away from the margins and these are also orientated north-south. Towards the south of the basin however a marked change in palaeocurrent direction is indicated. Grooves measured within 2 kilometres west of the Kirkkavak fault close to the village of Kepez have NNW-SSE direction (Fig. 4.16). A few kilometres further south, channels exposed in road cuttings are orientated NW-SE. Slumps measured just to the east of the Kirkkavak fault near the village of Karabucak show a wide variety of directions, but there is a conspicuous absence of slumping towards the north.

Although the slump data in the north of the basin indicate that there was a west facing slope close to the present day eastern margin of the Köprü basin, there is no related change in the grain-size of the turbidites from east to west. Thus, as in the Aksu basin the major source of turbidites seems to have been to the north.

The change in direction from axial flow documented by the groove marks in the north of the basin to flow directed to the south-east, towards and over the present day basin margin (Kirkkavak fault) in the south

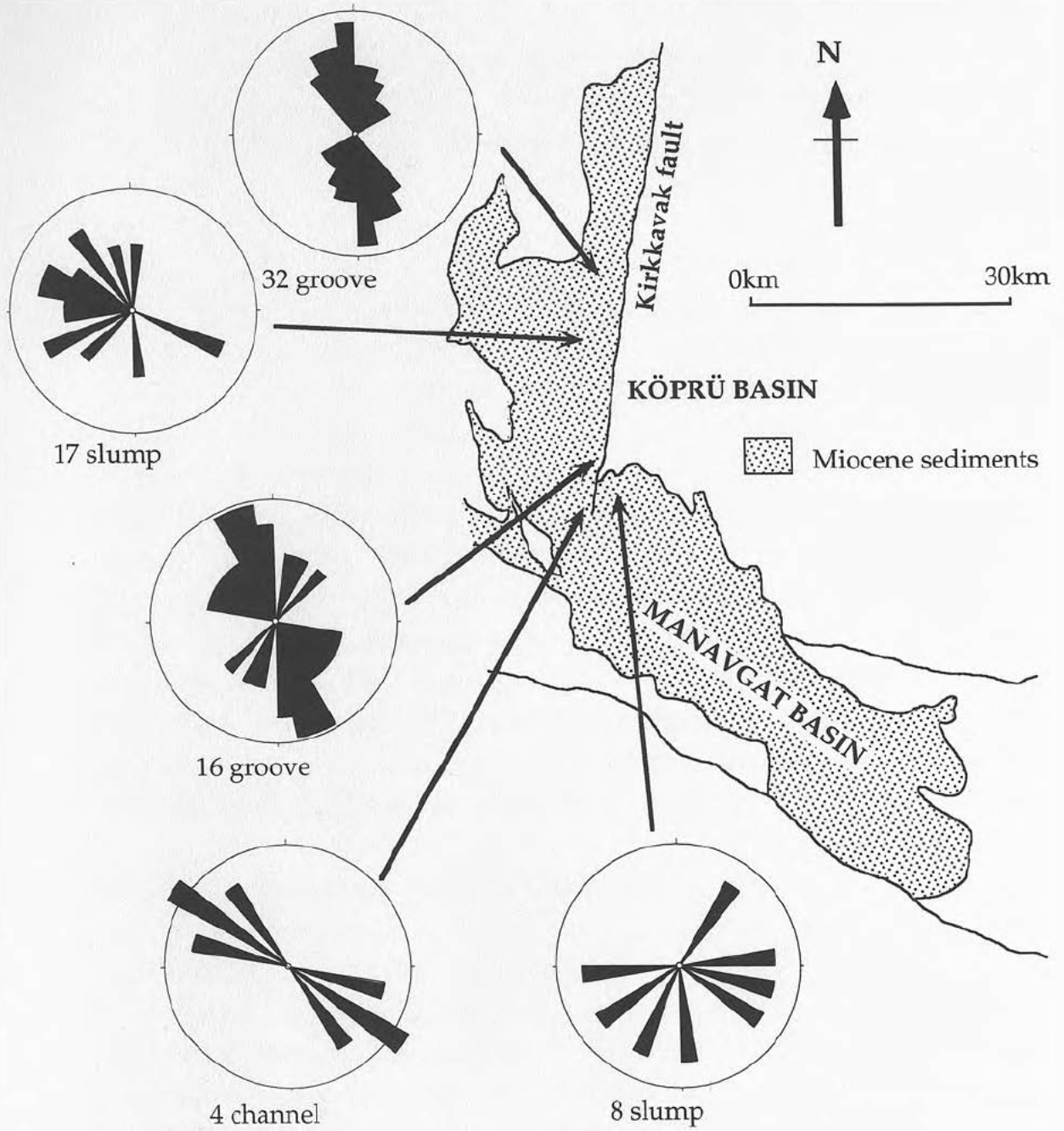


Figure 4.16 A map of the Köprü and Manavgat basins showing the location and orientation of some directional structures in the Karpuzçay Formation units.

indicates either that the Kirkkavak fault did not exist at the time of deposition or, if it did, that it had no marked topographic expression. At any rate the south of the Köprü basin appears to have been overfilled during the Early Miocene allowing turbidites to spill out towards the south east.

There is little evidence to suggest that the Kirkkavak fault was overstepped by turbidites along its entire length, although it is possible that due to subsequent uplift at the end of the Miocene (the Aksu Phase; chapter 7) much of what was deposited to the east of the Kirkkavak fault has been removed as a result of footwall uplift. Miocene outcrop east of the Kirkkavak fault occurs in only two places (Fig. 4.16), both in the far north close to a palaeo-incised valley which breaches the Kirkkavak Fault (chapter 5; Fig. 5.16). The exposures at Dumanli, though of similar age (Serravallian; Appendix 3.A.2) constitute shallow-water carbonates and conglomerates interbedded with marls that are rich in benthic foraminifera. The other exposure located between the villages of Çetmi and Gencek consists of a single small bank outcrop of marls containing no nannoplankton and abundant large oysters. Both these localities are discussed further in chapters 3, 5 and 6.

4.5.2.4 Spatial and temporal variations

Akay's M.T.A. report (1985) indicates that the Karpuzçay Formation in the Köprü basin is generally older and represents a much shorter time span (uppermost Burdigalian- Langhian) than that found in the Aksu basin (Langhian to Tortonian, Fig. 4.2). Nannoplankton analysis of sections in the south west of the basin (e.g. Aspendos and Deniztepesi; Fig. 4.1; C. Müller pers. com., 1994) suggest that here, Langhian shallow-water carbonates pass up into Early Serravallian turbidites (Appendix, 3.A.2; Fig. 4.32) thus extending the time period over which Karpuzçay turbidites are thought to have been deposited in the Köprü basin. Once again, because of the redeposited nature of the material, these dates must be regarded as providing an estimate of the maximum age of deposition (section 4.5.1.3). Potentially however, if the older samples do reflect Burdigalian-Langhian deposition of the Karpuzçay Formation in the east of the basin coeval

with shallower-water carbonates deposition in the west, this indicates an asymmetric geometry to the Köprü basin at this time (Fig 4.17).

Monod (1977) suggested that there was a north to south decrease in the grain-size of the Karpuzçay Formation in the Köprü basin. This trend was not observed, although local coarsening is associated with the transition to the conglomeratic Aksu Formation near Yesilbag in the north-eastern part of the basin.

4.5.3 Manavgat basin

Outcrop of the Karpuzçay Formation is abundant in the Manavgat basin, but particularly spectacular exposures are found along the new road from the coast towards Akseki. Every road cutting exposure of Karpuzçay Formation along this road was logged and is summarised in the upper half of the Ahmetler section (Fig. 4.18). References to sites and samples in the following text can be located in Appendix 5 where a detailed centimetre-meter scale log of the entire Ahmetler section is presented. Elsewhere in the basin, the outcrop is more patchy, but good road cutting sections can be found at Alarahan, Akdam, Oymapinar and on the road to Yaylaalan (Fig. 4.1).

The Karpuzçay Formation in the Manavgat basin is different from that exposed in the other two basins in the following ways:

- ◆ Nannoplankton analysis of samples from the Ahmetler section reveals that the Karpuzçay Formation in the south-east of the Manavgat basin is Tortonian to Upper Messinian in age (Fig. 4.18; Appendix 3a) much younger than Aksu and Köprü basin exposures which are mainly Serravallian.
- ◆ In the Manavgat basin, the Karpuzçay Formation is characterised by much coarser deposits than in either the Köprü or Aksu basins.

The Karpuzçay Formation in the Manavgat basin overlies conglomerates and sandstones of the Kizildag Formation in the north-west of the basin (Fig. 3.23). In this area, nannoplankton analyses (Akay & Uysal, 1985) suggest that deposition occurred during the Late Burdigalian-Early Langhian or at some time there after. In the south-east of the basin, the

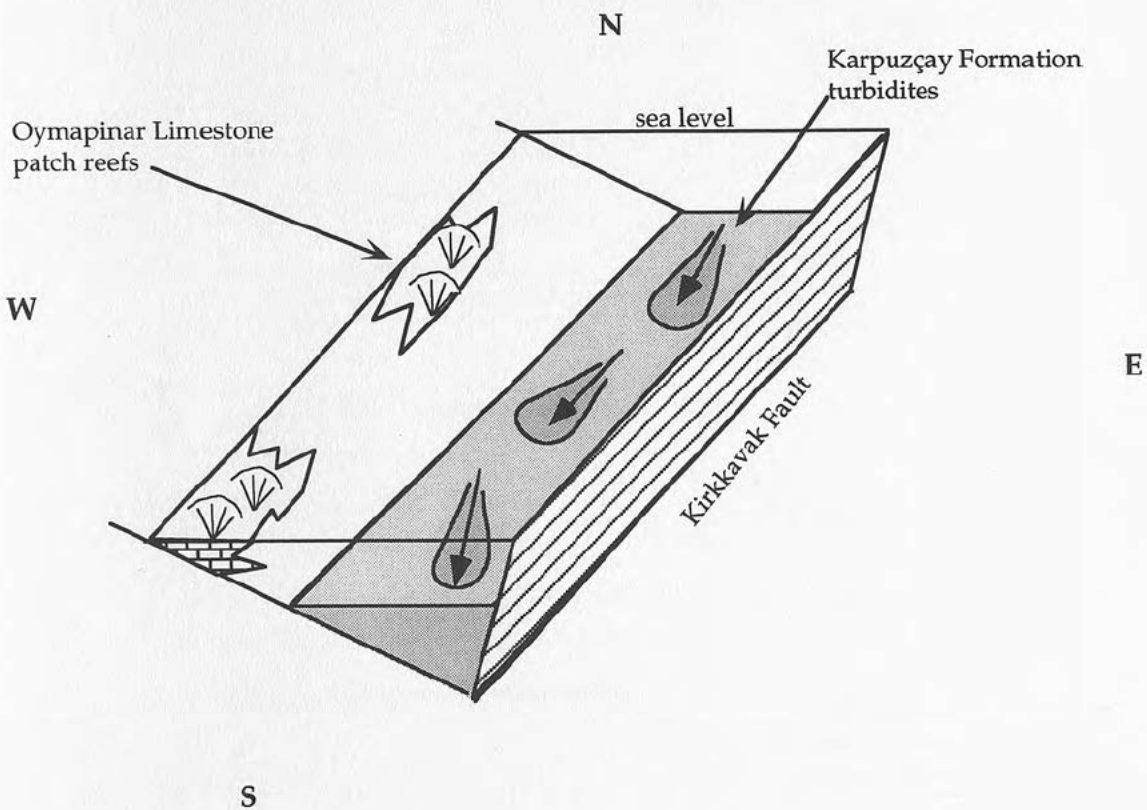


Figure 4.17 Schematic palaeogeographic reconstruction of the Köprü basin based on the apparent coeval deposition of turbidites in the east of the basin and shallow-water carbonates in the west in the Burdigalian. Note however that there is little evidence to suggest that the carbonates were shedding material east into the basin at this time and it is possible that the ages of the turbidites reflect reworking of older material rather than the age of deposition of the Karpuzçay Formation.

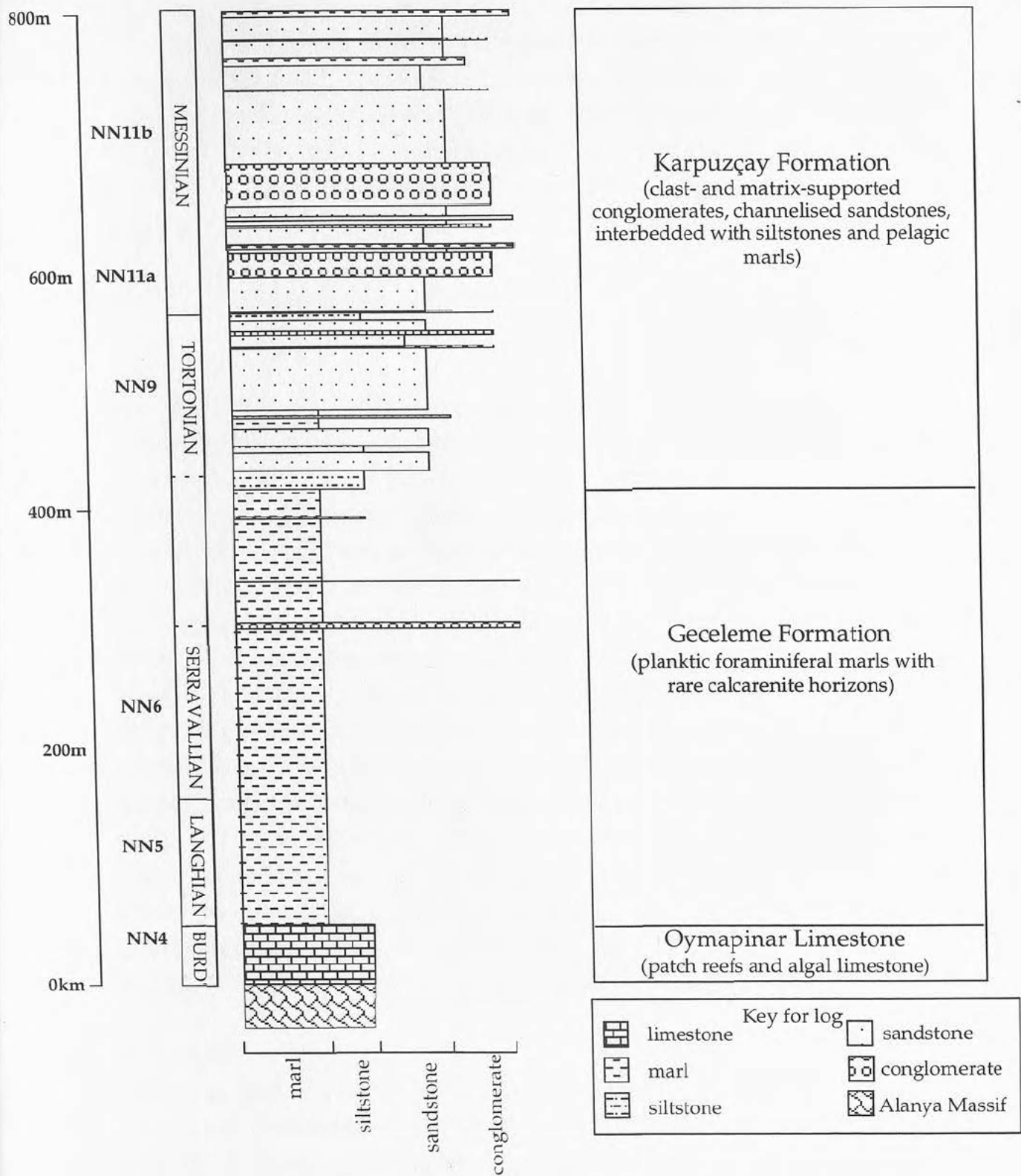


Figure 4.18 Summary log of the Ahmetler section showing the lithology, formation and the ages derived from nannoplankton analysis (modified after Flecker *et al.*, 1995).

Karpuzçay Formation overlies Serravallian planktic foraminiferal marls (Geceleme Formation). This contact is gradational over ~20m. The upper contact of Karpuzçay Formation is poorly exposed, but can be seen in a few places in the south of the Manavgat basin along the coast road where there is a subtle, shallow angular discordance with the overlying Pliocene succession. The implications of this unconformity are discussed in chapter 7.

4.5.3.1 Texture and composition

Thickness:

Bed thickness generally increases up section in the Manavgat basin. Siltstones and mudstones are rarely more than 10cm thick and have an average thickness of less than half that. At the base of the Karpuzçay Formation in the Ahmetler section (exposed at the junction between the road to Akseki and the track to Ahmetler), sandstone horizons 5cm thick or less are interbedded with 20-40cms of thinly bedded siltstones and mudstones (Appendix 5). Occasionally, coarser sandstone horizons up to 40cm thick are observed, e.g. just south of Alarahan near the village of Ulugüney. Higher up in the succession however, the variability of sandstone thickness increases and some massive sandstones are several metres thick. Near the base of the Karpuzçay exposure in the Ahmetler section, rare pebble horizons are thin, generally only a few centimetres thick. Conglomerates and debris flows further up the section, however, vary in thickness, but can be up to 8m thick. Channelised beds vary in thickness from 10cm to 2-3m as can be seen in the central region of the Ahmetler section (near sample 18S.344.7, Appendix 5). The thickness of slumped beds varies from 0.5-10m within the Ahmetler section.

Bed shape:

Siltstones and mudstone beds are dominated by parallel-sided geometry, as are the sandstones in the lower parts of the succession. Occasionally, sandstone lenses in mudstone are seen as at site 308 (Appendix 5). Further up the succession however, sandstones become increasingly erosively bedded and channelised (Fig. 4.15). The superimposition of conglomerate and sandstone channels produces abundant wedging out geometries in the central and upper parts of the succession (Fig. 4.12).

Some of these channelised conglomerates pass laterally into sandstones. Large scale slumps, several meters thick (Fig. 4.15), often have undulating exterior bedding surfaces.

Grain size:

The Karpuzçay Formation in the Ahmetler section contains a full range of grain-sizes from mud-grade to conglomerate with detached blocks 7-10m in diameter (Fig. 4.15). Siltstones and mudstones dominate the lower half of the section and over the transitional interval from the Geceleme Formation (planktic foraminiferal marls). Higher up the section sandstones and conglomerates become increasingly dominant.

Composition:

Figure 4.19 is a triangular diagram plotting the relative proportions of various groups of clast types found in the conglomerates and debris flows in the Ahmetler section. The analyses plotted include measurements from the Çakallar and Geceleme formations and these can be clearly distinguished from the Karpuzçay Formation measurements. What this indicates is that there was a change in the composition of coarse clastic deposits with time. Early calcirudites in the Geceleme and Çakallar Formations contain only Alanya Massif metacarbonates and Miocene shallow-water carbonate detritus. The later clast-supported and matrix-supported conglomerates of the Karpuzçay Formation by contrast, contain much more varied clast-types. In detail this change occurs abruptly over about 20m of stratigraphic thickness and coincides with both the appearance of sandstone in the section for the first time and quartz grains in the siltstones. Subsequently the quantity of Miocene shallow-water carbonate detritus gradually decreases whilst the percentage of Alanya Massif metacarbonate remains relatively constant. Almost without exception, the mega-detached blocks in the debris flows are made of Alanya Massif metacarbonate.

Rip-up clasts of marl make up a significant part of many of the clast-supported and matrix-supported conglomerates, particularly at the base of beds. They are also found at the base of many of the coarser sandstone units. Marl and marly siltstone is the most common matrix of the

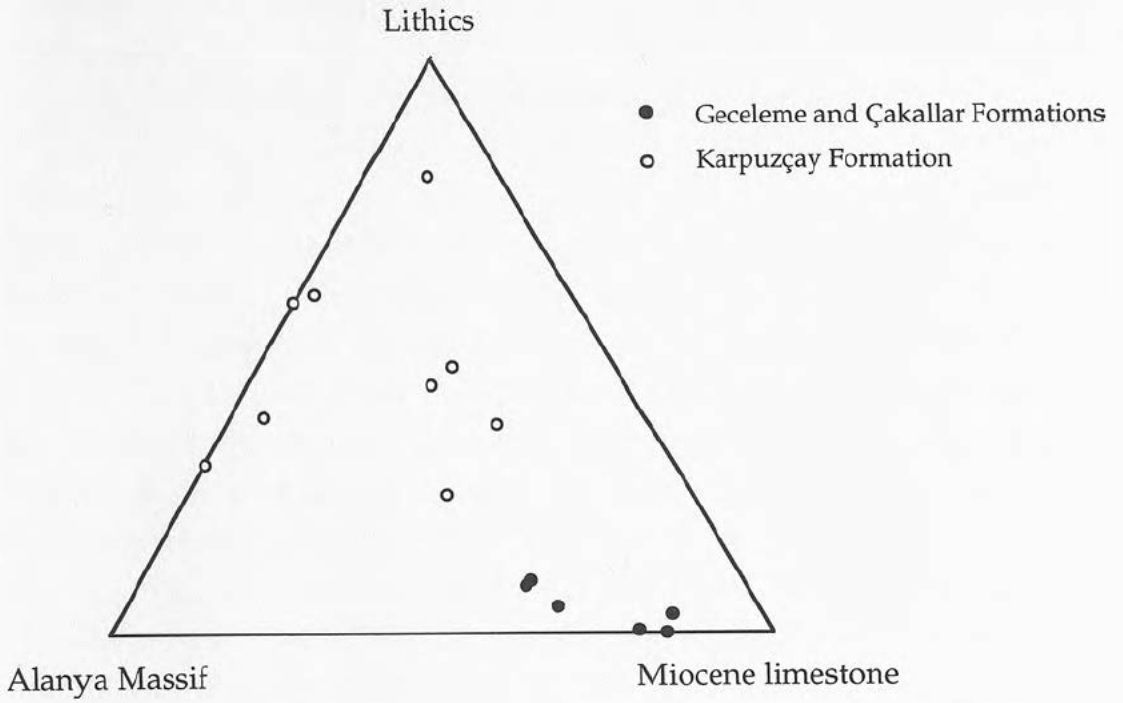


Figure 4.19 Triangular diagram plotting the relative proportions of Alanya Massif metacarbonate, Miocene shallow-water carbonate and lithic clasts in conglomerates from the Çalallar, Geceleme and Karpuzçay Formation in the Ahmetler section, east Manavgat basin.

matrix-supported conglomerates in the Manavgat basin, often making up 40% or more by volume of the rock.

In the Messinian, extremely rare, thin horizons of concentrated, fresh-looking, detrital Biotite are found. It is not clear what this represents and it is only seen in one other locality, in Middle Miocene marls (C. Müller pers. com., 1994) to the south east of Gebiz. Akay *et al.* (1985) report occasional volcanic tuff interbeds in the Karpuzçay Formation, but no such beds were identified during this study. The freshness of the biotite suggests that it has not been transported far and may have a volcanic origin. Lower Pliocene-Quaternary volcanism in the area has been reported by Lefevre *et al.* (1983) and K-Ar studies of Pliocene ignimbrites are currently being undertaken by C. Glover as part of a Ph.D. project. Miocene aged tuffs were noted in the Kithrea Flysch in northern Cyprus (A. Robertson pers. com., 1994) suggesting that Miocene volcanism is not entirely unknown in the area.

Sandstones, particularly massive sandstones, often contain shell fragments entrained along the base of beds. The fauna identified from these beds includes, bivalves, coral, rhodoliths, bryozoa and the large benthic foraminifera, *Operculina sp.* Slumps can also be rich in shell fragments. Brown plant material is common throughout the Karpuzçay succession in the Manavgat basin, but organic detritus is dominated by coal fragments of varying sizes which occurs in marls, siltstones and sandstones alike. Although ubiquitous on the large scale, millimetre thick horizons of concentrated coal fragments are the most common form of occurrence. One 7cm thick coal detritus layer which occurs towards the top of the section (sample 20S.352.3, Appendix 5), thins laterally, having a channel-shaped geometry. The biogenic components of the marls and siltstones resemble those of the Geceleme and Çakallar Formations and are described in section 3.6.4.1.

Sorting and physical maturity:

One of the most major differences between the clast-supported and matrix-supported conglomerates in the Manavgat basin, is that the clast-supported conglomerates tend to be moderately sorted, while the matrix-supported conglomerates are generally very poorly sorted. In the latter,

detached blocks several metres in diameter and often wider than the thickness of the debris flow horizon in which they have been transported, are surrounded by clasts with an average grain-size of a few tens of centimetres and sometimes less. The sorting of sandstones varies from moderately well sorted to poorly sorted. The latter are sometimes associated with bioturbation traces.

The physical maturity of clasts in the Manavgat basin, as in the Köprü basin, depends to some extent on the nature of the clasts (section 4.5.2.1). Miocene shallow-water carbonate clasts tend to be angular in the lower part of the section and more rounded towards the top. Alanya Massif metacarbonate schist clasts are also angular. The dark grey recrystallised form of Alanya Massif limestone occurs as both rounded and angular clasts in the lower part of the succession, but becomes increasingly rounded at the top.

Grading:

Normal-graded beds of sandstone to siltstone or marl are found with increasing abundance towards the top of the Ahmetler section. Clast-supported and matrix-supported conglomerates also sometimes show normal grading as do some of the debris flow deposits. Figure 4.20 is an example of a matrix-supported conglomerate unit with a normally-graded, imbricated, clast-supported basal layer.

Clast alignment and grain interaction:

Both Pteropod moulds and organic fragments show bedding parallel alignment. However, alignment within the plane of the bed was rarely observed. Imbrication in both clast- and matrix-supported conglomerates is relatively common particularly in the upper parts of the succession (Fig. 4.20).

Structures-:

Parallel laminations were observed relatively frequently in sandstones and siltstones. Some mudstones at the base of the Ahmetler section are laminated to the point of appearing fissile.



Figure 4.20 Photograph of a unit with a clast-supported, imbricated basal layer and an upper layer of matrix-supported conglomerate from the Karpuzçay Formation, Ahmetler section, east Manavgat basin.



Figure 4.21 Photograph of distorted beds interpreted as a water escape structure intruding into an imbricated conglomerate, Karpuzçay Formation, Ahmetler section, east Manavgat basin.

In comparison with both the Köprü and Aksu basins the Manavgat basin has a much lower frequency of cross-laminations and ripples. They occur in both sandstones and siltstones with increasing frequency at the top of the succession and are often capped with a mud drape, a few millimetres to several centimetres in thickness. Many coal-rich layers are also rippled. No wave ripples have been observed in this section. Cross-stratification was not observed in the Ahmetler section, but outcrops of cross-bedded sandstones and conglomeratic sandstones occur in a channel to the south of Akdam (the palaeocurrent direction indicated by these cross-sets is discussed in section 4.5.3.4) and in the Messinian section to the south of Alarahan.

3) Several spectacular examples of different types of distorted beds interpreted as water escape structures can be seen at the top of the Ahmetler section. These include the vertical structure 1.5m in height, shown in figure 4.21 (site 348, Appendix 5); a large load structure shown in figure 4.22 (site 356, Appendix 5) and a series of 6 asymmetrical flame structures (0.5-1m in height) along a single bed.

The Geceleme and Çakallar formations are largely free of burrowing traces whilst the Karpuzçay Formation in contrast is extensively burrowed. Burrowing, generally *Chondrites*, was first observed fairly low down the Ahmetler section (site 316, Appendix 5). The diversity of trace fossils increases upwards reaching a maximum diversity in the Tortonian (site 327, Appendix 5) where extensive networks of the branching echinoid burrow, *Thalassinoides* are found with *Chondrites*, *Zoophycos*, *Lophoctenium*, *Arenicolites* and other unidentified traces. Upper parts of the Ahmetler section contain a lower diversity of burrowing traces, but *Chondrites* is fairly ubiquitous. According to Chamberlain (1978) and Pemberton (1992) *Chondrites*, *Zoophycos*, *Lophoctenium*, and *Arenicolites* are common as an assemblage associated with turbidites in off-shore to bathyal environments, indicating an approximate water depth range of 150-3000m (Fig. 4.24). *Thalassinoides* however is characteristic only of off-shore environments. Thus, the ichnofacies assemblage found at site 327 indicates that the water depth of the basin was in the region of 150m or less. *Chondrites* outside this assemblage can be found in bathyal to nearshore environments (Chamberlain 1978,



Figure 4.22 Photograph of a large load structure located in the Messinian of the Karpuzçay Formation, Ahmetler section, south eastern Manavgat basin.



Figure 4.23 Photograph of layered bioturbation at site 327, Karpuzçay Formation, in the Ahmetler section, north-eastern Manavgat basin.

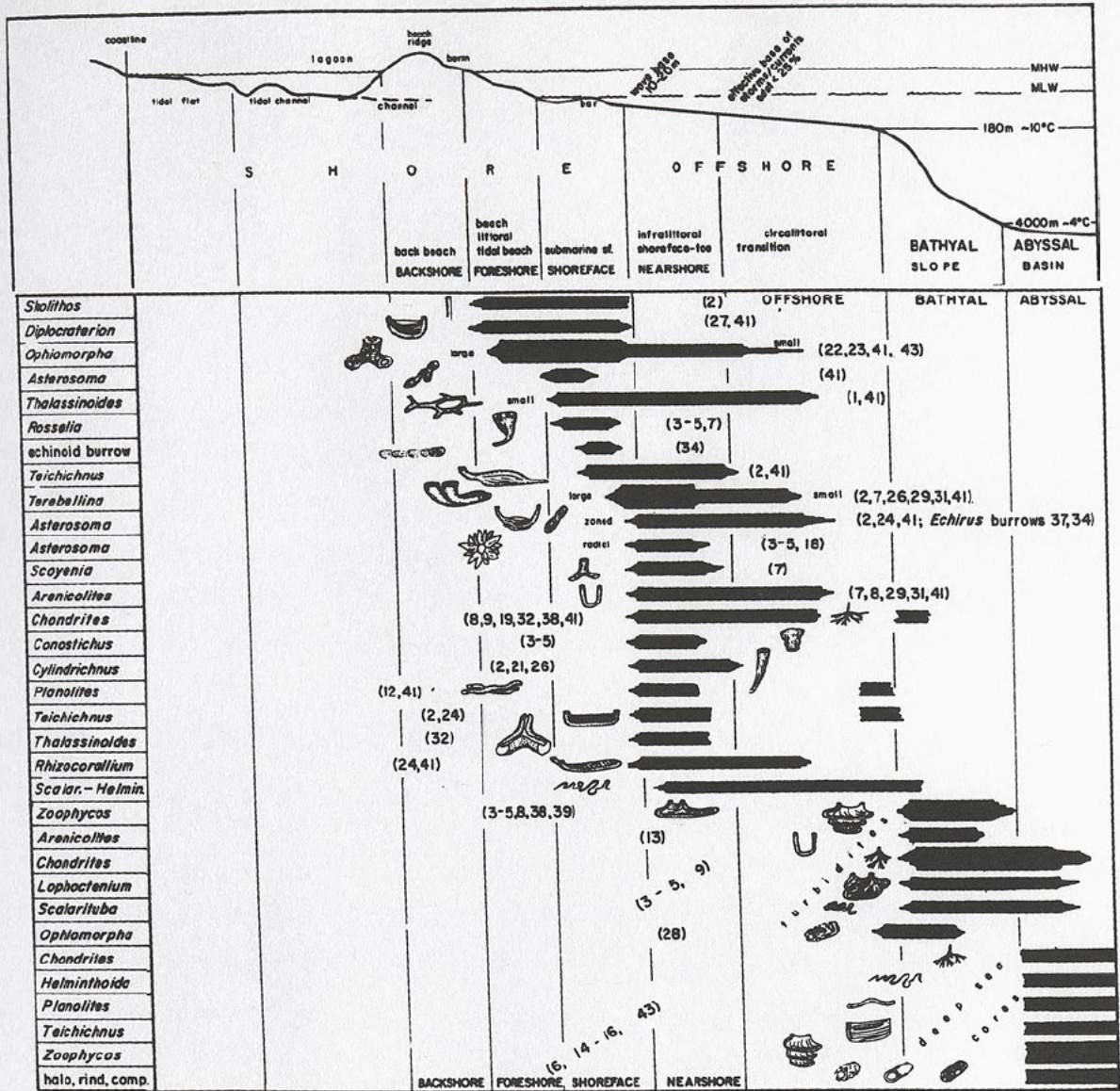


Figure 4.24 Chart of ichnofossils plotted against depth (after Chamberlain, 1978; Pemberton, 1992). Numbers refer to references in the original text.

Pemberton 1992). Figure 4.23 shows a more common exposure of burrowing, where contrasting layers of marl and sandstone allow clear trace identification.

Tool Marks are far less abundant than in the Köprü and Aksu basins, but they are common enough from site 344 up-section (Appendix 5) to give convincing palaeocurrent directions which are discussed in section 4.5.3.4.

Slumps are common from site 344 onwards (Appendix 5; Fig. 4.15), but vary greatly in thickness and grain-size. Where the exposure permits towards the top of the sequence a slump has been observed, passing laterally into a matrix-supported conglomerate with no discernible slump structures. This is in agreement with the common consideration of debris flows as being part of a continuum between slumps and turbidity currents (Rupke 1978). The orientation of the palaeoslope deduced from these slumps is discussed below (section 4.5.3.4).

Syn-sedimentary deformation structures

Syn-sedimentary faulting was occasionally observed within the Karpuzçay Formation in the Manavgat basin, but it is not common. Figure 4.25 shows a locality where approximately 1.5m of marls interbedded with siltstones and sandstones have been fractured and forced up into the overlying matrix-supported conglomerate. Both brittle and ductile deformation have taken place in the processes.

4.5.3.2 Interpretation

Many of the finer-grained units (medium-grained sandstone to clay grain-size populations) exposed in the Manavgat basin can be interpreted in a similar way to the Karpuzçay Formation in the Köprü and Aksu basin (section 4.5.1.2). Tables 4.1 and 4.2 summarise the turbidite sub-facies identified using a classification scheme after Pickering *et al.*, (1989). Exposure of the coarser grain-size population (coarse sandstone to detached blocks several meters in diameter) is restricted to the Manavgat basin and the small locality near the Bucak junction in the Aksu basin (section 4.5.1.3 and 4) and the processes of deposition of these facies are briefly described below.



Figure 4.25 Photograph of the "snapped beds" at site 345, where both ductile and brittle deformation have occurred during deposition of the overlying conglomerate unit, Karpuzçay Formation, Ahmetler section, south-eastern Manavgat basin.

The coarsest grain-size population can be divided into 3 facies: clast-supported conglomerates; matrix-supported conglomerates and sandstones. These have been subdivided into sub-facies as shown in Tables 4.3 and 4.4.

The internal structures of matrix-supported conglomerates can be explained in terms of debris flow processes. The flow rheology and particle-support mechanism have been briefly described in section 4.5.1.2. Chaotic structureless units with clasts dispersed fairly uniformly through the matrix suggest the existence of weak intergranular dispersive pressure (Lowe, 1976; 1979) or flow turbulence (Enos, 1977) and are thought to be preserved by freezing of the flow due to intergranular friction and cohesion. In some units, an upper cap of structureless matrix-supported conglomerate overlies a clast-supported conglomerate base (e.g. Fig 4.20). Typically, this basal layer is coarser and the grainsize distribution reflects the particle size limit that the matrix was capable of supporting during flow, such that clasts larger than this were able to settle through the matrix (Lowe, 1982). Imbrication of such layers is common and indicates intense grain interaction. Much of the variety of structures observed in debris flows is dependent on the percentage of matrix and whether the flow was turbulent at any time during its depositional history. Enos (1977) suggested that a fully turbulent flow could support much larger clasts than matrix cohesiveness and buoyancy alone. The size of some of the detached blocks (i.e. up to ~10m across) suggests that even a fully turbulent flow is unlikely to have been able to support them. Instead, they may have slid and bounced down slope, lubricated by the water-sediment mix. Turbulent flow is likely to have been active however, in the deposition of units with a relatively coarse matrix (e.g. sand-grade).

Debris flows also occur in subaerial environments and are discussed within the context of alluvial sedimentation in chapter 5 (section 5.6.1.3). Nemeč and Steel (1984) suggested a number of internal structural criteria that could be used to distinguish the two environments of deposition (Table 5.5). The structures generally associated with subaqueous debris flow units can be seen in figure 4.26 (after Nemeč and Steel, 1984).

Table 4.3 Description and classification of matrix-supported conglomerates in the Manaogat basin.

Structures	Sub-facies (Pickering <i>et al.</i> 1989)	Depositional process	Current type
Clast supported, thickly bedded, flat bedded-deeply scoured, poorly sorted clasts, plastically deformed mud clasts common	A1.1 Disorganised gravel	Freezing on decreasing bottom slopes due to intergranular friction and cohesion	High concentration turbidity flow or debris flow
Matrix supported, 10-50% mud-grade material, medium-thick bedded, often little erosion into underlying beds but upper surface hummocky, large boulders dispersed throughout, enormous detached blocks	A1.2 Disorganised muddy gravel	Freezing on decreasing bottom slopes due to intergranular friction and cohesion	Cohesive debris flow. Detached blocks may slide into place on a cushion of over-pressured or liquefied mud (Labaume <i>et al.</i> 1983)
Similar to A1.2, but contains 50-95% mud, irregular shape over short distance	A1.3 Disorganised gravely mud	Freezing on decreasing bottom slopes as the shear stress at the base of the flow becomes less than the cohesive strength	Cohesive mud flows (debris flows)
Similar to A1.1, but clasts are dispersed through a sand matrix	A1.4 Disorganised pebbly sand	Rapid collective grain deposition of a pebble sand mixture due to increased intergranular friction as the flow decelerates	High concentration turbidity flow

Table 4.4. Description and classification of clast-supported conglomerates and sandstones in the Manavgat basin.

Structures	Sub-facies (Pickering <i>et al.</i> 1989)	Depositional process	Current type
Imbrication, cross-stratification, lenticular to wedge-shaped bodies	A2.1 Stratified gravel	Grain-by grain deposition from suspension and then traction transport as bed-load	High concentration turbidity flow
Erosive, laterally thinning, poorly sorted, imbricated, inverse grading with or without overlying normal grading	A2.2 Inversely graded gravel	Rapid deposition of a concentrated traction carpet due to increased intergranular friction. Inverse grading and Imbrication are caused by intense grain interaction	High concentration turbidity currents
Normal grading, scour, clast-supported	A2.3 Normally graded gravel	Grain-by grain deposition from suspension with little subsequent tractional transport	High concentration turbidity currents
Normal grading, scour, clast-supported	A2.7 Normally graded pebbly sand	Grain-by grain deposition from suspension with little subsequent tractional transport	High concentration turbidity currents
Laterally continuous, grading absent or poorly developed, water escape structures,	B1.1 Thick-medium bedded disorganised sands	Rapid mass deposition due to intergranular friction in a concentrated dispersion near the bed. Resultant open grain packing may collapse during or after deposition resulting in the escape of poor fluids and formation of fluid escape structures	High concentration turbidity currents

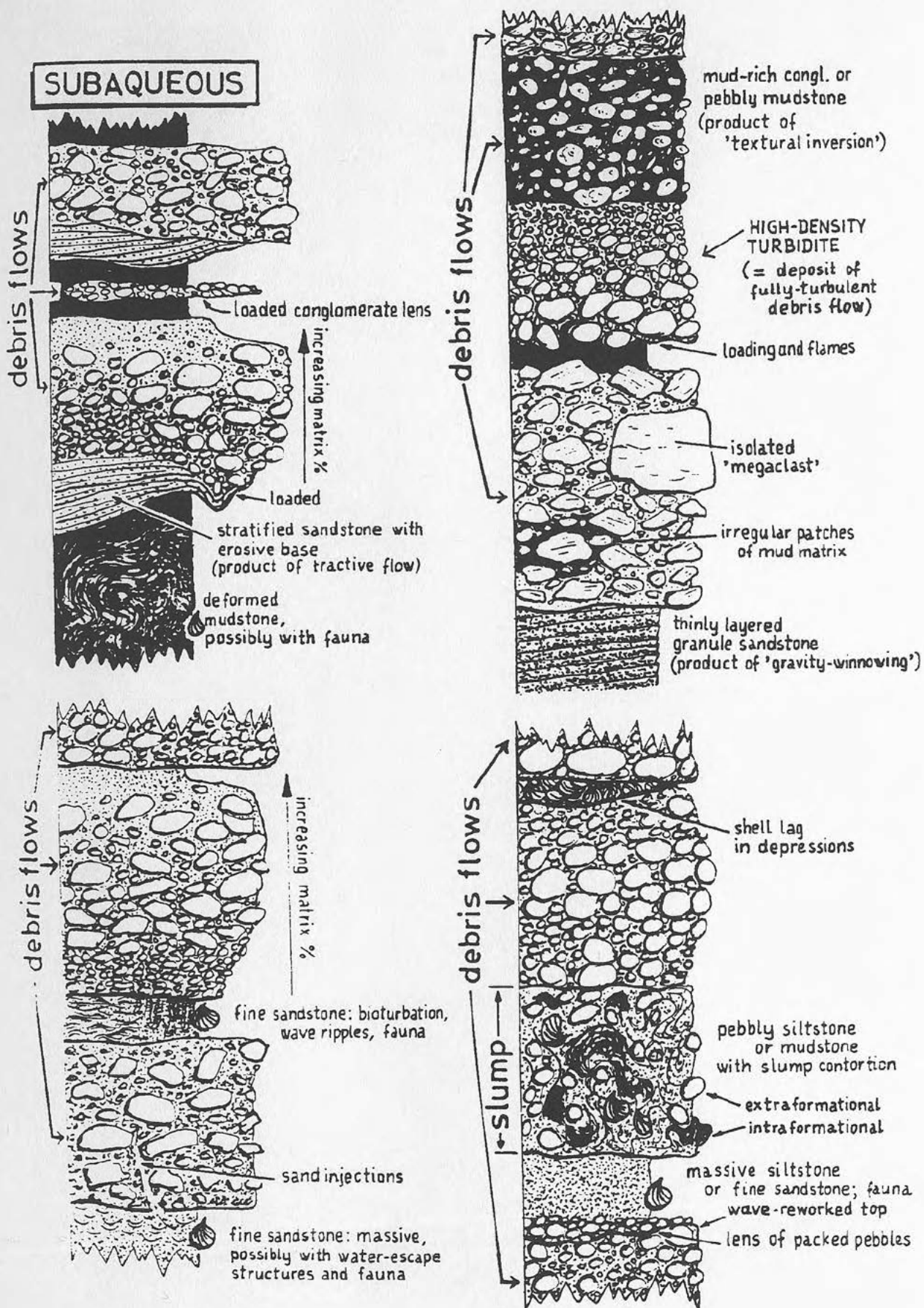


Figure 4.26 Characteristics of subaqueous debris flows (Nemec and Steel, 1984).

The disorganised character of some clast-supported conglomerates and coarse sandstones allows comparison with debris flow deposits. Where the amount of medium sand to mud grade matrix is <5% by volume, this suggests a non-cohesive transport mechanism (Ineson, 1989). In the field this was difficult to assess accurately, but it is thought that units with <5% matrix were relatively uncommon so that some buoyant lift from the matrix would have been active in reducing the effective weight of clasts (Rodine and Johnson, 1976). This may help to explain the generally coarse nature of the clast-supported conglomerates, although fully turbulent high-density flow is also capable of supporting and depositing coarse units. The internal structures observed such as imbrication, cross-stratification, inverse and normal grading result from various combinations of the processes active during deposition from high-density turbidity currents and debris flows e.g. traction sedimentation, deposition from suspension and frictional intergranular freezing.

4.5.3.3 Spatial and temporal variations

69 samples from the Ahmetler section were analysed for nannoplankton by C. Müller (pers. comm., 1992). With an average sampling rate of just under one sample for every 10m a far more detailed nannoplankton biostratigraphy has been set up than had been attempted by previous workers (Fig. 4.18; Appendices 5 and 3a). Other sections in the Manavgat basin were not sampled in so much detail due partly to the lack of such good exposure as that along the Ahmetler section, and because of time constraints. Because in general the exposure of vertical successions is so good in the Manavgat basin, a far more detailed study of spatial and temporal variations is possible here than in the Köprü or Aksu basins.

Analyses of the benthic/planktic foraminiferal ratio of nearly 40 marl samples from the Ahmetler section are shown in figure 4.27. The trend has been interpreted as indicating a shallowing-upwards sequence beginning as soon as shallow-water carbonate deposition had ceased (Latest Burdigalian- Early Langhian) and continuing throughout the Miocene. No evidence of emergence was observed at the top of the section (i.e. no wave ripples, desiccation cracks, evidence of continental or

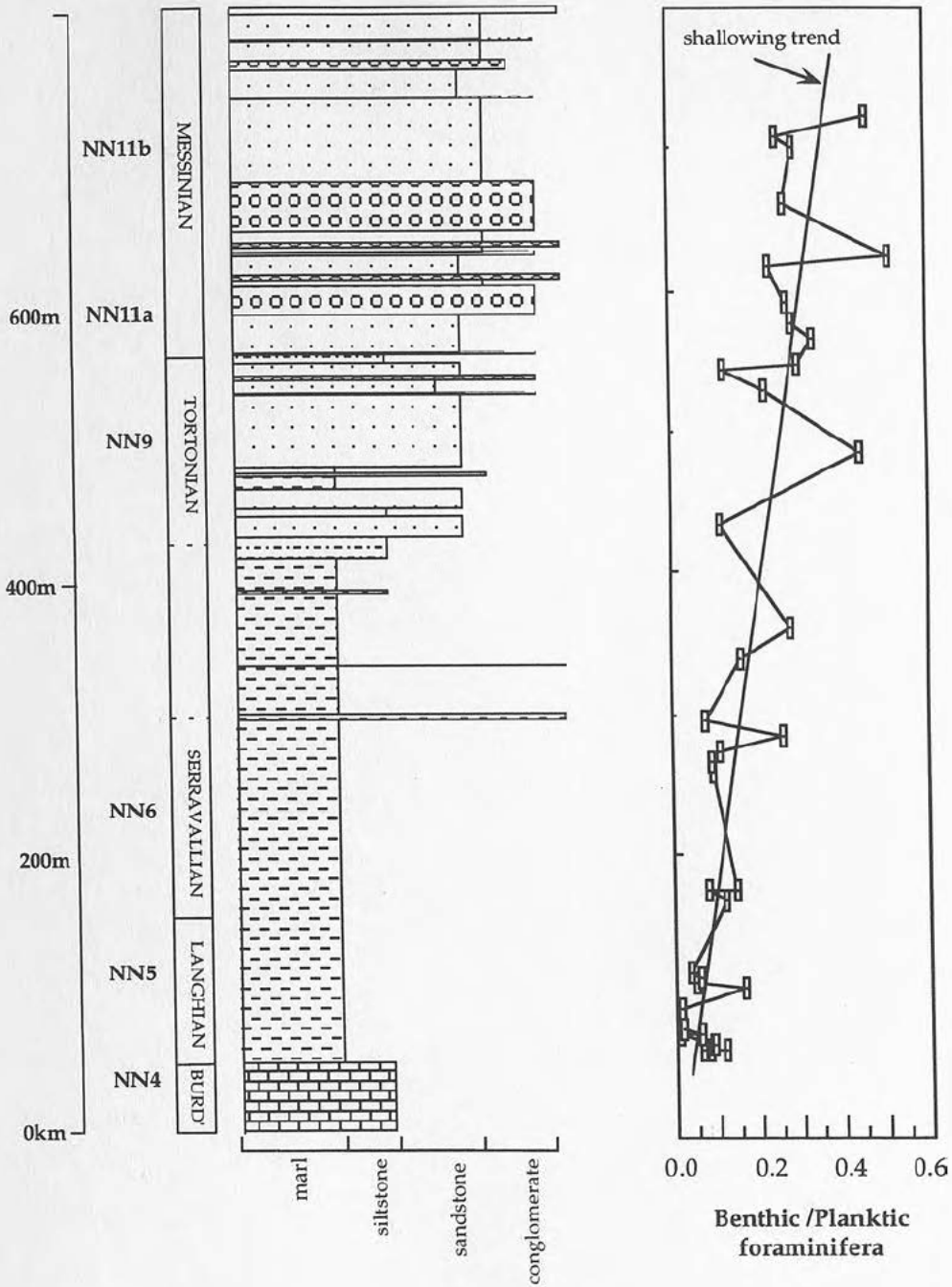


Figure 4.27 Plot of the benthic to planktic foraminiferal ratio for the Ahmetler section in the north of the Manavgat basin, showing a shallowing upwards trend.

estuarine conditions), so it is assumed that the depositional setting remained below wave base even at its shallowest.

Interpretation of this shallowing upwards trend is not without its difficulties however. As noted in section 3.6.4.1, the marls in the Geceleme and Çakallar formations consist both of horizons containing shallow-water detritus, which is thought to have been transported and others which contain little shallow-water debris. The Karpuzçay Formation has been interpreted as the product of turbiditic and debris flow activity and therefore, by their very nature contain reworked components. Some of the scatter in benthic/planktic ratios may, therefore, be explained, at least in part, by transport of shallow-water material including benthic foraminifera. Despite this scatter, however, a trend is clearly visible and it seems likely that this reflects a real shallowing upwards of the basin. The palaeobathymetry indicated by the benthic foraminifera, however, only provides an estimate of the minimum water depth (table 3.12). The ichnofacies identified in the central part of the Ahmetler section indicate slightly deeper water than the benthic foraminifera, but the absence of burrowing traces in the lower part of the section means that the palaeobathymetry for the first 200m of this section can only be estimated. The Late Miocene abundance of *Chondrites* traces may indicate either a stable water depth or a decreasing one. The increasingly dominant nature of the conglomerates and debris flows particularly in the Messinian part of the section indicates the increasing proximity of the source area and this may well have been caused by a relative sea level fall.

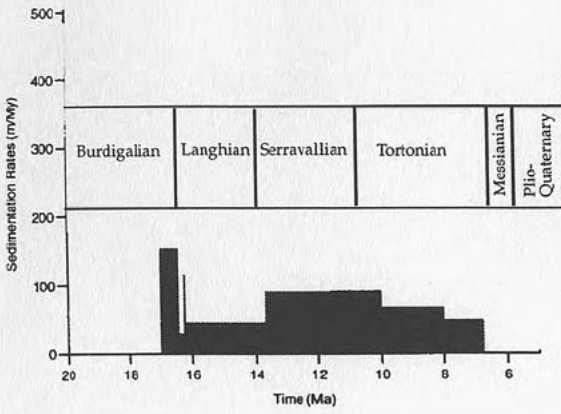
The sudden influx of sand detritus in the Ahmetler section occurs over a sampling period which failed to produce the characteristic nannoplankton markers to identify NN7 and NN8. The close proximity of this part of the succession to samples containing nannoplankton characteristic of NN9 indicates that the sand input probably occurred in the Early Tortonian. Correlation of the timing of the sand input with other sections in the Manavgat basin is hampered by this ambiguity, but it seems likely that the change in provenance was a relatively synchronous event affecting all parts of the basin.

Nannoplankton characteristic of zone NN10 were not identified in the Ahmetler section. This may indicate a period of non-deposition, although given that the dominant deposits from NN9 onwards are coarse clastics, this seems unlikely. It is possible that though deposited, all traces of NN10 in the Ahmetler section were subsequently removed by the erosive power of NN11a deposits. However, the most likely scenario is that NN10 lies within a sampling gap which, in this part of the section is about 100m.

None of the other sections in the Manavgat basin show anything like the concentration of coarse-grained, high-energy deposits such as those seen in the Ahmetler section. The absence of debris flows containing huge detached blocks anywhere other than the Ahmetler section is an obvious expression of this. In part this is due to the spectacularly continuous nature of the exposure seen along the road to Akseki, but it must also be admitted that some of the difference is due to lateral variation. It seems likely that the region south of Ahmetler was some sort of a broad channelised system, away from which to both east and west the deposits fined (Fig. 4.29). This channelised system may represent the highest energy deposits of a fan-delta system, similar, but on a larger scale to that seen in the Aksu basin, concentrated in a relatively restricted north-south trending area. The patchy distribution of the Çakallar Formation calcirudites and reef talus is concentrated in the same area as the coarse-grained Karpuzçay Formation in the Manavgat basin. This systematic distribution of coarse material throughout the Middle-Upper Miocene is discussed further in chapter 7 (section 7.5.1.2) where a structural hypothesis is suggested for this geographical relationship through time.

There is an increase in sedimentation rate from the Geceleme Formation planktic foraminiferal marls through the Late Serravallian and into the Early Tortonian Karpuzçay Formation in both the Ahmetler and the Alarahan sections (Fig. 4.28). The more limited data set from the Oymapinar section to the NW shows no such increase. Despite this, sedimentation rate information (Fig. 4.28) and field observations (Fig. 4.29) suggest that there is a correlation between high sedimentation rate and the occurrence of coarse, conglomeratic Karpuzçay Formation.

Ahmetler



Alarahan

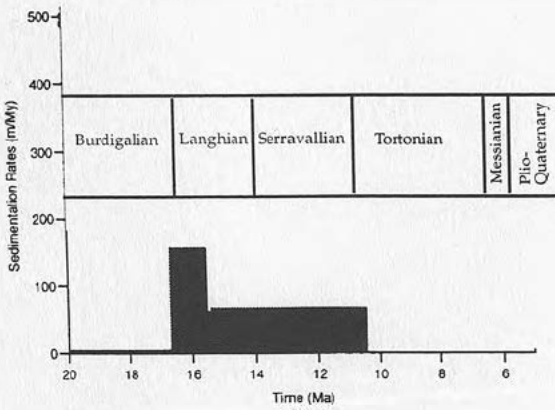
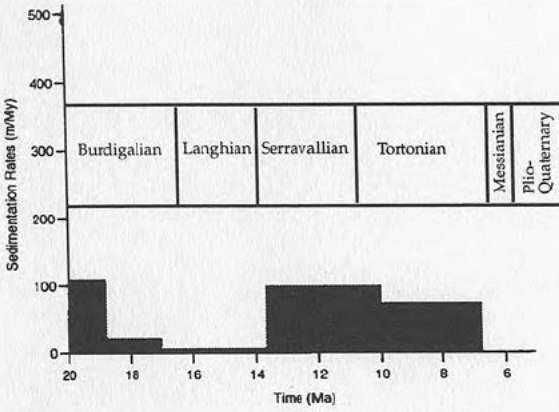


Figure 4.28 Miocene sedimentation rates for the Ahmetler, Oymapinar and Alarahan sections in the Manavgat basin (see Appendix 6).

SOUTH EAST

NORTH WEST

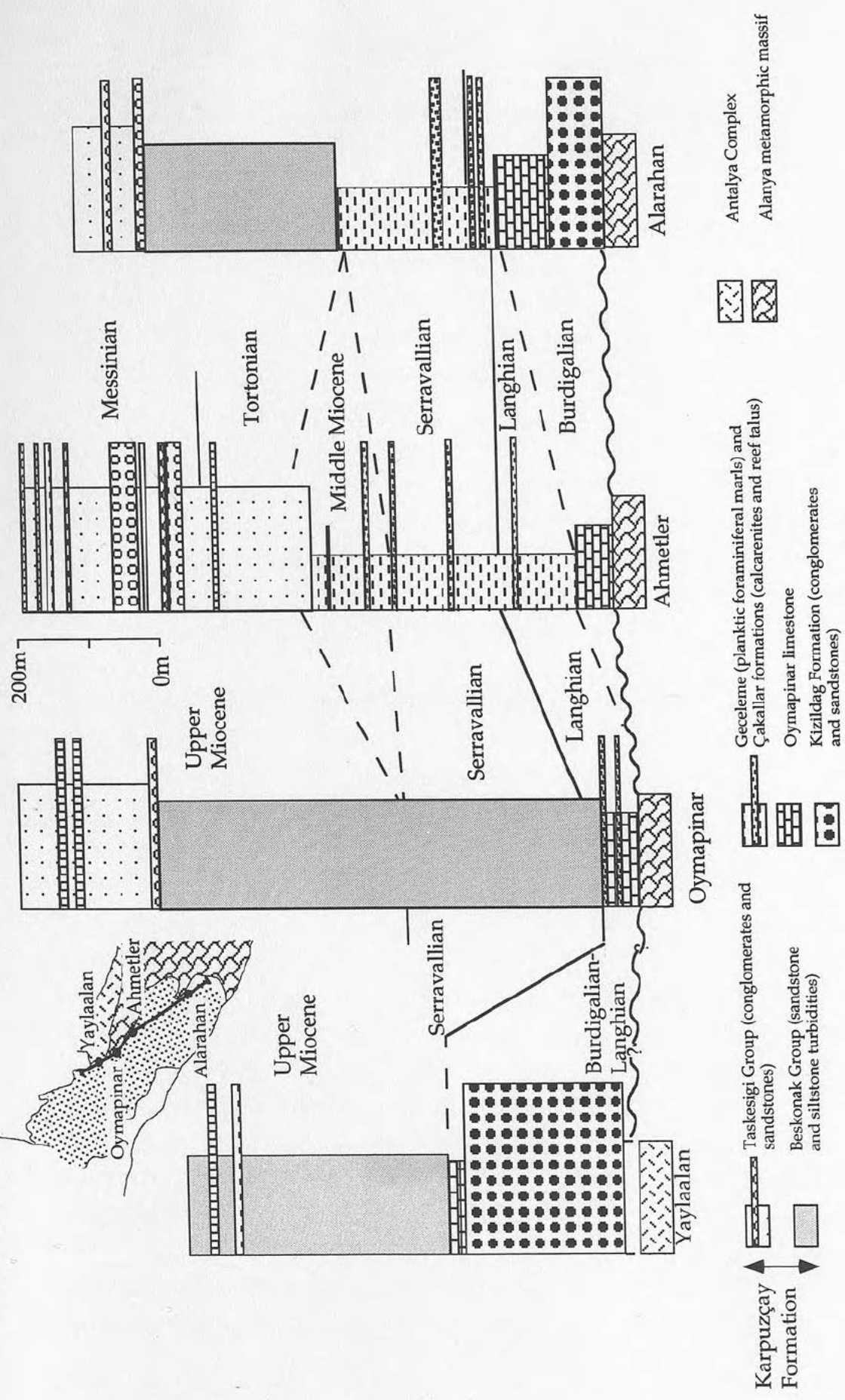







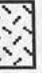
Figure 4.29 Correlation of four sections from the Manavgat basin.

4.5.3.4 Palaeocurrent analysis

Rose diagrams for the Karpuzçay Formation in the Manavgat basin are displayed in figure 4.30. The prevailing palaeocurrent direction for the formation is towards the south west although south and south east directions are also sometimes indicated. There appears to be little disparity between the palaeocurrent directions measured along the Ahmetler section and those from other parts of the basin and this probably indicates that the Karpuzçay Formation was deposited from a series of channels along its northern margin, the most high-energy of which was located in the Ahmetler area. The north and west directed cross-sets from a channel system in the far south east of the basin near Akdam, are unusual and may represent a sediment source to the east or south east. This system does not appear to have been a powerful one since there is no indication of further penetration of the west and north directed currents into the main part of the Manavgat basin. No difference in composition of the sandstones was noted.

4.7 Summary interpretation and reclassification of the Karpuzçay Formation

Study of the Karpuzçay Formation in the Aksu and Köprü basins suggests that the interbedded sandstones and siltstones found here can be interpreted mainly in terms of low- and high-density turbidity currents. The exposure mapped as Karpuzçay Formation in the Manavgat basin however, is dominated by clast-supported and matrix-supported conglomerates. These have been interpreted in terms of high density turbidity currents and debris flow processes. The age of this coarse-grained sequence is significantly younger (Tortonian-Messinian) than the turbidites in the Aksu and Köprü basin (mainly Serravallian and Lower Tortonian). To reflect these differences, the Karpuzçay Formation has been sub-divided into two groups: the Beskonak Member, comprising the Aksu and Köprü basin sandstone and siltstone dominated succession, and the Taskesigi Member comprising the coarse, conglomeratic sequence exposed in the Manavgat basin. A summary of the features, type section localities and synonyms is given in Table 2.3.

-  Karpuzçay Formation (turbidites and debris flows)
-  Geceleme Formation (planktic foraminiferal marls) and Çakallar Formation (calcareenites and reef talus)
-  Oymapinar Limestone (shallow-water carbonate)
-  Kizildag Formation (conglomerates and sandstones)
-  Alanya Massif
-  Antalya Complex

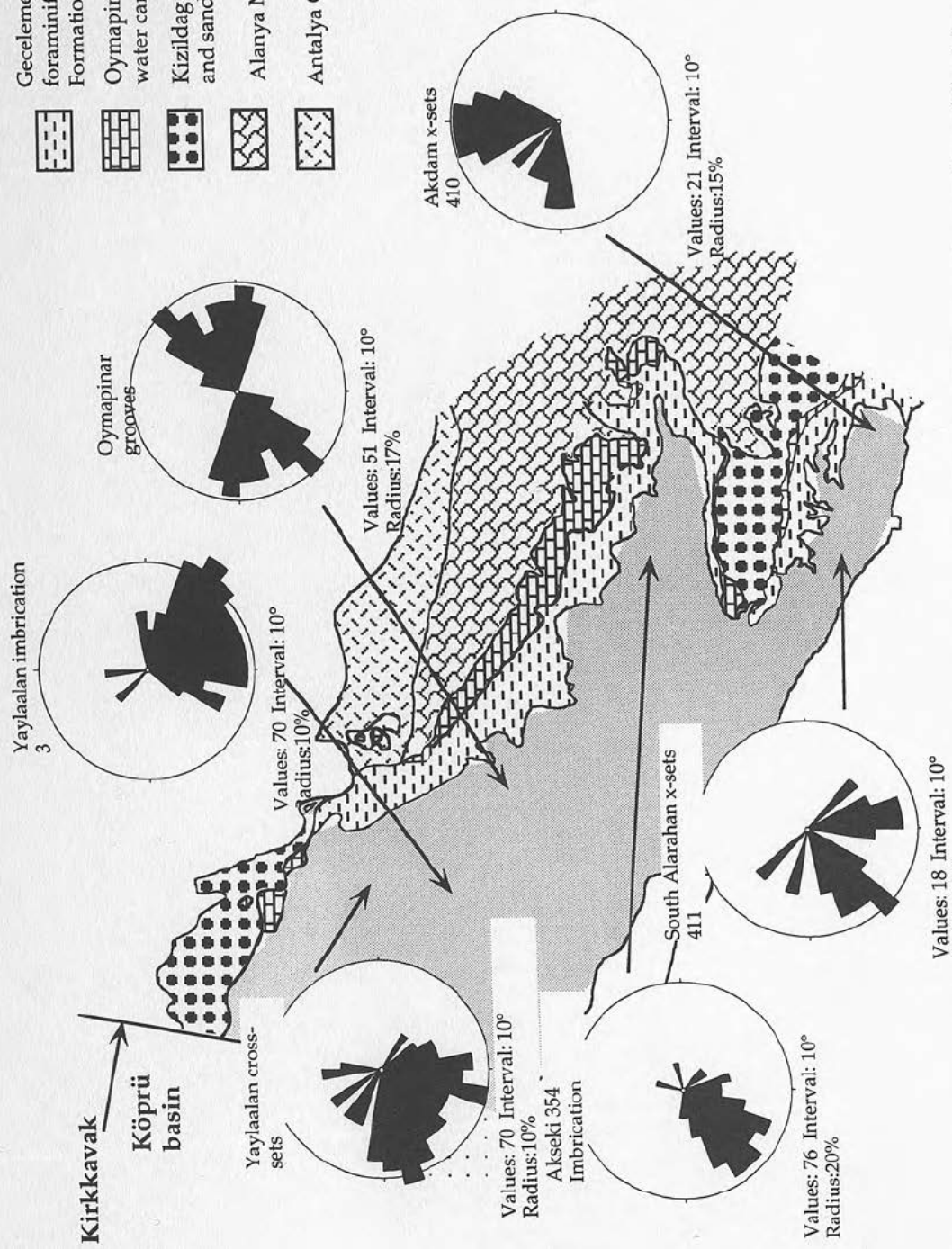


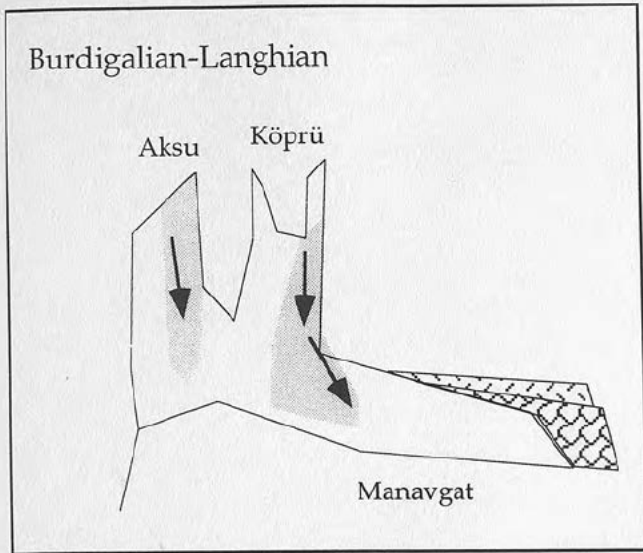
Figure 4.30 Rose diagrams indicating the palaeocurrent directions in the Karpuzçay Formation of the Manavgat basin.

Figure 4.31 is a schematic representation of the possible development of the three basins from Late Burdigalian to Messinian times as deduced from age (Figs. 4.2 and 4.29) and palaeocurrent data (Figs. 4.10, 4.16 and 4.30) for the Karpuzçay Formation. In this diagram it is suggested that the finer-grained deposits of the Karpuzçay Formation represent distal turbidites sourced mainly from the north. The conglomeratic succession in the Aksu basin has been interpreted as an ephemeral coarse-grained fan-delta sourced from the west. A similar interpretation may also apply to the Manavgat basin Taskesigi Member, although its north-south linear geometry suggests that it may represent the channel system of a fan-delta active throughout the Mid-Late Miocene from which finer-grained turbidity currents were also sourced.

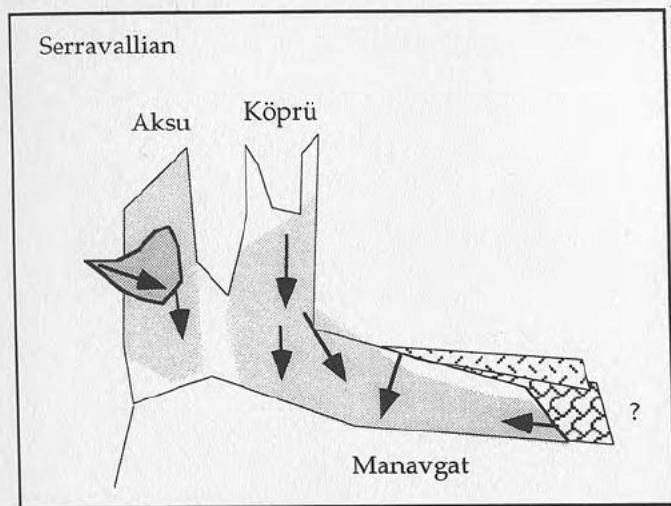
4.8 Correlation of the Karpuzçay Formation across the Isparta Angle

Nannoplankton dating of sections across the Isparta Angle by C. Müller has allowed the correlation of seven logged successions which contain Karpuzçay Formation. This correlation is displayed in figure 4.32. The following general observations can be made, always bearing in mind the biostratigraphic uncertainty inherent in redeposited rocks:

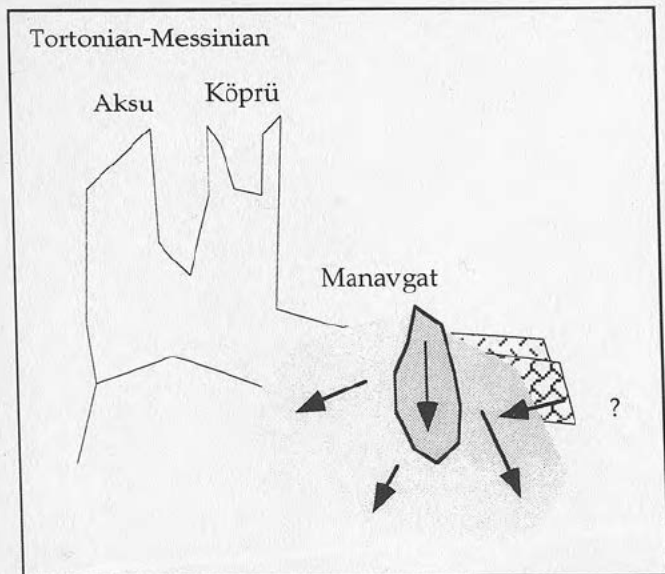
- ◆ There is a basinward shift in facies from shallow-water carbonates (Oymapinar Formation) to deeper water deposits (Karpuzçay or Geceleme Formations) during Latest Burdigalian-Langhian times (Fig. 4.32).
- ◆ This basinward shift in facies is observed throughout the Isparta Angle, but it appears to have started earlier in the south of the Manavgat basin than elsewhere (Fig. 4.32).
- ◆ Exposure of the Geceleme Formation is geographically restricted to the eastern part of the Manavgat basin. Elsewhere, coeval fine-grained Beskonak Member turbidites are found (Fig 4.29).
- ◆ Rapid coarsening of the succession in the Serravallian-Tortonian occurred in the eastern part of the Manavgat basin (Taskesigi Member). This is associated with an increase in sedimentation rate.



Burdigalian turbiditic flow inferred down the east side of the Aksu and Köprü basins from palaeocurrent and nannoplankton evidence. Coeval shallow-water carbonates forming on the west side of the Aksu and Köprü basins and in the east of the Manavgat basin.



Karpuzçay Formation deposited throughout the area on top of Burdigalian and Langhian shallow-water carbonates. Axial flow (north to south) is documented by tool marks in the turbidites in the Aksu and Köprü basins. Imbrication from a conglomeratic sequence in the Aksu basin suggests the ephemeral development of a fan-delta on the western margin. In the Manavgat basin, planktic foraminiferal marls were deposited in the north and east, whilst finer-grained turbidites flowed from the Köprü basin, over the Kikkavak fault. A small source of material is inferred to have been in the south east of the basin.



No Karpuzçay Formation younger than Lower Tortonian is preserved in the Aksu and Köprü basins. A thick succession of Beskonak Group turbidites is found in the Manavgat basin, with a core of coarse conglomeratic units (Taskesigi Group) orientated north-south in the east of the basin. The eastern source of material may still have been active at this time.





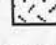
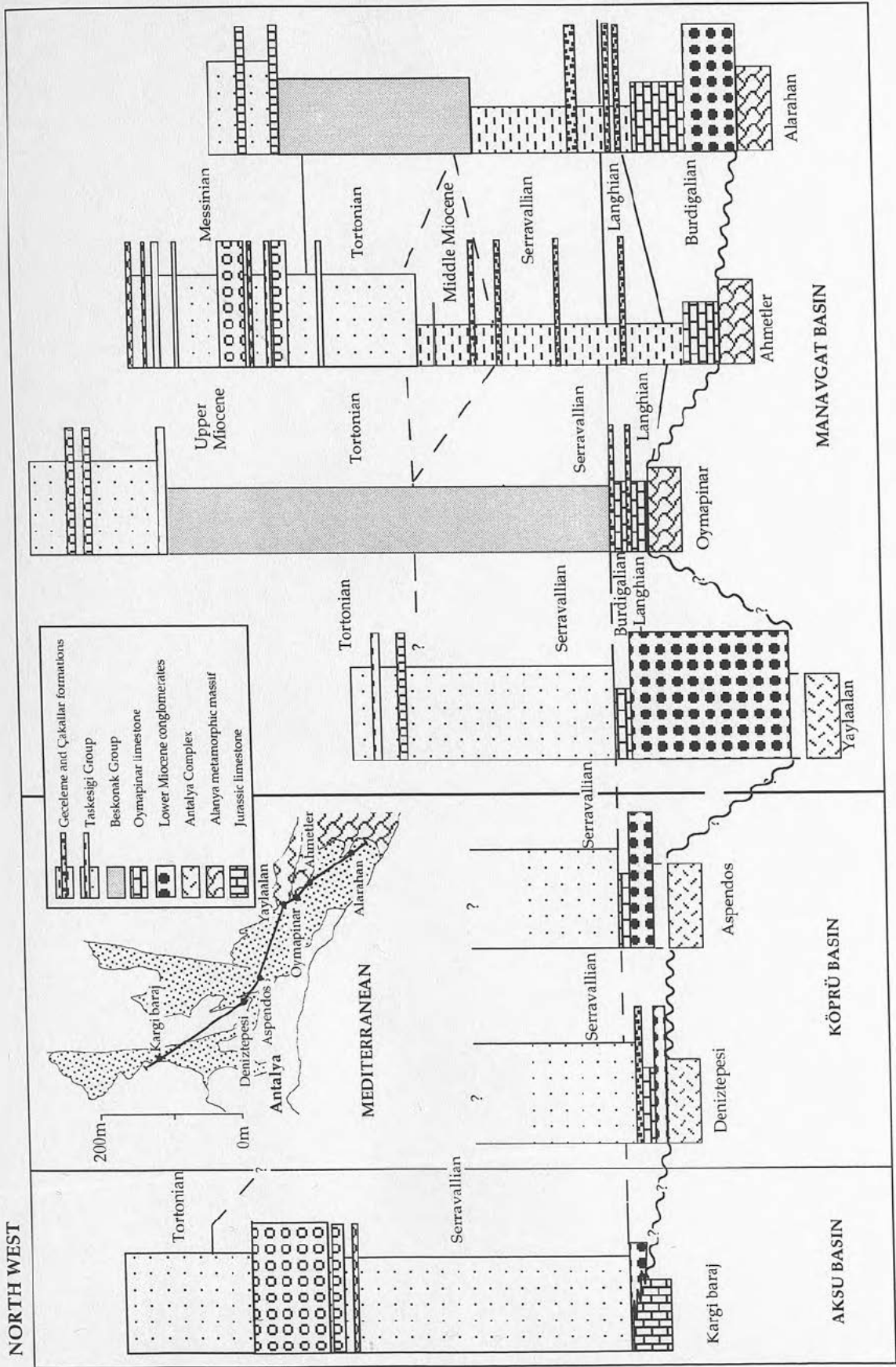
-  Turbidites (Beskonak Group)
-  Coarse fan-delta (Taskesigi Group)
-  Other Miocene sediments
-  Alanya Massif
-  Antalya Complex

Figure 4.31 Schematic representation of the deposition of the Karpuzçay Formation throughout the Miocene.

SOUTH EAST

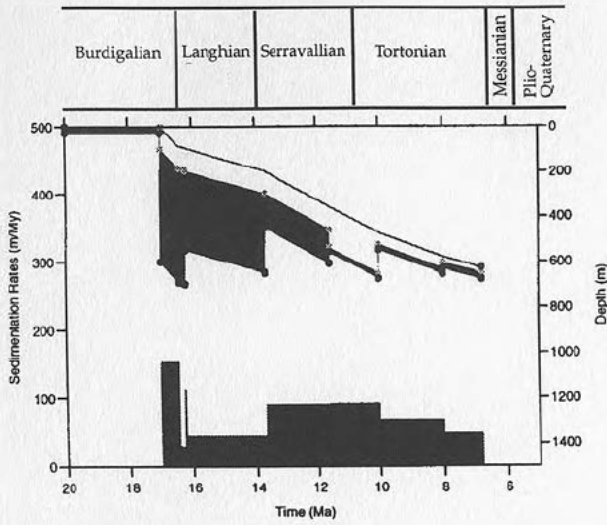


NORTH WEST

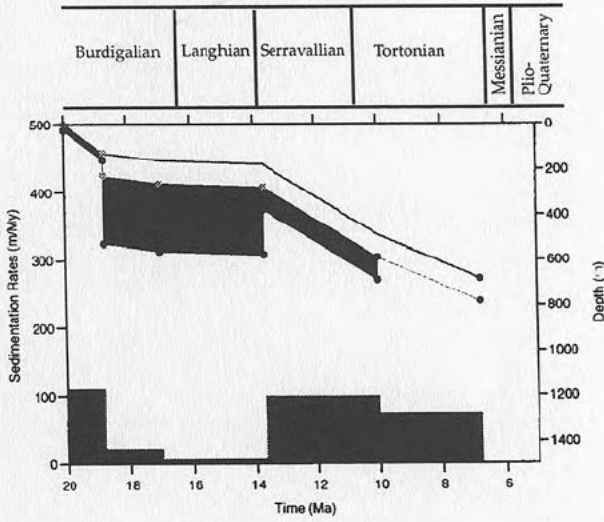
North-west to south-east correlation diagram of Miocene sections across the Isparta Angle.

Figure 4.32

Ahmetler



Oymapinar



Alarahan

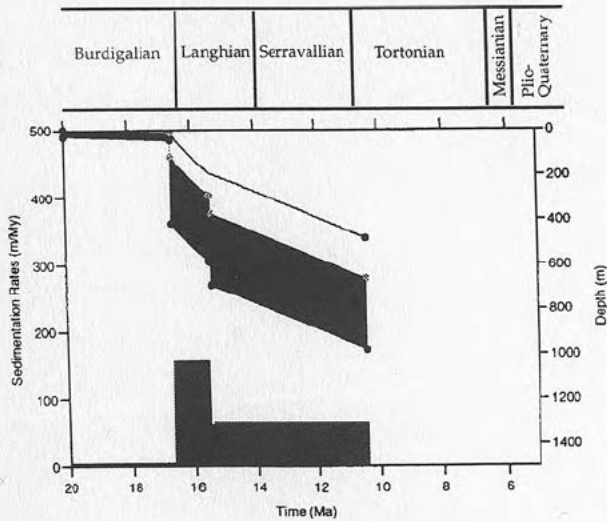


Figure 4.33 Miocene subsidence curves for the Ahmetler, Oymapinar and Alarahan sections in the Manavgat basin plotted with sedimentation rates along the bottom. (Diagram prepared using software written by J. Turner.)

These points will be discussed further in chapters 7 and 8 in terms of their tectonic and eustatic sea level implications for the Isparta Angle.

4.9 Conclusions

- ◆ The Karpuzçay Formation has been subdivided into the Beskonak and Taskesigi Members.
- ◆ The Beskonak Member has been interpreted as having been deposited mainly by low- and high-density turbidity currents.
- ◆ Some storm generated currents may have deposited and reworked material in the Aksu basin, but there is little evidence to suggest that this process had a widespread effect on the Karpuzçay Formation rocks preserved.
- ◆ The coarse-grained units in the Taskesigi Member have been interpreted as having been deposited mainly by high-density turbidity currents and debris flow processes.
- ◆ Low-density turbidity currents are also thought to have deposited the finer-grained sediments in the Taskesigi Member.
- ◆ The Taskesigi Member contains beds which document an extremely high energy of deposition.
- ◆ Coarse-grained successions in the Aksu and Manavgat basin may represent deposition on the shelfal part of a fan-delta.
- ◆ Major source of turbidite material is in the north for all basins.
- ◆ There is no evidence to suggest that western and eastern margins of the Aksu and Köprü basins were important sediment sources.
- ◆ The Kirkkavak fault had little topographic expression during the Lower Miocene allowing the Köprü basin to overflow in the south east.
- ◆ A rapid basinward shift in facies from shallow-water carbonates to deeper water foraminiferal marls occurred in the Manavgat basin near the Burdigalian-Langhian boundary.
- ◆ A decrease in water depth has been deduced from benthic/planktic ratios in the Manavgat basin.
- ◆ A shallowing up into the Tortonian is inferred for the Aksu and Köprü basins during the transition into the Aksu Formation.

Chapter 5

FAN-DELTA SEDIMENTATION, PROCESSES AND CONTROLS: THE AKSU AND KIZILDAG FORMATIONS.

5.1 Context

Sedimentary data from alluvial, coastal and subaqueous environments is discussed and interpreted in terms of fan-delta sedimentation. This concept integrates sediment transport, deposition and reworking in each of these environments so that basin-wide sedimentation processes can be studied. This results in information on palaeogeography, climate, sea level change, the mechanisms of basin fill and the tectonic process active during deposition and preservation.

5.2 Organisation of this chapter

Following a brief introduction to the temporal and spatial distribution of the sediments discussed in this chapter (5.3) a review of previous work on the conglomerate-dominated successions (Aksu and Kizildag Formations) is given in section 5.4. Section 5.5 contains descriptions of all the sub-facies observed within these successions. These have been divided into four groups (A-D) according to their sub-facies associations. A paragraph on the interpretation of the sub-facies association is given at the end of each sub-section. Palaeocurrent and provenance data is presented for the Aksu, Köprü and Manavgat basins (section 5.6). This is followed by an overview of the sedimentary system as a whole and the classification of the Fan-delta type (sections 5.7 and 5.8). Finally, section 5.9 discusses the controls on fan-delta development, e.g. climate, tectonics and eustacy and is followed by the conclusions (section 5.10).

5.3 Temporal and Spatial distribution

The sequences studied here are predominantly coarse sandstones and conglomerates. They are concentrated in northern and western parts of the Köprü and Aksu basins (Fig. 5.1) where they are Tortonian in age (Aksu Formation) and constitute the basal Miocene sediments in the far north and east of the Manavgat basin (Kizildag Formation). Figure 5.1 also indicates the key localities of the fan-delta sections mentioned on the text.

5.4 Previous work

5.4.1 *The conglomerate successions*

The basal formation in the classification of Miocene and Pliocene sediments in the area between Alanya and the Köprü basin devised by Blumenthal (1951) is called "les Conglomérats de base". Undated, these conglomerates were classified by their stratigraphic position beneath the Lower Miocene reefs (Calcaire récifal bordier; Fig. 5.2) and were only recognised along the northern margin of the Manavgat basin. Monod (1972) renamed these Manavgat conglomerates "les Conglomérats de Sevinç" after a small village to the south east of Yaylaalan, for his map of the Taurides south of Beysehir (1972; Fig. 5.2). In his thesis five years later however he refers to these conglomerates as "les Conglomérats de Tepekli" (Fig. 5.2). Monod (1977) describes these conglomerates as a formation of greatly variable thickness, up to 1000m thick, with clast-types representing "all the facies of the autochthonous and allochthonous formations of the Taurides". He notes that this succession almost always forms the basal transgressive horizon during the Miocene and suggests that the thickness variation is due to infill of an Oligo-Miocene erosion surface with palaeo-valleys developed orthogonally to the strike of the Tauride chain. He goes on to point out that the absence of this formation on the top of the Bey Daglari and Lycian Nappes (Poisson, 1974; Graciansky, 1972) in the west of the area indicates "a fundamental difference between the two arms of the Isparta Angle".

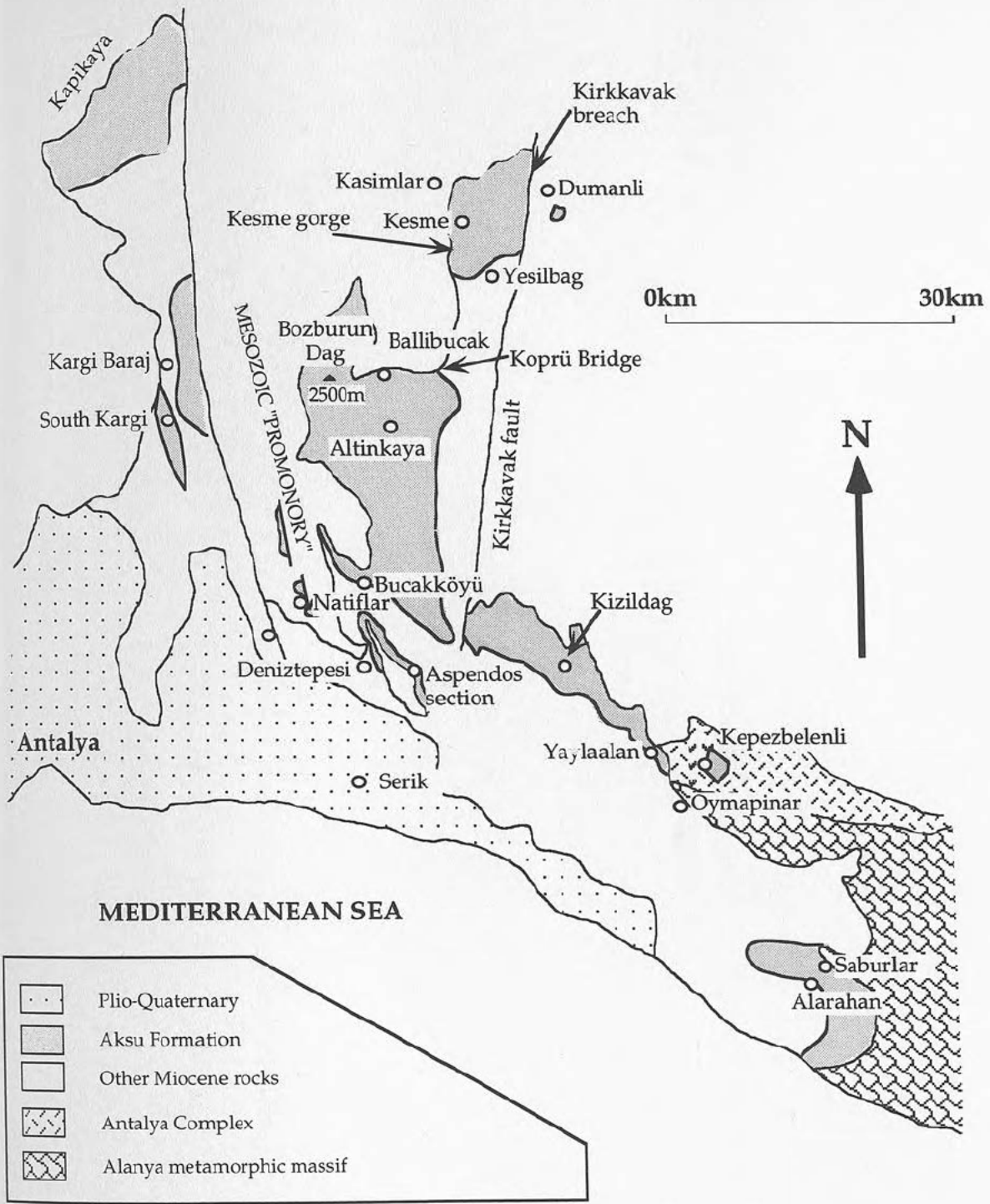


Figure 5.1 Geographic areas covered by Aksu Conglomerate Formation and the localities mentioned in the text. (Modified after Akay, 1985)

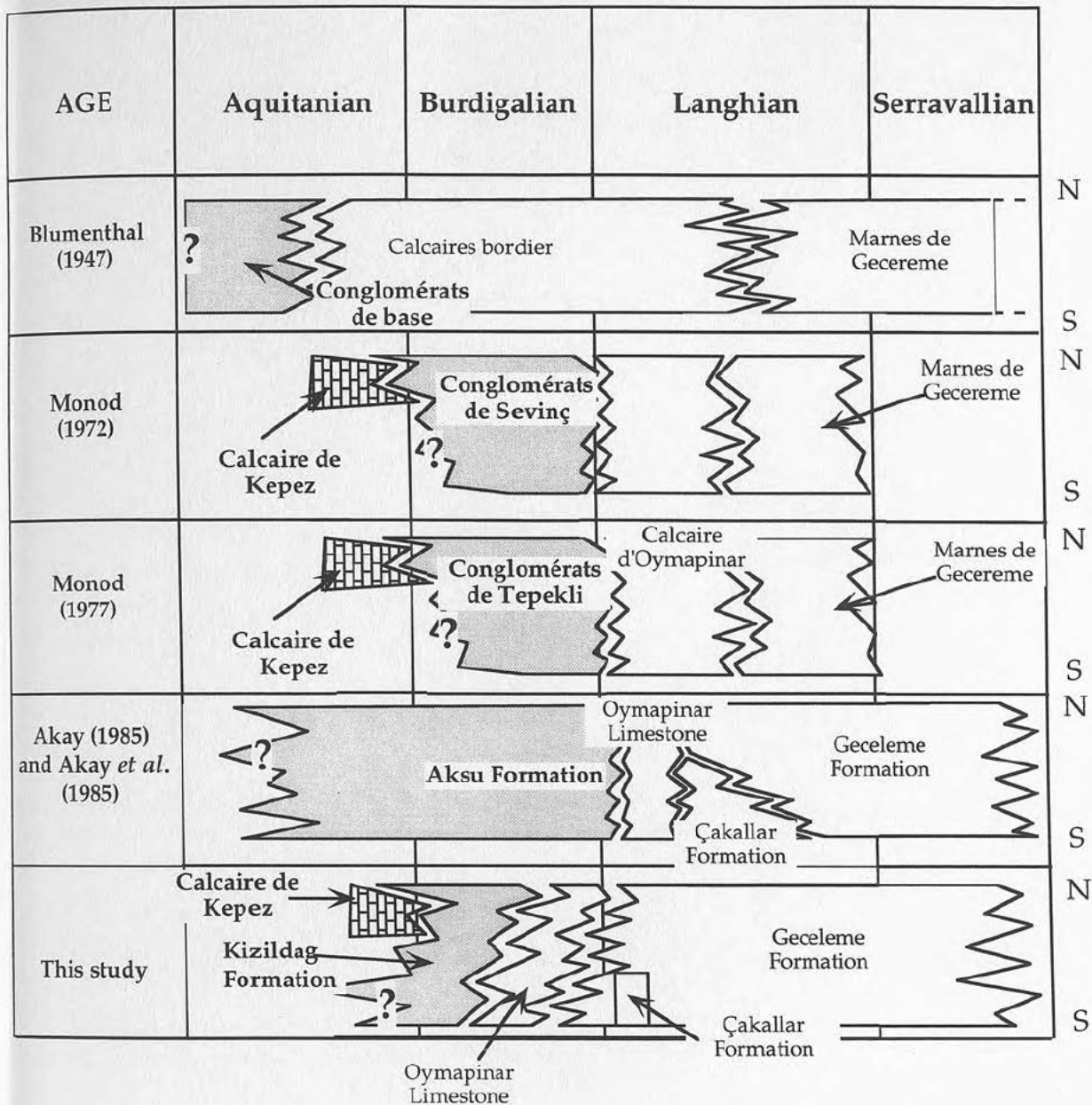


Figure 5.2 Table showing the various names and inferred ages of the basal conglomerate succession in the Manavgat basin (Kizildag Formation). For each box, the south of the basin is at the bottom and the north at the top. Thus, a south-north diachronous change from conglomerates to shallow marine carbonates is suggested as part of this study.

The Köprü basin conglomerates were undifferentiated from the turbidite succession (Karpuzçay Formation) by Monod (1972; 1977). Dumont (1974) studied the north eastern limb of the Köprü basin, named the conglomerates found around the village of Kesme in the Köprü basin (Fig. 5.1), "les Conglomérats de Kesme". He noted that conglomerates generally made up 90% of the formation and that these horizons are often laterally discontinuous. Interbedded with these highly heterogeneous, rounded conglomerates he observed lenses of reef limestone and marl, or sandstone horizons rich in oysters and gastropods. The marls in this area failed to yield age-diagnostic foraminifera. However, by studying a similar succession to the east of the Kirkkavak fault, south of the village of Dumanli (Fig. 5.1), Dumont (1974) obtained a Tortonian age (chapter 3; section 3.6.3.3) and made the assumption that the conglomerates on both sides of the Kirkkavak fault are age equivalent.

Akay and Uysal (1985) was the first person to study the Neogene sediments of the entire study area (i.e. Aksu, Köprü and Manavgat basins). He classified all the conglomerate-dominated successions in both the Upper and Lower Miocene as Aksu Formation (Fig. 5.2; Tables 2.1 and 2.4). Akay *et al.* (1985) defined this formation as consisting of terrigenous conglomerate-siltstone successions, marine conglomerate-sandstone successions and lenses of reef limestone. His generalised chronostratigraphic section across the area (Fig. 2.4) indicates that in his opinion this formation varies in age from Upper Tortonian in the Aksu basin, to Upper Oligocene near Serik in the south of the Köprü basin (Fig. 5.1). A TPAO report (Akay and Uysal, 1985) submitted on the subject of these basins reveals however, that very little data on the age of these conglomerates actually exists. The majority of the nannoplankton analyses on samples from the north of the Aksu basin yielded NN10-11 (Tortonian-Lower Messinian). A few however, produced NN3 and NN4 zones. Akay suggested that most of these are reworked. Gutnic *et al.* (1979) also quote a Tortonian age for the conglomerates onlapping onto the northern margin of the Aksu basin (Kapikaya). In conjunction with other workers, including Poisson, Akay and Uysal (1985) mapped the study area and differentiated between the conglomerate-dominated successions on the west side of the Köprü basin and the turbidite-

dominated (Karpuzçay Formation) succession on the east side of the basin.

5.4.2 *Lacustrine limestone*

Monod (1972; 1977) observed and named the thin (20m) sequence of lacustrine limestones found at Kepezbelenli beyond the northern margin of the Manavgat basin, the Calcaire de Kepez. Overlain by the Conglomérats de Tepekli/Sevinç (see above) and Calcaire d'Oymapinar (Fig. 5.2) he identified this limestone as part of the Miocene succession. Although Monod (1977) reported abundant plant traces including roots and leaf debris and rare *Charophytes*, pollen analysis failed to produce an age for this unit. No other worker has subsequently documented this limestone (Fig. 5.2).

5.5 **Facies description**

The sub-facies described below have been sub-divided, by their sub-facies association into 4 groups (A-D). A table showing the sub-facies discussed in each group, their localities (with reference to Fig. 5.1) and the formation in which they were found is shown at the beginning of each sub-facies association section. A summary table containing information concerning each sub-facies is also provided.

5.5.1 *Sub-facies association A*

A list of the sub-facies discussed in this section, their localities with reference to figure 5.1 and the formations in which they are found is given in table 5.1.

5.5.1.1 Clast-supported angular conglomerate.

Description

This sub-facies was only observed in the far north of the Aksu basin, overlapping at a high angle the Lycian remnant (Kapikaya) which forms the northern margin of the basin (Fig. 5.1). Gutnic *et al.* (1979) suggest that the sediments banked up against Kapikaya (Fig. 5.3) are Tortonian in

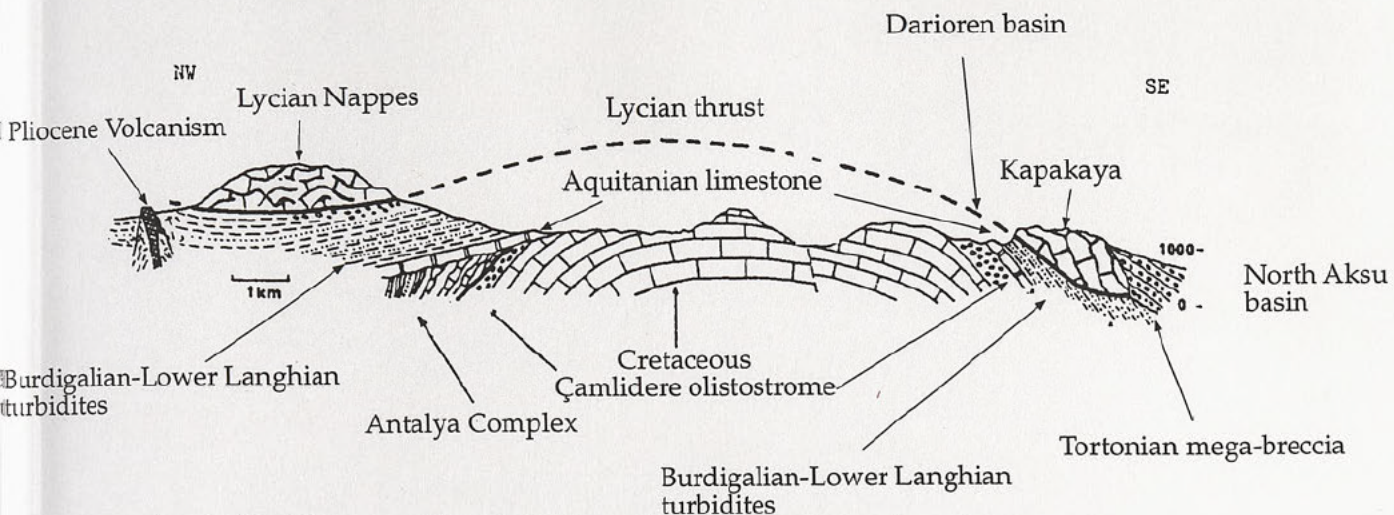


Figure 5.3 Diagram showing the onlapping relationship of the angular clast-supported conglomerate onlapping onto the Lycian Kapikaya ridge in the north of the Aksu basin (Modified after Gutnic *et al.*, 1979).



Figure 5.4 Photograph of some of the large clasts in the angular clast-supported conglomerate at Kapikaya in the north of the Aksu basin.

Table 5.1 List of the sub-facies in sub-facies association A, their localities and formations.

Sub-facies	Localities	Formation
Clast-supported angular conglomerate	Kapikaya	Aksu
Clast-supported conglomerates and coarse sandstones	Natiflar Aspendos Yaylaalan Bozburun Kapikaya Kesme Dumanli	Kizildag Aksu
Matrix-supported conglomerates	Yaylaalan Natiflar	Kizildag
Laminated sandstones	South Kargi Yaylaalan Aspendos Saburlar Dumanli	Kizildag
Calcretes and associated fine sediments	S Kargi Aspendos Kepezbelenli Yaylaalan Kapikaya	Kizildag Aksu

age. This is corroborated by Akay and Uysal (1985) who dated the conglomerate and sandstone sequences to the south of Kapikaya into which the angular conglomerate passes, as Tortonian. This sub-facies is laterally very restricted, hugging the margin of Kapikaya and perhaps extending only a few tens of metres from it. There is a clear wedge-shaped geometry associated with the exposure of the angular conglomerates such that the deposit thins to nothing <100m to the south. Clasts within this conglomerate consist of huge (up to 3m in diameter) blocks of Mesozoic limestone identical to that of which the Kapikaya is formed (Fig. 5.4) and a mass of smaller angular blocks of basalt and radiolarite. The fabric is clast supported and dramatically poorly sorted.

A consistent matrix is virtually absent, but smaller angular fragments fill some interstices. The thickness of the unit as a whole is difficult to estimate, as the base of the succession cannot be seen, but it must be >50m.

Interpretation

The nature of the poorly sorted angular clast-supported conglomerate with its limited lateral extent and wedge-shaped geometry banked up against the Kapikaya ridge, suggest formation as a talus deposit. Its similarity to other talus deposits particularly the reef limestone talus seen at Akseki road (section 3.6.2.3) and the modern talus deposited along the Kirkkavak fault on the eastern margin of the Köprü basin (Fig 5.1) is marked . The geographical association with the Kapikaya ridge and the similarity of the limestone of which it is made with respect to the large limestone blocks in the conglomerate, indicate that Kapikaya was a high at the time of deposition and a source of material. There is abundant evidence of faulting within the Kapikaya and Gutnic *et al.*, (1979) suggest that it itself was emplaced from the NW along a low angle thrust plane in the final stages of the Lycian Nappe movement (Fig. 5.3; chapter 7). There is also evidence of higher-angle faulting on the south face of the Kapikaya in the form of slickenside striated surfaces. Poisson (pers. com., 1995) suggested that these faults represent a later, Pre-Tortonian faulting event. It is suggested however, that the talus described above is fault generated, so that some of the faulting may be Tortonian in age. The lateral facies change to calcretes, sandstones (section 5.5.1.2) and conglomerates (section 5.5.1.5) suggests that the talus was deposited in a subaerial environment.

5.5.1.2 Clast-supported conglomerates and coarse sandstones

Description

Clast-supported conglomerates and coarse sandstones constitute 60-70% of all the Aksu and Kizildag Formation exposures. Beds are often characterised by limited lateral extent and erosive lower boundaries. This sub-facies is generally interbedded with finer-grained sandstones and calcretes, but in the southern central part of the study area near the village of Natiflar (Fig. 5.1) it can be seen directly overlying basement

rocks (Fig. 5.5). The upper surface of these units is generally fairly flat and at Yaylaalan this surface is often overlain by red marls containing caliche.

Bed thickness varies from 50cm to several metres. In rare cases conglomerates fine up to coarse or medium sands, but the vast majority are massive and only moderately sorted. Less frequently, large scale planar cross-bedding and imbrication such as that seen at Aspendos (Fig. 5.6) have been recorded from these clast-supported conglomerates. Clasts are generally angular to moderately rounded dependent on clast composition (section 4.6.2.2 for discussion). The composition of the conglomerate clasts is extremely heterogeneous comprising Mesozoic limestone, chert, igneous material, siltstone and sandstone (Appendix 4a, for full list of clast-types found here). Shallow water limestone clasts derived from the Miocene are almost entirely absent. They occur exceptionally at the very base of the Saburlar section overlying bored and oyster-encrusted Alanya Massif basement. Provenance data from these and other conglomerates is discussed in more detail in section 5.6 below.

The matrix is variable in both quantity and grainsize, but red, angular micro-conglomerates dominate with compositions similar to those of the clasts. In some cases a clear bimodal grainsize distribution is observed with coarse often imbricated conglomerates surrounded by a micro-conglomerate-silt grade matrix.

Interpretation

The general absence of marine fauna, the red colouration and the association of these conglomerates with red muds and calcrete horizons (section 5.5.1.5) suggest a continental environment of deposition. It seems likely however, that the conglomerates and sandstones described here represent more than one facies. Collinson (1986) described two sorts of traction deposited conglomerates common in coarse-grained alluvial fan environments: sheet or stream floods and stream channel conglomerates. In the former, conglomerates and gravels initially develop a sheet-like morphology under upper flow regime conditions. Later, the flow splits up into small channels dissecting the deposited sheet and reworking it. This may result in well sorted sands and

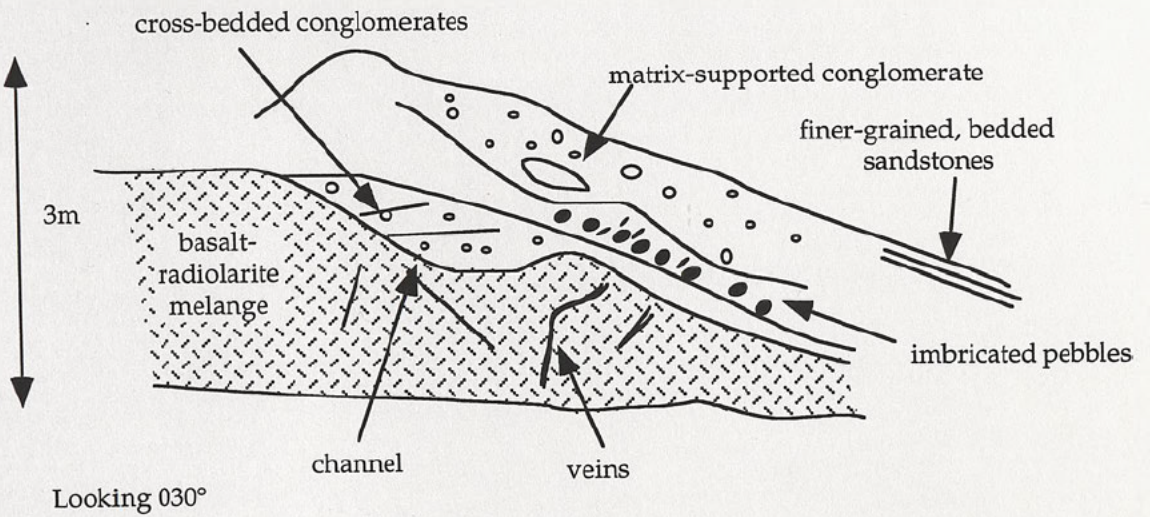


Figure 5.5 Photograph and field sketch of channelised red conglomerates directly overlying basement melange near the village of Natiflar on the Mesozoic "promontory" between the Asku and Köprü basins.

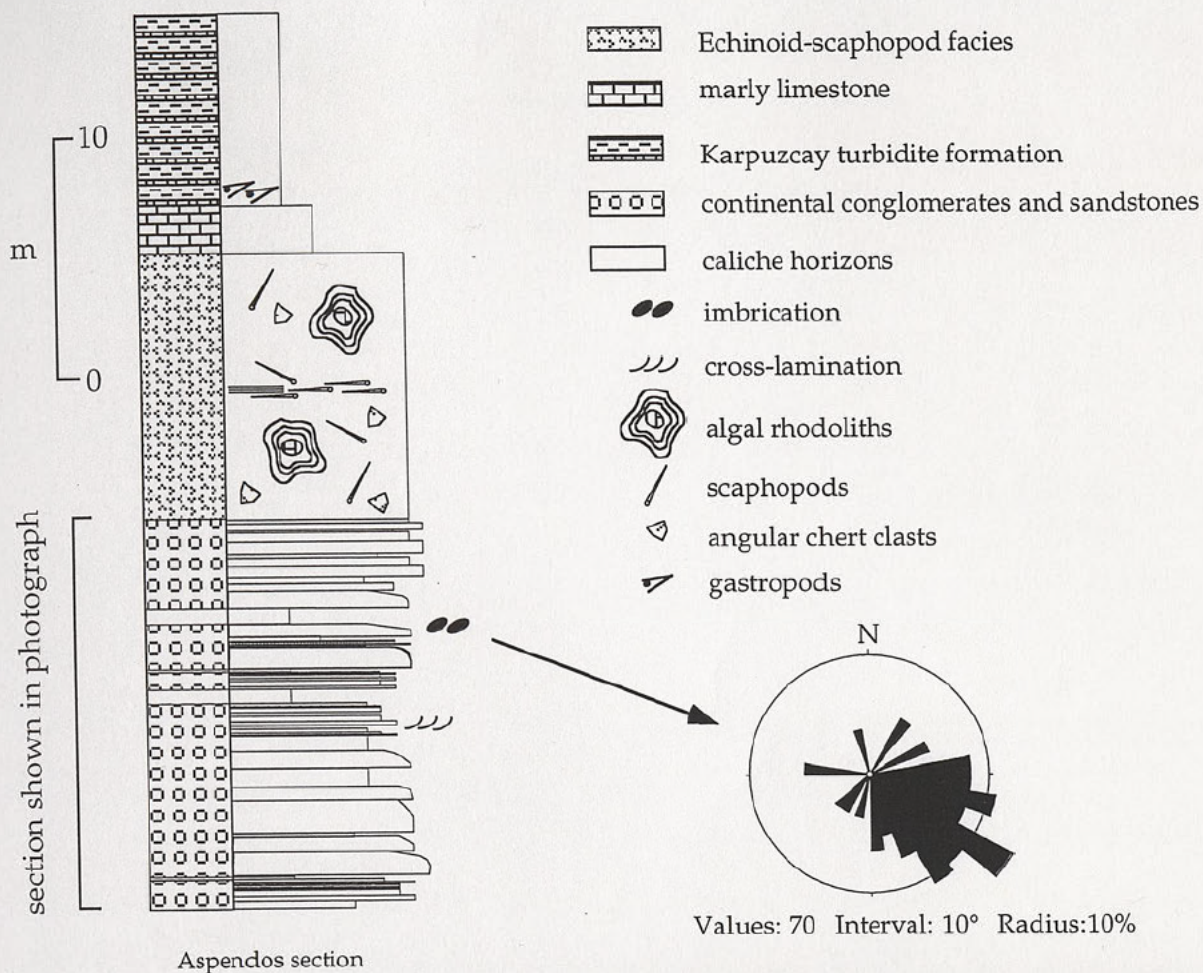


Figure 5.6 Log and photograph of the continental section at Aspendos with rather thinly bedded sandstones and conglomerates interbedded with quite well developed caliche. Imbrication data from this section is also displayed. Overlying these red beds is an exposure of the shallow marine echinoid-scapopod facies which also contains well developed rhodoliths (Fig. 3.18). Some of the scaphopods are strongly aligned in small parallel laminated sandstone horizons. This is overlain by marly limestone and then increasingly sandy turbidites with a gastropod-rich layer at the base.

conglomerates with lenticular bed forms and locally scoured bases. Cross-bedding and lamination may also develop.

Stream channel conglomerates are markedly laterally impersistent. They are deposited during the waning flood when the flow reworks less well sorted deposits within the channel. Vigorous grain transport either along the channel floor or on the top of a longitudinal bar results in the development both of stratified and unstratified bodies which are often lenticular and commonly display traction structures such as imbrication and cross-bedding. These features are typical of braided stream environments (Tucker, 1981). Table 5.2 is a list of the criteria used by Steel and Wilson (1976) for distinguishing between stream flood and braided stream deposits.

Table 5.2 Criteria for distinguishing between streamflood and braided stream deposits (Modified after Steel and Wilson, 1976).

Criteria	Streamflood deposits	Braided stream deposits
Sedimentation unit	Conglomerate bed usually overlain by sandstone beds	Conglomerate pass vertically or laterally into sandstones. Thin impersistent siltstones sometimes present
Sorting	Conglomerates usually poorly sorted, but normally with pebble and cobble frameworks	Conglomerates usually fine-grained and well sorted
Structures	Conglomerates often planar cross-stratified, sometimes on a very large scale (set thickness > 1.5m). Sandstones cross-stratified or flat-bedded	Abundance of trough cross-stratification in sandstones and conglomerates. Sandstones are also flat-bedded
Clasts	Extraformational clasts	Intraformational clasts are common
Basal erosion	Marked basal erosion	Abundance of concave-up erosion surfaces
Geometry of units	Laterally impersistent along depositional strike; often filling large channels	Always laterally impersistent, usually filling smaller channels than the stream-flood deposits

The development of cross-stratification is dependent on the availability of space (i.e. depth; Rust, 1975; Church and Gilbert, 1975) and thus has been recognised as a depth indicator (Kraus, 1984). Hein and Walker (1977) suggest that it forms during rapid decrease in fluid and sediment discharge across a bar and that this therefore is evidence for flashy, ephemeral flow. The steepness of this cross-stratification depends on the angle of repose of a gravel sheet foreset margin, the growth of which is governed by the flow symmetry, fluid discharge and sediment discharge (Hein and Walker, 1977).

It seems likely therefore that some of the conglomerates and sandstones described constitute either formation as a sheet flow or as channelised deposits, with traction processes dominating in a semi-arid environment with ephemeral flow. Stream/flood power must have been great to transport the quantity of coarse bedload that has been preserved. However, many of the massive, structureless conglomerates may be the product of mass flows similar to those described by McCallum and Robertson (in press) from the Pliocene of Cyprus. These are discussed further in the next section.

5.5.1.3 Matrix-supported conglomerates

Description

Interbedded with clast-supported conglomerates, sandstones, calcrete, siltstones and mudstones, the matrix-supported conglomerate units are laterally discontinuous on a scale of 100m or less. Within a single outcrop little scour is associated with the lower surface of the unit and the upper surface is generally flat to irregular.

Matrix-supported conglomeratic units are uncommon in the Aksu and Kizildag Formations. Most of the exposure of this sub-facies can be found near the base of the Lower Miocene succession on top of the Mesozoic "promontory" between the Aksu and Köprü basins (Fig. 5.1). Individual horizons are 50cm to several metres thick and vary greatly in appearance from one unit to the next. At Aspendos (Fig. 5.1), red siltstone with widely spaced rounded clasts up to 16cm in diameter are found interbedded with clast-supported fabrics (Fig. 5.6; section 5.5.1.2). At

Yaylaalan (Fig. 5.1) the grainsize of the clasts is much larger (up to 0.75m) and the fabric is only just matrix-supported. The matrix in these rocks is dominantly micro-conglomerate. Other structures associated with these units include crude fining up sequences and sandstone caps on matrix-supported conglomerate units seen near the village of Natiflar (Figs. 5.1 and 5.5).

Interpretation

The colour, and association with calcrete horizons (section 5.5.1.5) and conglomerates interpreted as braided stream or sheet flood deposits suggest that these matrix-supported conglomerates were deposited in a subaerial environment. The fabric and general lack of internal organisation of these units suggest that they are the product of subaerial debris flows. Massive, clast-supported conglomerates with coarse matrix were probably deposited by non-cohesive mass flow processes (Lowe, 1982) and these resemble the sandy mass flows documented by McCallum and Robertson (in press) from the Pliocene of Cyprus. Poole (1992) reported similar conglomerates from the Pleistocene of the same area and to the west of the study area, Hayward (1982) documented sandy mass flows from the Mid-Late Miocene of the Kas basin. The similarity of these conglomerates with those already described above indicates that there is a continuum of mass-flow processes which lead to a variety of different fabrics and structures. Indeed it is possible that imbrication observed in clast-supported conglomerates was produced by sandy mass-flows with density modified grain-flow processes active.

Hooke (1967) suggested that mass flows occur preferentially on the upper and middle reaches of alluvial fans. The greater abundance of debris flows overlying the basement potentially indicates a higher energy of deposition at the base of Miocene sedimentation, possible related to early subsidence of the basin. This idea is discussed further in chapter 7 in the light of structural evidence.

Nemec and Steel (1984) indicate that the lack of cohesive structures is indicative of non-cohesive flow which may well be related to the small quantity of mud and clay. It is interesting to note that even when matrix-supported debris-flows do occur in this environment, the matrix is

generally silt grade or coarser. Harvey (1984) noted that the lack of debris flows is typical of semi arid fans where soil cover is poor due to lack of abundant vegetation. This statement should be modified in recognition of the important role non-cohesive debris-flows play in transporting coarse-grained material, e.g. the lack of soil and fine material typical of a poorly vegetated semi-arid environment results in the deposition of few fine-grained, matrix-supported debris flows.

The crude fining up sequences in these units are probably caused by settling of larger clasts through the matrix during flow (Lowe, 1979). Lowe (1982) and other authors (e.g. Rodine and Johnson, 1976) have suggested that where in some cases a partially clast-supported fabric is observed and the quantity of the matrix is small, the largest clasts are not actually suspended during flow. Instead the clay-water matrix provides some buoyant lift reducing the effective weight of the clasts and lubricating them allowing them to intermittently roll, bounce and slide down slope. This type of deposit is often associated, as at Yaylaalan with small clay percentages (Winn and Dott, 1977).

Distinguishing subaerial and subaqueous mass-flow deposits

Mass-flow mechanisms have been discussed in Chapter 4 (sections 4.5.1.2 and 4.5.3.2) with reference to turbidite and large scale debris flow deposition in subaqueous environments. However, subaerial mass-flows were not covered in chapter 4 and for this reason they are touched on here.

Although in most cases it was possible to identify whether the mass-flow deposits observed in the field were subaerially or subaqueously deposited from their sub-facies associations, and their diagnostic components and structures, in other cases this was difficult or the relationships ambiguous (e.g. Bucak, Bucakköyü and Kizildag sections; Fig. 5.1). Nemec and Steel (1984) suggested a number of criteria that should be helpful in distinguishing the two environments. These are summarised in table 5.3 below and in figures 5.7 and 4.26.

Table 5.3 The differences between subaqueous and subaerial debris flows.

SUBAERIAL DEBRIS FLOWS	SUBAQUEOUS DEBRIS FLOWS
Mud-rich matrix-supported - clast-supported	Bimodal mud-rich conglomerates due to mixing with marine or lacustrine muds (Larsen and Steel, 1978; Nemeč <i>et al.</i> , 1984)
Usually ungraded and represent plug-flow deposition (Johnson, 1970)	Better internal organisation with well developed grading (Inverse/normal/both).
Inverse grading restricted to basal few cm (Gloppen and Steel, 1981)	
Signs of turbulent flow are generally transient	More often fully turbulent, but surges are still common.
Upward fining sandstone caps sometimes with erosive bases and stratified may result from turbulent fluidal flow or heavily sediment-laden stream flow following the debris flow. May also represent intersurge deposits	Sandy caps here are far more common. This is due to the tendency of subaqueous flows to evolve towards high density turbidity currents (Lowe, 1982; Nemeč and Steel, 1984)
Stream flow reworking may also produce interflow caps of tightly packed conglomerates.	Resedimentation processes common off active slump scars and unstable debris flow noses, density modified grain flows to high density turbidity currents due to partial selective liquefaction and later a series of continuous surging flows. Particularly in the lower reaches of fan-delta slopes debris flows are associated with sand-granule layers of stuff very similar to their matrix because of these processes (Postma, 1984; Nemeč <i>et al.</i> , 1984)
Composite units may result from rapidly surging flows	Composite units may result from rapidly surging flows
Where abundant units are variably channelised, clast-supported textures, crudely stratified, imbricated and have well stratified sandstone caps, this suggests depositional systems conducive to more watery flows (e.g. wet fans)	
Tend to terminate upwards with finer-grained tightly packed conglomerates.	Many show marked upward increase in matrix content particularly near top (Nemeč <i>et al.</i> , 1980; Kelling and Holroyd, 1979)
	On passing into water, debris flow may reduce its thickness and distally pass into lobes. This is particularly true of low viscosity debris flows and results in gravel lenses with little basal scour, and possible loading interbedded with marine or lacustrine fines.

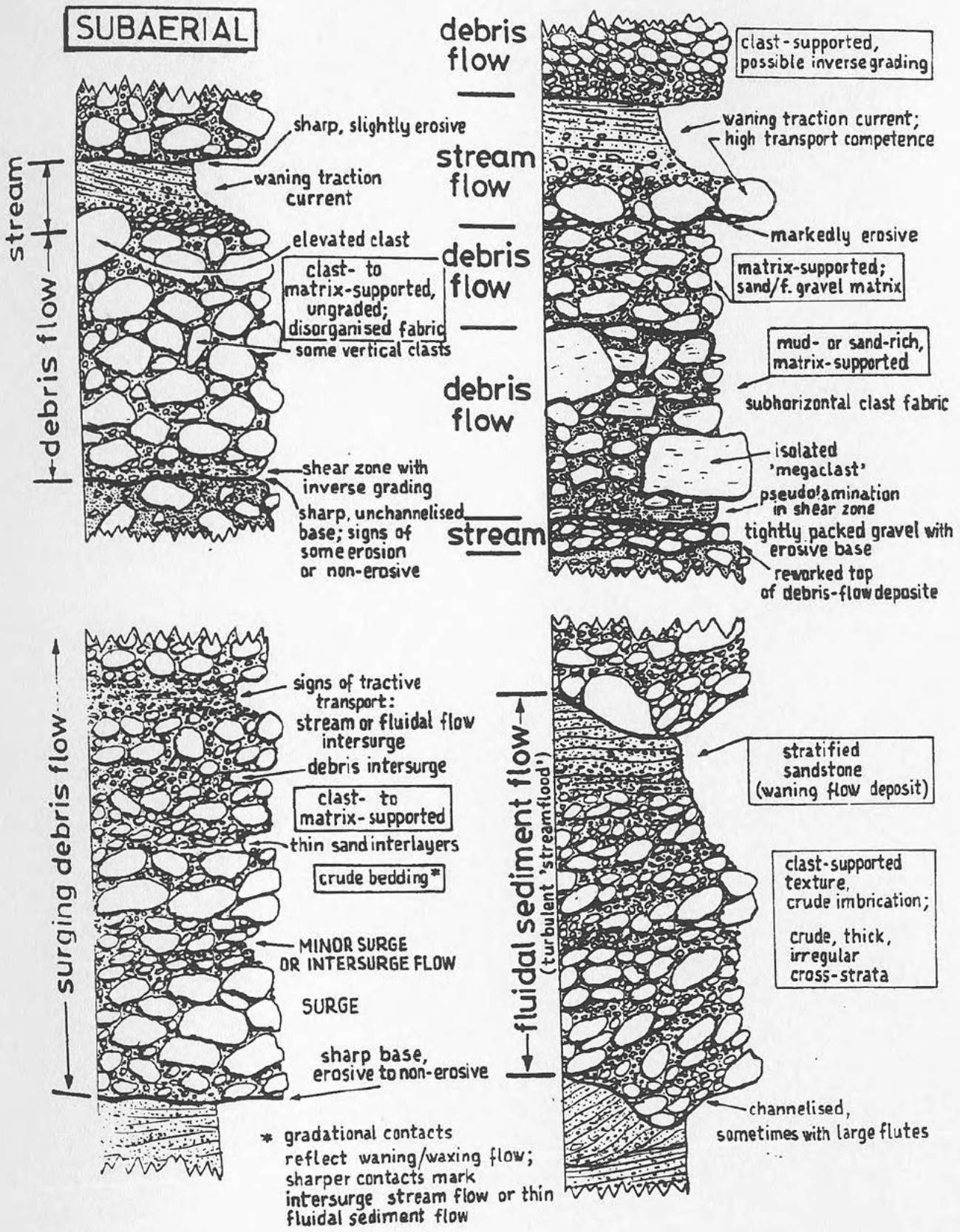


Figure 5.7 Some of the typical features of subaerial mass-flow deposits (Nemec and Steel, 1984).

5.5.1.4 Laminated sandstones

Description

Interbedded with both finer and coarser reddened sediments, the sandstones are commonly associated with a calcrete cap. Although occasionally showing scour and channel-shaped geometries, they are more often flat bedded and are in some cases slightly more laterally persistent than the conglomerates and sandstone facies described above. Wedging out geometries can still be seen on a scale of 100m or more.

Maximum bed thickness for these red sandstones recorded during this study was 30cm and generally they were 10-20cm thick. Structures within the beds varied greatly with well developed cross-bedding observed in the Yaylaalan section and cross-lamination at South Kargi. Parallel- and cross-laminations are common in the thinner units of the Saburlar section, while cross-sets characterise the thicker units which also tend to be the most laterally impersistent. Massive sandstones with no structures or grading were observed in the Aspendos section. This is rather exceptional in the context of outcrops elsewhere in the study area as normal grading is common.

Interpretation

Once again, despite the facies association with caliche horizons, red colouration and lack of marine fossils which suggests a ubiquitous subaerial environment of deposition, the variety of structures in this group almost certainly indicates deposition by more than one mechanism. It is suggested that channelised sandstones showing cross-bedding were deposited by the migration of braided stream bars (Collinson, 1986). These are generally uncommon however and the dominant sharp-bedded sandstone units with parallel and cross laminations interbedded with siltstone and developed caliche horizons may have been deposited by over bank flows (Steel and Aasheim, 1978; Tunbridge, 1981). Towards the top of the continental part of the Saburlar section which is progressively more muddy, the sandstone units may represent sheet floods distal to the active fan channel (Steel and Aasheim, 1978; Tunbridge, 1981; Hubert and Hyde, 1982). These overbank

sandstones resemble those described by McCallum (1989) from the Kakkaristra Formation in southern Cyprus.

5.5.1.5 Calcretes and associated fine-grained sediments

Description

Calcrete observed in the study area occurs in three broad morphological groups:

- ◆ as laterally continuous layers;
- ◆ as semi-continuous lenses and
- ◆ as more isolated nodules or pipes (Fig. 5.8).

Occasionally a continuum between these morphological states is visible most commonly between the lenses and the laterally continuous layers. Calcrete is intimately associated with the finest grained sediments, generally red mudstones and siltstones which are often bioturbated. Where most abundant, as at South Kargi (Fig. 5.1), calcrete horizons are interbedded with sandstones and siltstones and rare fine-grained conglomerate. Coarser conglomerate is generally absent.

Although abundant throughout the study area, laterally continuous calcrete layers are rarely thicker than 3-4cm, considerably thinner than the 2-3m reported by Allen (1974) and Leeder (1975). Siltstone, fine sandstone or mudstone layers containing lenses of calcrete can be up to 20cm thick, but in some cases it is not clear whether all the lenses are *in situ*. The dimensions of the vertical pipe structures vary from 2cm to rather irregular structures up to 10cm in length (Fig. 5.8). It is perhaps worthy of note that these vertical structures are rarely found in mudstone where the best continuous and semi-continuous calcrete layers are developed. Instead, they are found in coarser-grained siltstone. Root traces are very uncommon, but can be found at the Kirkkavak breach locality near Dumanli in the north of the Köprü basin (Fig. 5.1). Figure 5.9 shows rootlets picked out in green in medium-grained sandstone.

a)



b)



Figure 5.8 Morphologies of calcrete. a) Laterally continuous layers (South Kargi, central Aksu basin); b) nodular calcrete (Yaylaalan, northern margin of the Manavgat basin).



Figure 5.9 Evidence of roots in a medium sandstone at the Kirkkavak breach locality near Dumanli, North Kopru basin.

Interpretation

Calcite pedogenesis is a common form of mineralisation in red sequences (Collinson, 1986) indicating soil formation in an arid to semi-arid climate (Butzer, 1964). It has been suggested that vertical pipes, sheets and more isolated nodules may compare with modern rhizoliths (e.g. Klappa, 1980). Mature soil profiles require about 10,000 yrs and imply that for periods of this sort of duration little or no deposition took place, the water table was deep and the alluvial plain well drained (Leeder, 1975). In general however, none of the even continuous calcrete horizons showed a really mature soil profile i.e. substantial thickness and laminar structures (Allen, 1974). This immaturity probably indicates that periods of low sediment supply were not long enough to allow soil maturation and this is born out by the association of calcretes with coarse clastics even when best developed. Soil development is generally thought to be due to a period of incision and terrace development (cf. Tandon and Narayan, 1981) although it may also be caused by avulsion away from the site of pedogenetic activity. No evidence of terrace development was observed and it is suggested that as the argument for the immature development of the soils is dependent on high sediment influx, avulsion may be the primary control.

The paucity of evidence of plant material bears out the lack of vegetation, suggested as one possible reason for the lack of soils and associated fine-grained material (Harvey, 1984).

5.5.1.6 Interpretation of sub-facies association A

A summary of the description and interpretation of the sub-facies discussed above is given in table 5.4. The sub-facies in group A have all been interpreted as being deposited under continental conditions. The successions containing the facies described above are dominated by clast-supported conglomerates and coarse sandstones with lenticular geometries whose structures and fabric indicate deposition by mass flow and braided-stream processes. Immature caliche is observed associated with finer sediments, indicating palaeosol development when sediment influx and drainage conditions were suitable. The association of these sub-facies suggest that they were deposited as part of an alluvial fan

Table 5.4 Summary of the features of sub-facies association A.

Name	Lower boundary	Upper boundary	Lateral variation	Thickness	Sorting	Current structures	Matrix	Interpretation
Clast-supported angular conglomerate	unconformable	?	wedges out over 100m	>50m total	very poor		little	fault talus
Clast-supported conglomerate and coarse sandstone	erosive	planar	thins to nothing over several hundred meters	0.5-2m/bed	massive-moderately sorted	planar cross-bedding, rare channel structures, imbrication	red, grit-silt	sheet flood and channelised braided stream deposits.
Matrix-supported conglomerates	possibly undulating, but not very erosive	planar-irregular	wedges out over 100m	0.5-several meters	poorly sorted to crudely stratified	crude fining upward sequences	red, silt-grit	debris flow
Laminated sandstones	generally planar, occasional scour and channel shapes	planar	laterally impersistent on a scale of >100m	up to 30cm	cross-bedding, cross-lamination, parallel lamination, often normally graded	moderately sorted		braided stream bars, over bank flows, sheet floods
Calcretes and associated fine-grained sediment	gradational	gradational-sharp	rarely laterally continuous	<3-4cm	continuous layers, lenses, nodules, pipes.		mud-siltstone	palaeosol

system (Nemec and Steel, 1984). Within the alluvial conglomerate association, braided stream processes are thought to be the generally the most active (Nemec and Steel, 1984). Evidence reported here suggests that there is a continuum between traction deposition in streams and mass flow deposition, leading to a difficulty in identifying the dominant depositional process.

Historically, alluvial fans and fan-deltas are associated with tectonically active basin margins (e.g. Bull, 1977 on Death Valley). Here, coarse-grained successions resemble the alluvial sequences seen in the Humbolt Range, Nevada, at present the subject of a Ph.D. study by M. Stewart at Leeds University. Maizels and McBean (1990) suggest that the controls on alluvial fan development are primarily precipitation regime, base level changes and network expansion together with tectonic, pedogenic and fluvial processes.

Humid conditions would result in more persistent river flow resulting in meander development (Jackson, 1978; Arch, 1983; Bridge, 1985). It would also promote more extensive vegetation increasing slope stability and therefore reducing both the quantity and grainsize of the sediments supplied to the fan. Thus the preserved record of humid climatic conditions would be meandering channels through relatively fine-grained bank material (Maizels and McBean, 1990). By contrast, arid conditions would result in flashy ephemeral flow accommodated in large distributary channel systems (Maizels and McBean, 1990). Sub-facies association A described above, resembles sequences documented by Maizels and McBean (1990) in the upper part of a Cenozoic alluvial fan under semi-arid climatic conditions and the conglomerates of the Quaternary of Cyprus (Poole, 1990). They have therefore been interpreted as having been deposited under semi-arid conditions.

The dominantly coarse grainsize suggests, both that the sequences discussed here are proximal with respect to the source and that the hinterland was tectonically active and therefore able to maintain coarse clastic dominance. Fining upwards sequences typical of lobe abandonment and of prograding alluvial-fan sequences are rare, occurring potentially only at Saburlar and Bozburun Dag. Possible

reasons for the absence of such sequences are that either active tectonic subsidence or rising eustatic sea level or a balance between the two results in relative sea level keeping pace with progradation and either maintaining the gradient of deposition or steepening it.

5.5.2 *Sub-facies association B*

A list of the sub-facies discussed in this section, their localities with reference to figure 5.1 and the formations in which they are found is given in table 5.5.

Table 5.5 *List of the sub-facies in sub-facies association B, their localities and formations.*

Sub-facies	Localities	Formation
Organic-rich facies	Bozburun Yaylaalan	Kizildag
Green clays	Bozburun Yaylaalan	Kizildag
Laminated limestone and lime mud	Kepezbelenli Yaylaalan Bucakkoyu	Calcaire de Kepez (Kizildag)
Gastropod siltstones	Kapikaya	Aksu
Limestone breccia	Kesme gorge Köprü bridge	Aksu

5.5.2.1 Organic rich horizons

Description

Organic-rich horizons occur very infrequently and are generally merely thin concentrations of redeposited detrital plant material. However in two localities, Bozburun Dag and Yaylaalan, thicker organic-rich horizons are developed. In both cases the organic-rich horizons are associated with a sequence of coarse continental clastics described in section 5.5.1 above overlain by green clays discussed below in section 5.5.2.2 (Figs. 5.10 and 5.11). At Yaylaalan the organic horizon is poorly exposed and is not thought to be laterally extensive (e.g. on a scale of 10-15m). At Bozburun

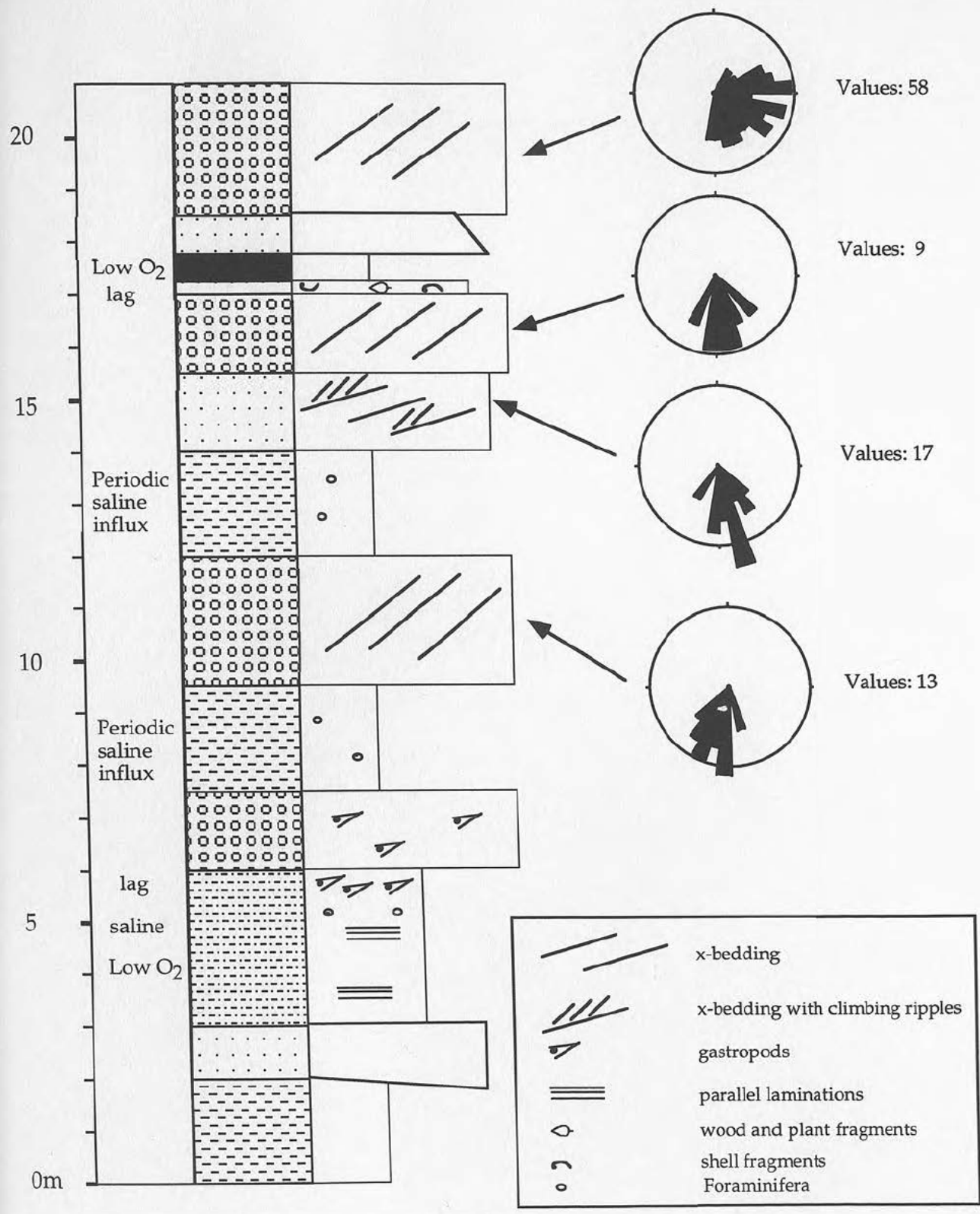


Figure 5.10 Log of the Bozburun coal section showing the interbedded marine and alluvial facies with cross-sets indicating that the current direction for the conglomerates was to the south and east.

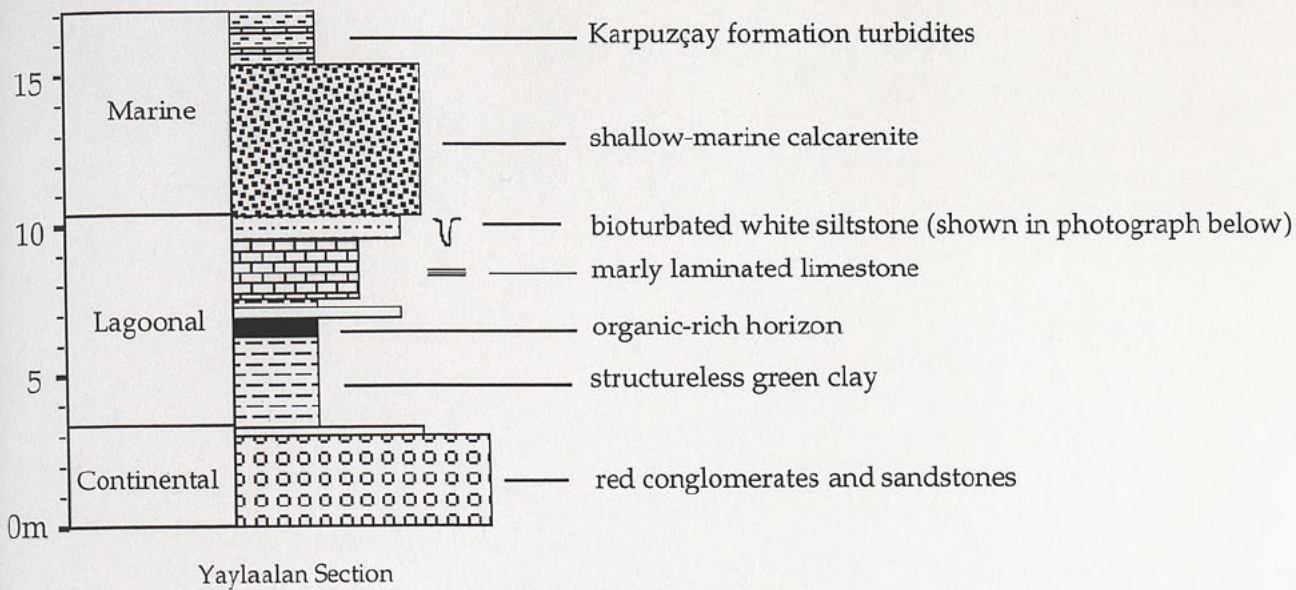


Figure 5.11 Log of the Yaylaalan transition from continental conglomerates to fully marine shallow-water limestones. Photograph of the bioturbated limemud part of the succession.

Dag however, two organic-rich layers have been mined by local inhabitants for 10 years and they can be traced for several hundred metres along strike. To the west they eventually disappear underneath the huge pile of coarse clastics that makes up the Bozburun Dag recumbent fold, while to the east they are faulted out by a high angle reverse fault (chapter 7).

The organic-rich layers at Yaylaalan and Bozburun Dag differ considerably from each other. At Yaylaalan, the layer is 60cm thick and consists of a dark, clay-rich, poorly lithified horizon which contains no identifiable organic or clastic components. At Bozburun Dag, by contrast, the two organic-rich horizons are 75cm to 1m thick and are much better indurated. A polished section revealed, in reflected light, that they consist of concentrated organic fragments (dominantly fusain) and strands with abundant fine-grained silt and biogenic detritus, much of which was broken. Rare whole, but small *Potamid* gastropods were identified preserved in primary aragonite, but flattened along the plane of fissility. No vitrinite was identified.

Interpretation

The environment required to preserve organic-rich material is still a matter of debate (e.g. sapropel formation in the Mediterranean; Ryan and Cita, 1977; Calvert, 1987; Lucci *et al.*, 1994). At Bozburun Dag, however, there is evidence from the lack of bioturbation and the preservation of primary aragonite, of an anoxic environment, at least periodically, allowing the build up of non-decomposed organic material. The microscopic structure of these horizons reveal that the organics are not entirely *in situ* although some of them may be. Influx of terrigenous and biogenic detritus led to less concentrated organic-rich layers and it is along these that the bedding-parallel fissility at Bozburun Dag has developed. The Yaylaalan organic-rich horizon is perhaps best interpreted as an oil shale. It is patently immature and was probably never deeply buried.

The lack of vitrinite in both of the samples collected implies that either the depth of burial, or the time of burial, or both, were not sufficient to mature these horizons to high quality coal, although it is clearly good enough to maintain a local mining industry. The current height of the

Bozburun Dag peak above the coal seams is in the order of 1.5km and it is therefore safe to assume that it must have been buried to at least this depth at the time the nappe formed, during the Aksu Phase of compressional deformation at the end of the Messinian (e.g. 5.5Ma; chapter 7).

5.5.2.2 Green clays

Description

These occur in two localities, Yaylaalan and Bozburun Dag (Fig. 5.1) and in both cases they are intimately associated with organic-rich layers (Figs. 5.10 and 5.11). At both localities the clays are underlain by thick successions of continental conglomerates and sandstones and at Bozburun Dag they are overlain by a similar succession (Fig. 5.10). At Yaylaalan however, green clays and an associated organic-rich horizon are overlain by non-marine limestones (Fig. 5.11 and section 5.6.2.3, below). The exposure of this facies is poor and does not allow lateral facies changes to be observed, but they are not thought to be laterally extensive.

These sticky, green and structureless clays contain no fauna at Yaylaalan. At Bozburun however some horizons contain abundant *Potamid sp.* gastropods which XRD analysis showed to have preserved their original primary aragonite mineralogy. All three washed clay samples revealed rare benthic and planctic foraminifera including *Orbulina*. The thickness of these horizons varies from a few centimetres up to 3m at Yaylaalan.

Interpretation

Potamid gastropods are well known for their lagoonal affinities (e.g. Plaziat, 1991; 1993) and their setting here, in fine-grained clays associated with anoxic sediments resembles that described by Plaziat (1984) from the Eocene of Corbières region of southern France. Periodic marine incursions possibly due to storms, washed foraminifera into this low energy environment and may well have altered salinities and oxygen levels. The structureless nature of the clays and the abundance of *Potamids* at Bozburun suggest that bioturbation was active and this indicates that anoxia was only periodically present, allowing the

accumulation of organic-rich horizons described above. The presence of *Orbulina* indicates that the succession at Bozburun is Langhian, or younger (Berggren *et al.*, 1985; Bizon *et al.*, 1974). The potential for dating the primary aragonite preserved in these gastropods using Sr dating techniques is limited by the probability that some of the $^{87}\text{Sr}/^{86}\text{Sr}$ signature is derived from a continental source, thus invalidating the use of the Sr sea water curve (e.g. McKenzie, 1988, Müller *et al.*, 1990, Elderfield, 1994).

5.5.2.3 Laminated limestone and lime mud

Description

In the Miocene laminated limestone and lime mud only occur in two localities. Both of these are on the northern margin of the Manavgat basin, at Yaylaalan and Kepezbelenli (Figs. 5.1 and 5.12). The Kepezbelenli locality was documented by Monod (1977) and he named this limestone "le Calcaire de Kepez", (section 5.3.2.2 above). Monod did not study the sediments far enough west to incorporate the similar limestone at Yaylaalan into his thesis.

Kepezbelenli, the thicker succession of the two, spans 17m of vertical stratigraphy and comprises a variety of different carbonate textures. The carbonates directly overlie Mesozoic radiolarian chert and are overlain by coarse conglomerates (Fig. 5.13). Mapping (Monod, 1972) shows that these carbonates are of limited lateral extent (Fig. 5.12). The limestone contains abundant plant debris and rare Charophytes. Pollen analysis carried out by Monod (1977) failed to produce age-diagnostic species. The succession at Yaylaalan (Fig. 5.11) is significantly different from that at Kepezbelenli. A thick pile of continental conglomerates and sandstones with less frequent interbedded finer-grained siltstones and variably developed caliche are overlain by interbedded sticky, green clays, fine sandstones and one organic-rich layer (sections 5.5.2.1 and 5.5.2.2). This is overlain by 2m of carbonate and is itself overlain by fossiliferous shallow water limestone (chapter 3).

The dominant structure of the limestone at Kepezbelenli is millimetre to centimetre, sometimes irregular, algal laminations in variable beige to

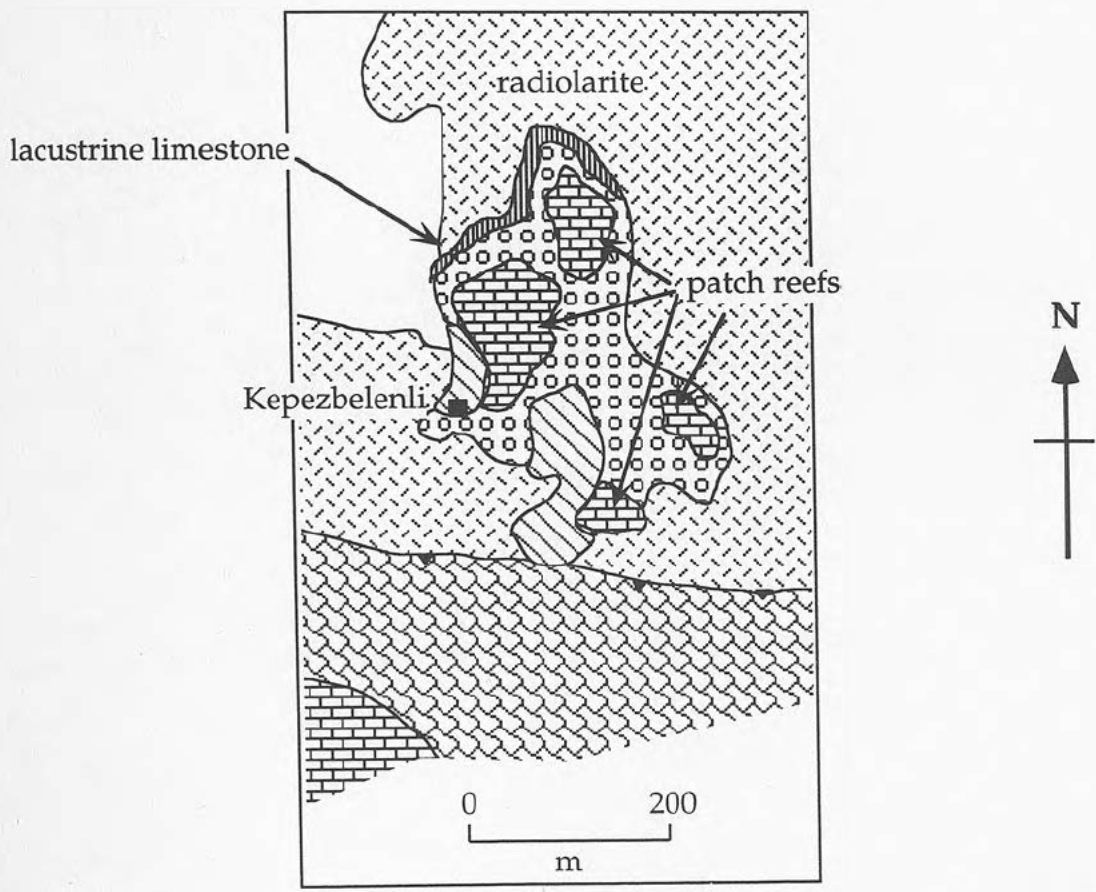
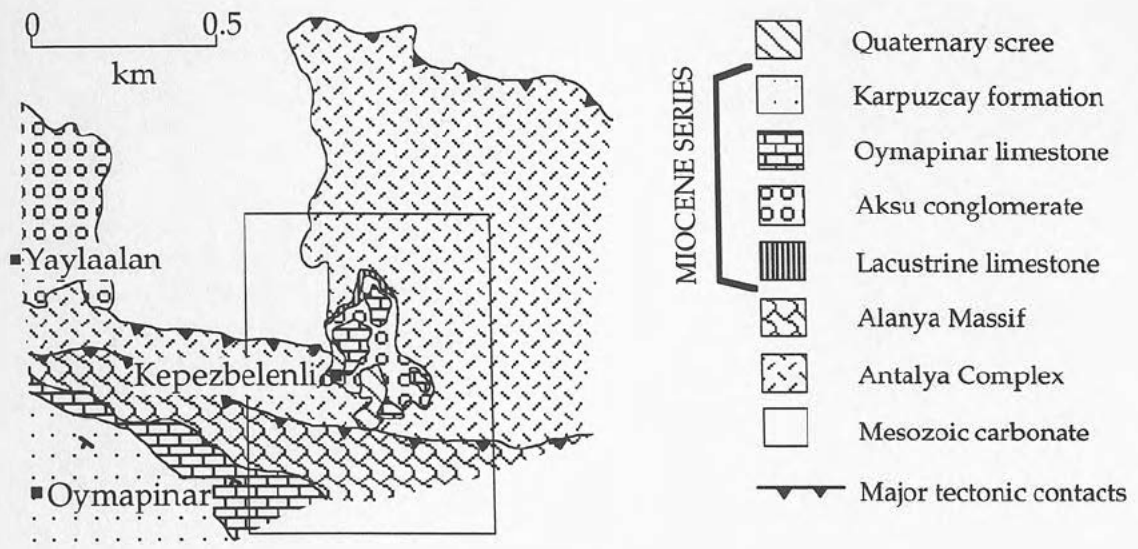


Figure 5.12 Location map of the Kepezbelenli section on the northern margin of the Manavgat basin showing the limited lateral extent of the basal lacustrine limestone and its relationship to the other Miocene sediments in the area (after Monod, 1977).

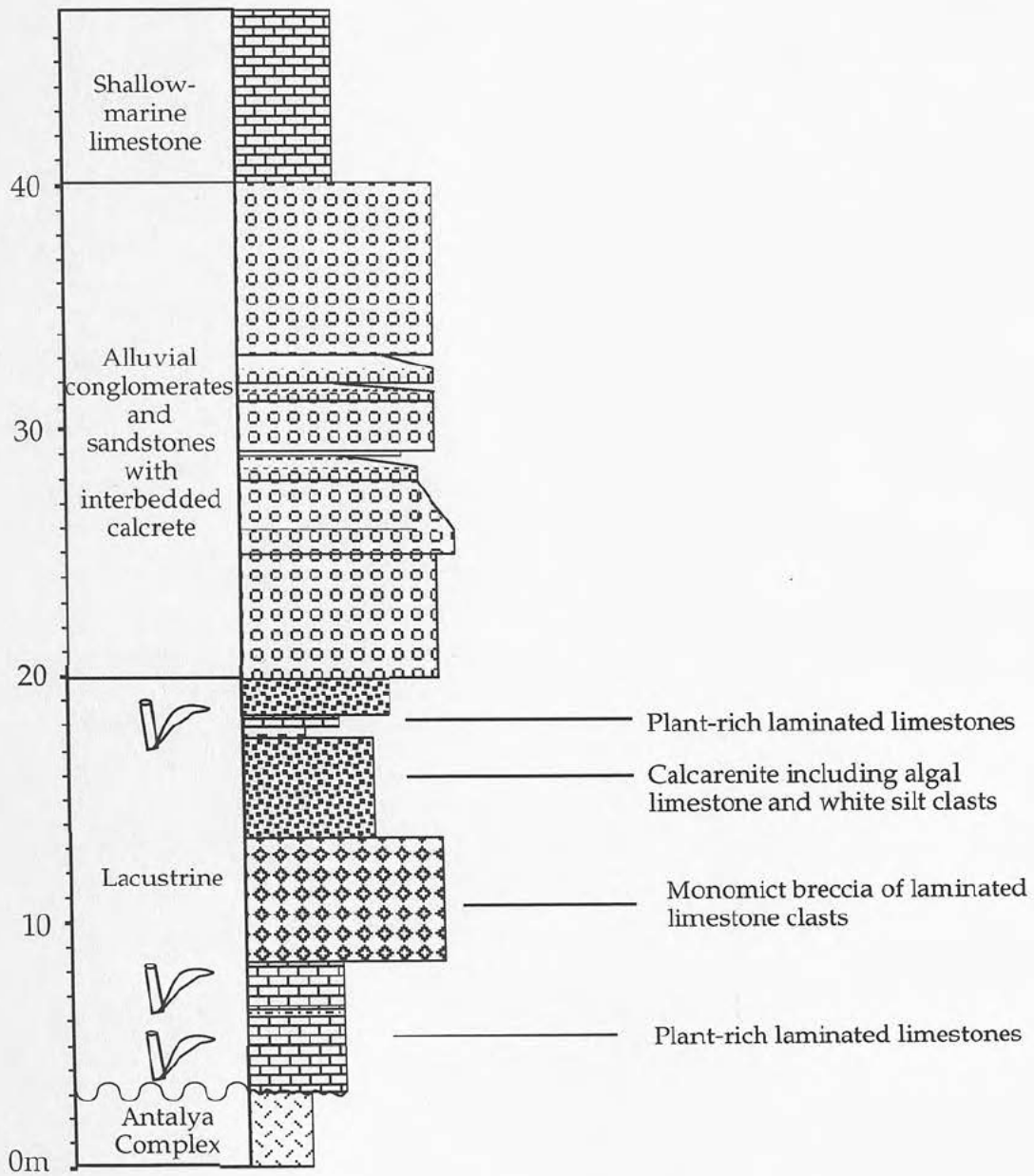


Figure 5.13 Log of the Kepezbelenli section on the northern margin of the Manavgat basin (Fig. 5.1).

brown carbonate, rich in plant fragments. Large numbers of holes less than a millimetre across can be seen throughout the rock. This facies also occurs as clasts in a breccia bound with algal strands in the same sequence. Similar carbonate, but with a different texture occurs towards the top of the section at Kepezbelenli. Here, beige-brown carbonate forms concentric rings around casts of tube structures assumed to be plant stems. White powdery lime mud occurs both at Kepezbelenli and at Yaylaalan, but in the latter locality it is heavily burrowed with a network of large branching structures (Fig. 5.11). Laminated limestones similar to those described at Kepezbelenli underlie this burrowed horizon, but the laminations are contorted. Beds either side of this deformed layer do not show deformation structures.

Interpretation

A lacustrine setting is inferred from the absence of marine fauna, the presence of algal laminations and the abundance of plant material. Quaternary tufas occur in abundance in the study area and are currently the subject of part of a Ph.D. project undertaken by C. Glover at Edinburgh University. She defines tufa as a cold water deposit which is controlled by algal growth in carbonate-rich waters producing a generally porous texture. Algal strands around plant stems at Kepezbelenli, closely resemble freshwater tufa textures in Quaternary deposits of the area. These have been interpreted as forming in association with fresh-water springs. (Glover, 1995). Lime mud horizons generally indicate slightly deeper water conditions in small lakes associated with the pools (C. Glover, pers. com., 1994). The proximity of the fully marine carbonates in the Yaylaalan forces the question of whether the lake in which these carbonates were deposited was influenced by marine conditions. It was hoped that the presence of brackish-water ostracods would shed light on this question, but no ostracods of any sort were detected. There is no evidence of marine fossil lags indicating periodic inundation by sea water in either locality, but as laminated algal structures can form in brackish and hypersaline water (e.g. Burdur Lake; Price and Scott, 1991) marine incursions cannot be ruled out particularly at Yaylaalan.

The contorted laminated limestones have been interpreted as slump structures formed whilst the algal laminations were only partially

cemented. This may have been triggered merely by slope steepening or by tectonic activity. The brecciation seen at Kepezbelenli may also have been generated by one of these two mechanisms and subsequently bound by recurrent algal colonisation.

5.5.2.4 Gastropod siltstones

Description

This facies is only found in one locality, in the far north of the Aksu basin, to the south of Kapikaya (Fig. 5.1). It consists of a 10-20m thick sequence of homogenous-looking siltstones some of which are very rich in a monospecific gastropod. No lateral variations in bed thickness of the siltstones was observed, but exposure is limited to a track cutting only half a kilometre in length. Basal facies relations here were not exposed, but the siltstones pass upwards into an increasingly coarse-grained succession of sandstones and conglomerates. Interbedded with these in the finer horizons immature caliche is developed.

The siltstones are bedded in a 5-10 cm scale and show few sedimentary structures. Horizons containing abundant gastropods were sampled and resemble the freshwater gastropod, *Viviparus*. (Further investigation into the identity of this gastropod is being undertaken in conjunction with a specialist at Université d'Orsay, France.) Previously, mammal vertebra have been found in this succession by Akay (A. Poisson, pers. com., 1994), none were discovered during this study however.

Interpretation

If, as suggested by the initial identification, the gastropod found here is a freshwater species, taken in conjunction with the mammal vertebra this suggests that these silts were deposited in a fresh water, lake environment. During silt deposition, conglomerate incursions were few, but these increased with time and the transition from lacustrine facies to alluvial facies suggests that either infill or dessiccation of the lake led to this transition. No evidence of dessiccation was observed and considering the proximity of Kapikaya and fault generated talus (section 5.5.1.1), infill of lacustrine accommodation space due to avulsion of alluvial channels is more likely to have caused the facies change.

Dating of this succession has proved extremely difficult. Both Akay and Poisson attempted to find diagnostic ostracods within these siltstones, but failed. Gutnic *et al.* (1979) and Akay and Uysal (1985) give a Tortonian age for the conglomerate sandstone sequence overlying these siltstones and it is therefore assumed that in the absence of an unconformity surface between the two, the siltstones are Middle-Late Miocene in age.

5.5.2.5 Limestone breccia

Description

This facies occurs only in the north of the Köprü basin and is best exposed at the Kesme gorge locality and at the Köprü bridge (Fig. 5.1). It unconformably overlies folded and faulted basement limestone in laterally continuous sheets (Fig. 5.14) and is itself overlain by a sequence of matrix supported conglomerates and sandstones described in section 5.6.4.1 and 5.6.4.3 above. This facies has not been previously recognised probably because of its similarity of the appearance in weathered exposure to basement limestone (Fig. 5.14). In 1974, when Dumont was writing his thesis on the area, he noted that the road south from Egirdir stops at the village of Kesme and it is quite possible therefore that he never saw the exposures created by the dirt track that now runs south from Kesme, through the Kesme gorge to Beskonak in the central part of the Köprü basin.

The age of all the Neogene sediments in the North of the Köprü basin is still a largely unsolved problem. The overlying polymict conglomerates are thought to be Miocene in age for the following reasons:

- ◆ Similar conglomerates on the east side of the Kirkkavak fault have been dated as Tortonian (Dumont, 1974);
- ◆ A polymict conglomerate-filled "breach" in the Kirkkavak fault exists just to the north of the Kesme gorge area (Fig. 5.16) which contains palaeocurrents which indicate that the transport direction into the north of the Köprü basin is likely to have been at least in part from the north east, through this conduit (Fig. 5.36).



Figure 5.14 Photograph of limestone breccia at Kesme (north Köprü basin) unconformably overlying Mesozoic carbonates.



Figure 5.15 Interbedded limestone breccia and polymict conglomerate at Kesme gorge, north Köprü basin.

This "breach" is now exposed along the scarp of the Kirkkavak fault indicating that it pre-dates the last movement on the fault. The last large scale uplifting event of the fault was probably in the latest Messinian during the Aksu Phase (chapter 7). If this is the case then the polymict conglomerates are pre-Messinian in age. It is suggested that the underlying limestone breccias can be included in the discussion of the Miocene sedimentary system because towards the top of the breccias they are interbedded with the overlying polymict conglomeratic succession. This is illustrated in figures 5.15 and 5.17 which is a log of this transition section 100m to the north of the Kesme Gorge.

The limestone breccia sub-facies is distinctive comprising of 30cm - 1.5m beds of moderately sorted angular breccia whose clasts are entirely limestone of various sorts (Fig. 5.17). Within the clast-supported fabric no structures are visible that indicate traction deposition. Intraclast space is filled with white carbonate silt, similar to that described in section 5.5.2.3 as lime mud.

Interpretation

The clast-supported fabric and angular nature of the clasts suggests that this breccia may have been deposited as slope talus. The fine-grained carbonate matrix indicates that deposition occurred in subaqueous conditions. In the rest of the study area, angular limestone clasts are incredibly rare and relative roundness has not proved a useful tool in deducing distance from the source area. In this case however, the angularity of the limestone clasts indicates that deposition must have occurred very proximally relative to the source and that very little reworking took place subsequently. It is for this reason that it is suggested that the interbedded succession of limestone breccia and polymict conglomerates shown in figures 5.15 and 5.17 is not the result of reworking and redeposition of an older, potentially Mesozoic limestone breccia, but rather primary deposition from different sources at the same time.

Although the angular clast-supported conglomerate at Kapikaya (section 5.5.1.1) and the limestone breccia discussed above, differ markedly in terms of their composition, matrix, sorting and inferred environment of

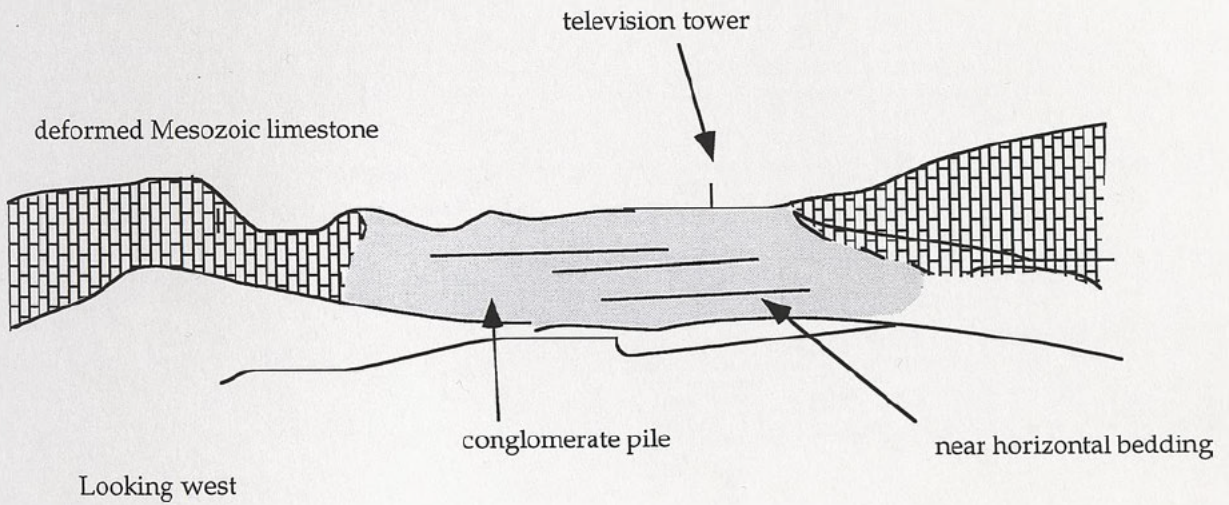


Figure 5.16 "Breach" in the Kirkkavak fault to the west of Dumanli in the north of the Köprü basin. Deformed Triassic limestone walls are filled with polymict conglomerate thought to be of Miocene age. Note television tower for scale.

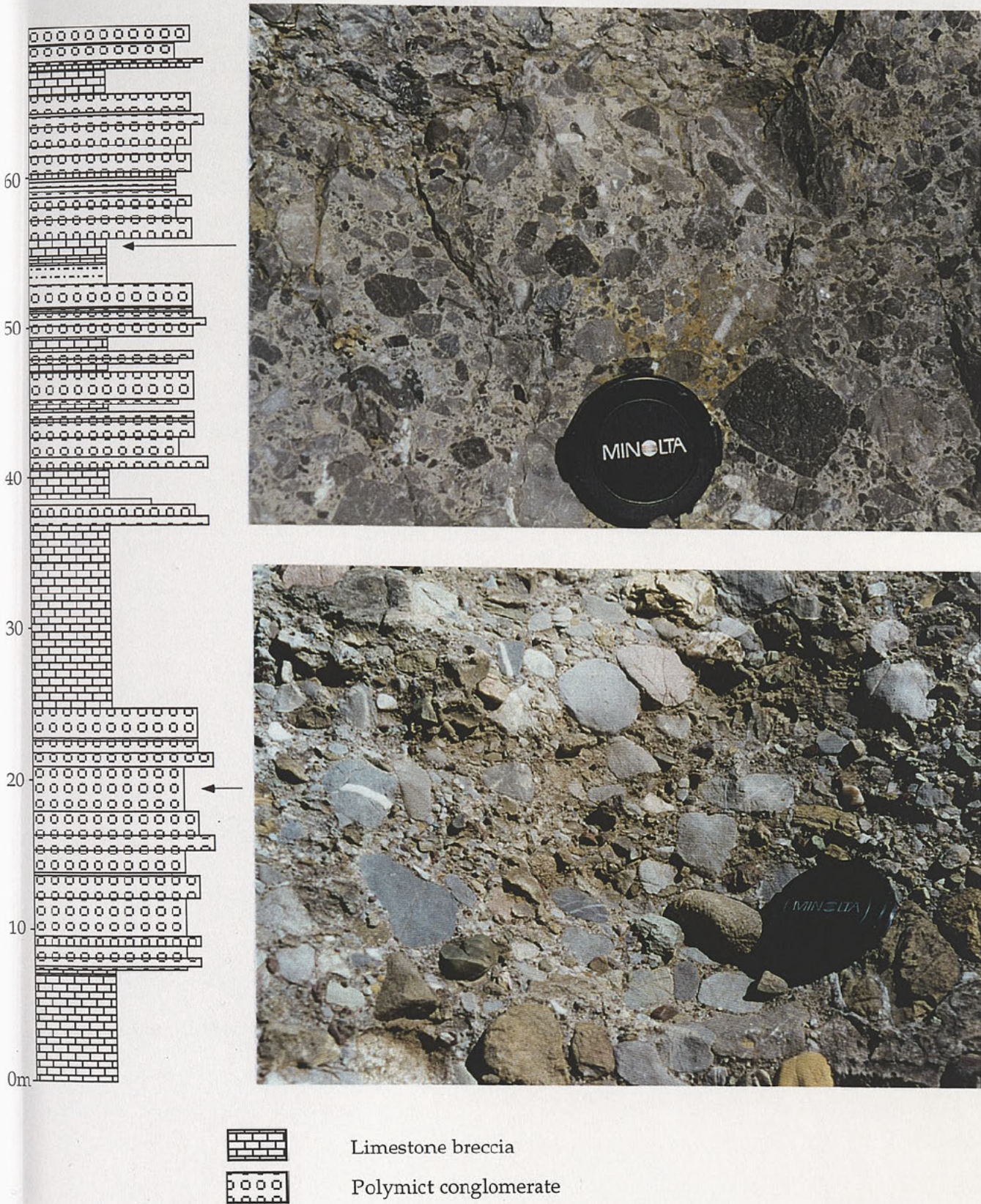


Figure 5.17 Log of the interbedding of limestone breccia to polymict conglomerate at the Kesme gorge locality, North Köprü basin. Photographs show the different appearance of the two rock types.